

# **Polymers with Upper Critical Solution Temperature in Aqueous Solution**

## **Kumulative Dissertation**

zur  
Erlangung des Doktorgrades  
der Naturwissenschaften  
(Dr. rer. nat.)

dem  
Fachbereich Chemie der Philipps-Universität Marburg  
vorgelegt von

Dipl.-Chem. Jan Seuring  
von  
Frankfurt am Main

Marburg an der Lahn 2012

Vom Fachbereich Chemie der Philipps-Universität Marburg am 13.08.2012 als Dissertation  
angenommen.

Erstgutachter: Prof. Dr. Seema Agarwal

Zweitgutachter: Prof. Dr. Andreas Greiner

Tag der mündlichen Prüfung: 14.08.2012

Hochschulkennziffer: 1180

You can know the name of a bird in all the languages of the world, but when you're finished, you'll know absolutely nothing whatever about the bird... So let's look at the bird and see what it's doing — that's what counts.

I learned very early the difference between knowing the name of something and knowing something.

*Richard Feynman*



# Contents

Introduction.....	1
Thermoresponsive Polymers.....	1
Upper and Lower Critical Solution Temperature .....	3
Prior State of Science.....	5
Motivation.....	7
Outline and Concept of the Thesis.....	8
References.....	9
Publications.....	13
List of Publications .....	15
Publication 1 .....	17
Publication 2 .....	33
Publication 3 .....	57
Publication 4 .....	67
Publication 5 .....	85
Publication 6 .....	95
Lectures.....	119
Summary .....	121
Outlook .....	123
Zusammenfassung.....	125
Curriculum Vitae .....	127
Acknowledgments.....	131



# Introduction

## Thermoresponsive Polymers

All compounds react to changes in their environment. Properties change more or less with external stimuli like temperature, pressure, radiation, magnetic fields or the chemical environment, in most cases gradually which is a form of stimuli-sensitivity. However, some compounds exhibit a drastic change of their physical properties upon only a small change in the environment. These are called stimuli-responsive. Stimuli-responsive polymers are of special interest because polymer engineering allows to unite the responsivity with the huge range of chemical and mechanical properties that polymeric materials can display. The facile production of composite materials as well as materials of high tensile strength should be named in particular.

This work deals with thermoresponsive polymers. Temperature is a stimulus that can be applied easily and reversibly in contrast to, for instance, chemical additives. For this reason thermoresponsive polymers have been subject to extensive research in academic and applied polymer science over the last decades. Among them water-soluble thermoresponsive polymers are most attractive since water is the cheapest and safest solvent as well as the solvent of living systems allowing application in the huge field of biochemistry and medicine. Although other property changes are conceivable (e.g. thermochrome polymers) the vast majority exhibits a change of hydrophilicity. This change of hydrophilicity causes phase separation from solution at a distinct temperature. In analogy to the solution properties the switch of hydrophilicity can also occur when the thermoresponsive polymer is bound to a surface or when the polymer is part of a three-dimensionally crosslinked gel. This versatility allowed the development of numerous so called “smart” applications that exploit this kind of responsivity. An illustrative example are switchable hydrophilic-hydrophobic surfaces<sup>[1-3]</sup> that were the basis of the first commercial applications as coatings for cell culture dishes. The adhesion of cells depends on the hydrophilicity of the surface. In the hydrophobic state cells can adhere and proliferate. Using a thermoresponsive polymer coating the cells can be detached just by a slight temperature change (Figure 1). This makes the use of proteases like trypsin unnecessary avoiding unwanted side reactions. Other promising application areas for thermoresponsive polymers are chromatography<sup>[4]</sup>, temperature triggered drug release<sup>[5,6]</sup>, targeted drug delivery<sup>[7]</sup>, gene therapy<sup>[8,9]</sup>, thermally switchable

optical devices<sup>[10]</sup>, or bioseparation<sup>[11-13]</sup>. However, with few exceptions applications were demonstrated only for polymers with inverse temperature dependent solubility (hydrophobic at high temperature) and due to the need of special monomers commercial applications remained restricted to small scales like cell-culture dishes<sup>[14-16]</sup> or bioseparation<sup>[17]</sup>. Both are key issues that are addressed in this thesis.

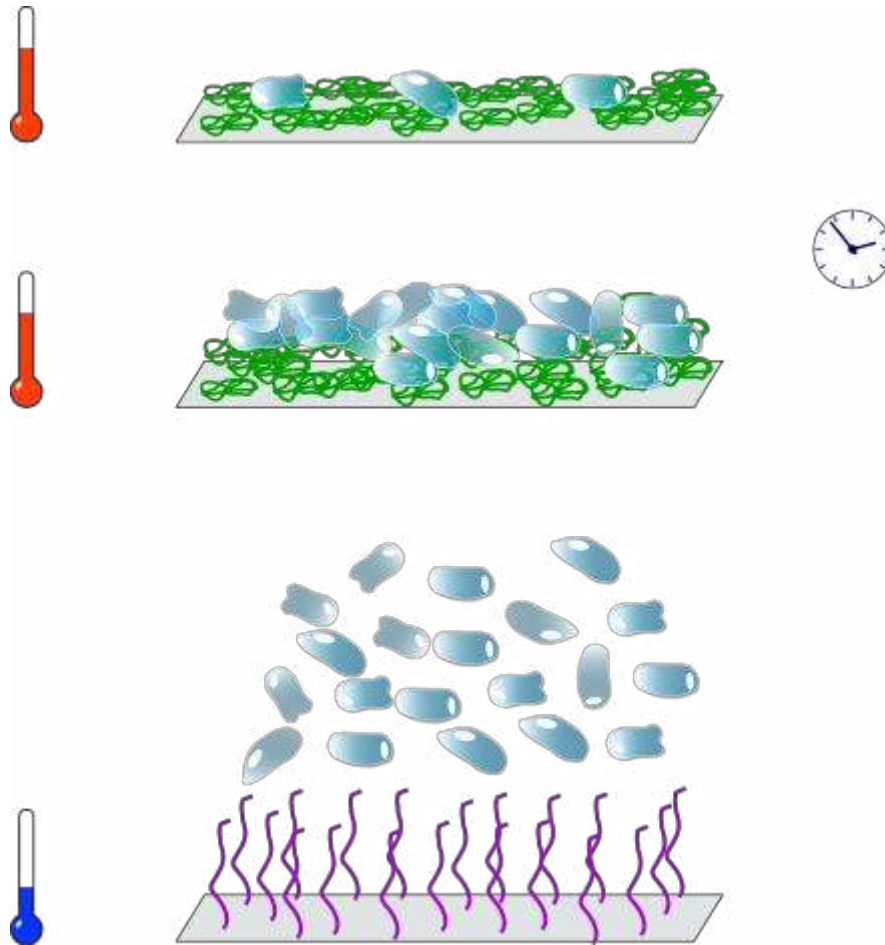


**Figure 1.** Application of thermoresponsive polymer coatings for cell sheet tissue engineering. Displayed is a polymer with inverse temperature dependence of the solubility (LCST-behavior). Image by Guillaume Paumier (CC BY 3.0 licence).



## Upper and Lower Critical Solution Temperature

The group of thermoresponsive polymers is divided into polymers that can phase separate from solution upon heating and those that can phase separate upon cooling. Above the upper critical solution temperature (UCST) and below the lower critical solution temperature (LCST) a polymer is miscible with a solvent in all proportions.<sup>[18]</sup> This definition implies that below the UCST and above the LCST there is a miscibility gap over a certain range of concentrations in which phase separation occurs. The phase behavior is conveniently displayed by isobaric phase diagrams where temperature is plotted versus the polymer concentration (Figure 2).

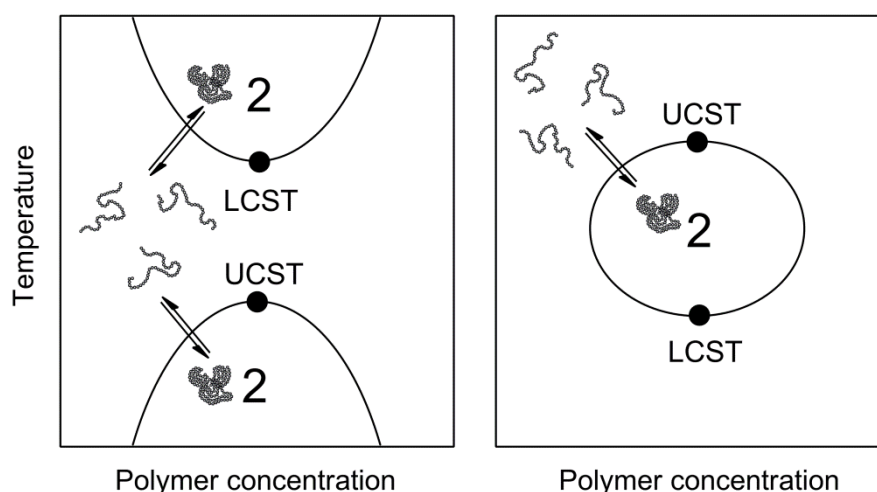


**Figure 2.** Phase diagrams displaying both UCST and LCST. “2” denotes the two phase region. left:  $LCST > UCST$ ; right: loop-shaped miscibility gap with  $UCST > LCST$ .

Coming from the one phase region (homogeneous solution) the binodal curve denotes the temperature-concentration pairs where phase separation into a polymer rich and polymer poor phase sets in. The UCST and LCST are defined as the maximum and minimum of the binodal, respectively, and can only be found at a distinct critical concentration. At other concentrations phase separation occurs simply at the “phase transition temperature”. At the binodal the solvent quality changes from a good to a bad solvent. In response the conformation of the polymer chains changes from the open coil state to the collapsed globule state.<sup>[19]</sup> To minimize solvent contact these globuli further aggregate to particles of increasing size. The appearance of aggregates is accompanied by an increasing turbidity of the mixture which can be followed by recording the transmittance or light scattering of the solution as shown in Figure 3. The temperature at which cloudiness appears or disappears is called cloud

point. Because of kinetic hindrance and aging in the collapsed state the cloud points upon cooling and heating measured by a turbidity photometer do not coincide with the phase separation temperature at the binodal. Typically, heating/cooling rates of 1 °C/min are employed. The resulting difference between the cloud point upon cooling and heating is called hysteresis.

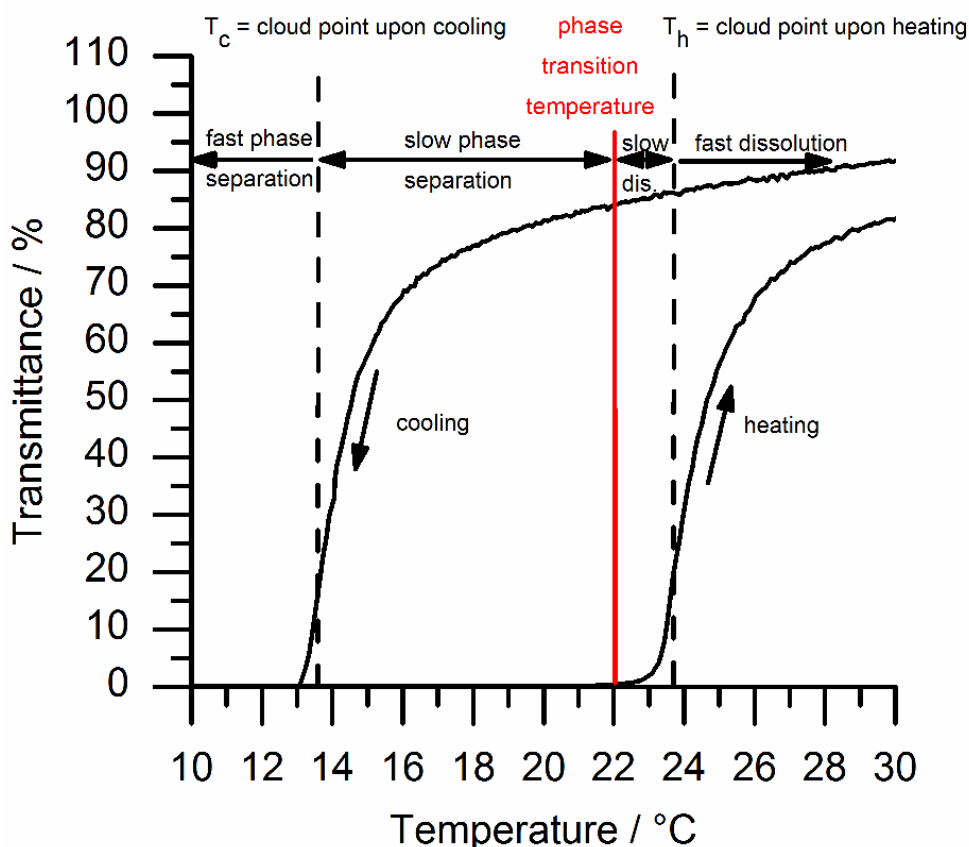


**Figure 3.** Turbidity curve of a polymer with UCST-type phase transition and a large hysteresis of about 10 °C. The heating/cooling rate was 1.0 °C/min and the inflection points were defined as cloud points. Reprinted with permission from reference [20]. Copyright (2012) American Chemical Society.

The thermodynamic reasons for phase separation can be understood on the basis of the Legendre transformation of the Gibbs equation (1).

$$\Delta G_m = \Delta H_m - T \cdot \Delta S_m \quad (1)$$

For simplicity, we assume that the polymer solution separates into pure polymer and pure solvent phases. On this assumption, a polymer dissolves in a solvent when the change of the Gibbs energy of mixing  $\Delta G_m$  is negative. In this model the enthalpy of mixing  $\Delta H_m$  and entropy of mixing  $\Delta S_m$  must both be positive for UCST polymers. At low temperature  $\Delta H_m$  exceeds the  $T \cdot \Delta S_m$  term, thus  $\Delta G_m$  is positive and the polymer is insoluble. When the temperature exceeds the phase separation temperature  $T_p$  the  $T \cdot \Delta S_m$  term outweighs  $\Delta H_m$ , thus  $\Delta G_m$  becomes negative and the polymer dissolves. Vice versa, polymers with LCST have negative  $\Delta H_m$  and  $\Delta S_m$  values and the same logic can be applied to explain phase separation upon heating.  $\Delta H_m$  and  $\Delta S_m$  are the sum of many different contributions that vary with the particular polymer structure. Generally it can be said that UCST polymers exhibit stronger polymer-polymer interactions than LCST polymers. The entropy of mixing that originates from the random distribution of chains (combinatorial entropy) is small but always positive for polymers. However, this is not the only contribution to the entropy of mixing. LCST polymers possess hydrophobic groups which exhibit a strong hydrophobic effect. This negative contribution outweighs the combinatorial part. Understanding the hydrophobic effect is not straight forward and it should be mentioned here that the classical model of ordered hydration shells (clathrate cages) around hydrophobic moieties is losing support and is likely to be replaced by a new theory.<sup>[21,22]</sup> A detailed discussion about the different contributions and of their sign and magnitude is part of the review article “Polymers with Upper Critical Solution Temperature in Aqueous Solution” (Publication 6). Moreover, this review explains phase diagrams of polymer solutions on the basis of the Flory-Huggins-Staverman (FHS) model.

## Prior State of Science

Reviews on water-soluble thermoresponsive polymers are numerous. The reader is referred to an excellent recent review of Aseyev et al.<sup>[23]</sup> As they have already pointed out there are about 60 reviews on “stimuli-responsive polymers” or “thermoresponsive polymers” each year (Scifinder scholar, word search, 2005-2010). It is suspicious, however, that the reviews deal almost exclusively with polymers that show a LCST in water (Figure 4) and the few examples of UCST polymers are merely a side note, if at all. 2005-2010 about 330 publications per year were on “LCST” in contrast to only 44 on “UCST” of which just one

per year dealt with UCST behavior in water. To the best of my knowledge Figure 5 shows all polymers with UCST in water that were known prior to this work. Among them are established polymers like poly(ethylene oxide)<sup>[24]</sup> (PEO, **1**), poly(vinyl methyl ether) (PVME, **2**)<sup>[25,26]</sup>, hydrophobically modified poly(vinyl alcohol) (PVA, **3**)<sup>[27,28]</sup> and poly(hydroxyethylmethacrylate) (PHEMA, **4**)<sup>[29]</sup>. However, these polymers show a UCST either below 0 °C or above 100 °C. Also long known were the UCST behavior of some polybetaines (**5-7**)<sup>[30-34]</sup> and poly(acrylic acid) (PAAc, **8**)<sup>[35,36]</sup>. It is important to note that due to the ionic nature of these polymers their UCST behavior is heavily affected by the addition of electrolytes. Polybetaines only display a UCST at very low ionic strength while PAAc only at very high ionic strength. The nonionic polymers **9-13** are considerably less sensitive to the ionic strength of the solution and, therefore, were most promising for a broad application. However, information about their basic properties was scarce in the publications of Aoki et al.<sup>[37,38]</sup> and patents of Ohnishi et al.<sup>[39,40]</sup> For an in depth literature review the reader is referred to Publication 6.

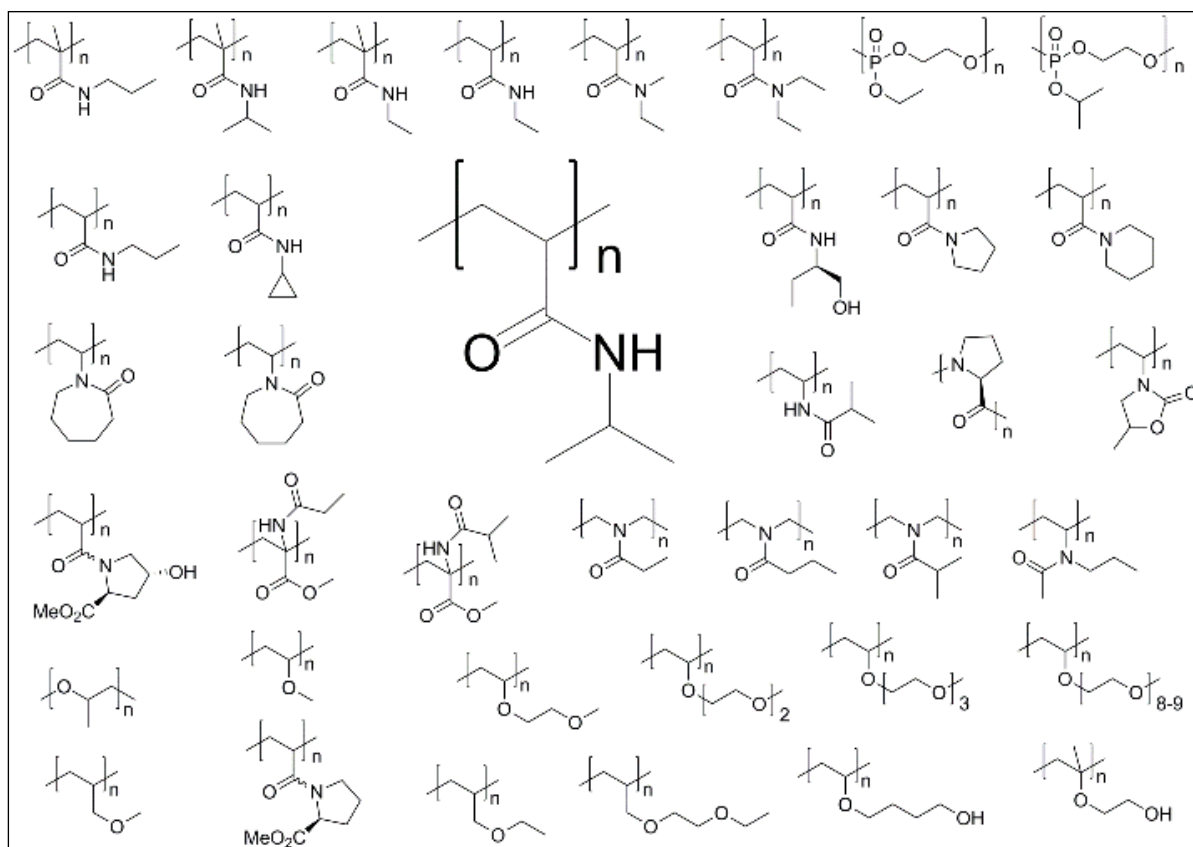


**Figure 4.** Collection of nonionic polymers showing a lower critical solution temperature (LCST) in water. Copolymers are not included. The most prominent example poly(*N*-isopropylacrylamide) (PNiPAAm) is displayed in the center.

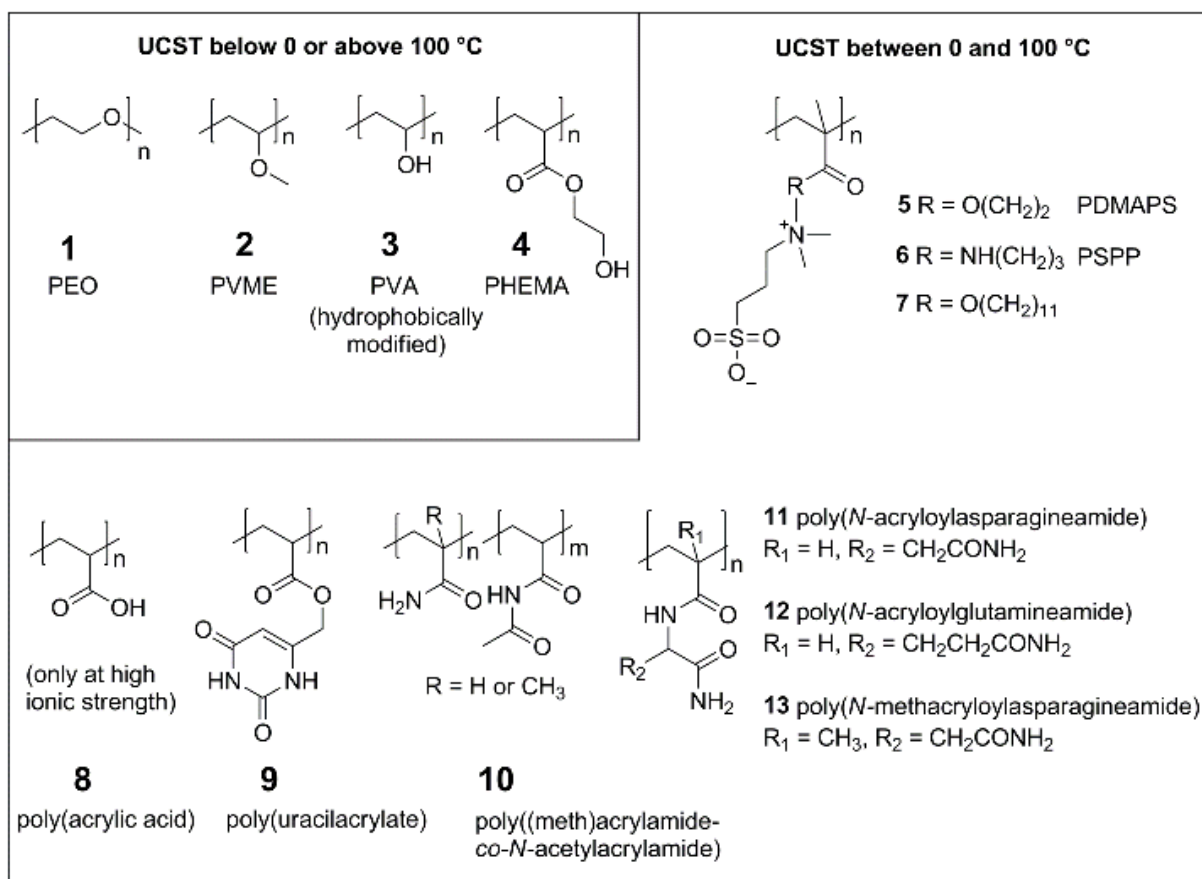


**Figure 5.** Polymers with UCST in water that were known prior to this work. Copolymers are not included except when copolymerization was necessary to observe UCST behavior.

## Motivation

The motivation of this work was to investigate why the few examples of polymers with UCST in water got no attention of the scientific community and to develop reliable synthetic strategies for the synthesis of new UCST polymers. Furthermore, structure property relationships concerning important features of the phase transition like the sharpness, hysteresis or reversibility should be evaluated.

### Outline and Concept of the Thesis

In a patent of Ohnishi et al. a copolymer of *N*-acryloylglycinamide (NAGA) and *N*-acetylacrylamide (NAAcAm) was shown to exhibit a UCST-type cloud point in water. On this basis a series of these copolymers was synthesized with the intention to study their UCST behavior. During the study it turned out that the homopolymer poly(NAGA) alone showed a UCST-type phase transition which had not been reported previously. Both the UCST behavior of the homopolymer as well as of the copolymers were investigated (Publication 1).

The subsequent work dealt with the question why this key feature remained unpublished although poly(NAGA) is known since 1964. It was found that traces of ionic groups drastically decrease the cloud point until complete water-solubility. In order to ensure a reproducible preparation of thermoresponsive aqueous solutions in the future the different possibilities for unintentional introduction of ionic groups had to be investigated. Studies focused on monomer purity, ionic initiators, ionic chain transfer agents and hydrolysis of the amide groups in the side chains (Publication 2). Furthermore, it was intended to gather basic information about the phase separation mechanism. Theory predicted that a UCST-type phase transition should be accompanied by an endothermic heat of transition upon heating. After failed attempts with conventional differential scanning calorimetry the expectation could be confirmed by ultrasensitive differential scanning calorimetry. For getting insight into the phase separation mechanism on the molecular scale dynamic and static light experiments were conducted in cooperation with Prof. Klaus Huber in Paderborn (Publication 2).

During optimization of the monomer synthesis high purity monomer could be received. Since the crystal structure was unknown and the hydrogen bonding pattern in the crystal may help to understand intra- and intermolecular hydrogen bonding in the polymers x-ray crystallography was performed in cooperation with Dr. Klaus Harms (Publication 3).

For tailored applications it is desirable that the phase transition temperature can be tuned freely over a wide range of temperatures. In analogy to LCST polymers it was tried to influence the phase transition temperature by changing the hydrophilic-lipophilic balance by copolymerization. A controlled increase of the phase transition temperature could be achieved. Simultaneously it became clear that the choice of comonomer has crucial influence on the sharpness of transition and chemical stability in aqueous solution (Publication 4). Knowledge from this work paired with knowledge gained during previous works allowed setting up rules which requirements have to be fulfilled in order to observe a UCST in water.

This hypothesis was confirmed by showing that actually very old polymer systems like poly(acrylamide-*co*-acrylonitrile) show a freely tunable UCST in water if polymerized under appropriate conditions (Publication 4).

The driving force behind the synthesis of thermoresponsive polymers is the design of so called “smart” materials. Many of these applications require attachment of the thermoresponsive polymer to surfaces. This way one can, for instance, trigger a drastic change of the wetting properties or properties as diffusion barrier for drugs by just small changes of temperature. Covalent binding of polymers onto surfaces can be done by either grafting from or onto the surface. Grafting from the surface can be achieved by controlled radical polymerization methods. For grafting onto approaches these methods are also suitable as they provide precise control of the polymer endgroups which are necessary for “grafting onto reactions”. To lay the basis for future grafting reactions a controlled radical polymerization procedure was developed using the RAFT process. Although RAFT polymerization of NAGA had been achieved previously by Lutz et al. the conditions had to be revised in order to receive a polymer that shows a UCST in water (Publication 5).

Finally, all knowledge obtained during literature research and this PhD thesis was condensed into a review article. From the sum of available data a simple qualitative approach for the tuning of the phase transition temperature could be developed based on the sign and relative magnitude of enthalpic and entropic contributions to the Gibbs energy of mixing. This approach may help to develop new UCST polymers. Furthermore, other apparent structure property relationships concerning important features of the phase transition like the sharpness, hysteresis or reversibility were discussed in detail (Publication 6).

## References

- [1] N. Yamada, T. Okano, H. Sakai, F. Karikusa, Y. Sawasaki, Y. Sakurai, *Macromol. Rapid Commun.* **1990**, *11*, 571-576.
- [2] N. Mori, H. Horikawa, H. Furukawa, T. Watanabe, *Macromol. Mater. Eng.* **2007**, *292*, 917-922.
- [3] P. Muthiah, S. M. Hoppe, T. J. Boyle, W. Sigmund, *Macromol. Rapid Commun.* **2011**, *32*, 1716-1721.
- [4] H. Kanazawa, K. Yamamoto, Y. Matsushima, *Anal. Chem.* **1996**, *68*, 100-105.

- [5] Y. H. Bae, T. Okano, R. Hsu, S. W. Kim, *Macromol. Rapid Commun.* **1987**, *8*, 481-485.
- [6] Y. Oni, W. O. Soboyejo, *Mater. Sci. Eng., C* **2012**, *32*, 24-30.
- [7] V. Bulmus, S. Patir, S. A. Tuncel, E. Piskin, *J. Controlled Release* **2001**, *2001*, 265-274.
- [8] W. L. J. Hinrichs, N. M. E. Schuurmans-Nieuwenbroek, P. van de Wetering, W. E. Hennink, *J. Controlled Release* **1999**, *60*, 249-259.
- [9] S. Dincer, A. Tuncel, E. Piskin, *Macromol. Chem. Phys.* **2002**, *203*, 1460-1465.
- [10] S. A. Asher, J. M. Weissman, H. B. Sunkura (University of Pittsburgh of the Commonwealth of Higher Education), U.S. patent 6,165,389, **2000**.
- [11] J. P. Chen, A. S. Hoffman, *Biomater.* **1990**, *11*, 631-634.
- [12] A. Kondo, T. Kaneko, K. Higashitani, *Biotechnol. Bioeng.* **1994**, *44*, 1-6.
- [13] S. Anastase-Ravion, Z. Ding, A. Pelle, A. S. Hoffman, D. Letourneur, *J. Chromatogr., B: Anal. Technol. Biomed. Life Sci.* **2001**, *761*, 247-254.
- [14] J. Kobayashi, T. Okano, *Sci. Technol. Adv. Mater.* **2010**, *11*, 014111.
- [15] M. Nakayama, T. Okano, F. M. Winnik, *Mater. Matters* **2010**, *5*, 56-62.
- [16] Cosmo Biosciences Inc., Online-Shop,  
[http://www.cosmobrands.com.cn/product/transplant-medical/22\\_eb9a98efc499464b9e88b6d66cc67423.shtml](http://www.cosmobrands.com.cn/product/transplant-medical/22_eb9a98efc499464b9e88b6d66cc67423.shtml) (May 2012).
- [17] Magnabeat Inc., Online-Shop Therma-Max,  
[http://www.magnabeat.com/e\\_thermamax.html](http://www.magnabeat.com/e_thermamax.html) (May 2012).
- [18] A. D. McNaught, A. Wilkinson, *IUPAC. Compendium of Chemical Terminology (the "Gold Book")*, Blackwell Scientific Publications, Oxford, **1997**.
- [19] Y. Lu, K. Zhou, Y. Ding, G. Zhang, C. Wu, *Phys. Chem. Chem. Phys.* **2010**, *12*, 3188-3194.
- [20] J. Seuring, F. M. Frank, K. Huber, S. Agarwal, *Macromol.* **2012**, *45*, 374-384.
- [21] T. P. Silverstein, *J. Chem. Edu.* **1998**, *75*, 116-118.
- [22] T. P. Silverstein, *J. Chem. Edu.* **2008**, *85*, 917-918.
- [23] V. Aseyev, H. Tenhu, F. M. Winnik, *Adv. Polym. Sci.* **2010**, *242*, 29-89.
- [24] B. Hammouda, D. Ho, S. Kline, *Macromol.* **2002**, *35*, 8578-8585.
- [25] K. Van Durme, G. V. Assche, E. Nies, B. Van Mele, *J. Phys. Chem. B* **2007**, *111*, 1288-1295.
- [26] G. V. Assche, B. Van Mele, T. Li, E. Nies, *Macromol.* **2011**, *44*, 993-998.
- [27] K. Shibatani, Y. Oyanagi, *Kobunshi Kagaku* **1971**, *28*, 361-367.
- [28] T. Shiomi, K. Imai, C. Watanabe, M. Miya, *J. Polym. Sci., Polym. Phys. Ed.* **1984**, *22*, 1305-1312.



- [29] R. Longenecker, T. Mu, M. Hanna, N. A. D. Burke, H. D. H. Stöver, *Macromol.* **2011**, *44*, 8962-8971.
- [30] D. N. Schulz, D. G. Pfeiffer, P. K. Agarwal, J. Larabee, J. J. Kaladas, L. Soni, B. Handwerker, R. T. Garner, *Polym.* **1986**, *27*, 1734-1742.
- [31] M. B. Huglin, M. A. Radwan, *Polym. Int.* **1991**, *26*, 97-104.
- [32] M. Arotcarena, B. Heise, S. Ishaya, A. Laschewsky, *J. Am. Chem. Soc.* **2002**, *124*, 3787-3793.
- [33] J. Virtanen, M. Arotcarena, B. Heise, S. Ishaya, A. Laschewsky, H. Tenhu, *Langmuir* **2002**, *18*, 5360-5365.
- [34] P. Köberle, A. Laschewsky, T. D. Lomax, *Makromol. Chem., Rapid Commun.* **1991**, *12*, 427-433.
- [35] P. J. Flory, J. E. Osterheld, *J. Phys. Chem.* **1954**, *58*, 653.
- [36] R. Buscall, T. Corner, *Eur. Polym. J.* **1982**, *18*, 967-974.
- [37] T. Aoki, K. Nakamura, K. Sanui, N. Ogata, A. Kikuchi, T. Okano, Y. Sakurai, *Proceed. Int. Symp. Control. Rel. Bioact. Mater.* **1996**, *23*, 767.
- [38] T. Aoki, K. Nakamura, K. Sanui, A. Kikuchi, T. Okano, Y. Sakurai, N. Ogata, *Polym. J.* **1999**, *31*, 1185-1188.
- [39] H. Nagaoka, N. Ohnishi, M. Eguchi (Chisso Corporation), U.S. patent 2007/0203313 A1, **2007**.
- [40] N. Ohnishi, H. Furukawa, K. Kataoka, K. Ueno (National Institute of Advanced Industrial Science and Technology; Chisso Corporation), U.S. patent 7,195,925 B2, **2007**.



# **Publications**



## List of Publications

- Publication 1** Non-Ionic Homo- and Copolymers with H-Donor and H-Acceptor Units with a UCST in Water **17**  
Jan Seuring, Seema Agarwal, *Macromolecular Chemistry and Physics* **2010**, *211*, 2109-2117
- Publication 2** Upper Critical Solution Temperature of Poly(*N*-acryloyl glycinamide) in Water: A Concealed Property **33**  
Jan Seuring, Frank M. Bayer, Klaus Huber, Seema Agarwal, *Macromolecules* **2012**, *45*, 374-384
- Publication 3** *N*-Acryloyl glycinamide **57**  
Jan Seuring, Seema Agarwal, Klaus Harms, *Acta Crystallographica Section E* **2011**, *E67*, o2170
- Publication 4** First Example of a Universal and Cost-Effective Approach: Polymers with Tunable Upper Critical Solution Temperature in Water and Electrolyte Solution **67**  
Jan Seuring, Seema Agarwal *Macromolecules* **2012**, *45*, 3910-3918
- Publication 5** Controlled Radical Polymerization of *N*-Acryloylglycinamide and UCST-type Phase Transition of the Polymers **85**  
Fangyao Liu, Jan Seuring, Seema Agarwal, *Journal of Polymer Science, Part A: Polymer Chemistry* **2012**, DOI: 10.1002/pola.26322
- Publication 6** Polymers with an Upper Critical Solution Temperature in Aqueous Solution **95**  
Jan Seuring, Seema Agarwal, *Macromolecular Rapid Communications* **2012**, DOI: 10.1002/marc.201200433



# Publication 1

## Non-Ionic Homo- and Copolymers with H-Donor and H-Acceptor Units with a UCST in water

Jan Seuring, Seema Agarwal, *Macromolecular Chemistry and Physics* **2010**, *211*, 2109-2117.

doi: 10.1002/macp.201000147

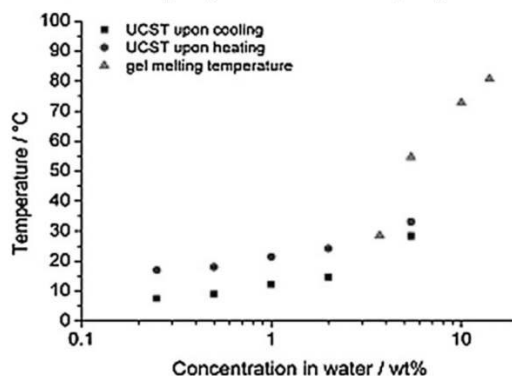
### Author contributions

Experimental work and writing of the manuscript was done by Jan Seuring. Prof. Seema Agarwal was responsible for supervision and correction of the manuscript.

# Non-Ionic Homo- and Copolymers with H-Donor and H-Acceptor Units with an UCST in Water<sup>a</sup>

Jan Seuring, Seema Agarwal\*

A well-studied example of a thermoresponsive polymer is PNiPAAm, which exhibits a sharp coil-to-globule transition in water at its LCST. A study relating to the missing counterpart of LCST polymers is presented: *N*-acryloylglycinamide (NAGA) homopolymer and copolymers from NAGA and *N*-acetylacrylamide (NAAcAm) that show a sharp UCST (where the sharpness depends on the composition). The polymers were synthesized by free-radical copolymerization and the copolymerization parameters were determined by the method of Kelen-Tüdös. The UCST was investigated by turbidimetry, regarding the influence of the copolymer composition, the polymer concentration and the addition of electrolytes.



## Introduction

Stimuli-responsive polymers, or “smart” polymers, exhibit a predictive and sharp change in properties upon only small changes in environment (e.g., temperature, pH, ionic strength, radiation, or mechanical stimuli).<sup>[1]</sup> These changes can result in phase separation from aqueous solution or order-of-magnitude changes of hydrogel size and water content. One class of smart polymers are thermoresponsive polymers, the best-known example being poly(*N,N*-isopropylacrylamide) (PNiPAAm), which

undergoes phase separation from aqueous solution at approximately 33 °C.<sup>[2]</sup> Above this lower critical solution temperature (LCST), the dissolved polymer changes from the coil to the globule conformation. PNiPAAm and related polymer systems have been well characterized and are widely used to design smart materials.<sup>[3]</sup> Current applications are bioseparation and drug delivery, the development of new biocatalysts, biomimetic actuators, and surfaces with switchable hydrophobic/hydrophilic properties.<sup>[1,4]</sup>

In contrast to LCST polymers, there are only a few polymeric materials known that show an upper critical solution temperature (UCST) in water.<sup>[5–10]</sup> Furthermore, in non-patent literature, there have been no reports on non-ionic polymers that show a UCST in water with a sharp phase transition. A typical UCST system is based on a combination of acrylamide (AAm) and acrylic acid (AAc) in the form of an interpenetrating polymer network (IPN). This system makes interpolymer complexes via hydrogen bonding at lower temperatures, which dissociate at higher temperatures.<sup>[5]</sup> To make the system more efficient, with suppressed intramolecular complexation, a variation is to

J. Seuring, S. Agarwal  
 Philipps-Universität Marburg, Fachbereich Chemie, Hans-  
 Meerwein Strasse, D-35032 Marburg, Germany  
 E-mail: agarwal@staff.uni-marburg.de

<sup>a</sup> Supporting information for this article is available at the bottom of the article’s abstract page, which can be accessed from the journal’s homepage at <http://www.mcp-journal.de>, or from the author.

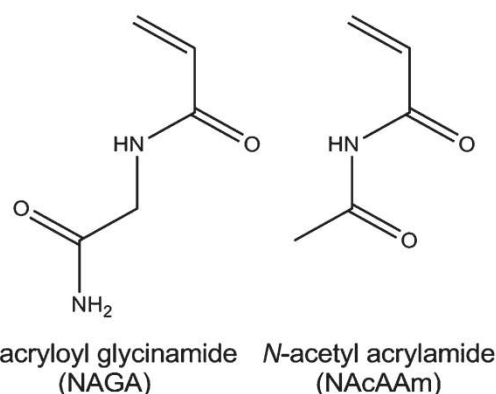


use *N,N*-dimethylacrylamide (DMAAm) instead of AAm for IPN formation with poly(acrylic acid) (PAAc).<sup>[6]</sup>

In one of the studies in the literature, IPNs composed of poly[AAm-*co*-(butyl methacrylate)] and PAAc demonstrated positive swelling changes with an abrupt transition as the temperature increased. Temperature-modulated, controlled drug release using the swelling-shrinking responses of UCST interpenetrating hydrogels as an on-off switch for drug release has also been reported by Katono et al.<sup>[7]</sup> Recently, there was an interesting article by Jiang and Deng et al.<sup>[8]</sup> reporting the effect of microstructure on thermal phase transitions of a particular block-copolymer system, poly(caprolactone-*co*-glycolide)-*block*-poly(ethylene glycol)-*block*-poly(caprolactone-*co*-glycolide), made by ring-opening polymerization. There was a switch from LCST behavior to UCST behavior on changing the microstructure, keeping the polymer composition the same.

UCST polymers based on ionic interactions are also known, for example, polybetaines (PBs). Among the synthetic PBs currently available, polysulfobetaine has been shown to exhibit a UCST in aqueous solution.<sup>[9]</sup> Laschewsky et al.<sup>[10]</sup> showed both an LCST and a UCST in their schizophrenic copolymer of PB with *N*-isopropylacrylamide (NiPAAm). The change in the polarity of the micellar core in the process of a reversible phase transition provided the possibility of solubilizing different compounds in a given solution just by simple heating and cooling. Both of the above systems have, however, major disadvantages that limit their applicability. Blends rely on intermolecular interactions; hence, equimolar concentrations are needed to provide a sufficient number of proton donors and proton acceptors. Electrostatic interactions of polyelectrolytes (the PBs) are disturbed by the presence of salts, which makes them unsuitable for application in biological fluids. This is why novel polymer systems that show a sharp UCST over a wide range of concentrations and that are tolerant to electrolytes are highly desirable.

This work reports, to the best of our knowledge for the first time, the UCST of aqueous solutions of the homopolymer of *N*-acryloylglycinamide (NAGA) bearing H-donor and H-acceptor sites. Thermally reversible gelation of concentrated aqueous solutions of poly(NAGA) was first observed and studied by Haas et al.<sup>[11a-f]</sup> in the late 1960s. Haas showed that thiocyanate as a hydrogen-bond-interrupting agent prevents the formation of gels.<sup>[11b]</sup> Furthermore, they calculated that the average number of groups involved in a crosslink is too low to form crystallites.<sup>[11c]</sup> This was supported by the extremely low heat of formation per crosslink. They estimated it to be  $-5$  to  $-12$  kcal·mol<sup>-1</sup> crosslinks, which was impossible to be detected by differential thermal analysis.<sup>[11e]</sup> They concluded that the crosslinking is based on randomly



■ Scheme 1. Monomers used for the copolymer synthesis.

distributed hydrogen bonds. More recently this was supported by dynamic light scattering and Raman spectroscopy.<sup>[12,13]</sup>

Despite all these findings concerning thermally reversible gelation of concentrated solutions, phase separation at an UCST has never been reported. We investigate the influence of the polymer concentration on the UCST. A UCST copolymer system based on H-donor NAGA and H-acceptor *N*-acetylacrylamide (NAAAm) monomers (Scheme 1) made by free-radical polymerization was mentioned in a patent.<sup>[14]</sup> We present a detailed study of the system where the copolymerization parameters, as well as the correlation between the UCST and the copolymer composition, polymer concentration and presence of electrolytes are examined.

## Experimental Part

### Materials

2,2'-Azobisisobutyronitrile (AIBN, Fluka) was recrystallized from ethanol. AAm (98.5%, Acros), acryloyl chloride (96%, Fluka), glycine hydrochloride (98%, Acros) and *N,N*-dimethylacetamide dimethylacetal (98%, Alfa Aesar) were used as received. Solvents were distilled prior to use.

### Analytical Techniques

#### Gel-Permeation Chromatography (GPC)

The molecular weights and molecular-weight distributions of the polymers were determined using GPC in one of two set-ups. One set-up comprised a Knauer pump equipped with two NOVEMA columns (particle size 10  $\mu$ m, dimension 8  $\times$  300 mm<sup>2</sup>, porosity 1 000 and 30  $\text{\AA}$ , respectively), calibrated with poly(2-vinylpyridine) standards, and a differential-refractive-index detector. The eluent was 0.3 M aqueous formic acid with a flow rate of 1 mL·min<sup>-1</sup>. The other set-up comprised a Knauer pump equipped with two GRAM

columns (particle size 10  $\mu\text{m}$ , dimension  $8 \times 300 \text{ mm}^2$ , porosity 100 and 3 000  $\text{\AA}$ , respectively), calibrated with poly(methyl methacrylate) (PMMA) standards, and a differential-refractive-index-detector as well as a UV-detector. The eluent was *N,N*-dimethylformamide (DMF) with 5  $\text{g} \cdot \text{L}^{-1}$  lithium bromide added. For both set-ups, the molecular-weight distributions were calculated using the Win GPC Unity software, version 5403.

### NMR Spectroscopy

$^1\text{H}$  and  $^{13}\text{C}$  NMR spectra were recorded either on a Bruker Avance DRX-500 (500 MHz) or a Bruker Avance 300 A (300 MHz) spectrometer, with  $\text{D}_2\text{O}$  used as solvent. One drop of methanol was added as a standard for the  $^{13}\text{C}$  NMR measurements, and was calibrated to  $\delta = 49.50$ .

### Thermal Analysis

For thermal characterization, Mettler thermal analyzers having 851 TG and 821 DSC modules were utilized. Indium and zinc standards were used for temperature and enthalpy calibration of the 821 DSC module. DSC scans were recorded under a nitrogen atmosphere (flow rate = 80  $\text{mL} \cdot \text{min}^{-1}$ ) at a heating rate of 10  $^\circ\text{C} \cdot \text{min}^{-1}$ . The melting temperatures ( $T_m$ ) were determined from the endothermic-peak maxima of the first heating cycle. The glass-transition temperature ( $T_g$ ) was taken as the inflection point of the observed shift in the base line of the second heating cycle of the DSC scan. The thermal stability was determined by thermogravimetric analysis (TGA) with a nitrogen atmosphere (flow rate = 50  $\text{mL} \cdot \text{min}^{-1}$ ) using powdered samples. A heating rate of 10  $^\circ\text{C} \cdot \text{min}^{-1}$  and a sample size of 5–20 mg was used in each experiment.

### Turbidity Measurements

Turbidity measurements were performed on a Tepper turbidity photometer, TP1-D, at a wavelength of 670 nm, a heating rate of 1  $^\circ\text{C} \cdot \text{min}^{-1}$  and with magnetic stirring. The polymer solutions (above the UCST) were filtered through a warm 0.45  $\mu\text{m}$  poly(ethylene terephthalate) (PET) syringe filter before measurement. Unless stated otherwise, each measurement was repeated at least five times and the mean value and standard deviation were calculated. The turning point of the transmittance curve was considered as the UCST. It was graphically determined by the maximum of the first derivative of the heating or cooling curve. The sharpness of the transition was determined as the interval in  $^\circ\text{C}$  from 0.1 to 0.9 or 0.9 to 0.1 transmittance for the heating or cooling curve, respectively. The very low UCST of the NAGA82 sample was determined visually.

### Gel Melting Temperature

The gel melting temperature was determined using the falling-ball method.<sup>[15]</sup> Concentrated polymer solutions were heated above the gel melting temperature and filled into a glass tube ( $d = 15 \text{ mm}$ ). The liquid sample was cooled below the gel melting temperature and a steel ball ( $d = 3.2 \text{ mm}$ ,  $m = 136 \text{ mg}$ ) was carefully placed onto the gel in the center of the tube. The tube was heated at a heating rate of about 1  $\text{K} \cdot \text{min}^{-1}$ . With the help of video analysis the distance the steel ball traveled was recorded as a function of the temperature. At the gel melting temperature, the ball dropped. After repeating the procedure three times, an average value was calculated.

## Syntheses

### Synthesis of NAGA

The synthesis of NAGA was adapted from a synthesis by Haas et al.<sup>[11a]</sup> that was slightly modified. Glycinamide hydrochloride (24.50 g, 222 mmol, 1.00 equiv.) was slurred in dry, cold (10  $^\circ\text{C}$ ) diethyl ether (250 mL) containing acryloyl chloride (17.64 mL, 217 mmol, 0.98 equiv.) in a 1 L, three-necked round-bottom flask equipped with a mechanical stirrer. It was a suspension of a fine powder. The suspension was stirred at 10  $^\circ\text{C}$  for 3 h and 125 mL of a saturated aqueous potassium carbonate solution was added and further stirred for 1 h at room temperature (RT). The solvents were removed at 40  $^\circ\text{C}$  to complete dryness and the residue was subjected to Soxhlet extraction with diethyl ether. The solvent was removed at 40  $^\circ\text{C}$ . To remove small amounts of homopolymer, the solid was dissolved in warm methanol and filtered. The methanol was removed by rotary evaporation at 40  $^\circ\text{C}$  to yield 18.17 g (64%) of the desired product.

DSC (rate of heating = 10  $\text{K} \cdot \text{min}^{-1}$ ):  $T_m = 139 \text{ }^\circ\text{C}$  (ref.<sup>[11a]</sup>:  $T_m = 129 \text{ }^\circ\text{C}$ ). IR (ATR):  $\nu = 3\ 380$  (m, NH), 3 312 (s, NH), 3 187 (m, NH), 1 652 (vs, C=O), 1 621 (vs, C=O), 1 551 (vs, NH)  $\text{cm}^{-1}$ .  $^1\text{H}$  NMR (300 MHz,  $\text{D}_2\text{O}$ ):  $\delta = 3.93$  (s, 2H,  $-\text{CH}_2-\text{CONH}_2$ ), 5.77 [dd, J(doublet 1) = 2.0 Hz, J(doublet 2) = 9.5 Hz, 1H,  $\text{H}_{\text{olef}}$ ], 6.20 [dd, J(doublet 1) = 2.0 Hz, J(doublet 2) = 17.1 Hz, 1H,  $\text{H}_{\text{olef}}$ ], 6.29 [dd, J(doublet 1) = 9.5 Hz, J(doublet 2) = 17.2 Hz, 1H,  $\text{H}_{\text{olef}}$ ].  $^{13}\text{C}$  NMR (75 MHz,  $\text{D}_2\text{O}$ ):  $\delta = 42.7$  ( $-\text{N}-\text{CH}_2-$ ), 128.8 ( $\text{C}_{\text{olef}}$ ), 130.0 ( $\text{C}_{\text{olef}}$ ), 169.6 ( $-\text{CO}-$ ), 174.8 ( $-\text{CO}-$ ).

### Synthesis of NACAAM

The synthesis of NACAAM was performed according to Onishi et al.<sup>[16]</sup> (for details see Supporting Information). Colorless crystals were obtained in a 37% yield.

DSC (rate of heating = 10  $\text{K} \cdot \text{min}^{-1}$ ):  $T_m = 109 \text{ }^\circ\text{C}$  (ref.<sup>[17]</sup>:  $T_m = 100.5 \text{ }^\circ\text{C}$ ). IR (ATR):  $\nu = 3\ 266$  (m, NH), 3 172 (m, NH), 3 007 (w), 1 726 (s, C=O), 1 628 (m), 1 504 (vs, NH)  $\text{cm}^{-1}$ .  $^1\text{H}$  NMR (300 MHz,  $\text{CHCl}_3$ ):  $\delta = 2.23$  (s, 3H,  $-\text{NH}-\text{CO}-\text{CH}_3$ ), 5.97 [dd, J(doublet 1) = 2.1 Hz, J(doublet 2) = 9.3 Hz, 1H,  $\text{H}_{\text{olef}}$ ], 6.36 [dd, J(doublet 1) = 9.3 Hz, J(doublet 2) = 17.1 Hz, 1H,  $\text{H}_{\text{olef}}$ ], 6.44 [dd, J(doublet 1) = 2.1 Hz, J(doublet 2) = 17.1 Hz, 1H,  $\text{H}_{\text{olef}}$ ].  $^{13}\text{C}$  NMR (75 MHz,  $\text{D}_2\text{O}$ ):  $\delta = 24.9$  ( $-\text{CO}-\text{CH}_3$ ), 130.2 ( $\text{C}_{\text{olef}}$ ), 132.6 ( $\text{C}_{\text{olef}}$ ), 167.5 ( $-\text{CO}-$ ), 175.2 ( $-\text{CO}-$ ).

### Synthesis of Poly(*N*-acryloyl glycinamide) (PNAGA) Homopolymer

NAGA (500 mg, 3.90 mmol) was dissolved in dimethyl sulfoxide (DMSO, 18 mL) in a nitrogen flask and was degassed by three freeze/thaw cycles. Then, an aliquot of a separately degassed AIBN solution in DMSO containing 3.5 mg of AIBN (0.0055 equiv.) was added. The flask was placed in a preheated oil bath of 70  $^\circ\text{C}$  and the NAGA was polymerized for 2 h. The reaction was stopped by cooling in an ice bath and the polymer was precipitated in 200 mL of methanol. It was centrifuged (10 min, 6 000 rpm) and washed with methanol three times. It was dried in vacuum at 80  $^\circ\text{C}$  for 72 h to obtain 297 mg (59%) of the homopolymer as a white powder.

IR (FT-ATR):  $\nu = 3\ 283$  (mb, NH), 3 198 (mb, NH), 2 932 (w, CH), 1 639 (vs), 1 539 (s), 1 400 (m), 1 258 (m)  $\text{cm}^{-1}$ .  $^1\text{H}$  NMR (500 MHz,  $\text{D}_2\text{O}$ ,  $T = 70 \text{ }^\circ\text{C}$ , the residual solvent peak was calibrated

to  $\delta = 4.20$ ):  $\delta = 1.3$ – $1.7$  (Hc, polymer backbone,  $-\text{CH}_2-$ ),  $2.0$ – $2.3$  (Hb, polymer backbone,  $-\text{CH}-$ ),  $3.6$ – $4.05$  (Ha,  $\text{NH}-\text{CH}_2-\text{CONH}_2$ ).  $^{13}\text{C}$  NMR (125 MHz,  $\text{D}_2\text{O}$ ,  $T = 70^\circ\text{C}$ ):  $\delta = 35.0$ – $36.6$  (C5, polymer backbone,  $-\text{CH}_2-$ ),  $41.5$ – $42.9$  (C4,  $\text{NH}-\text{CH}_2-\text{CONH}_2$ ),  $42.1$ – $43.2$  (C3, polymer backbone,  $-\text{CH}-$ ),  $174.1$ – $174.7$  (C2,  $-\text{NH}-\text{CH}_2-\text{CONH}_2$ ),  $177.0$ – $178.0$  (C1,  $-\text{CO}-\text{NH}-$ ).

### Synthesis of Poly(NAcAAm-co-NAGA) Copolymers

As an example, the copolymer synthesis of the copolymer, NAGA78, is described: NAGA (335 mg, 2.61 mmol, 0.78 eq) and NAcAAm (83 mg, 0.74 mmol, 0.22 eq) were dissolved in DMSO (15 mL) in a nitrogen-flask and degassed by three freeze-thawing cycles. Then, an aliquot of a separately degassed AIBN solution in DMSO containing 3 mg of AIBN (0.0055 equiv.) was added. The flask was placed in a preheated oil bath at  $70^\circ\text{C}$  and polymerization was carried out for 45 min. The reaction was stopped by cooling in an ice bath and the polymer was precipitated in 200 mL of methanol. It was centrifuged (10 min, 6 000 rpm) and washed with methanol three times. It was dried in vacuum at  $80^\circ\text{C}$  for 72 h to obtain 163 mg (39%) of the copolymer as a white powder. Several different copolymers were made using the same procedure. The time of polymerization was varied between 20 and 60 min to keep the yield of the copolymers always less than 50%.

$^1\text{H}$  NMR (300 MHz,  $\text{D}_2\text{O}$ ): The following NMR data is for the sample NAGA78 (Figure 1). It was recorded at RT. The NAGA90, NAGA95 and NAGA98 copolymers possessed a UCST in  $\text{D}_2\text{O}$  higher than RT. For these, the NMR spectra were recorded at  $70^\circ\text{C}$  and therefore the chemical shifts may slightly differ.  $\delta = 1.3$ – $2.0$  (Hd, polymer backbone,  $-\text{CH}_2-$ ),  $2.14$  (Hc,  $\text{N}-\text{CO}-\text{CH}_3$ ),  $2.0$ – $2.6$  (Hb, polymer backbone,  $-\text{CH}-$ ),  $3.5$ – $4.2$  (Ha,  $\text{NH}-\text{CH}_2-\text{CONH}_2$ ).

## Results and Discussion

The homopolymer of *N*-acryloyl glycine (PNAGA) was synthesized by free-radical polymerization. Structural characterization was carried out using NMR. The  $^1\text{H}$  and  $^{13}\text{C}$  NMR spectra are shown in Figure 2 and Figure 3. 2D NMR techniques like heteronuclear multiple quantum coherence (HMQC) and heteronuclear multiple bond coherence (HMBC) were used for the correct peak assignments (for details see supporting information). PNAGA synthesized by free-radical polymerization shows a UCST in water, as determined by turbidimetry (Figure 4).

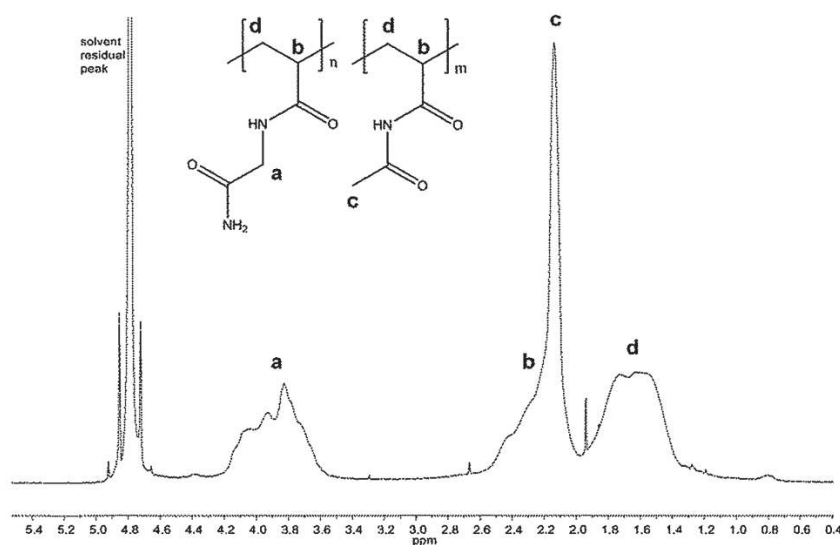


Figure 1. 300 MHz  $^1\text{H}$  NMR spectrum of NAGA78 copolymer in  $\text{D}_2\text{O}$  at room temperature.

PNAGA has already been shown to build interpolymer complexes with PAAc via hydrogen bonding.<sup>[18]</sup> The glycine moiety of PNAGA can act both as a hydrogen donor (mainly primary amide) and acceptor (carbonyl groups). As our experiments regarding the UCST of PNAGA indicate, the polymer is capable of forming intra- and intermolecular complexes between its side groups on its own. The results made us speculate that hydrogen bonds form below the UCST (intramolecular and intermolecular). At this stage, it is not possible to comment which one dominates: inter- or intramolecular. Aggregation continued until the sedimentation of visible polymer particles was

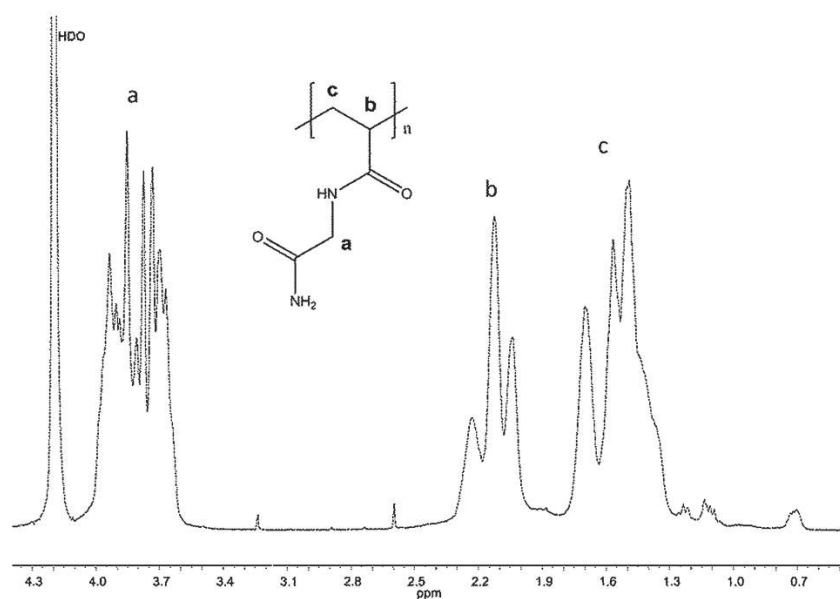


Figure 2. 500 MHz  $^1\text{H}$  NMR spectrum of PNAGA in  $\text{D}_2\text{O}$  at  $70^\circ\text{C}$ .

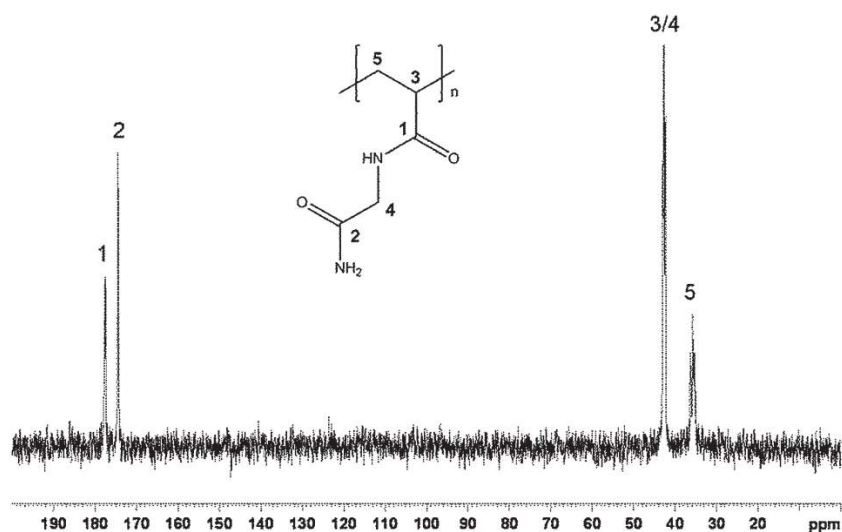


Figure 3. 125 MHz  $^{13}\text{C}$  NMR spectrum of PNAGA in  $\text{D}_2\text{O}$  at  $70^\circ\text{C}$ .

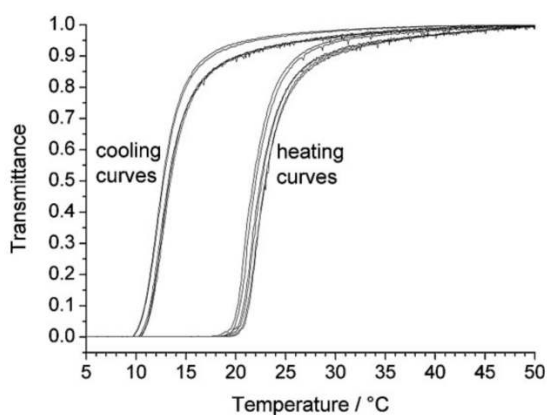


Figure 4. Six turbidity curves of the same 1 wt.% solution of PNAGA (NAGA100) in deionized water at a heating/cooling rate of  $1\text{K}\cdot\text{min}^{-1}$ .

observed after a few hours. When the temperature was raised above the UCST, the hydrogen bonds between the polymer chains were broken and the polymer was dissolved again. At a concentration of 1 wt.% ( $\bar{M}_n = 13\,200\text{ g}\cdot\text{mol}^{-1}$ ) and a heating rate of  $1\text{K}\cdot\text{min}^{-1}$ , the UCST was found to be  $21.5 \pm 2.2^\circ\text{C}$  upon heating and  $12.3 \pm 0.3^\circ\text{C}$  upon cooling. A UCST was found over a wide range of concentrations and was slightly increased at higher concentrations (Figure 5). At concentrations greater than 2 wt.% in water, PNAGA can form physical gels that reversibly melt and reform at distinct temperatures: a behavior first described by Haas et al.<sup>[11a]</sup> Haas prepared the polymer by precipitation polymerization in ethanol and found a gel melting temperature of  $38\text{--}39^\circ\text{C}$  for a 5 wt.% solution in water. In our work, we made an attempt to determine the gel

melting temperatures by DSC, but it was unsuccessful. Neither peaks nor steps distinguishable from noise were found in the heating or cooling curves from  $20$  to  $85^\circ\text{C}$  at heating rates of 1 and  $10\text{K}\cdot\text{min}^{-1}$ . This is in agreement with previous estimations that the heat of formation per crosslink is only  $-5$  to  $-12\text{ kcal}\cdot\text{mol}^{-1}$ .<sup>[11c]</sup> Therefore, the falling-ball method was employed to determine the gel melting temperatures (Figure 6).<sup>[15]</sup> There was an increase in the gel melting temperature from  $55^\circ\text{C}$  to about  $81^\circ\text{C}$  on changing the concentration from 5.4 to 14 wt.% (Table 1). Like PNAGA, the poly(*N*-acetylacrylamide) (PNAAcAm) homopolymer also possesses both hydrogen donor (secondary amide) and acceptor (carbonyl groups) sites. It has been shown that it exhibits a UCST in aqueous alcoholic solution.<sup>[16,19]</sup> However, in pure water, it is readily soluble and does not show a UCST.

Furthermore, we used an external H-acceptor monomer, NAAcAm, in combination with NAGA to study the behavior of the resulting copolymers with respect to the UCST. Different copolymers of NAGA and NAAcAm were synthesized using different feed compositions. The samples were designated by their feed content of NAGA in mol-%: for example, the polymer NAGA78 contained 78 mol-% NAGA in the feed mixture. The structural characterization was carried out using  $^1\text{H}$  NMR techniques. A representative  $^1\text{H}$  NMR spectrum of the NAGA78 copolymer (the molar ratio of NAGA:NAAcAm in the feed was 3.545) is shown in the Figure 1. The  $^1\text{H}$  NMR spectrum shows the characteristic signals of both the NAGA and the NAAcAm. The copolymer

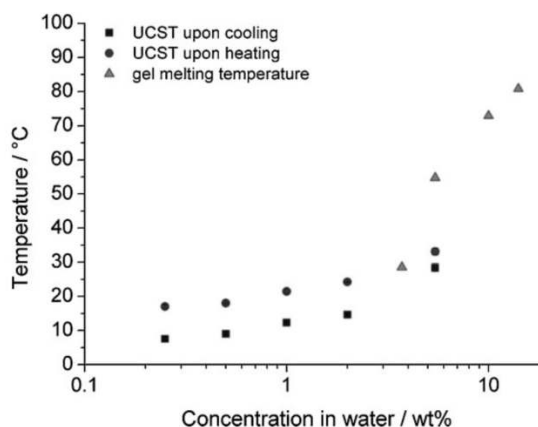


Figure 5. UCST and gel melting temperature of PNAGA as a function of the concentration in deionized water. The heating rate was  $1\text{K}\cdot\text{min}^{-1}$ .

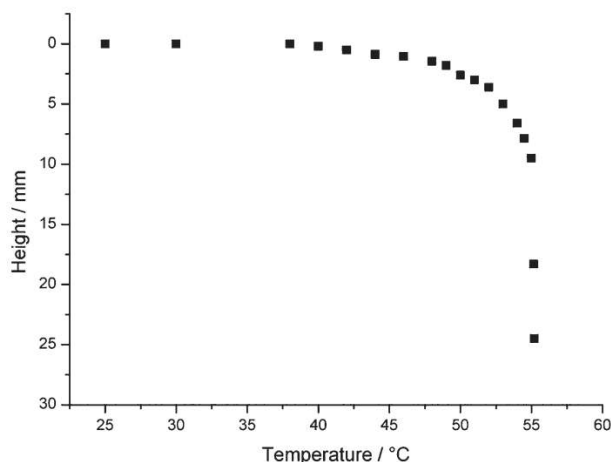


Figure 6. Determination of the gel melting temperature of 5.4 wt.-% PNAGA in water by the falling-ball method. At the gel melting temperature, the ball drops.

composition was determined by taking the ratio of the integral of the methylene group of the glycinamide side group ( $\delta = 3.5\text{--}4.2$ ) and the integral of the remaining proton signals ( $\delta = 1.2\text{--}2.6$ ). The results are summarized in Table 2. Although the amount of NAGA in the copolymers was always less than in the feed, different copolymers with

Table 1. UCST and gel melting temperature of PNAGA as a function of concentration in deionized water. The UCST value is an average of at least 5 runs (indicated  $\pm$  standard deviation), the gel melting temperature an average of 3 runs.

Concentration in water	UCST upon cooling <sup>a)</sup>	UCST upon heating <sup>a)</sup>	Gel melting temperature
wt.-%	°C	°C	°C
14.0	n.d.	n.d.	81
10.0	n.d.	n.d.	73
5.4	$28.4 \pm 1.2$	$33.1 \pm 1.0$	55
2.00	$14.7 \pm 0.2$	$24.2 \pm 0.1$	none
1.00	$12.3 \pm 0.3$	$21.5 \pm 0.5$	none
0.50	$9.0 \pm 0.04$	$18.0 \pm 0.2$	none
0.25	$7.6 \pm 0.4$	$17.0 \pm 0.4$	none

<sup>a)</sup>At higher concentrations (5.4 wt.-%), reversible physical gelation occurred at a distinct temperature that was higher than the UCST. Since heat transfer within a gel and the mobility of polymer chains are different from liquid samples, the comparability is limited.

Table 2. Copolymer composition and molecular weight of poly(NAcAam-co-NAGA) as a function of feed composition.

Sample	Feed ratio NAGA:NAcAam	NAGA in feed	NAGA:NAcAam molar ratio in copolymer <sup>a)</sup>	NAGA in copolymer <sup>a)</sup>	$\overline{M}_n$ <sup>b)</sup>	$\overline{M}_w/\overline{M}_n$
		molar fraction		molar fraction		
NAGA30	0.430	0.300	0.18	0.155	14 5000	1.98
NAGA50	1.000	0.500	0.41	0.291	78 800	2.25
NAGA60	1.500	0.600	0.75	0.428	57 400	2.10
NAGA68	2.125	0.680	1.12	0.528	48 800	2.14
NAGA70	2.333	0.700	1.19	0.543	49 000	2.27
NAGA78	3.545	0.780	1.82	0.645	–	–
NAGA82	4.556	0.820	2.32	0.698	–	–
NAGA85	5.667	0.850	2.96	0.747	10 700	2.35
NAGA88	7.333	0.880	3.82	0.793	12 300	2.31
NAGA90	9.00	0.900	4.80	0.826	12 800	2.20
NAGA95	19.00	0.950	10.0	0.909	11 300	2.18
NAGA98	49.0	0.980	17.6	0.946	11 600	2.15

<sup>a)</sup>The polymer composition was determined by means of NMR spectroscopy. The integral area of the methylene proton signals adjacent to the primary amide group of the NAGA was compared to the integral of all of the residual protons; <sup>b)</sup>For NAGA30, NAGA50, NAGA60, NAGA68 and NAGA70, DMF with  $5 \text{ g} \cdot \text{L}^{-1}$  LiBr added was used as the eluent. The molecular weights are relative to PMMA standards. For NAGA78–NAGA98,  $0.3 \text{ M}$  formic acid was used as the eluent. The molecular weights are relative to poly(2-vinylpyridine) standards. NAGA78 and NAGA82 were not soluble in DMF; samples with NAGA content lower than 75 mol-% (NAGA78 and NAGA82) also proved unsuitable for the GPC set-up with formic acid as eluent (weak detector signals).

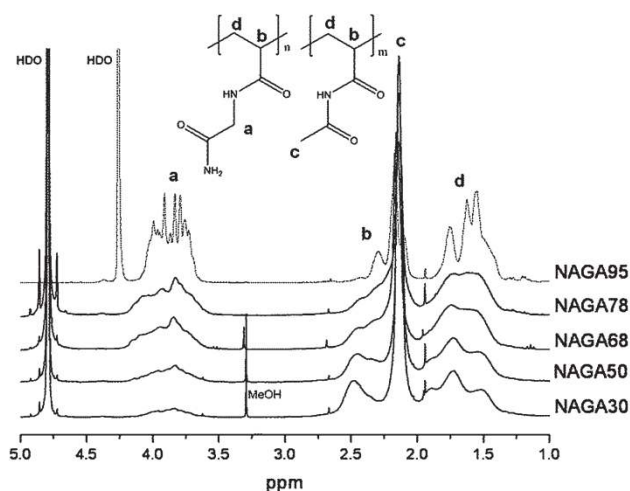


Figure 7. Different copolymer compositions, analyzed using  $^1\text{H}$  NMR spectroscopy, in  $\text{D}_2\text{O}$ . The spectra of NAGA30, NAGA50, NAGA68 and NAGA78 were recorded at room temperature at a frequency of 300 MHz. The spectrum of NAGA95 was recorded at  $70^\circ\text{C}$  at a frequency of 500 MHz. The peak integrals' intensities change gradually according to the copolymer composition.

different ratios of NAGA and NAcAAm could be prepared by changing the amount in the feed (their NMR spectra are shown in Figure 7). The copolymerization parameters were quantitatively calculated from these data using the method of Kelen-Tüdös.<sup>[20]</sup> The copolymerization parameters were found to be  $r_{\text{NAGA}} = 0.56 \pm 0.05$  and  $r_{\text{NAcAAm}} = 2.39 \pm 0.11$ . This showed that the copolymers were statistical copolymers, as the product of  $r_{\text{NAGA}}$  and  $r_{\text{NAcAAm}}$  ( $r_{\text{NAGA}} \times r_{\text{NAcAAm}}$ ) is 1.34. The copolymerization equation plotted from the copolymerization parameters is in good agreement with the experimental data (for the  $\xi/\eta$  plot and linear fit, please see the Supporting Information).

The copolymers showed very high glass-transition temperatures that depended upon the copolymer composition (Table 3). The glass-transition temperature increased with an increase in the amount of NAGA in the copolymers and correlated linearly with the mole fraction of NAGA in the copolymers (Figure 8).

The UCSTs of the poly(NAcAAm-co-NAGA) copolymers were determined by measuring the turbidity of 1 wt.-% solutions in water as a function of the temperature (Figure 9). The pure PNAcAAm and copolymers with a NAGA mole fraction of up to 0.645 did not show a UCST above  $0^\circ\text{C}$ . Table 4 lists the UCSTs upon cooling and heating. Increasing the mole fraction from 0.645 to 1.000, the UCST increased from around  $-1$  to  $+12.3^\circ\text{C}$  upon cooling and from  $6$  to  $21.5^\circ\text{C}$  upon heating. As already known for polymers exhibiting a LCST, the cooling and heating curves did not coincide. The hysteresis was about  $10^\circ\text{C}$  for the samples studied here. The increase of the UCST with increasing mole fraction of NAGA may be explained by the

Table 3. Glass-transition temperature as a function of the copolymer composition determined by DSC at a heating rate of  $10\text{ K} \cdot \text{min}^{-1}$ .

Sample	NAGA in copolymer	Glass transition temperature
	molar fraction	$^\circ\text{C}$
PNAcAAm	0	118
NAGA30	0.155	125
NAGA50	0.291	134
NAGA60	0.428	142
NAGA68	0.528	154
NAGA70	0.543	164
NAGA78	0.645	159
NAGA82	0.698	165
NAGA85	0.747	167
NAGA88	0.793	170
NAGA90	0.826	172
NAGA95	0.909	175
NAGA98	0.946	180
PNAGA	1	186

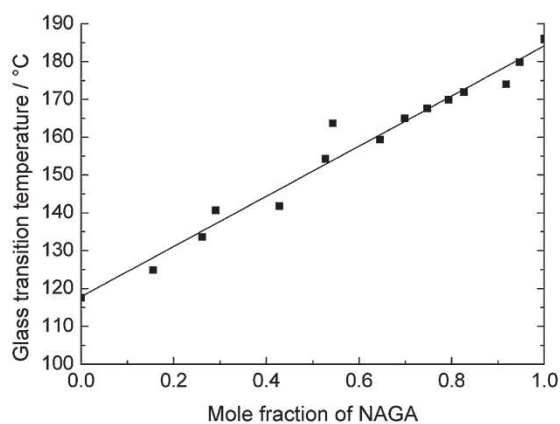
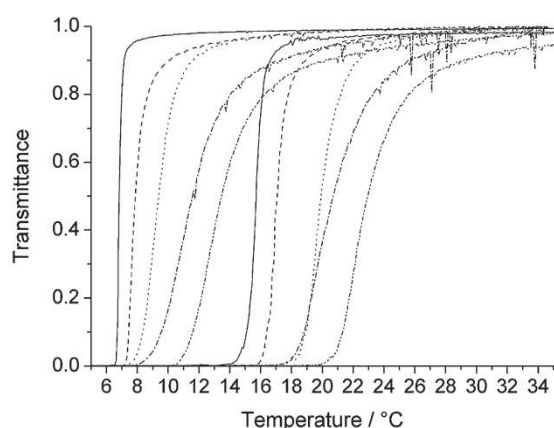


Figure 8. Glass-transition temperatures of poly(NAcAAm-co-NAGA) as a function of the copolymer composition determined by DSC at heating rate of  $10\text{ K} \cdot \text{min}^{-1}$ .

overall hydrophobicity of the copolymer. Higher mole fractions of NAGA lead to more-hydrophobic copolymers and consequently to an increase in the UCST. Similar phenomena are known for interpolymer complexes of PAAc.<sup>[5,21]</sup> Interestingly there was also a correlation between the copolymer composition and the sharpness of the coil-to-globule transition. Higher mole fractions of NAGA lead to less-sharp transitions (Figure 10). To exclude an influence of the molecular weight on the UCST



**Figure 9.** Turbidity measurements of 1 wt.-% poly(NAcAAm-co-NAGA) solutions in water: representative curves for different copolymer compositions. The left and the right sets of the curves are from cooling and heating the solutions, respectively. From the left to the right: solid line = NAGA85, dashed line = NAGA90, dotted line = NAGA95, dash-dot line = NAGA98, dash-dot-dot line = NAGA100 (homopolymer).

sharpness, GPC was performed (Table 2, for details see Supporting Information). The molecular weights of all of the polymers exhibiting a UCST above 0 °C were in the range from 10 700 to 13 200 g · mol<sup>-1</sup>, so differences in the molecular weight could not have had a significant influence on the UCST or on the sharpness of the transition. The polydispersity was between 2.10 and 2.35, which is common for polymers synthesized by free-radical polymerization. Preliminary studies were carried out to study the influence of electrolytes on the UCST behavior. The UCST of a 1 wt.-% solution of NAGA95 in water containing 0.9 wt.-% of sodium chloride or in phosphate-buffered saline (PBS, pH = 7.4) was little affected (Table 5). In contrast to NaCl and PBS solutions, the UCST did decrease drastically in sodium

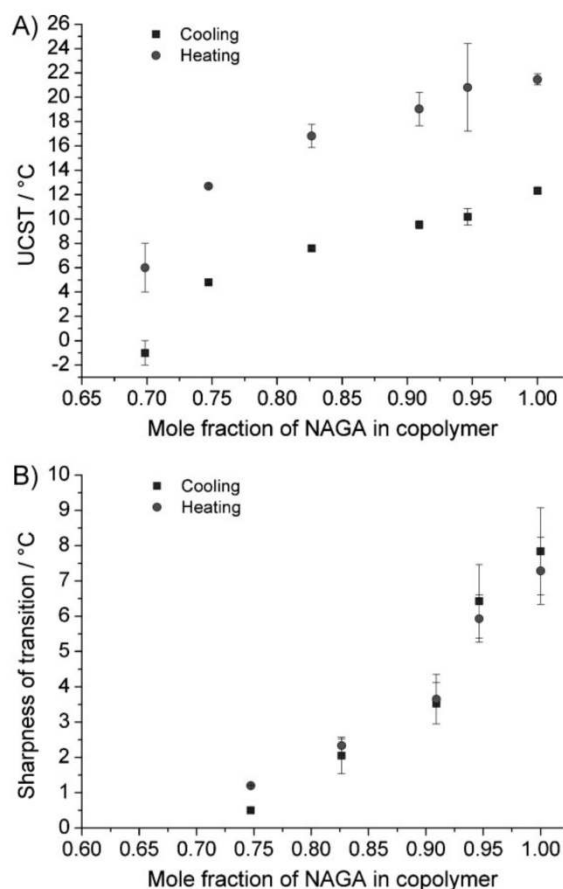


**Figure 10.** A) UCST of 1 wt.-% solutions of poly(NAcAAm-co-NAGA) in deionized water determined by turbidimetry as a function of the copolymer composition, at a heating rate of 1 K · min<sup>-1</sup> and a wavelength of 670 nm. B) Temperature interval in which the transmittance changes from 0.9 to 0.1 (cooling) or from 0.1 to 0.9 (heating) as a function of the copolymer composition.

**Table 4.** UCST upon cooling of 1 wt.-% poly(NAcAAm-co-NAGA) solutions in deionized water as a function of copolymer composition at a heating rate of 1 K · min<sup>-1</sup> and a wavelength of 670 nm.

NAGA in copolymer	Cooling		Heating	
	UCST	Sharpness	UCST	Sharpness
	°C	°C	°C	°C
0.645	no UCST (<0 °C)	–	–	–
0.747	4.8 ± 0.1	0.5 ± 0.04	12.7 ± 0.1	1.2 ± 0.02
0.826	7.6 ± 0.2	2.1 ± 0.5	16.4 ± 0.9	2.3
0.909	9.5 ± 0.3	3.5 ± 0.6	19.0 ± 1.4	3.7
0.946	10.2 ± 0.7	6.4 ± 1.1	20.8 ± 3.6	5.9
1	12.3 ± 0.3	7.8 ± 1.2	21.5 ± 2.2	7.3

**Table 5.** Influence of electrolytes on the UCST of a 1 wt.-% solution of sample NAGA95 (mole fraction of NAGA in copolymer = 0.909) at a heating rate of  $1\text{ K} \cdot \text{min}^{-1}$  and a wavelength of 670 nm. The UCST values are average values of three runs.

Medium	UCST	
	°C	
	Cooling	Heating
deionized water (0.06 $\mu\text{S}$ )	9.5	19.0
0.9 wt.-% (0.15 M) sodium chloride	9	21
phosphate-buffered saline (pH = 7.4)	10	22
0.10 M sodium thiocyanate	4	13
0.20 M sodium thiocyanate	2	10
0.50 M sodium thiocyanate	no UCST	no UCST

thiocyanate (NaSCN) solution, which is a strong hydrogen-bond-breaking agent. At a NaSCN concentration of  $0.10\text{ mol} \cdot \text{L}^{-1}$ , the UCST decreased by  $6\text{ }^\circ\text{C}$ , at  $0.20\text{ mol} \cdot \text{L}^{-1}$  by a further  $2\text{ }^\circ\text{C}$ , and polymer aggregation was completely prevented at a concentration of  $0.50\text{ mol} \cdot \text{L}^{-1}$ . This is a strong indication that hydrogen bonding is the main driving force for phase separation below the UCST.

## Conclusion

PNAGA prepared by free-radical polymerization showed a UCST, as determined by turbidimetry, at different concentrations and the reversible formation of a physical gel was observed at higher concentrations. Copolymers of NAGA and NAcAAm were also synthesized with different feed compositions. The copolymer compositions were determined using NMR spectroscopy and the copolymerization parameters were determined using the method of Kelen-Tüdös to be  $r_{\text{NAGA}} = 0.56 \pm 0.05$  and  $r_{\text{NAcAAm}} = 2.39 \pm 0.11$ . The copolymers were thermally characterized using TGA and DSC, and the UCST in water was found to depend on the copolymer composition. Copolymers with a NAGA mole fraction ratio between 0.698 and 1.000 showed a sharp UCST between  $-1$  and  $+12.3\text{ }^\circ\text{C}$  upon cooling and  $6$  and  $21.5\text{ }^\circ\text{C}$  upon heating. The sharpness of the transition decreased with increasing NAGA mole fraction. These experiments showed the possibility of controlling the UCST in the stated temperature intervals by choosing the desired copolymer composition. The UCST was present over a wide range of concentrations and was unaffected in 0.9 wt.-% NaCl solution or PBS. This could open a new field of using such polymers for different biomedical applications.

Acknowledgements: Authors would like to thank *Rajat Agarwal* for technical help.

Received: March 23, 2010; Accepted: June 15, 2010; Published online: September 6, 2010; DOI: 10.1002/macp.201000147

Keywords: *N*-acetylacrylamide; *N*-acryloylglycinamide; smart polymers; thermoresponsive polymers; upper critical solution temperature (UCST)

- [1] A. Cameron, K. M. Shakesheff, *Adv. Mater.* **2006**, *18*, 3321.
- [2] H. G. Schild, *Prog. Polym. Sci.* **1992**, *17*, 163.
- [3] L. Ren, S. Agarwal, *Macromol. Chem. Phys.* **2007**, *208*, 245.
- [4] L. Jun, W. Bochu, W. Yazhou, *Int. J. Pharm.* **2006**, *2*, 513.
- [5] H. Katono, K. Sanui, N. Ogata, T. Okano, Y. Sakurai, *Polym. J.* **1991**, *23*, 1179.
- [6] T. Aoki, M. Kawashima, H. Katono, K. Sanui, N. Ogata, T. Okano, Y. Sakurai, *Macromolecules* **1994**, *27*, 947.
- [7] H. Katono, K. Sanui, N. Ogata, T. Okano, Y. Sakurai, *J. Controlled Release* **1991**, *16*, 215.
- [8] Z. Jiang, Y. You, Q. Gu, J. Hao, X. Deng, *Macromol. Rapid Commun.* **2008**, *29*, 1264.
- [9] [9a] Z. Zhang, T. Chao, S. Chen, S. Jiang, *Langmuir* **2006**, *22*, 10072; [9b] B. L. Andrew, A. B. Lowe, C. L. McCormick, *Chem. Rev.* **2002**, *102*, 4177.
- [10] M. Arotçaréna, B. Heise, S. Ishaya, A. Laschewsky, *J. Am. Chem. Soc.* **2002**, *124*, 3787.
- [11] [11a] H. C. Haas, N. W. Schuler, *J. Polym. Sci. Part B: Polym. Lett.* **1964**, *2*, 1095; [11b] H. C. Haas, R. D. Moreau, N. W. Schuler, *J. Polym. Sci. Part A-2: Polym. Phys.* **1967**, *5*, 915; [11c] H. C. Haas, C. K. Chiklis, R. D. Moreau, *J. Polym. Sci. Part-A1: Polym. Chem.* **1970**, *8*, 1131; [11d] H. C. Haas, R. L. MacDonald, A. N. Schuler, *J. Polym. Sci. Part A-1: Polym. Chem.* **1970**, *8*, 1213; [11e] H. C. Haas, M. J. Manning, M. H. Mach, *J. Polym. Sci. Part A: Poly. Chem.* **1970**, *8*, 1725; [11f] H. C. Haas, R. L. MacDonald, A. N. Schuler, *J. Polym. Sci. Part A: Polym. Chem.* **1970**, *8*, 3405.
- [12] O. Marstokk, B. Nyström, J. Roots, *Macromolecules* **1998**, *31*, 4205.
- [13] D. Ostrovskii, P. Jacobsson, B. Nyström, H. B. M. Kopperud, *Macromolecules* **1999**, *32*, 5552.
- [14] US 7 195 925 B2 (2007) National Institute of Advanced Industrial Science and Technology, Chisso Corporation, invs.: N. Ohnishi, H. Furukawa, K. Kataoka, U. Katsuhiko.
- [15] A. Takahashi, M. Sakai, T. Kato, *Polym. J.* **1980**, *12*, 335.
- [16] EP 0922715 A2 (1999) Agency of Industrial Science and Technology MITI (Ibaraki, JP), Japan Chemical Innovation Institute (Ibaraki, JP), invs.: N. Ohnishi, K. Aoshima, K. Kataoka, U. Katsuhiko.
- [17] T. Miyake, *Kogyo Kagaku Zasshi* **1961**, *64*, 422.
- [18] H. Sasase, T. Aoki, H. Katono, K. Sanui, N. Ogata, *Macromol. Rapid Commun.* **1992**, *13*, 577.
- [19] N. Kato, M. Takeda, Y. Sakai, T. Uyehara, *Anal. Sci.* **2001**, *17*, supplement i1137.
- [20] F. Tüdös, T. Kelen, T. Földes-Bereznich, B. Turcsányi, *J. Macromol. Sci., Part A* **1976**, *10*, 1513.
- [21] M. Koussathana, P. Lianos, *Macromolecules* **1997**, *30*, 7798.



Supporting Information for  
*Macromolecular Chemistry and Physics*

**Nonionic Homo- and Copolymers with H-donor and H-Acceptor  
Units having an Upper Critical Solution Temperature in Water**

**Jan Seuring and Seema Agarwal\***

Philipps-Universität Marburg, Fachbereich Chemie, Hans-Meerwein Strasse, D-35032

Marburg, Germany

E-mail: agarwal@staff.uni-marburg.de

**Synthesis of 1-(acryloyl)imino-N,N-dimethyl ethanamine**

A 250 mL roundbottom flask equipped with condenser was charged with acrylamide (16.59 g, 233 mmol, 1.00 eq), N,N-dimethylacetamide dimethylacetal (42.75 g, 289 mmol, 1.24 eq) and THF (100 mL). It was a slightly turbid and brown solution. The mixture was stirred at 65 °C for 3 h. The solvent was removed by rotary evaporation at 40 °C. The residue was subjected to vacuum distillation to obtain 22.00 g (67%) of a slightly yellow liquid. The product was used for the next step without further purification.

<sup>1</sup>H NMR (300 MHz, CHCl<sub>3</sub>): δ = 2.10-2.20 (m, 3H, N=C(CH<sub>3</sub>)-N), 2.95-3.05 (m, 6H, N(CH<sub>3</sub>)<sub>2</sub>), 5.50-5.60 (m, 1H, H<sub>olef.</sub>), 6.10-6.30 (m, 2H, H<sub>olef.</sub>).

**Synthesis of N-acetyl acrylamide (NAcAAm)**

A 250 mL roundbottom flask was charged with hydrochlorid acid 2N (110 mL), 1-(Acryloyl)imino-N,N-dimethyl ethanamine (22 g, 157 mmol, 1.00 eq) and acetic acid (22 mL, 384 mmol, 2.45 eq). The solution was stirred for 6 h at RT. Thereafter, 55 mL water and 110 mL ethyl acetate were added. The organic phase was washed with saturated aqueous sodium hydrogencarbonate solution until it became neutral (3 x 50 mL). The aqueous phases were combined and extracted with ethyl acetate (2 x 100 mL). The new organic phase was washed with sodium hydrogencarbonate solution until it became neutral (3 x 100 mL), combined with the first organic phase and then dried over magnesium sulfate. The solvent was removed by rotary evaporation and it was recrystallized from ethyl acetate to yield 6.60 g (37%) of colorless crystals.

DSC (rate of heating = 10 K/min):  $T_m = 109\text{ }^\circ\text{C}$  (lit.<sup>[16]</sup>  $T_m = 100.5\text{ }^\circ\text{C}$ ). IR (ATR): 3 266 (m, NH), 3 172 (m, NH), 3 007 (w), 1 726 (s, C=O), 1 628 (m), 1 504  $\text{cm}^{-1}$  (vs, NH).  $^1\text{H}$  NMR (300 MHz,  $\text{CHCl}_3$ ):  $\delta = 2.23$  (s, 3H, -NH-CO- $\text{CH}_3$ ), 5.97 (dd,  $J(\text{doublet } 1) = 2.1\text{ Hz}$ ,  $J(\text{doublet } 2) = 9.3\text{ Hz}$ , 1H,  $\text{H}_{\text{olef.}}$ ), 6.36 (dd,  $J(\text{doublet } 1) = 9.3\text{ Hz}$ ,  $J(\text{doublet } 2) = 17.1\text{ Hz}$ , 1H,  $\text{H}_{\text{olef.}}$ ), 6.44 (dd,  $J(\text{doublet } 1) = 2.1\text{ Hz}$ ,  $J(\text{doublet } 2) = 17.1\text{ Hz}$ , 1H,  $\text{H}_{\text{olef.}}$ ).  $^{13}\text{C}$  NMR (75 MHz,  $\text{D}_2\text{O}$ ):  $\delta = 24.9$  (-CO- $\text{CH}_3$ ), 130.2 ( $\text{C}_{\text{olef.}}$ ), 132.6 ( $\text{C}_{\text{olef.}}$ ), 167.5 (-CO-), 175.2 (-CO-).

### Structural characterization of poly(N-acryloyl glycinamide)

The structural characterization of homopolymer of N-acryloyl glycinamide (PNAGA) was carried out using NMR spectroscopic techniques. 2D NMR techniques like HMQC (Heteronuclear Multiple Quantum Coherence) and HMBC (Heteronuclear Multiple Bond Coherence) were used for the correct peak assignments in  $^1\text{H}$  and  $^{13}\text{C}$  NMR spectra. Carbon signal **1** shows  $^2\text{J}$ - and  $^3\text{J}$ -coupling to the polymer backbone protons in the HMBC spectrum (Figure S1) and therefore can be assigned to the secondary amide group. Hence, carbon signal **2** must be the primary amide group further from the backbone. The backbone proton signals **b** ( $\delta = 2.0$ - $2.3$ , peak integral = 1) and **c** ( $\delta = 1.3$ - $1.7$ , peak integral = 2) can be clearly distinguished by their chemical shift and peak integrals. With all proton signals assigned the location of the carbons **3**, **4** and **5** could be determined with the help of the HMQC spectrum (Figure S2).

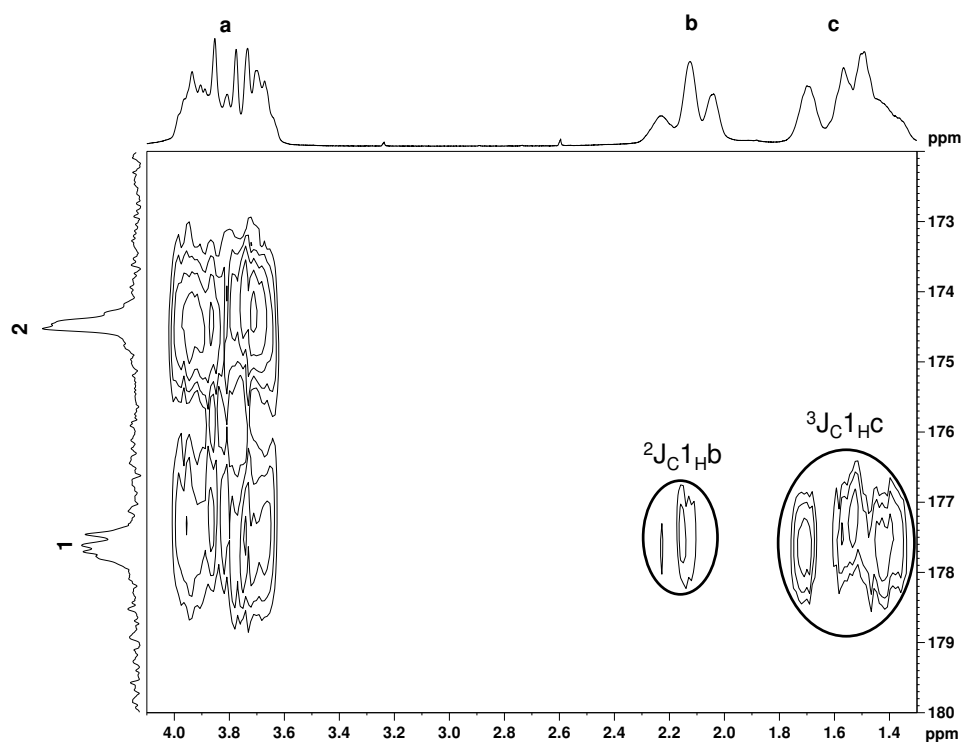


Figure S1.  $^1\text{H}^{13}\text{C}$  HMBC spectrum of poly(N-acryloyl glycinamide) in  $\text{D}_2\text{O}$  at  $70\text{ }^\circ\text{C}$ .

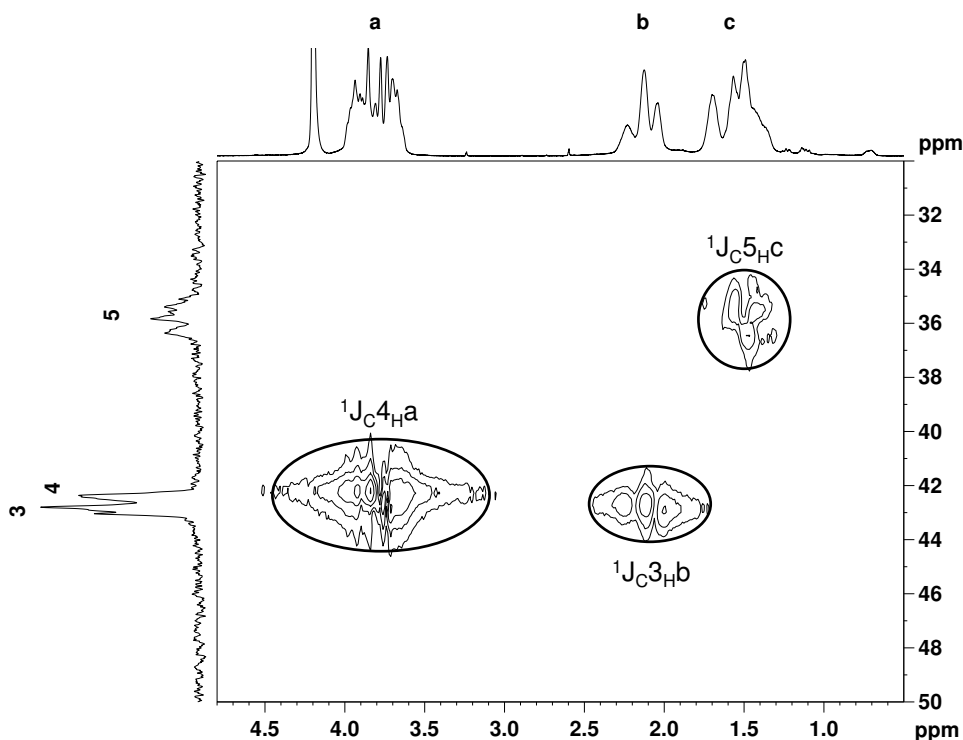


Figure S2.  $^1\text{H}^{13}\text{C}$  HMQC spectrum of poly(N-acryloyl glycinamide) in  $\text{D}_2\text{O}$  at  $70\text{ }^\circ\text{C}$ .

### Molecular weight determination by gel permeation chromatography (GPC)

The molecular weight determination by GPC was not trivial since the polymers are insoluble in most common GPC solvents like chloroform, tetrahydrofurane, chlorobenzene or hexafluoroisopropanol. DMF is a solvent for copolymers with a NAGA content of 54 mol-% or below. Copolymers with higher NAGA contents were only soluble in water at temperatures higher than UCST. Although soluble in the eluent (0.3M formic acid) with decreasing NAGA content the refractometer signal decreased in intensity until the setup was unsuitable for the molecular weight determination. Probably, the refractive index of the polymer solution comes closer to the refractive index of the eluent causing weaker detector signals.

We do not claim accuracy in respect to absolute values of molecular weights. The polymers used for calibration of both GPC setups are certainly very different from the polymers we studied. Especially in case of polymers that are able to form aggregates GPC results should be treated with care. The molecular weights measured in DMF are not comparable to the molecular weights measured in acid solution. However, GPC can determine the relative molecular weight of a number of samples measured in the same experimental setup. All copolymers that showed UCST behavior could be measured using the same experimental

setup (acid solution). The molecular weights of all those polymers were in the range from 10700 to 13200 g/mol so differences in molecular weight could not have had a significant influence on the UCST or the sharpness of the transition.

### Determination of the copolymerization parameters by the method of Kelen and Tüdös

The copolymerization parameters were determined by the method of Kelen and Tüdös.<sup>[1]</sup> The copolymerization equation plotted from the copolymerization parameters is in good agreement with the experimental data (Figure S3). The  $\xi$ - $\eta$ -plot and linear fit is shown in figure S4. The error of the linear fit ( $\eta = 0.956\xi \pm 0.032\xi - 0.397 \pm 0.018$ ) was used to estimate the error of the calculated copolymerization parameters.

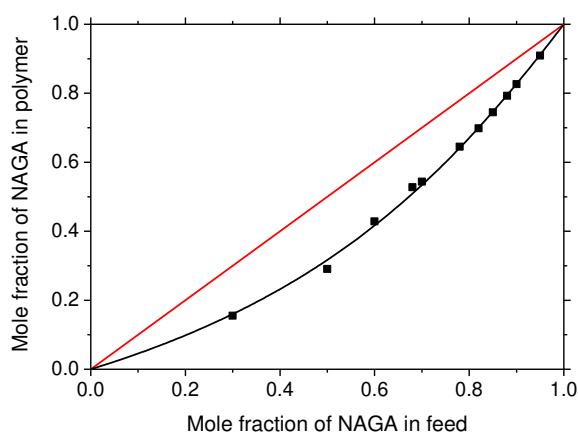


Figure S3. Determination of the copolymerization parameters by the method of Kelen-Tüdös. Bended line = plot of the copolymerization equation derived from calculated copolymerization parameters, straight line = ideal copolymerization.

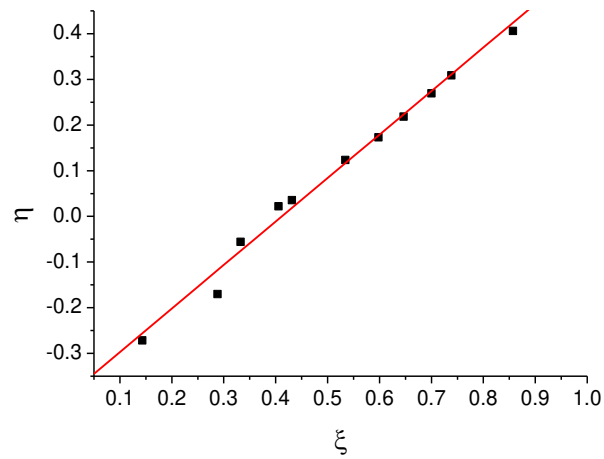


Figure S4. Determination of the copolymerization parameters by the method of Kelen-Tüdös.<sup>[1]</sup> The graph shows the  $\xi$ - $\eta$ -plot and linear fit.

## References

- [1] F. Tüdös, T. Kelen, T. Földes-Bereznich, *J. Macromol. Sci., Part A* **1976**, *10*, 1513.



## Publication 2

### Upper Critical Solution Temperature of Poly(*N*-acryloyl glycinamide) in Water: A Concealed Property

Jan Seuring, Frank M. Bayer, Klaus Huber, Seema Agarwal,

*Macromolecules* **2012**, *45*, 374-384.

doi: 10.1021/ma202059t

#### Author contributions



All experiments were conducted by Jan Seuring with exception of light scattering and ultrasensitive differential scanning calorimetry. Light scattering experiments were conducted in cooperation with Prof. Klaus Huber (University of Paderborn). The sample preparation was done by Jan Seuring in the laboratories of Prof. Huber in Paderborn. Frank M. Bayer was responsible for operating the goniometer and performing the CONTIN analysis of the dynamic light scattering data. Data from static light scattering was analyzed by Jan Seuring. The discussion concerning light scattering experiments was corrected by Prof. Klaus Huber. The manuscript was written by Jan Seuring. Apart from the light scattering experiments Prof. Seema Agarwal was responsible for supervision and correction of the manuscript.

# Upper Critical Solution Temperature of Poly(*N*-acryloyl glycinamide) in Water: A Concealed Property

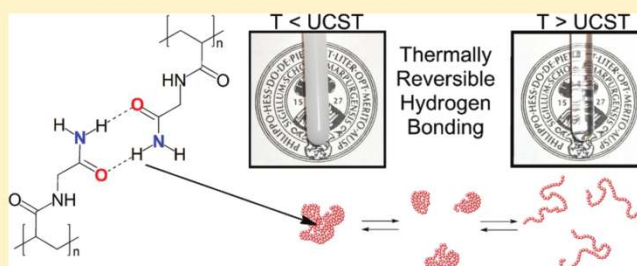
Jan Seuring,<sup>†</sup> Frank M. Bayer,<sup>‡</sup> Klaus Huber,<sup>‡</sup> and Seema Agarwal<sup>\*,†</sup>

<sup>†</sup>Fachbereich Chemie, Philipps-Universität Marburg, Hans-Meerwein Straße, D-35032 Marburg, Germany

<sup>‡</sup>Department Chemie—Physikalische Chemie, Universität Paderborn, Warburger Straße 100, D-33098 Paderborn, Germany

 Supporting Information  Web-Enhanced

**ABSTRACT:** Polymers showing an upper critical solution temperature (UCST) in water are rare. Recently, the nonionic homopolymer poly(*N*-acryloyl glycinamide) (poly(NAGA)) has been shown to exhibit a sharp upper critical solution temperature in pure water as well as in electrolyte solution. Although poly(NAGA) is known for decades the UCST behavior had not been reported. The first controlled radical polymerization of poly(NAGA) by the RAFT (reversible addition–fragmentation transfer) process was also achieved recently, but no UCST was observed. The present study shows that traces of ionic groups in the polymer prevent phase separation. Failure to notice the UCST in the past was because ionic groups have been introduced unintentionally by either acrylate impurities in the monomer, hydrolysis of the polymer side chains, and/or usage of ionic initiators or chain transfer agents. A synthetic procedure for high purity NAGA monomer free of ionic impurities is reported. It is also shown how to obtain stable aqueous solutions of nonionic poly(NAGA) so that the UCST behavior can be exploited in pure water as well as in a physiological milieu. Further, ultrasensitive differential scanning calorimetry and light scattering were used to get insights into the phase separation mechanism. We believe that this knowledge is transferable to other systems and will greatly accelerate research in the field of macromolecules that feature thermally reversible hydrogen bonding.



## 1. INTRODUCTION

Stimuli-responsive polymers or “smart” polymers exhibit a predictive and sharp change in properties upon only small changes in the environment (e.g., temperature, pH, ionic strength, radiation, mechanical stimuli).<sup>1</sup> These changes can result in phase separation from aqueous solution or order-of-magnitude changes of hydrogel size and water content. One class of smart polymers are thermoresponsive polymers, the best known example being Poly(*N,N*-isopropylacrylamide) (PNiPAAm) which shows a lower critical solution temperature (LCST). It undergoes phase separation from dilute aqueous solution at approximately 33 °C.<sup>2</sup> Above this temperature the dissolved polymer changes from the coil to the globule conformation. PNiPAAm and related polymer systems have been well characterized and are widely used to design smart materials.<sup>3</sup> Current applications are bioseparation and drug delivery, the development of new biocatalysts, biomimetic actuators, and surfaces with switchable hydrophobic–hydrophilic properties.<sup>1,4,5</sup>

In contrast to the LCST polymers, only a few polymeric materials with an upper critical solution temperature (UCST) in water are known.<sup>6–13</sup> In most cases, the UCST is based on either ionic interactions or hydrogen bonding. The first is observed for some polybetaines.<sup>11–13</sup> However, the electrostatic interactions of polyelectrolytes (e.g., polybetaines) are disturbed by the presence of salts which makes them unsuitable for the application under physiological conditions. For this reason, novel nonionic polymer systems showing sharp UCST-type phase transitions

over a wide range of concentrations and being tolerant to electrolytes are highly desirable. Despite the high potential of such systems, research had been limited to a few scattered publications and patents that focused on the application instead on the phase transition itself and lacked important aspects concerning sample preparation and stability.<sup>6,14–17</sup> We believe that progress has been hindered because of poor reproducibility. In this study, drawing on the example of poly(*N*-acryloyl glycinamide) (poly(NAGA)), sample preparation, sample stability and the basic features of its thermoresponsive behavior are discussed in particular.

Poly(*N*-acryloyl glycinamide) (Chart 1) is long known. It has first been synthesized by Haas and Schuler in 1964.<sup>18</sup> They found that poly(NAGA) can form thermoreversible gels in concentrated aqueous solutions.<sup>18–23</sup> Haas and Schuler showed that hydrogen bond interrupting agents like thiocyanate or urea can prevent the formation of the gel.<sup>19</sup> Furthermore, they calculated that the average number of groups involved in a cross-link is too low to form crystallites.<sup>20</sup> This was supported by the extremely low heat of formation per cross-link. They estimated it to be –5 to –12 kcal/mol of cross-links.<sup>22</sup> They concluded that the cross-linking is based on randomly distributed hydrogen bonds.

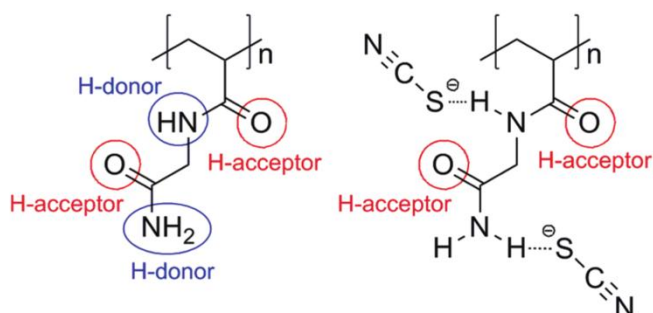
**Received:** September 9, 2011

**Revised:** November 14, 2011

**Published:** December 16, 2011



Chart 1. Poly(NAGA) Bearing H-Donor and H-Acceptor Sites (Left) That Can Be Blocked by Thiocyanate Salts (Right)



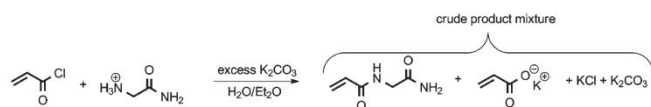
In dilute solutions, poly(NAGA) does not show thermoreversible gelation. However, despite looking transparent and homogeneous, the solution contains polymer aggregates. This was first evidenced by a nonlinear dependency of the reduced viscosity from the polymer concentration in pure water and the fact that the viscosity dropped significantly upon addition of sodium thiocyanate.<sup>19</sup> Later, the conclusions of Haas and Schuler were confirmed by light scattering<sup>24</sup> and Raman spectroscopy.<sup>25</sup>

Despite studying the thermoreversible gelation of poly(NAGA) an upper critical solution temperature has not been reported in the publications mentioned above. The UCST of poly(NAGA) and derivatives like poly(*N*-asparagine amide) was first mentioned in some patents by Ohnishi et al.<sup>15–17</sup> On the basis of these patents we published the first study on the UCST behavior of poly(NAGA) and its copolymers with *N*-acetyl acrylamide as a comonomer.<sup>26</sup> The copolymerization parameters as well as the correlation between the cloud point and the copolymer composition, polymer concentration and presence of electrolytes were examined.

The first controlled radical polymerization of poly(NAGA) and poly(*N*-asparagine amide) by the RAFT process was achieved by Lutz et al. but no UCST was observed for poly(NAGA)<sup>27</sup> and a strong positive molecular weight dependence for poly(*N*-asparagine amide).<sup>28</sup> Both phenomena will be discussed and explained in this study.

We were surprised by the fact that the UCST behavior of poly(NAGA) has not been reported in open literature although the polymer is known since 1964. In this work we demonstrate that the upper critical solution behavior in water of poly(NAGA) is suppressed by traces of ionic groups that can be introduced unintentionally by monomer impurities prior to polymerization, by polymer hydrolysis, by the use of ionic radical initiators or ionic chain transfer agents. We believe that poly(NAGA) used in previous studies contained traces of ionic groups that were responsible for the absence or irreproducible UCST behavior, thus explaining why this key feature remained unpublished. In this work, it is shown how to obtain stable aqueous solutions of nonionic poly(NAGA) including the monomer synthesis, polymer synthesis and the dissolution of the polymer in water. From the dissolution conditions the temperature, time and the surprisingly strong influence of the material of the vessel used for dissolution are highlighted. It is also shown that these findings do not interfere with the applicability in aqueous solution or biological fluids. Finally, it is demonstrated how the phase transition can be analyzed by employing powerful methods such as microcalorimetry or light scattering.

Scheme 1. Synthesis for *N*-Acryloyl Glycinamide According to Haas et al.<sup>18 a</sup>



<sup>a</sup> The crude product mixture contains potassium acrylate as a side product.

## 2. RESULTS AND DISCUSSION

### 2.1. Synthesis of Acrylate Free *N*-Acryloyl Glycinamide.

The procedure used for the synthesis of NAGA had crucial influence on the UCST behavior of the corresponding polymer (poly(NAGA)). The conventional synthesis of the monomer *N*-acryloyl glycinamide as reported many years ago by Haas and Schuler followed by others is troubled by the fact that potassium acrylate is a side product of the synthesis (Scheme 1).<sup>18,25,27</sup>

If residues of potassium acrylate remain in the monomer subsequent polymerization leads to the incorporation of acrylic acid units into the polymer backbone. Even small amounts of carboxylic groups in the resulting polymers caused a dramatic suppression of the UCST (further discussion in the section Suppression of the UCST by Ionic Groups in the Polymer). Also, the formation of readily polymerizable potassium acrylate during synthesis bears a high risk of premature polymerization during synthesis and work-up. To prevent the formation of large amounts of potassium acrylate during synthesis and to minimize the risk of premature polymerization a new modified synthetic procedure is developed. Acryloyl chloride should not be used in excess as done in previously reported procedures because it is not necessary for obtaining good yields. An excess would result in quantitative formation of potassium acrylate. The potassium carbonate solution should not be added to a solution of glycinamide hydrochloride and acryloyl chloride as done by Haas and Schuler. This facilitates the hydrolysis of acryloyl chloride to potassium acrylate, and in our experiments, we experienced premature polymerization 4 times out of 7 during synthesis. Instead, acryloyl chloride should be added dropwise to the glycinamide solution. Another critical step of the synthesis is the removal of water from the crude product mixture during work-up. To prevent unwanted polymerization water should be removed by lyophilization instead of rotary evaporation. Also, recrystallization alone is not sufficient to obtain an acrylate free monomer. Suitable methods are the Soxhlet extraction with diethyl ether or column chromatography. Soxhlet extraction, however, is inconvenient because of long extraction times, varying yields due to poor penetration of the crude product mixture and the formation of polymeric impurities. Extraction with acetone followed by column chromatography and subsequent recrystallization from a mixture of methanol and acetone was found to yield an acrylate free monomer as colorless, transparent crystals in a reproducible good yield (75%). Recently, we published the crystal structure of NAGA.<sup>29</sup> Standard methods such as NMR, IR, TLC, and CHN analysis are not sensitive enough to detect significant differences in monomer purity. Separation by liquid chromatography using a conventional C18 column was also unsuccessful. Instead, the determination of the melting point by DSC (Figure 1), determination of residual potassium by flame atomic absorption spectroscopy and direct quantification of acrylate by capillary electrophoresis

(Figure 2) proved to be useful. Table 1 compares the conventional method of preparation with our newly modified method in terms of product purity. Previously reported melting points (129,<sup>18</sup> 140–141,<sup>21</sup> and 136–136.5 °C<sup>30</sup>) were lower than observed for NAGA made in this work. A direct proof for the presence of acrylate impurities in conventionally synthesized NAGA could be obtained by capillary electrophoresis. In contrast, NAGA synthesized by our method did not show an acrylate signal. As the majority of impurities are potassium salts (Scheme 1) determination of the residual potassium content by flame atomic absorption spectroscopy is also suitable for controlling the product purity. The residual potassium content of NAGA

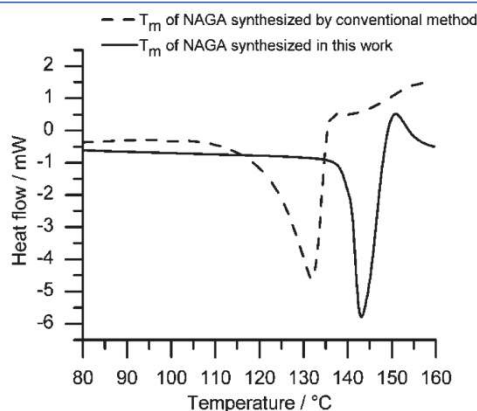


**Figure 1.** Melting point of *N*-acryloyl glycinamide determined by differential scanning calorimetry at a heating rate of 10 K/min. After melting, the monomer polymerizes, causing an exothermic heat flow.

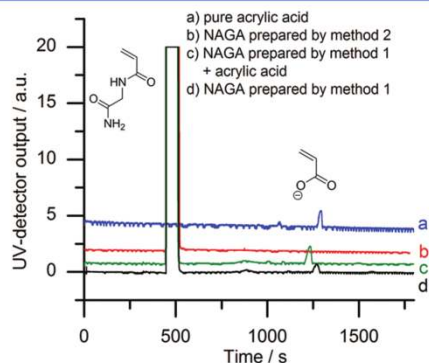


**Figure 2.** Capillary electrophoresis for the detection and quantification of acrylate impurities in *N*-acrylate glycinamide after different methods of preparation.

synthesized by our method was 4.6 ppm and negligible in comparison to NAGA made by the conventional procedure (9700 ppm). Both NAGAs were polymerized under similar reaction conditions i.e. in DMSO using AIBN as initiator at 70 °C. The poly(NAGA) made from monomer that was synthesized according to the conventional literature procedure showed no UCST while acrylate free NAGA (this work) showed an UCST.

**2.2. Turbidity Curve of Poly(NAGA) in Water: Basic Considerations.** To follow changes in the UCST behavior, the cloud points upon cooling and heating were determined using turbidimetry as a major tool (a movie of the UCST transition is available in the HTML version of this paper). Therefore, it is necessary to discuss the basic features and major influences on the turbidity curve. The turbidity curve of poly(NAGA) shows a large hysteresis (Figure 3). At a polymer concentration of 1.0 wt % and a heating rate of 1.0 °C/min it is 10 °C. From a thermodynamic point of view the cloud point upon cooling and heating must be identical when the system has got sufficient time for relaxation. Indeed, the hysteresis observed is a kinetic phenomenon. According to our synthesis and sample preparation the phase transition temperature of a 1.0 wt % poly(NAGA) solution is about 22–23 °C. Cooling at a rate of 1.0 °C/min led to a cloud point of 13.7 °C. Between the phase transition temperature and the cloud point upon cooling the solution is thermodynamically unstable although relaxation occurs very slowly. When cooled from 50 to 18.5 °C followed by keeping the temperature constant for 5 d, the slow growing of aggregates could be followed by conventional dynamic light scattering and turbidimetry (Figure 4). In another experiment, the same solution was cooled and kept constant at 22 °C. Still phase separation took place, although it proceeded extremely slowly. The transmittance

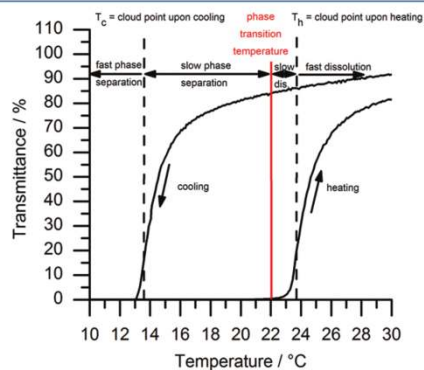


**Figure 3.** Turbidity curve of a 1.0 wt % poly(NAGA) solution in pure water at a heating rate of 1.0 °C/min.

**Table 1. Comparison of the Purity of *N*-Acryloyl Glycinamide after Two Different Methods of Preparation**

method	1 (conventional procedure)	2 (this work)
eq acryloyl chloride used in synthesis <sup>a</sup>	1.20	0.98
purification <sup>b</sup>	extraction with methanol/acetone (v/v = 1/2) + recrystallization therefrom <sup>b</sup>	extraction with acetone + column chromatography + recrystallization from methanol/acetone (v/v = 1/2)
$T_m$ (DSC)/°C <sup>c</sup>	132	143
K-content/ppm	9700 (acrylate <0.7 mol %)	4.6 (acrylate <0.00033 mol %)
acrylate content (capillary electrophoresis)/wt %	0.12	<0.01
UCST behavior of resulting polymers <sup>d</sup>	no	yes

<sup>a</sup> 1.20 equiv were used in all previous publications.<sup>18,25,27</sup> <sup>b</sup> Haas and Schuler recrystallized from methanol/acetone (v/v = 1/2), Marstokk et al. from methanol/acetone (v/v = 1/1) and Lutz et al. from pure acetone. <sup>c</sup> Previously reported melting points: 129, 140–141, and 136–136.5 °C.<sup>18,21,30</sup>

<sup>d</sup> No UCST = no phase separation of a 1.0 wt % solution in pure water upon cooling in an ice bath.

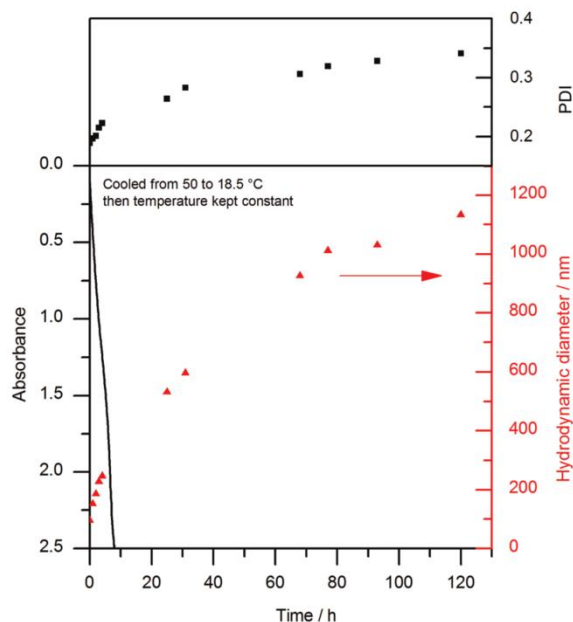


**Figure 4.** Slow formation of aggregates in a 1.0 wt % aqueous solution of poly(NAGA) after a drop of temperature from 50 to 18.5 °C. The temperature was kept constant for 120 h.

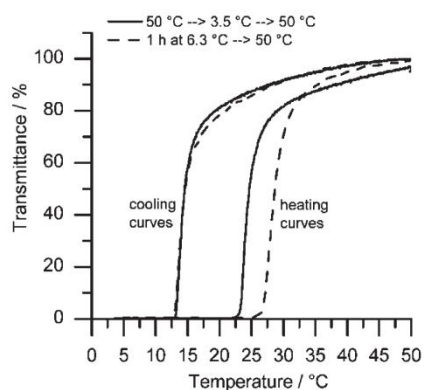


**Figure 5.** Influence of thermal history on the cloud point upon heating. Two turbidity measurements of the same 1.0 wt % aqueous solution of poly(*N*-acryloyl glycinamide) at a heating rate of 1.0 °C/min. Solid curve = cooled from 50 to 3.5 °C and heated back to 50 °C. Dashed curve = sample was tempered at 6.3 °C for 1 h before heating to 50 °C followed by cooling to 3.5 °C.

dropped to 7% (absorbance of 1.1) within 37 h and was still decreasing when the experiment was aborted. From this experiment and the fact that the phase transition temperature must be below the cloud point upon heating it was concluded that the phase transition temperature is between 22 and 23 °C. When the complementary experiment was performed involving heating from 4 to 18.5 °C, no dissolution was observed. This showed the cloud point upon cooling being dependent on the cooling rate. The cloud point upon heating, on the other hand, is dependent on the thermal history below the phase transition temperature and thereby indirectly dependent on the heating rate. In a separate experiment, we could show that the cloud point upon heating is shifted to higher values when the sample is tempered for longer time intervals below the phase transition temperature (Figure 5).

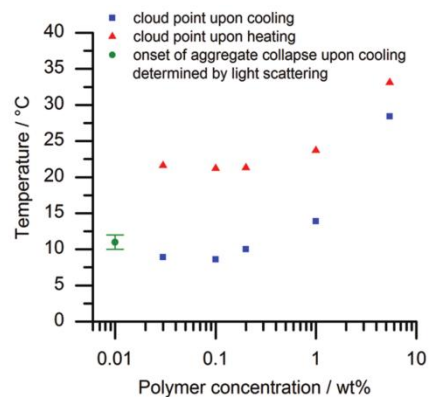


**Figure 6.** Phase transition temperature as a function of concentration (note the logarithmic scale) of poly(NAGA) in pure water. The heating rate for the cloud point measurements was 1.0 °C/min except for  $c = 0.03$  wt % where it was 0.1 °C/min.

Recently, we have shown that the cloud point of aqueous poly(NAGA) solutions increases with increasing polymer concentration<sup>26</sup> as it is expected for polymers showing UCST behavior. In dilute solutions the concentration dependence of the cloud point is less prominent (Figure 6, note the logarithmic scale). This observation is similar to the phase transition behavior of PNiPAAm.<sup>31,32</sup>

For all the reasons mentioned above it is important to keep the polymer concentration as well as the heating program constant when comparing the UCST behavior of different polymers. In respect to time exposure and sensitivity a concentration of 1.0 wt % and a heating rate of 1.0 °C/min were considered most appropriate for the majority of turbidity measurements.

**2.3. Suppression of the UCST by Ionic Groups in the Polymer.** The role of ionic groups in suppressing the UCST of poly(NAGA) was confirmed by deliberately adding acrylic acid prior to polymerization of NAGA. The corresponding polymers were designated according to the acrylic acid content in the feed in mol %, i.e., AA0.01, AA0.10, AA0.21, AA1.00, and AA5.00. It was found that just small amounts of carboxyl groups dramatically suppress the UCST (Table 2).

Poly(NAGA) synthesized from acrylate free monomer (acrylate content <4 ppm) showed a cloud point at 13.7 and 23.5 °C in cooling and heating cycles, respectively. The addition of acrylic acid in even very low amounts (AA0.01 and AA0.10) led to a decrease in UCST. The UCST disappeared completely on increasing the amount of acrylic acid to 0.21 mol % and beyond. The shielding of the carboxylate groups by electrolytes counteracts these effects. In phosphate buffered saline the cloud point of the polymers AA0.01 and AA0.1 with low carboxylate content recovers to the level of the cloud point of nonionic poly(NAGA). Having no cloud point in pure water AA1.00 shows a cloud point in PBS, although it is slightly lower than this of nonionic poly(NAGA). If the acrylic acid content is further increased to 5.0 mol % the cloud point is absent even in PBS showing that carboxyl contents higher than 1 mol % started to influence the hydrophilic–lipophilic balance in a significant manner.

This fact of suppression of UCST by ionic groups was further supported by functionalization of the chain end groups by using chain transfer agents or ionic initiators. The results showed that ionic groups in general are the cause of cloud point/UCST suppression. Recently, Lutz et al. performed RAFT polymerization

**Table 2. Influence of Ionic Groups on the Cloud Point of 1.0 wt % Poly(NAGA) in Pure Water and Phosphate Buffered Saline, Respectively<sup>a</sup>**

polymer code	CTA	acrylic acid in feed/mol %	polymerization medium	initiator	cloud point/°C			
					pure water		phosphate buffered saline	
					cooling	heating	cooling	heating
poly(NAGA)-std	-	<4 ppm <sup>b</sup>	DMSO	AIBN	13.7	23.5	10.2	21.3
AA0.01	-	<b>0.01</b>	DMSO	AIBN	11.4	19.9	9.7	20.4
AA0.10	-	<b>0.10</b>	DMSO	AIBN	2.5	13.0	10.0	20.9
AA0.21 <sup>c</sup>	-	<b>0.21<sup>c</sup></b>	DMSO	AIBN	none	none	n.d.	n.d.
AA1.00	-	<b>1.00</b>	DMSO	AIBN	none	none	8.1	19.1
AA5.00	-	<b>5.0</b>	DMSO	AIBN	none	none	none	none
RAFT_1	<b>BCPS<sup>d</sup></b>	<4 ppm <sup>b</sup>	DMSO	AIBN	none	none	3.8	10.5
RAFT_2	DBTC <sup>f</sup>	<4 ppm <sup>b</sup>	DMSO	<b>VA-044<sup>e</sup></b>	none	none	13.4	22.2
RAFT_3	DBTC <sup>f</sup>	<4 ppm <sup>b</sup>	DMSO	AIBN	15.7	25.7	11.4	22.6
poly(NAGA)-KPS	-	<4 ppm <sup>b</sup>	water/isopropanol	<b>KPS<sup>g</sup></b>	11.8	22.1	8.1	18.9

<sup>a</sup>The source of ionic groups that caused depression or absence of the cloud point was printed in bold letters. <sup>b</sup>Acrylic acid originating from the monomer synthesis is present in the form of potassium acrylate. According to flame atomic absorption spectroscopy the potassium content was 4.6 ppm; hence, the potassium acrylate content is below 4 ppm. <sup>c</sup>Polymer resulting from the polymerization of NAGA that was synthesized using method 2 (Table 1). Acrylic acid is present in the form of a potassium acrylate impurity that was quantified by capillary electrophoresis. <sup>d</sup>BCPS = sodium 3-(((benzylthio)carbonothioyl)thio)propane-1-sulfonate. <sup>e</sup>2,2'-Azobis[2-(2-imidazolin-2-yl)propane]dihydrochloride. <sup>f</sup>DBTC = dibenzyl trithiocarbonate. <sup>g</sup>KPS = potassium persulfate.

of NAGA in water using sodium 3-(((benzylthio)carbonothioyl)thio)propane-1-sulfonate as CTA and VA-044 as initiator.<sup>27</sup> The resulting polymers possessed sulfonate groups at the  $\omega$  chain ends and partly imidazolium chloride moieties at the  $\alpha$  chain ends originating from the initiator VA-044 which was used in the ratio CTA/initiator = 3/1. These polymers did not display a cloud point in pure water at least up to a degree of polymerization of 500. The absence of an UCST could be due to acrylate impurities in the monomer as the monomer was synthesized by the conventional monomer synthesis or hydrolysis during the polymerization in water (overnight at 60 °C). For this reason the polymer synthesis reported by them was repeated with acrylate free monomer in DMSO as a solvent with substitution of either the CTA and/or the initiator with a nonionic compound (polymers RAFT\_1, RAFT\_2, and RAFT\_3 in Table 2). In all cases the chain ends were functionalized by the RAFT agent as determined by NMR spectroscopy. The average degree of polymerization ( $P_n$ ) was estimated from the integral ratio of the phenylic protons compared to the methylene protons adjacent to the nitrogen (NMR spectra in the Supporting Information). It was calculated to be 189, 160, and 118 for RAFT\_1, RAFT\_2, and RAFT\_3, respectively. Some of the  $\alpha$  chain ends were functionalized by the initiator. Since the initiator signals overlap with polymer signals it was not possible to estimate the amount of initiator derived chain ends. Hence, the real  $P_n$  will be slightly lower than calculated. However, for the conclusions drawn it is sufficient to know that the  $P_n$  was in the range of 100 to 200. If the  $\omega$  chain end was functionalized with sulfonate (RAFT\_1) the cloud point was absent in pure water. Switching to nonionic dibenzyl trithiocarbonate as CTA while using the ionic initiator VA-044 led to the same observation. This demonstrates that, despite being commonly neglected, a considerable amount of  $\alpha$  chain ends was derived from the initiator in the RAFT process. At  $P_n = 100$ –200 the chain end counts for 0.5–1.0% in respect to NAGA units. Thus, the absence of a cloud point in pure water is

in agreement with the findings for carboxyl groups where cloud points are absent for contents >0.10%. If the initiator as well as the transfer agent are nonionic (RAFT\_3) a cloud point could be observed. Free radical polymerization of NAGA in a water/isopropanol mixture using potassium persulfate as initiator leads to a polymer with a molecular weight of 230 kDa ( $P_n = 1800$ ).<sup>25</sup> This corresponds to only 0.06% in respect to NAGA units and explains why the cloud point is just slightly depressed compared to nonionic poly(NAGA).

**2.4. Suppression of the UCST by the Hydrolysis of Amide Bonds of NAGA.** Amides are relatively stable against hydrolysis, especially at neutral pH. However, despite proceeding slowly hydrolysis does occur as shown for poly(acrylamide).<sup>33,34</sup> Hence, hydrolysis must be taken into account and it is necessary to choose the dissolution conditions carefully. Bringing the solid nonionic polymer into aqueous solution is not trivial. Temperatures greater 60 °C were necessary. On the other hand, higher temperatures accelerate the hydrolysis, which may result in loss of the UCST behavior. The influence of the temperature on the dissolution state and UCST behavior was investigated qualitatively (Table 3). On the basis of our observations the process of dissolution at elevated temperatures was categorized as follows: Category 1: swollen physically cross-linked hydrogel particles exist along with dissolved polymer. Category 2: the solution is clear and homogeneous above the cloud point and complete phase separation occurs below the cloud point. When the polymer precipitates an intransparent (path length = 1 cm) milk is formed. Within minutes further flocculation leads to visible particles that slowly sediment. Category 3: the solution shows decreasing turbidity upon cooling and decreasing tendency to flocculate. Category 4: the cloud point has disappeared, and the solution is clear over the whole temperature range. At 60 °C the polymer did not completely dissolve (category 1). At 70, 80, and 90 °C all four categories of dissolution are observed depending on the time of heating. At 70 °C in PP-tubes the cloud point

**Table 3. Influence of the Temperature and the Surface of the Used Vessel on the Progress of Dissolution and the Cloud Point of Poly(NAGA) in Pure Water<sup>a</sup>**

temperature/°C	vessel material	category of dissolution								
		0.25 h	0.5 h	1 h	2 h	3 h	4.5 h	7 h	12 h	18 h
60	PP	1	1	1	1	1	1	1	1	1 + 4 <sup>b</sup>
70	PP	1	1	1	1	2	2	3	4	4
80	PP	1	2	2	3	3	3	4	4	4
90	PP	1	2	2	3	4	4	4	4	4
80	borosilicate glass <sup>c</sup> (acidic)	1	3	3	3	4	4	4	4	4
80	borosilicate glass <sup>c</sup> (neutral)	1	3	4	4	4	4	4	4	4
80	borosilicate glass <sup>c</sup> (basic)	1	3	4	4	4	4	4	4	4
80	fused silica (neutral)	1	2	2	3	3	3	4	4	4

<sup>a</sup> All samples were dissolved without agitation at a concentration of 1.0 wt %. The temperature stated is the temperature inside the vessels. The dissolution process was divided into four categories. 1 = swollen physically crosslinked hydrogel particles exist along with dissolved polymer, the dissolved fraction shows thermoresponsivity. 2 = the solution is clear and homogeneous above the cloud point and complete phase separation occurs below the cloud point. When the polymer precipitates an intransparent (path length = 1 cm) milk is formed. Within 10 min further flocculation leads to visible particles that slowly sediment. 3 = the solution shows decreasing turbidity upon cooling and decreasing tendency to flocculate. 4 = the cloud point has disappeared, and the solution is clear over the whole temperature range. <sup>b</sup> The cloud point of the dissolved polymer fraction disappeared.

<sup>c</sup> Two borosilicate glass vials (Macherey-Nagel, N8-425, 1.5 mL, 11.6 × 32 mm, hydrolytic class I) were filled with either 1 M hydrochloric acid or pure water or 1 M sodium hydroxide and let to stand for 1 h. Thereafter all vials were rinsed 10 times with pure water, dried at 80 °C for 1 h, and used the same day. The results of both experiments were identical.

**Table 4. Influence of the Hydrolysis at 75 °C on the Cloud Point of Poly(NAGA)**

time/h <sup>a</sup>	additive	cloud point/°C	
		cooling	heating
0.5	-	11	21
1.5	-	7	17
3.0	-	4	14
5.0	-	0–3 <sup>b</sup>	n.d.
5.0	9 mM NaCl	9.4	20.7
5.0	100 mM NaCl	9.0	20.4
8.5	100 mM NaCl	6.0	16.7

<sup>a</sup> Time that the polymer dispersion or solution was held at 75 °C. A 30 mg sample of dry polymer was dissolved in the measuring cuvette (Hellma, Suprasil, fused silica) at 75 °C in 2970 mg of pure water with magnetic stirring at 300 rpm to obtain a 1.0 wt % polymer solution. After 0.5 h, the solution appeared clear and the first measurement was conducted. <sup>b</sup> The cloud point was below the cooling limit of the turbidity photometer. The sample showed a cloud point when cooled in an ice bath for 5 min.

disappeared after 12 h, at 80 °C after 7 h and at 90 °C after 3 h. In fused silica vessels, the speed of hydrolysis is approximately the same whereas in borosilicate glass vessels the hydrolysis is much faster and the cloud point disappeared after 1 h at 80 °C. In addition to these qualitative results the proceeding decrease of the cloud point with prolonged heating was analyzed by turbidity measurements (Table 4).

As expected the thermoresponsivity could be recovered by adding a salt as long as the carboxyl content is low. Because of the small degree of hydrolysis a quantification of carboxyl groups was not possible. The presence of anionic moieties in the polymer backbone, however, could be proven by capillary electrophoresis (Figure 7). The migration time of a heat treated polymer solution (4 mL class vial, hydrolytic glass III, 4 h, 80 °C) was increased compared to a nonionic internal standard. The absolute

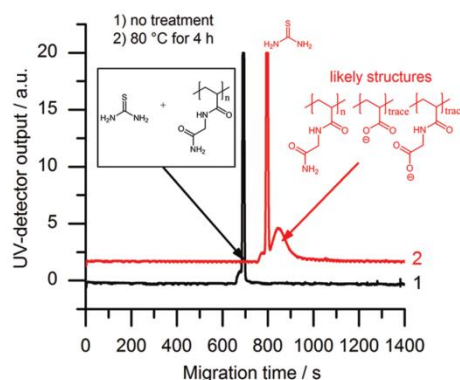


**Figure 7.** Proof for the formation of anionic units in poly(*N*-acryloyl glycinamide) by capillary electrophoresis. Curve 1 = electrophoresis of a 1 g/L solution of poly(NAGA) in 10 mM phosphate buffer. Curve 2 = electrophoresis of the same solution after heating it to 80 °C for 4 h in a glass vessel of hydrolytic class III. The migration time of the heat treated polymer is increased compared to the nonionic standard, hence indicating hydrolysis.

migration times of the nonionic standard are not identical because the polymers get partially adsorbed at the capillary walls.

**2.5. Influence of Surfaces on the Hydrolysis.** The reproducible preparation of aqueous solutions of poly(NAGA) is complicated by the fact that the speed of hydrolysis is a function of many parameters. Apart from the temperature the surface of the vessel used for dissolution is of importance. For instance, the degradation of gelatin has been observed to proceed faster in glass vessels than in poly(propylene) vessels.<sup>35</sup> Gelatin is a biopolymer that contains amide bonds between its amino acid units and also shows a similar thermoreversible gelation, providing a good comparison to poly(NAGA). The authors argued that gelatin adsorbs at the glass wall causing an unfolding of the macromolecule. An effect that has been described by others.<sup>36</sup> It was assumed that gelatin is more prone to hydrolysis in its unfolded state. Our findings suggest a different conclusion.

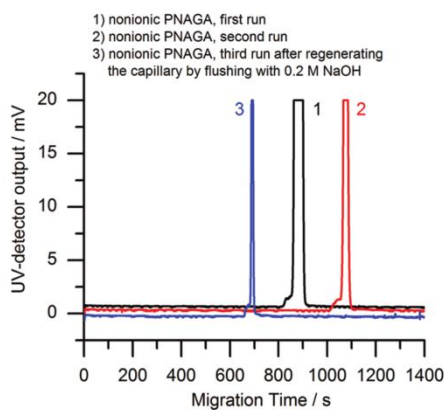


**Figure 8.** Capillary electrophoresis of nonionic poly(NAGA). In all runs, thiourea was used as nonionic internal standard. From run one to run two the migration time increased due to polymer adsorption to the wall of the fused silica capillary.

Indeed, poly(NAGA) adsorbs at glass walls which could be well observed in capillary electrophoresis experiments where capillaries from fused silica are used (Figure 8). The migration time of the neutral polymer increased strongly from one measurement to the next. This effect is well-known and a consequence of polymer adsorption.<sup>37</sup> Adsorbed polymer could be washed off with sodium hydroxide solution to regenerate an uncoated silica surface. However, the speed of hydrolysis which is indicated by the loss of the cloud point was not faster in fused silica vessels compared to poly(propylene) vessels (Table 2). In both vessels it took 7 h at 80 °C for the cloud point to disappear. Instead, hydrolysis was greatly accelerated in glass vessels containing alkali and alkaline earth metal oxides. The borosilicate vials used were of hydrolytic class I (alkaline release =  $0.35 \pm 0.05$  mL 0.02 N H<sub>2</sub>SO<sub>4</sub>/10 g of glass, measured according to USP 25) and it took only 1 h until the cloud point disappeared at 80 °C. This conclusion is supported by the fact that acid treatment of these glasses prior to the test increased the time until cloud point loss to 4 h while neutral and basic treatment had no effect. The pH increase in the bulk solution by the leaching of alkali bases is not significant. The polymer, however, is crowded at the source of alkali base formation, namely the interfacial area with a high local pH. Thus, it is most likely the combination of adhesion and basic glass components that is responsible for this surprising acceleration of hydrolysis.

Along with surface effects goes an influence of the polymer concentration and volume to surface ratio (not investigated in this study). The real surface area in turn strongly depends on the surface roughness which further complicates the matter. The results described above show that the choice of vessel and dissolution conditions is essential and needs to be stated in great detail in order to conduct reproducible and comparable experiments. Poly(propylene) vessels seem to be most appropriate for the handling of poly(NAGA) solutions. Paying attention to all relevant dissolution conditions previously discussed a reproducibility of sd (cloud point, four samples) =  $\pm 0.2$  °C for a 1.0 wt % solution of nonionic poly(NAGA) in pure water was achieved.

**2.6. UCST in Human Blood Serum.** The cloud point of poly(*N*-acryloyl glycinamide) can be influenced by additives. Chaotropic agents or hydrogen bond breaking agents like sodium thiocyanate reduce the cloud point<sup>26</sup> whereas kosmotropic agents like sulfate salt increase the cloud point. The question whether

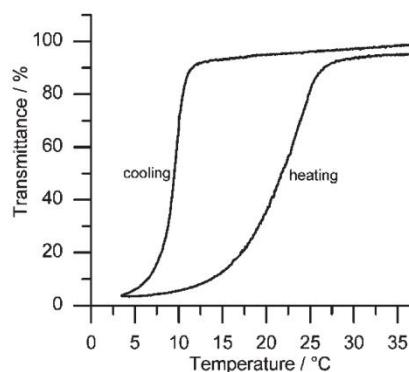


**Figure 9.** Turbidity curve of a 0.1 wt % solution of nonionic poly(*N*-acryloyl glycinamide) in 90 vol % human blood serum. Heating rate = 1.0 °C/min.

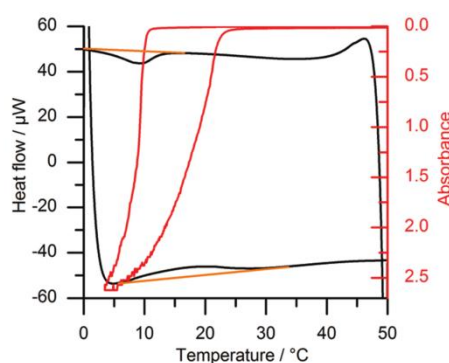


**Figure 10.** Differential scanning microcalorimetry (black curve) of a 1.0 wt % aqueous solution of poly(*N*-acryloyl glycinamide) overlaid with the turbidimetry curve (red curve) of a 0.2 wt % aqueous solution of the same polymer. A straight baseline (orange) has been added to the DSC curve for clarity. For both measurements, the heating rate was 1.0 °C/min. Measurement ranges of DSC: 50 to 0 °C, 10 min at 0 °C, and then 0 to 50 °C. Measurement ranges of turbidimetry: 50 to 3.5 °C, 3.5 to 50 °C. Note that the heat flow is scaled in  $\mu$ W.

the UCST transition of poly(NAGA) could be exploited in biomedical applications is of great interest and its answer will govern the path of further research in this field. As biological fluids are a complex mixture of compounds simple models like phosphate buffered saline are inadequate and tests in real biological fluids are necessary. For this purpose the human human blood serum was chosen. Figure 9 shows that poly(NAGA) displays a cloud point at 9.8 °C upon cooling and 24 °C upon heating at a heating rate of 1.0 °C/min despite the complex environment of blood serum. Although for specific applications the kinetics of the UCST transition need to be considered the results shown here are highly encouraging for further research in this direction.

**2.7. Ultrasensitive Differential Scanning Calorimetry.** For simplicity, we assume that the polymer solution separates into pure polymer and pure solvent phases. On this assumption, a polymer dissolves in a solvent when the change of the free enthalpy of dissolution  $\Delta G$  is negative (eq 1).

$$\Delta G = \Delta H - T\Delta S \quad (1)$$

The LCST of PNiPAAm is due to the fact that both the change of enthalpy ( $\Delta H$ ) and the change of entropy ( $\Delta S$ ) are negative.

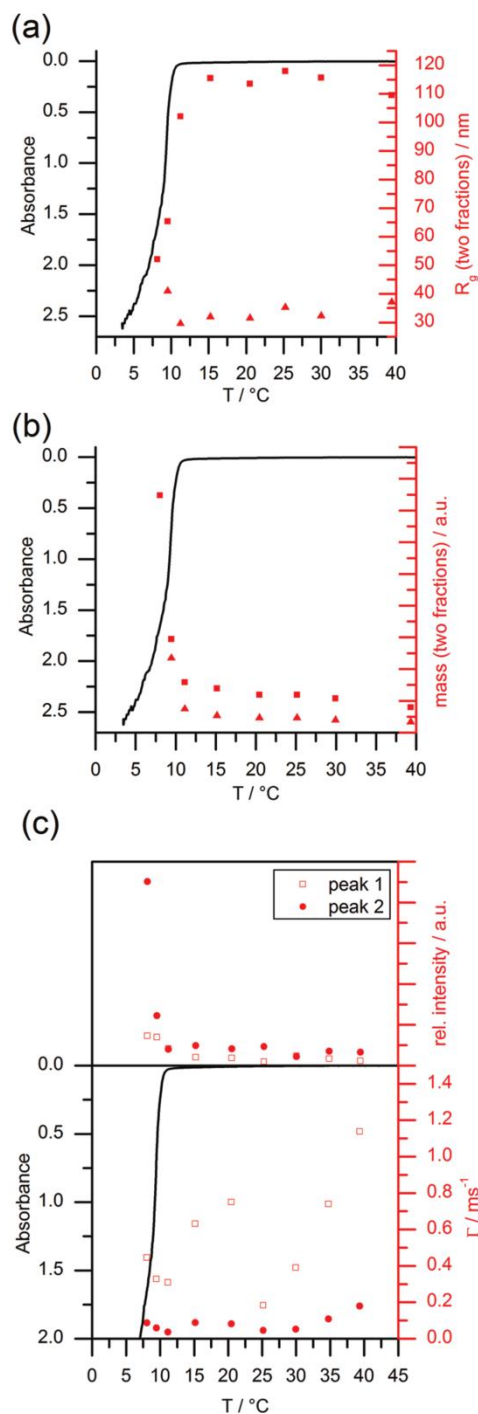
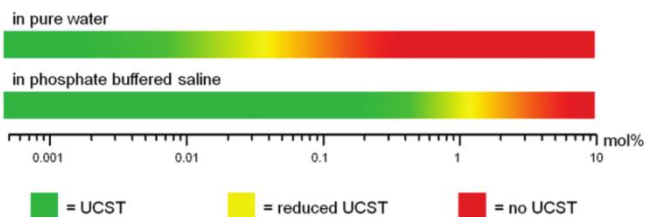


**Figure 11.** Light scattering results from a 0.01 wt % solution of poly(NAGA) in pure water. (a) Radii of gyration from static light scattering reveal two separable fractions (squares and triangles) which are plotted versus temperature. (b) Respective relative mass data are plotted for both fractions from static light scattering. (c) The inverse relaxation time of the fast mode (hollow squares) and the slow mode (solid circles) and their contribution to the overall scattering intensity are plotted versus temperature.

The negative change of entropy is explained by the highly ordered hydration shell of the isopropyl groups when the polymer is in solution (hydrophobic effect). With increasing temperature this effect contributes more to the change of free enthalpy until a critical temperature is reached where  $\Delta G$  gets positive.

## Scheme 2. Effect of Carboxyl Content on the UCST of Poly(*N*-acryloyl glycinamide) Solutions in Pure Water or Phosphate Buffered Saline, Respectively

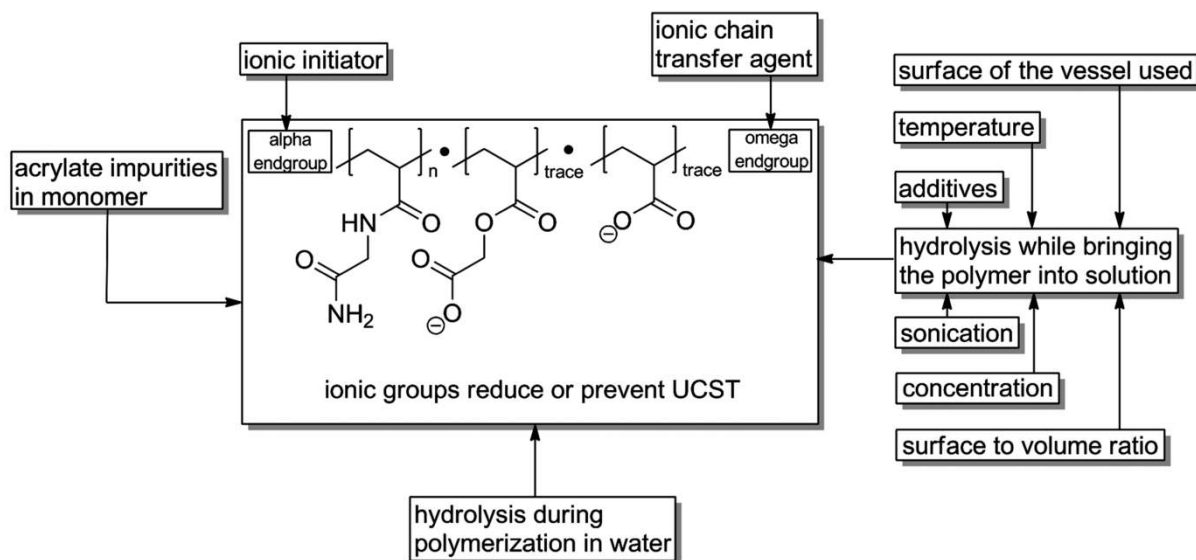
### Effect of carboxyl content on the UCST



The polymer precipitates. For a polymer showing an UCST the opposite situation is expected. Both  $\Delta H$  and  $\Delta S$  should be positive. Poly(NAGA) does not contain a hydrophobic side chain as PNiPAAm. Therefore, the hydrophobic effect is small and the entropy change is dominated by the random distribution of chains in solution and the increased chain flexibility. In the solid state poly(NAGA) is stabilized by hydrogen bonding which is indicated by the very high glass transition temperature of 186 °C.<sup>26</sup> In order to bring the polymer into solution, these hydrogen bonds have to be cleaved. While the cleavage of the interpolymer amide–amide hydrogen bonds is an endothermic process the simultaneous formation of amide–water hydrogen bonds is exothermic. This greatly diminishes the overall observable change of enthalpy. For low molecular weight amides in water, the heat of formation of hydrogen bonds has been shown to be close to zero.<sup>38</sup>

Previous experiments to detect an enthalpy change by conventional differential scanning calorimetry have not been successful. In this study we used a calorimeter of much higher sensitivity in order to detect the assumed transition. Indeed we observed an exothermic peak upon precipitation and an endothermic peak upon dissolution (Figure 10). The heat of transition was determined to be  $0.7 \pm 0.4$  J/g. The transitions were broad and close to the turning point of the heating profile which made it difficult to apply a reliable baseline. Therefore, a relatively large error has been introduced. To the best of our knowledge this is the first calorimetric evidence of a UCST transition of a poly(acrylamide) derivative. The  $\Delta H$  values calculated from the cooling and heating curves are identical, indicating that the transition is fully reversible. Over nine consecutive DSC runs, there is no significant decrease in  $\Delta H$  values. This is another indication for a good reversibility of the UCST transition.

**2.8. Static and Dynamic Light Scattering.** Polymers exhibiting a LCST like PNiPAAm undergo a coil-to-globule transition at a molecular level. The coil-to-globule transition of a single chain can be detected by dynamic and static light scattering.<sup>39</sup> Marstokk et al. have shown that poly(NAGA) does not molecularly dissolve in pure water.<sup>25</sup> Aggregates are present even at low concentrations. Only a 2 M solution of sodium thiocyanate was capable of breaking up the aggregates producing a molecular dispersion. Under these conditions, however, the UCST transition would also be suppressed. Although we were forced to accept the presence of aggregates, we will outline a brief qualitative discussion of our preliminary light scattering results referring to a temperature series in pure water at a poly(NAGA) concentration of 0.01 wt %. Below the cloud point curve key parameters like the radius of gyration and the molecular mass of

Scheme 3. Ionic Groups in Poly(NAGA) Reduce or Prevent the UCST in Pure Water<sup>a</sup>

<sup>a</sup>The introduction of such groups can occur prior to polymerization, during polymerization or after polymerization by hydrolysis. The kinetics of hydrolysis are influenced by a multitude of parameters.

the present polymer particles changed drastically. At 40 °C we observed two well separated slopes in static light scattering curves (Supporting Information), each revealing a radius of gyration (Figure 11, a and b). One is close to  $R_g = 110$  nm and a second one lies close to  $R_g = 37$  nm with a relative mass of 1.0 and 2.4, respectively. The two separable values correspond to two different species and may be attributed to a single coil fraction and to an aggregate fraction. The dispersion was stable for at least 24 h. Over a period of 8 h, the temperature was successively decreased stepwise. Once the temperature dropped below 15 °C the size of the larger fraction shrank drastically until the two fractions merged at 8 °C with  $R_g = 52$  nm. Simultaneously the relative mass of the aggregate fraction increased to 37, indicating that the polymer aggregates collapsed and became very compact. One can estimate that the density of the particles increased by more than 2 orders of magnitude during this temperature drop. To shed further light on this process and its participating species, we performed an inverse Laplace Transformation of the normalized electric field correlation function from dynamic light scattering at a scattering angle of 30°, where the signal-to-noise ratio is expected to be good enough. The transformation was based on the CONTIN routine representing the inverse relaxation times  $\Gamma$  of the contributing species and their intensity contributions (Figure 11c). In close agreement with the strongly bended curves from static light scattering, two well separated modes became discernible. As expected, the scattering intensity of the aggregates emphasized at this point that an evaluation of clear-cut trends from the CONTIN analysis always requires high precision data. Nevertheless, even with a preliminary analysis at a single angle a decrease to 1/3 occurs for  $\Gamma$  from the fast mode (1.2/ms to 0.4/ms) which indicates a significant contraction of the species identified as the single chains. The slow mode seems to follow a similar trend. However, it is difficult to attribute any mechanistic features to these variations since aggregation is certainly overlaid by a condensation/collapse of the constituent chains. The overlay of such trends may even result in a minimum. Considering the uncertainty of the

CONTIN analysis, such a minimum is also compatible with the trend in  $\Gamma$  of the slow mode.

### 3. CONCLUSION

Nonionic polymers bearing primary amide moieties, like poly(NAGA), can display an UCST in aqueous solution due to thermally reversible hydrogen bonding. In this study it was shown that traces of ionic groups in the polymer prevent phase separation of poly(NAGA) (Scheme 2). In the past, the UCST of poly(*N*-acryloyl glycinamide) had not been reported because ionic groups were introduced accidentally by either acrylate impurities in the monomer, hydrolysis of the polymer side chains and/or usage of ionic initiators (Scheme 3).

Monomer purity must be proven by stating physical properties and analytical data like the melting point and residual potassium content. The ionic groups can be shielded by counterions so that the addition of salts largely compensates the ionic groups UCST lowering effects. Nevertheless, the ability to control the electrostatics of the polymers is crucial. To avoid ionic groups in the polymer, some guidelines should be followed. During monomer synthesis acryloyl chloride should be used in deficit and acrylate impurities need to be thoroughly removed from the product, e.g., by column chromatography. To prevent hydrolysis of the polymer side chains polymerization should be performed in non-aqueous media or at lower temperatures. Also, when preparing aqueous solutions of poly(NAGA) the dissolution conditions have to be chosen with care. Prolonged heating to higher temperatures ( $T > 70$  °C,  $t > 3$  h) should be avoided to retain thermoresponsivity. In any case the dissolution conditions like temperature, time, concentration, material and dimensions of the vessel used and agitation should be stated in detail to ensure reproducibility. We believe that this knowledge is transferable to other systems and will greatly accelerate research in the field of UCST polymers.

Turbidity and DLS studies revealed that the phase transition temperature of a 1.0 wt % solution of poly(NAGA) in pure water



(according to our synthesis and sample preparation) is 22–23 °C. However, at conventional heating rates such as 1.0 or 0.1 °C/min, the turbidity curve displayed a large hysteresis. There was a temperature interval around the phase transition temperature where equilibration of the system was extremely slow. In dilute solutions (0.01 to 1.0 wt %) the phase transition temperature showed little concentration dependence. A combined static and dynamic light scattering goniometer was used in order to study the UCST transition on a molecular level. Solutions of poly(NAGA) in pure water contained aggregates even at 40 °C and very low concentrations such as 0.01 wt %. Below the phase transition temperature the radius of gyration of the aggregate fraction decreased, whereas its relative mass still increased. Hence, the density of the particles increased more than 2 orders of magnitude indicating that further aggregation took place simultaneously with a drastic shrinking of the aggregate dimensions.

We measured the first DSC trace of the UCST transition of this polymer class by employing an ultrasensitive calorimeter. As anticipated from basic thermodynamic considerations we found an endothermic heat of transition upon heating and an exothermic heat of transition upon cooling which corresponds to the cleavage and formation of polymer–polymer hydrogen bonds, respectively. The heat of transition is extremely low and was determined to be  $0.7 \pm 0.4$  J/g. The transition appeared to be fully reversible over a number of at least 9 consecutive runs which involved heating up to 50 °C.

The sum of experiments showed that polymers featuring primary amide groups, like poly(*N*-acryloyl glycinamide), represent a powerful tool for the preparation of responsive materials that retain their function under physiological conditions. With its upper critical solution temperature in water poly(*N*-acryloyl glycinamide) complements the well investigated polymers with lower critical solution temperature in water such as poly(*N*-isopropylacrylamide). This work has established the synthetic and analytical base needed to exploit the inherent thermoresponsive properties of poly(NAGA).

## ■ ASSOCIATED CONTENT

**S Supporting Information.** Materials, methods, experimental, and characterization details. **Web enhanced object.** A video of the UCST transition of two polymer samples with different cloud points is available online. This material is available free of charge via the Internet at <http://pubs.acs.org>.

**W Web Enhanced Feature.** A movie of the UCST transition is available in the HTML version of this paper.

## ■ AUTHOR INFORMATION

### Corresponding Author

\*E-mail: [agarwal@staff.uni-marburg.de](mailto:agarwal@staff.uni-marburg.de).

## ■ ACKNOWLEDGMENT

The authors would like to thank the Philipps-University of Marburg for funding and the group of Prof. Barner-Kowollik (KIT) for the provision of dibenzyltrithiocarbonate. Also, we would like to express our gratitude to Christian Ortmann from TA Instruments and Prof. Ute Pyell from the University of Marburg for providing the experimental setup and assistance for ultra sensitive differential scanning calorimetry and capillary electrophoresis, respectively.

## ■ ABBREVIATIONS

BCPS, sodium 3-(((benzylthio)carbonothioyl)thio)propane-1-sulfonate; CTA, chain transfer agent; DBTC, dibenzyltrithiocarbonate; DLS, dynamic light scattering; DSC, differential scanning calorimetry; KPS, potassium persulfate; LCST, lower critical solution temperature; NAGA, *N*-acryloyl glycinamide; PNIPAAm, poly(*N*-isopropylacrylamide); UCST, upper critical solution temperature; USP, United States Pharmacopeia; RAFT, reversible addition–fragmentation chain transfer polymerization; TLC, thin layer chromatography

## ■ REFERENCES

- (1) Cameron, A.; Shakesheff, K. M. *Adv. Mater.* **2006**, *18*, 3321–3328.
- (2) Schild, H. G. *Prog. Polym. Sci.* **1992**, *17*, 163–249.
- (3) Ren, L.; Agarwal, S. *Macromol. Chem. Phys.* **2007**, *208*, 245–253.
- (4) Jun, L.; Bochu, W.; Yazhou, W. *Int. J. Pharm.* **2006**, *2*, 513–519.
- (5) Kobayashi, J.; Okano, T. *Sci. Technol. Adv. Mater.* **2010**, *11*, 014111.
- (6) Aoki, T.; Nakamura, K.; Sanui, K.; Kikuchi, A.; Okano, T.; Sakurai, Y.; Ogata, N. *Polym. J.* **1999**, *31*, 1185–1188.
- (7) Katono, H.; Kohei, S.; Ogata, N.; Okano, T.; Sakurai, Y. *Polym. J.* **1991**, *23*, 1179–1178.
- (8) Aoki, T.; Kawashima, M.; Katono, H.; Sanui, K.; Ogata, N.; Okano, T.; Sakurai, Y. *Macromolecules* **1994**, *27*, 947–952.
- (9) Katono, H.; Maruyama, A.; Sanui, K.; Ogata, N.; Okano, T.; Sakurai, Y. *J. Controlled Release* **1991**, *16*, 215–228.
- (10) Jiang, Z.; You, Y.; Gu, Q.; Hao, J.; Deng, X. *Macromol. Rapid Commun.* **2008**, *29*, 1264–1268.
- (11) Zhang, Z.; Chao, T.; Chen, S.; Jiang, S. *Langmuir* **2006**, *22*, 10072–10077.
- (12) Lowe, A. B.; Mc Cormick, C. L. *Chem. Rev.* **2002**, *102*, 4177–4190.
- (13) Arotcarena, M.; Heise, B.; Ishaya, S.; Laschewsky, A. *J. Am. Chem. Soc.* **2002**, *124*, 3787–3793.
- (14) Ohnishi, N.; Aoshima, K.; Kataoka, K.; Ueno, K. *Stimuli-responsive polymer utilizing keto-enol tautomerization*. EP 0 922 715 A2, June 16, 1999.
- (15) Ohnishi, N.; Furukawa, H.; Kataoka, K.; Ueno, K. *Polymer Having An Upper Critical Solution Temperature*. US 7,195,925 B2, March 27, 2007.
- (16) Nagaoka, H.; Ohnishi, N.; Eguchi, M. *Thermoresponsive Polymer and Production Method Thereof*. US 2007/0203313 A1, August 30, 2007.
- (17) Eguchi, M.; Ohnishi, N. *Aqueous Solution of Polymer Having Upper Critical Solution Temperature, Aqueous Dispersion of Particle Modified with the Polymer and Method of Storing the Same*. EP 2 009 044 A1, December 31, 2008.
- (18) Haas, H. C.; Schuler, N. W. *J. Polym. Sci., Part C: Polym. Lett.* **1964**, *2*, 1095–1096.
- (19) Haas, H. C.; Moreau, R. D.; Schuler, N. W. *J. Polym. Sci., Part A-2* **1967**, *5*, 915–927.
- (20) Haas, H. C.; Chiklis, C. K.; Moreau, R. D. *J. Polym. Sci., Part A-1* **1970**, *8*, 1131–1145.
- (21) Haas, H. C.; MacDonald, R. L.; Schuler, A. N. *J. Polym. Sci., Part A-1* **1970**, *8*, 1213–1226.
- (22) Haas, H. C.; Manning, M. J.; Mach, M. H. *J. Polym. Sci., Part A-1* **1970**, *8*, 1725–1730.
- (23) Haas, H. C.; MacDonald, R. L.; Schuler, A. N. *J. Polym. Sci., Part A-1* **1970**, *8*, 3405–3415.
- (24) Ostrovskii, D.; Jacobsson, P.; Nyström, B.; Marstokk, O.; Kopperud, H. B. M. *Macromolecules* **1999**, *32*, 5552–5560.
- (25) Marstokk, O.; Nyström, B.; Roots, J. *Macromolecules* **1998**, *31*, 4205–4212.
- (26) Seuring, J.; Agarwal, S. *Macromol. Chem. Phys.* **2010**, *211*, 2109–2117.
- (27) Glatzel, S.; Badi, N.; Päch, M.; Laschewsky, A.; Lutz, J. *Chem. Commun.* **2010**, *46*, 4517–4519.

- (28) Glatzel, S.; Laschewsky, A.; Lutz, J. *Macromolecules* **2011**, *44*, 413–415.
- (29) Seuring, J.; Agarwal, S.; Harms, K. *Acta Crystallogr., Sect. E: Struct. Rep. Online* **2011**, *67*, o2170.
- (30) Heilmann, S. M.; Smith, H. K. *J. Appl. Polym. Sci.* **1979**, *24*, 1551–1564.
- (31) Fujishige, S.; Kubota, K.; Ando, I. *J. Phys. Chem.* **1989**, *93*, 3311–3313.
- (32) Winnik, F. M. *Macromolecules* **1990**, *23*, 233–242.
- (33) Kheradmand, H.; Francois, J. *Polymer* **1988**, *29*, 860–870.
- (34) Muller, G. *Polym. Bull.* **1981**, *5*, 31–37.
- (35) van den Bosch, E.; Gielens, C. *Int. J. Biol. Macromol.* **2003**, *32*, 129–138.
- (36) Egger, D. K.; Valentine, J. S. *J. Mol. Biol.* **2001**, *314*, 911–922.
- (37) Lucy, C. A.; MacDonald, A. M.; Glucev, M. D. *J. Chromatogr., A* **2008**, *1184*, 81–105.
- (38) Mitchell, J. B. *Chem. Phys. Lett.* **1991**, *180*, 517–523.
- (39) Wu, C.; Wang, X. *Phys. Rev. Lett.* **1998**, *80*, 4092–4094.

Supporting Information

**Upper Critical Solution Temperature of  
Poly(N-acryloyl glycinamide) in Water: A Concealed Property**

Jan Seuring,<sup>†</sup> Frank M. Bayer,<sup>‡</sup> Klaus Huber,<sup>‡</sup> and Seema Agarwal<sup>\*,†</sup>

<sup>†</sup>Philipps-Universität Marburg, Fachbereich Chemie, Hans-Meerwein Straße, D-35032  
Marburg, Germany

<sup>‡</sup>Universität Paderborn, Department Chemie – Physikalische Chemie, Warburger Str. 100,  
D-33098 Paderborn, Germany

E-mail: agarwal@staff.uni-marburg.de

**Experimental Section**

**Materials**

Azobisisobutyronitrile (Fluka) was recrystallized from ethanol. Acryloyl chloride (96%, Fluka), glycinamide hydrochloride (98%, Acros), acrylic acid (99%, Aldrich) and 2,2'-Azobis[2-(2-imidazolin-2-yl)propane]dihydrochloride (VA-044, Wako) were used as received. 3-(((benzylthio)carbonothioyl)thio)propane-1-sulfonate (BCPS) and dibenzyltrithiocarbonate (DBTC) were synthesized according to the literature.<sup>1,2</sup> Solvents were distilled prior to use. Ultra pure water was obtained from a TKA Micro UV system model 08.1005 (conductivity = 0.06  $\mu\text{S}/\text{cm}$ , filtered through 200 nm filter, UV treated). Phosphate buffered saline was prepared using precalibrated tablets (Aldrich). Human blood serum was freshly obtained from the author (Seuring, male) and used within 8 h.

**Analytical techniques**

<sup>1</sup>H and <sup>13</sup>C NMR spectra were either recorded on a Bruker Avance DRX-500 (500 MHz) or a Bruker Avance 300 A (300 MHz) spectrometer, with D<sub>2</sub>O used as solvent. A trace of methanol was added as a standard for <sup>13</sup>C NMR measurements and it was calibrated to 49.50 ppm.

Conventional differential scanning calorimetry was performed on a Mettler thermal analyzer having a821 DSC module. Indium and zinc standards were used for temperature and

enthalpy calibration of the 821 DSC module. Differential scanning calorimetric (DSC) scans were recorded in nitrogen atmosphere (flow rate = 80 mL/min) at a heating rate of 10 °C/min. The melting temperatures ( $T_m$ ) were determined from the endothermic peak maximum of the first heating cycle.

Ultrasensitive differential scanning calorimetry was performed on a TA Instruments Nano DSC that uses a fixed-in-place platinum capillary with a volume of 300  $\mu$ L. 30 mg of the dry polymer were dissolved in 2970 mg of pure water at 70 °C and sonicated for 1 h in 10 mL glass vial (hydrolytic class III) to obtain a 1 wt% aqueous solution. All samples were equilibrated at 50 °C for 10 min prior to measurements. In the first scan the sample was cooled at a constant rate to 0 °C. At 0 °C the temperature was held for 10 min followed by the heating back to 50 °C at the same rate as the cooling scan. Peak integration was performed using NanoAnalyze 2.1.13 software with a sigmoidal baseline fit.

Turbidity Measurements were performed on a custom-modified Tepper turbidity photometer TP1-D at a wavelength of 670 nm, a cell path length of 10 mm and magnetic stirring. The polymer solutions (above UCST) were filtered through a warm 1.2  $\mu$ m PET syringe filter before measurement. Unless stated otherwise the heating program started at 50 °C from where it was cooled to 3.5 °C at a constant cooling rate of 1.0 °C/min followed by heating back to 50 °C at the same rate. The inflection point of the transmittance curve was considered as cloud point. It was graphically determined by the maximum of the first derivative of the heating or cooling curve, respectively. In the stated temperature range the repeatability and reproducibility of the cloud point determination of a 1.0 wt% poly(NAGA) solution in pure water was very good. The repeatability was  $sd(9 \text{ consecutive runs}) = \pm 0.1$  °C and the reproducibility  $sd(4 \text{ samples}) = \pm 0.2$  °C for both heating and cooling. Sample preparation included four samples from two different polymer batches (two samples each), weighing the polymers into 2 mL polypropylene tubes, dilution with water in order to obtain a polymer content of 1.0 wt%, dissolution at 70 °C (inside the tube) for 60 min with sonication and filtration through a 1.2  $\mu$ m PET-filter into the cuvette.

The potassium content was determined by flame atomic absorption spectroscopy on a Perkin-Elmer 5000 system.

Capillar electrophoresis was performed on an ATI Unicam Crystal CE system model 310 equipped with a UV-absorbance detector TSP Spectra 100. The detection wavelength was set to 210 nm. A fused-silica capillary (TSP050375, 50  $\mu$ m id, 360  $\mu$ m od) was obtained from Polymicro Technologies, Phoenix, AZ, USA. The new capillary was conditioned by rinsing it first with NaOH solution (0.2 mol/L) for 60 min, water for 15 min, and phosphate buffer (10

mmol/L) as separation electrolyte for 15 min. Between runs the capillary was rinsed with separation electrolyte for 5 min. The total length of the capillary was 70 cm and the length to the detector 55 cm. N-acryloyl glycinamide samples were dissolved in diluted phosphate buffer (1 mmol/L) in order to exploit the so called “stacking effect” for a lower detection threshold. Pure acrylic acid and poly(N-acryloyl glycinamide) were dissolved in the undiluted separation electrolyte at concentrations of 1.2 g/L and 1 g/L, respectively. To determine whether poly(N-acryloyl glycinamide) contains charged groups the migration time was compared to the migration time of thiourea as nonionic internal standard.

The slow aggregation of a 1.0 wt% poly(NAGA) solution at 18.5 °C was followed by dynamic light scattering on a Beckman Coulter DelsaNano C particle analyzer at a scattering angle of 165°. The cuvette was rinsed with filtered water (200 nm pore size) and the warm and clear sample was filtered through a warm 1.2 µm PET syringe filter into the cuvette. The autocorrelation function was averaged over 70 runs of 3 seconds each (about 3 min total). Prior to each measurement the optimal measuring position inside sample cuvette was determined. Consequently, highly turbid samples were probed close to the cuvette wall in order to avoid multiple scattering. The average hydrodynamic diameter of aggregates was calculated by the CONTIN method using the software DelsaNano 3.73.

The temperature dependent behavior of a dilute (0.01 wt%) aqueous solution of poly(NAGA) was performed with a model 5000e compact goniometer system (ALV-Laser Vertriebgesellschaft, Germany), which allows the simultaneous recording of static and dynamic light scattering. A Nd:YAG laser (Soliton, Germany) with 300 mW, operating at a wavelength of 532 nm was used as the light source. Cylindrical quartz glass cuvettes with an outer diameter of 20 mm (Hellma, Germany) served as scattering cells. A C25 Haake thermostat was used to set the temperature with a precision of 0.01 °C. The scattering intensity was observed under 13 different scattering angles  $\theta$  in a range of  $30^\circ \leq \theta \leq 150^\circ$ . This corresponds to a  $q$  regime of  $0.0081 \text{ nm}^{-1} \leq q \leq 0.0304 \text{ nm}^{-1}$ . All samples were filtered with a 1.2 µm PET syringe filter (Macherey-Nagel, Germany) prior to the experiment.

For sonication a heated Bandelin Sonorex RK 102 H ultrasound device (HF power = 120 Weff, HF peak performance = 480 W, HF frequency = 35 kHz) was used.

### **Preparation of a solution of poly(NAGA) in human blood serum**

Human blood serum contains about 7 wt% of proteins which would denaturize during the harsh conditions needed for dissolution of poly(NAGA). To avoid this poly(NAGA) was

separately dissolved in pure water ( $c = 1 \text{ wt}\%$ ,  $70 \text{ }^\circ\text{C}$  inside the tube, sonication for 60 min). After dissolution 200  $\mu\text{L}$  of the polymer solution were diluted with 1800  $\mu\text{L}$  of blood serum to obtain a 0.1 wt% solution of poly(NAGA) in 90 vol% human blood serum.

## Syntheses

### **Synthesis of N-acryloyl glycinamide (N-(carbamoylmethyl)prop-2-enamide according to IUPAC nomenclature)**

N-acryloyl glycinamide has been prepared according to the route of Haas and Schuler.<sup>3</sup> However, relevant modifications have been made concerning reagent ratios, workup and purification.

In a 1 L three-necked round-bottom flask equipped with mechanical stirrer glycinamide hydrochloride (23.11 g, 209 mmol) and potassium carbonate (56.7 g, 410 mmol) were dissolved in 125 mL of water. The solution was cooled in an ice bath and acryloyl chloride (16.65 mL, 205 mmol) dissolved in 250 mL of diethylether was added dropwise over 30 min with fast stirring (300 rpm). The suspension was further stirred at RT for 2 h. The diethylether was removed by rotary evaporation at  $35 \text{ }^\circ\text{C}$ . The remaining aqueous phase was lyophilized. The crude brittle solid was extracted with acetone (6 times, 500 mL acetone,  $40 \text{ }^\circ\text{C}$ , stirring for at least 15 min). Insoluble potassium salts were filtered off and the acetone was removed by rotary evaporation at  $35 \text{ }^\circ\text{C}$ . 22.7 g (85%) of crude product were obtained. The crude product was dissolved in an eluent mixture of methanol and dichloromethane ( $v/v = 1/4$ , 600 mL) by heating to reflux once. The solution was filtered to remove polymeric impurities and purified by column chromatography ( $d = 9 \text{ cm}$ , 900 g silica, porosity 60 Angström, 0.063-0.2 mm mesh size, TLC:  $R_f(\text{N-acryloyl glycinamide}) = 0.40$ ;  $R_f(\text{potassium acrylate}) = 0.05$  (not detected on TLC plate)) to obtain 21.3 g (80%) of product which were recrystallized from 240 mL of a mixture of methanol and acetone ( $v/v = 1/2$ ) to yield 15.7 g (57%) and 4.4 g (75% total yield) second crop.

DSC (rate of heating =  $10 \text{ K}\cdot\text{min}^{-1}$ ):  $T_m = 143 \text{ }^\circ\text{C}$ . IR (ATR):  $\nu = 3380$  (m, NH), 3312 (s, NH), 3187 (m, NH), 1652 (vs, C=O), 1621 (vs, C=O), 1551 (vs, NH)  $\text{cm}^{-1}$ .  $^1\text{H}$  NMR (300 MHz,  $\text{D}_2\text{O}$ ):  $\delta = 3.93$  (s, 2H, N-CH<sub>2</sub>-CONH<sub>2</sub>), 5.77 [dd,  $J(\text{doublet } 1) = 2.0 \text{ Hz}$ ,  $J(\text{doublet } 2) = 9.5 \text{ Hz}$ , 1H,  $H_{\text{olef.}}$ ], 6.20 [dd,  $J(\text{doublet } 1) = 2.0 \text{ Hz}$ ,  $J(\text{doublet } 2) = 17.1 \text{ Hz}$ , 1H,  $H_{\text{olef.}}$ ], 6.29 [dd,  $J(\text{doublet } 1) = 9.5 \text{ Hz}$ ,  $J(\text{doublet } 2) = 17.2 \text{ Hz}$ , 1H,  $H_{\text{olef.}}$ ].  $^{13}\text{C}$  NMR (75 MHz,  $\text{D}_2\text{O}$ ):  $\delta =$

42.7 (-N-CH<sub>2</sub>-), 128.8 (C<sub>olef.</sub>), 130.0 (C<sub>olef.</sub>), 169.6 (-CO-), 174.8 (-CO-). Flame emission spectroscopy: potassium content = 4.6 ppm. LC-MS for C<sub>5</sub>H<sub>8</sub>N<sub>2</sub>O<sub>2</sub> MS M<sup>+</sup> Calcd: 129.0585, found: 129.0659.

Further recrystallization of NAGA from isopropanol led to uniform crystals that are suitable for x-ray analysis. The crystal structure was recently published by us.<sup>4</sup>

### **General procedure for the purification and isolation of polymers**

The reaction mixture was quickly cooled to room temperature in an ice bath and the polymer was precipitated in 10 fold excess volume of methanol. It was centrifuged (10 min, 8000 rpm) and after decantation the sediment was thoroughly slurried with methanol using a glass rod. The centrifugation-wash cycles were repeated three times. Subsequently the polymer was dried in the vacuum oven at 70 °C for 24 h. The brittle pellet was grinded to a powder using a glass rod and further dried for another 24 h to obtain a powdery polymer.

For some copolymers that precipitated in more compact particles, e.g. poly(acrylamide-co-acrylonitrile), other isolation techniques like filtration may be more convenient but for comparability reasons it was considered better to use the same work-up procedure for all polymers in this study.

### **Synthesis of homopolymer poly(N-acryloyl glycinamide) with potassium peroxodisulfate as initiator**

This polymer was synthesized in a mixture of water and isopropanol at 50 °C with potassium peroxodisulfate as initiator according to Marstokk et al.<sup>4</sup> Modifications have been made in order to minimize polymer hydrolysis. It was polymerized for 3 h instead of 16 h. After three hours the yield was already 84%.

### **Endgroup functionalization by using chain transfer agents**

In a 25 mL nitrogen NAGA (500 mg, 3.9 mmol, 500 eq) was dissolved in 8.8 mL of DMSO. From a stock solution 1 eq of chain transfer agent dissolved in 100 µL DMSO was added. The solution was degassed by three freeze-pump-thaw-cycles. 100 µL of a separately degassed DMSO solution containing 0.3 eq of initiator were added and the flask was placed into an oil bath which was preheated to 60 °C. It was polymerized for 16 h. The endgroups were analyzed by <sup>1</sup>H NMR spectroscopy. Yields: RAFT\_1 (78%), RAFT\_2 (90%), RAFT\_3 (76%).

## Further Discussion and Supporting Material

### Effect of the heating rate on the turbidity curve of poly(NAGA)

Figure S1 illustrates that the cloud point upon cooling increases at lower cooling rates and approaches the UCST. The cloud point upon heating also increases due to prolonged aging below the UCST.

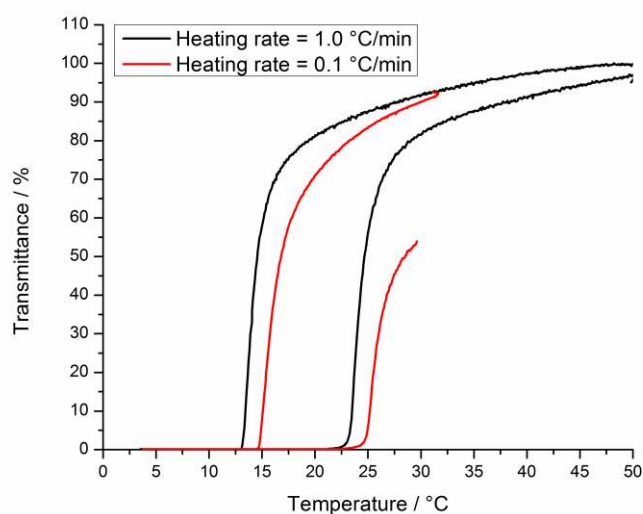


**Figure S1.** Influence of the heating rate on the turbidity curve of a 1 wt% solution of poly(NAGA) in pure water.

### Suppression of the UCST by ionic groups in the polymer

Figure S2 illustrates the influence of the carboxyl content in poly(NAGA) on the cloud point in pure water.



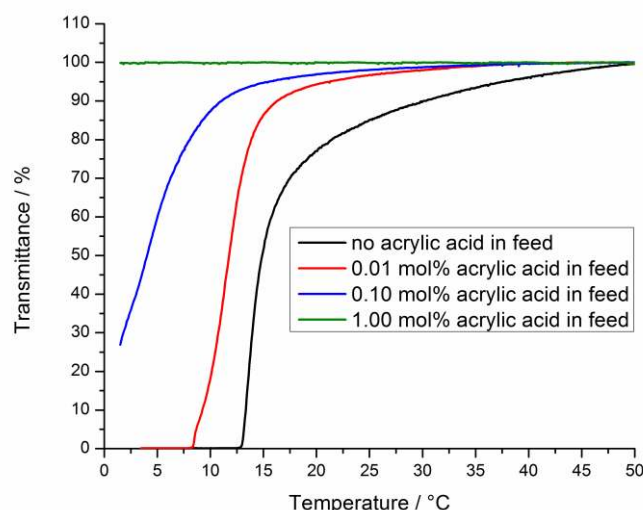


**Figure S2.** Cloud points upon cooling of poly(NAGA)s with different contents of acrylic acid units in the polymer backbone.

#### Endgroup detection by high temperature $^1\text{H}$ NMR spectroscopy

Endgroup functionalization of the samples RAFT\_1, RAFT\_2 and RAFT\_3 was achieved by the use of different chain transfer agents. The average degree of polymerization ( $P_n$ ) was estimated from the integral ratio of the phenylic protons (**a**) compared to the methylene protons adjacent to the nitrogen (**b**) (Figure S3, Figure S4, Figure S5). It was calculated to be 189, 160 and 118 for RAFT\_1, RAFT\_2 and RAFT\_3, respectively. Some of the alpha-chainends were functionalized by the initiator. Since the initiator signals overlap with polymer signals it was not possible to estimate the amount of initiator derived chain ends. Hence, the real  $P_n$  will be slightly lower than calculated. However, for the conclusions drawn it is sufficient to know that the  $P_n$  is in the range of 100 to 200.

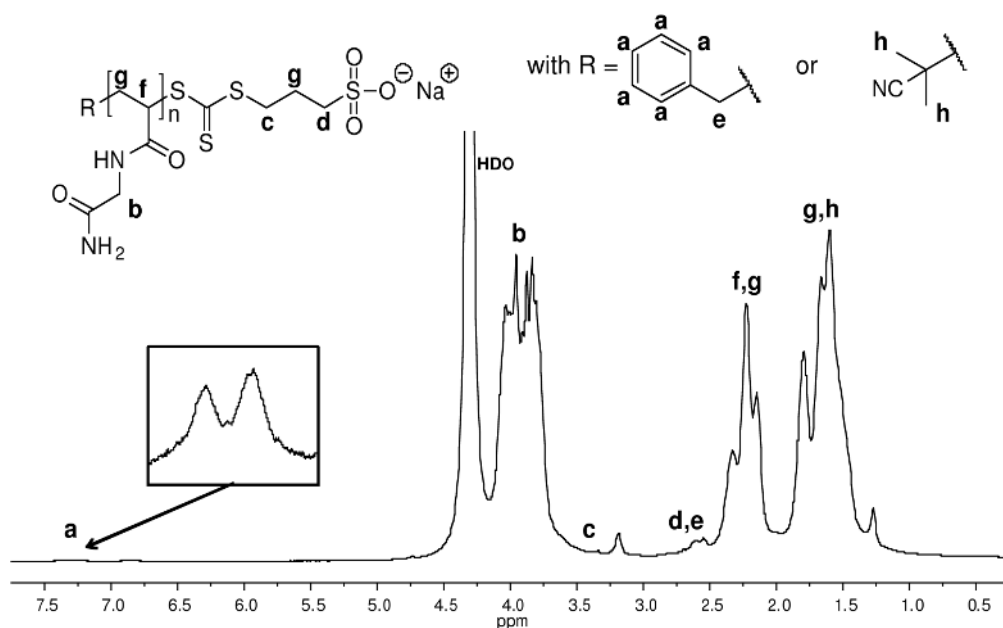


**Figure S3.** 500 MHz <sup>1</sup>H NMR spectrum of poly(N-acryloyl glycinamide) synthesized by the RAFT process using 3-(((benzylthio)carbonothioyl)thio)propane-1-sulfonate as chain transfer agent and the nonionic initiator AIBN. The spectrum was recorded in D<sub>2</sub>O at 70 °C.

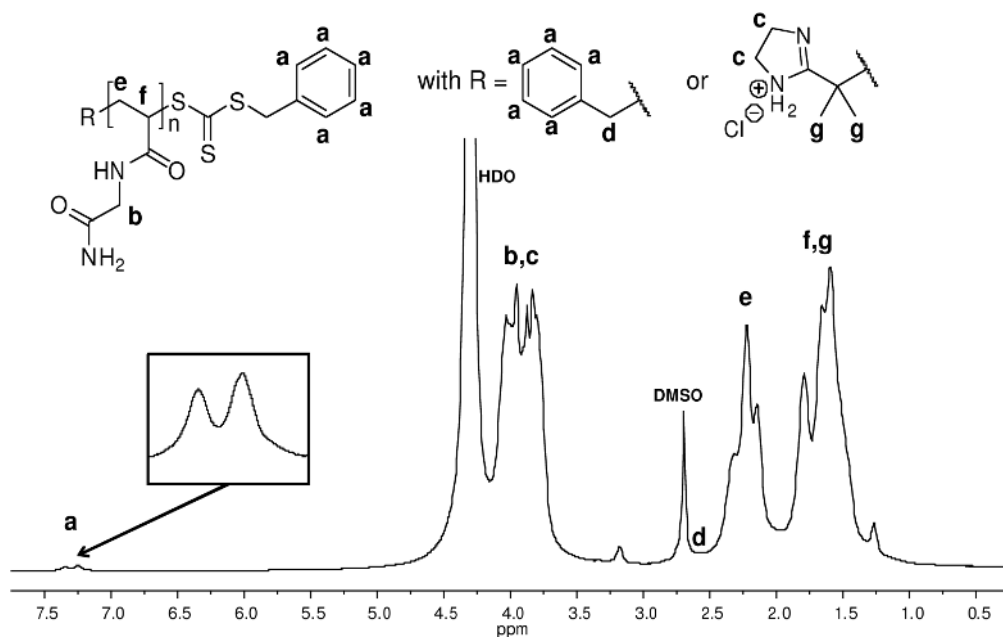


**Figure S4.** 500 MHz <sup>1</sup>H NMR spectrum of poly(N-acryloyl glycinamide) synthesized by the RAFT process using dibenzyltrithiocarbonate as chain transfer agent and the ionic initiator VA-044. The spectrum was recorded in D<sub>2</sub>O at 70 °C.

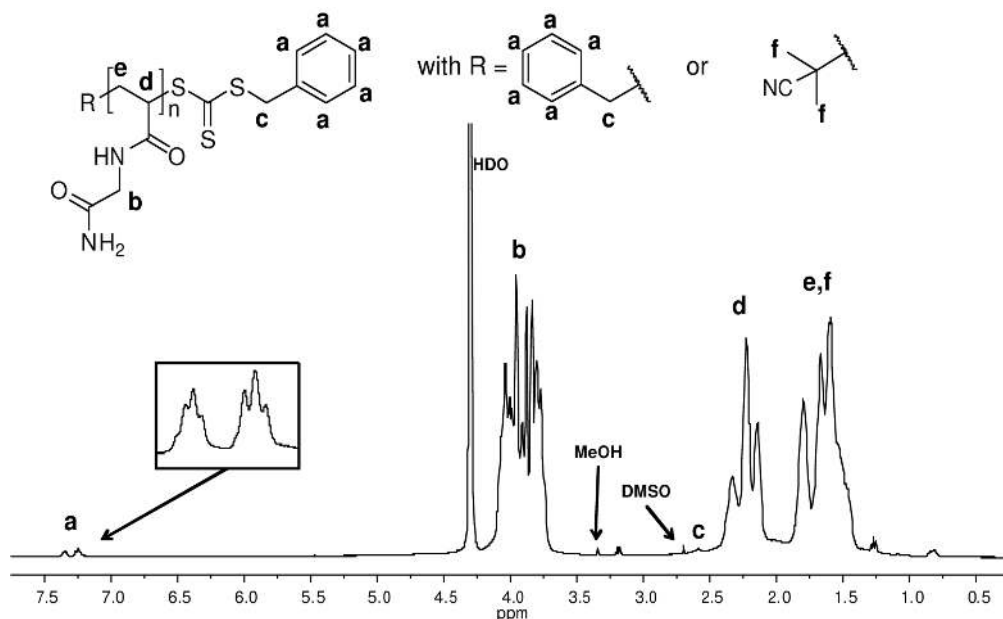


**Figure S5.** 500 MHz  $^1\text{H}$  NMR spectrum of poly(N-acryloyl glycinamide) synthesized by the RAFT process using dibenzyltrithiocarbonate as chain transfer agent and the nonionic initiator AIBN. The spectrum was recorded in  $\text{D}_2\text{O}$  at  $70^\circ\text{C}$ .

### Reversibility of UCST transition as determined by ultrasensitive differential scanning calorimetry

With exception of the runs four to six the  $\Delta H$ -values calculated from the cooling and heating curves are identical, indicating that the transition is fully reversible (Table S1). The discrepancy of run four to six is likely due to the high heating rate which makes it difficult to apply an appropriate baseline. Over nine consecutive DSC runs there is no significant decrease in  $\Delta H$ -values. This is another indication for a good reversibility of the UCST transition. The peak maxima remain constant over the runs 1, 2, 3, 7, 8, and 9. Hysteresis is about  $8^\circ\text{C}$  for these runs. The fact that the peak maxima of run 4 to 6 show a small shift in  $T_{\text{max}}$ -values resulting in a bigger hysteresis of about  $11^\circ\text{C}$  is also due to the higher heating rate which prevents the system from reaching the equilibrium in time.

**Table S1.** Differential scanning microcalorimetry of a 1 wt% solution of poly(NAGA) in pure water. For calculations of the  $\Delta H$ -values in this table the baseline was drawn in the same manner in order to detect whether there is a trend in  $\Delta H$  over a number of runs.

Run	Heating rate / $\text{K}\cdot\text{min}^{-1}$	UCST			
		Cooling		Heating	
		$T_{\text{max}} / ^\circ\text{C}$	$\Delta H / \text{J}\cdot\text{g}^{-1}$	$T_{\text{max}} / ^\circ\text{C}$	$\Delta H / \text{J}\cdot\text{g}^{-1}$
1	1.0	9.5	-0.94	17.3	+0.8
2	1.0	9.4	-0.89	17.5	+0.9
3	1.0	9.2	-0.85	17.3	+0.9
4	2.0	8.4	-0.95	18.8	+0.4
5	2.0	8.2	-0.83	20.6	+0.4
6	2.0	8.4	-0.74	19.3	+0.3
7	0.5	9.7	-0.84	17.9	+0.9
8	0.5	9.5	-0.89	17.8	+1.1
9	0.5	9.5	-0.84	17.7	+1.1

### Supporting information for static and dynamic light scattering

The radii gyration and relative mass values, recorded at variable temperatures have been calculated from the Guinier-plot (Figure S6) using the approximate equations (S2 and S3).<sup>6</sup> In the equations (S2) and (S3),  $K$  is a constant which accounts for the scattering contrast,  $c$  is the polymer concentration in  $\text{g/L}$ ,  $\Delta R$  is the scattering intensity of the dissolved polymers expressed as the Rayleigh ratios,  $M$  is the weight averaged molecular weight of the polymeric particles  $R_g^2$  is the  $z$ -averaged squared radius of gyration of the polymeric particles and  $A_2$  is the second virial coefficient, which had to be neglected in the present case as the system varies with concentration and an extrapolation to  $c = 0$  thus turns out to be impossible. As only relative molecular weights were discussed a specification of the contrast factor  $K$  was not necessary. In the temperature range between 40 and 11  $^\circ\text{C}$  the static light scattering represented by means of a Guinier-plot showed two well separated slopes, each revealing a radius of gyration. The two separable values correspond to two different species, well separated in size. The fraction with the smaller size may be attributed to single coils and the fraction with the larger size to aggregates formed by these coils. At 9.5  $^\circ\text{C}$  the two slopes converge and finally merge at 8  $^\circ\text{C}$ .

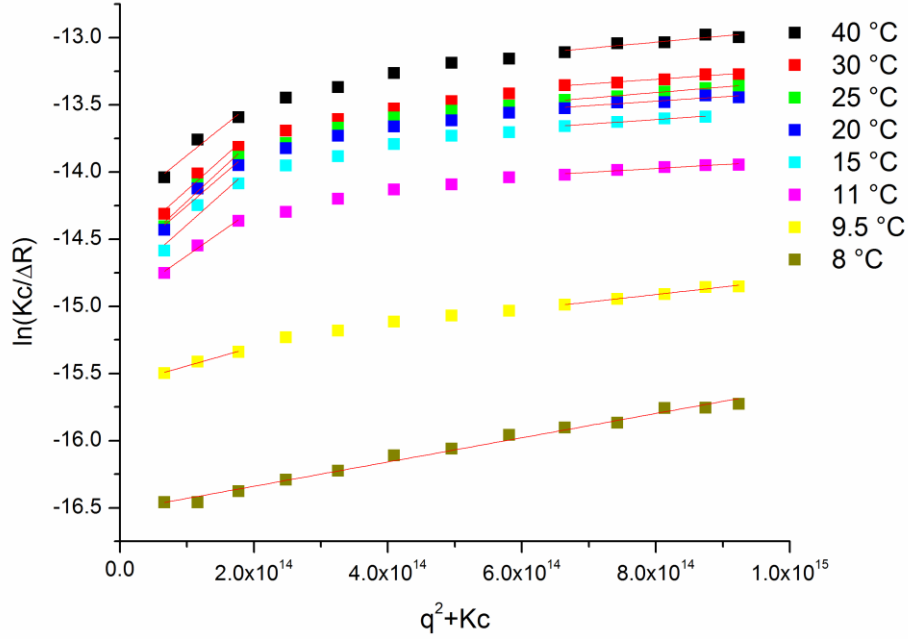


**Figure S6.** Guinier-plot<sup>6</sup> derived from static light scattering at different temperatures. A linear fit to the angular dependence reveals the radius of gyration (from slope) and the relative mass (from intercept with the y-axis).

$$\ln\left(\frac{Kc}{\Delta R}\right) = \frac{\langle R_g^2 \rangle}{3} \cdot (q^2 + Kc) \quad (\text{S2})$$

$$\ln\left(\frac{1}{M}\right) = \lim_{q \rightarrow 0} \left[ \frac{\langle R_g^2 \rangle}{3} \cdot (q^2 + Kc) \right] \quad (\text{S3})$$

To shed further light on this process and its participating species, we performed an inverse Laplace Transformation of the normalized electric field correlation function (S4) from dynamic light scattering at a scattering angle of 30°, where the signal to noise ratio is expected to be good enough. Equation S4 represents the electric field autocorrelation function as superposition of components  $i$  – represented as a sum.

$$g_1(t, q) = \sum_i \gamma_i \exp(-\Gamma_i \cdot t) \quad (\text{S4})$$

The transformation was based on the CONTIN routine<sup>7</sup> representing the inverse relaxation times  $\Gamma$  of the contributing species and their intensity contributions. The average value of  $\Gamma$  for a certain mode with a width of species  $m < j < n$  was calculated using equation S5.

$$\Gamma(t, q) = \sum_{j=m}^n \gamma_j \exp(-\Gamma_j \cdot t) \quad (\text{S5})$$

For the calculation of the intensity contribution of each mode equation S6 has been employed

$$\Delta R_{\Gamma}(q) = f_N \sum_{j=m}^n \gamma_j \quad (\text{S6})$$

with  $f_N$  being a normalization factor fixed to yield a value that represents the overall distribution (S7).

$$\Delta R(q) = f_N \sum_{j=m}^n \gamma_j \quad (\text{S7})$$

## References

- (1) Glatzel, S.; Badi, N.; Päch, M.; Laschewsky, A., Lutz, J. *Chem. Commun.* **2010**, *46*, 4517-4519.
- (2) Wood, M. R.; Duncalf, D. J.; Rannard, S. P.; Perrier, S. *Org. Lett.* **2006**, *8*, 553-556.
- (3) Haas, H. C., Schuler, N. W. *J. Polym. Sci., Part C: Polym. Lett.* **1964**, *2*, 1095-1096.
- (4) Seuring, J.; Agarwal, S., Harms, K. *Acta Crystallogr., Sect. E: Struct. Rep. Online* **2011**, *67*, o2170.
- (5) Marstokk, O.; Nyström, B., Roots, J. *Macromol.* **1998**, *31*, 4205-4212.
- (6) Guinier, A.; Fournet, G. *Small Angle Scattering of X-Rays*; Wiley-VCH: New York, 1955.
- (7) Provencher, S. W. *Comput. Phys.* **1982**, *27*, 213-227.

## Publication 3

### *N*-Acryloyl glycinamide

Jan Seuring, Seema Agarwal, Klaus Harms,  
*Acta Crystallographica Section E* **2011**, E67, o2170.  
doi: 10.1107/S1600536811029758

#### **Author contributions**

Synthesis of *N*-acryloylglycinamide and preparation of crystals was done by Jan Seuring. X-ray crystallography was conducted by Dr. Klaus Harms. The introduction of the manuscript was written by Jan Seuring, analysis and presentation of the crystal structure was done by Dr. Klaus Harms. Prof. Seema Agarwal and Dr. Klaus Harms shared the supervision of this work.

Acta Crystallographica Section E

## Structure Reports

Online

ISSN 1600-5368

## N-Acryloyl glycinamide

Jan Seuring, Seema Agarwal\* and Klaus Harms\*

Philipps Universität Marburg, Fachbereich Chemie, Hans-Meerwein-Strasse,  
D-35032 Marburg, Germany  
Correspondence e-mail: agarwal@staff.uni-marburg.de,  
klaus.harms@chemie.uni-marburg.de

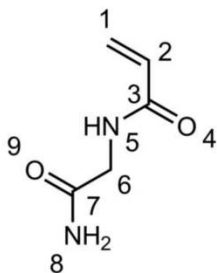
Received 12 July 2011; accepted 22 July 2011

Key indicators: single-crystal X-ray study;  $T = 100$  K; mean  $\sigma(\text{C}-\text{C}) = 0.002$  Å;  
 $R$  factor = 0.032;  $wR$  factor = 0.085; data-to-parameter ratio = 11.8.

The molecule of the title compound [systematic name: *N*-(carbamoylmethyl)prop-2-enamide],  $\text{C}_5\text{H}_8\text{N}_2\text{O}_2$ , which can be radically polymerized to polymers with thermoresponsive behavior in aqueous solution, consists of linked essentially planar acrylamide and amide segments [maximum deviations = 0.054 (1) and 0.009 (1) Å] with an angle of 81.36 (7)° between their mean planes. In the crystal,  $\text{N}-\text{H}\cdots\text{O}$  hydrogen bonding leads to an infinite two-dimensional network along (100).

## Related literature

For the first preparation of the title compound, see: Haas & Schuler (1964). For the properties of polymers of the title compound in aqueous solution, see: Haas *et al.* (1967, 1970*a,b,c,d*); Marstokk *et al.* (1998); Nagaoka *et al.* (2007); Ohnishi *et al.* (2007); Seuring & Agarwal (2010); Glatzel *et al.* (2010). For the structure of the related compound, 2-(2-acrylamidoacetamido)acetic acid monohydrate, see Gao *et al.* (2007).



## Experimental

## Crystal data

$\text{C}_5\text{H}_8\text{N}_2\text{O}_2$   
 $M_r = 128.13$   
Monoclinic,  $P2_1/c$   
 $a = 15.938$  (2) Å  
 $b = 4.8055$  (4) Å  
 $c = 8.4920$  (12) Å  
 $\beta = 98.109$  (11)°

$V = 643.91$  (14) Å<sup>3</sup>  
 $Z = 4$   
Mo  $K\alpha$  radiation  
 $\mu = 0.10$  mm<sup>-1</sup>  
 $T = 100$  K  
 $0.23 \times 0.19 \times 0.09$  mm

## Data collection

Stoe IPDS 2T diffractometer  
Absorption correction: integration  
(*X-RED*; Stoe & Cie, 2006)  
 $T_{\min} = 0.991$ ,  $T_{\max} = 0.997$

6001 measured reflections  
1362 independent reflections  
1065 reflections with  $I > 2\sigma(I)$   
 $R_{\text{int}} = 0.049$

## Refinement

$R[F^2 > 2\sigma(F^2)] = 0.032$   
 $wR(F^2) = 0.085$   
 $S = 0.97$   
1362 reflections

115 parameters  
All H-atom parameters refined  
 $\Delta\rho_{\max} = 0.18$  e Å<sup>-3</sup>  
 $\Delta\rho_{\min} = -0.15$  e Å<sup>-3</sup>

Table 1

Hydrogen-bond geometry (Å, °).

$D-\text{H}\cdots A$	$D-\text{H}$	$\text{H}\cdots A$	$D\cdots A$	$D-\text{H}\cdots A$
$\text{N5}-\text{H5}\cdots\text{O4}^i$	0.850 (19)	2.062 (19)	2.8946 (14)	166.3 (15)
$\text{N8}-\text{H8B}\cdots\text{O9}^{ii}$	0.881 (17)	2.081 (17)	2.9494 (14)	168.2 (15)
$\text{N8}-\text{H8A}\cdots\text{O9}^{iii}$	0.927 (18)	1.971 (18)	2.8855 (14)	168.6 (16)

Symmetry codes: (i)  $x, y + 1, z$ ; (ii)  $-x + 1, y - \frac{1}{2}, -z + \frac{3}{2}$ ; (iii)  $x, -y + \frac{1}{2}, z + \frac{1}{2}$ .

Data collection: *X-AREA* (Stoe & Cie, 2006); cell refinement: *X-AREA*; data reduction: *X-AREA*; program(s) used to solve structure: *SIR92* (Altomare *et al.*, 1994); program(s) used to refine structure: *SHELXL97* (Sheldrick, 2008); molecular graphics: *DIAMOND* (Brandenburg, 2007); software used to prepare material for publication: *publCIF* (Westrip, 2010), *PLATON* (Spek, 2009) and *WinGX* (Farrugia, 1999).

We acknowledge financial support from Philipps-Universität Marburg, Germany.

Supplementary data and figures for this paper are available from the IUCr electronic archives (Reference: SJ5179).

## References

- Altomare, A., Cascarano, G., Giacovazzo, C., Guagliardi, A., Burla, M. C., Polidori, G. & Camalli, M. (1994). *J. Appl. Cryst.* **27**, 435.
- Brandenburg, K. (2007). *DIAMOND*. Crystal Impact GbR, Bonn, Germany.
- Farrugia, L. J. (1999). *J. Appl. Cryst.* **32**, 837–838.
- Gao, X., Wu, C., Wang, H. & Wang, J. (2007). *Acta Cryst.* **E63**, o4580.
- Glatzel, S., Badi, N., Päch, M., Laschewsky, A. & Lutz, J.-F. (2010). *Chem. Commun.* **46**, 4517–4519.
- Haas, H. C., Chiklis, C. K. & Moreau, R. D. (1970*a*). *J. Polym. Sci. Part A Polym. Chem.* **8**, 1131–1145.
- Haas, H. C., MacDonald, R. L. & Schuler, A. N. (1970*b*). *J. Polym. Sci. Part A Polym. Chem.* **8**, 3405–3415.
- Haas, H. C., MacDonald, R. L. & Schuler, A. N. (1970*c*). *J. Polym. Sci. Part A Polym. Chem.* **8**, 1213–1226.
- Haas, H. C., Manning, M. J. & Mach, M. H. (1970*d*). *J. Polym. Sci. Part A Polym. Chem.* **8**, 1725–1730.
- Haas, H. C., Moreau, R. D. & Schuler, N. W. (1967). *J. Polym. Sci. Part B Polym. Phys.* **5**, 915–927.
- Haas, H. C. & Schuler, N. W. (1964). *J. Polym. Sci. Part B Polym. Lett.* **2**, 1095–1096.
- Marstokk, O. B., Nyström, B. & Roots, J. (1998). *Macromolecules*, **31**, 4205–4212.
- Nagaoka, H., Ohnishi, N. & Eguchi, M. (2007). US Patent No. 0203313 A1.
- Ohnishi, N., Furukawa, H., Kataoka, K. & Ueno, K. (2007). US Patent No. 7,195,925 B2.
- Seuring, J. & Agarwal, S. (2010). *Macromol. Chem. Phys.* **211**, 2109–2117.
- Sheldrick, G. M. (2008). *Acta Cryst.* **A64**, 112–122.
- Spek, A. L. (2009). *Acta Cryst.* **D65**, 148–155.
- Stoe & Cie (2006). *X-AREA and X-RED32*. Stoe & Cie, Darmstadt, Germany.
- Westrip, S. P. (2010). *J. Appl. Cryst.* **43**, 920–925.



## **supplementary materials**

*Acta Cryst.* (2011). E67, o2170 [ doi:10.1107/S1600536811029758 ]

## **N-Acryloyl glycinamide**

**J. Seuring, S. Agarwal and K. Harms**

### **Comment**

N-acryloyl glycinamide was first synthesized by Haas and Schuler (1964). It can be polymerized radically to obtain polymers that exhibit thermoresponsive behavior in aqueous solution. The polymers show gelatin-like thermoreversible gelation (Haas & Schuler, 1964; Haas *et al.*, 1967, 1970*a*, 1970*b*, 1970*c*, 1970*d*; Marstokk *et al.*, 1998; Seuring & Agarwal, 2010; Glatzel *et al.*, 2010) and an upper critical solution temperature (Seuring & Agarwal, 2010; Ohnishi *et al.*, 2007; Nagaoka *et al.*, 2007) in water. These phenomena rely on intermolecular hydrogen bonding. Therefore, investigating the intermolecular hydrogen bonding between monomer units in the crystal may contribute to the understanding of interpolymer interactions.

The molecular structure of the title compound shows two planar parts with C1, C2, C3, O4, N5, C6 and C6, C7, N8, O9 in plane. The angle between these mean planes is 81.36 (7)°. In the packing the molecule forms three hydrogen bonds to three different neighbouring molecules. For details see Table 1. The intermolecular N5—H5···O4<sup>i</sup> contacts form an infinite chain in the (0 1 0) direction. Two of these chains are linked *via* N8—H8A···O9<sup>iii</sup> and N8—H8B···O9<sup>ii</sup> interactions, respectively (symmetry codes: (i)  $x, y + 1, z$ ; (ii)  $-x + 1, y - 1/2, -z + 3/2$ ; (iii)  $x, -y + 1/2, z + 1/2$ ). Herein the N8—H8A···O9<sup>iii</sup> hydrogen bonds form a second chain with direction (0 0 1), and hydrogen bonded rings are generated. In conclusion, a two dimensional hydrogen bond network has been formed with the hydrophobic tails of the molecules as border planes.

For the crystal structure of a related compound, 2-(2-acrylamidoacetamido)acetic acid monohydrate, see Gao *et al.* (2007).

### **Experimental**

N-acryloyl glycinamide has been prepared according to the route of Haas and Schuler (1964). However, reagent ratios, workup and purification have been modified as follows.

In a 1 l three-necked round-bottom flask equipped with a mechanical stirrer glycinamide hydrochloride (23.11 g, 209 mmol) and potassium carbonate (56.7 g, 410 mmol) were dissolved in 125 ml of water. The solution was cooled in an ice bath and acryloyl chloride (16.65 ml, 205 mmol) dissolved in 250 ml of diethylether was added dropwise over 30 min with fast stirring (300 rpm). The suspension was further stirred at RT for 2 h. The diethylether was removed by rotary evaporation at 35 °C. The remaining aqueous phase was freeze dried. The crude brittle solid was extracted with acetone (6 times, 500 ml acetone, 40 °C, stirring for at least 15 min). Insoluble potassium salts were filtered off and the acetone was removed by rotary evaporation at 35 °C. 22.7 g (85%) of crude product were obtained. The crude product was dissolved in an eluent mixture of methanol and dichloromethane ( $v/v = 1/4$ , 600 ml) by heating to reflux once. The solution was filtered to remove polymeric impurities and purified by column chromatography ( $d = 9$  cm, 900 g silica, porosity 60 Å, 0.063–0.2 mm mesh size, TLC:  $R_f$ (N-acryloyl glycinamide) = 0.40) to obtain 21.3 g (80%) of product which was recrystallized from 240 ml of a mixture of methanol and acetone ( $v/v = 1/2$ ) to yield 15.3 g (57%) of colorless needle-like crystals.

For obtaining crystals that are suitable for X-ray analysis a small fraction of purified N-acryloyl glycinamide was again recrystallized from a dilute solution in 2-propanol.

## Refinement

All H atoms were located in a difference Fourier map and refined isotropically. The C—H bond distances vary from 0.937 (18) to 0.981 (18), the N—H bond lengths from 0.850 (19) to 0.927 (18) Å.

## Figures

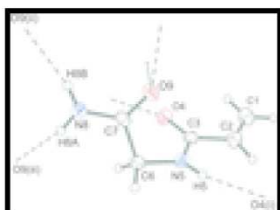


Fig. 1. View of the crystal structure of the title compound. The thermal ellipsoids are drawn at 50% probability level. Dashed lines indicate hydrogen bonding contacts.

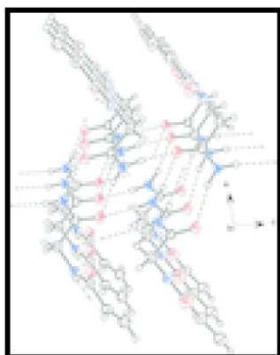


Fig. 2. Two dimensional hydrogen bond network with plane direction (1 0 0). Dashed lines indicate hydrogen bonds.

## *N*-(Carbamoylmethyl)prop-2-enamide

### Crystal data

$C_5H_8N_2O_2$

$M_r = 128.13$

Monoclinic,  $P2_1/c$

Hall symbol:  $-P 2ybc$

$a = 15.938 (2) \text{ \AA}$

$b = 4.8055 (4) \text{ \AA}$

$c = 8.4920 (12) \text{ \AA}$

$\beta = 98.109 (11)^\circ$

$V = 643.91 (14) \text{ \AA}^3$

$Z = 4$

$F(000) = 272$

$D_x = 1.322 \text{ Mg m}^{-3}$

Melting point: 143 K

Mo  $K\alpha$  radiation,  $\lambda = 0.71073 \text{ \AA}$

Cell parameters from 7769 reflections

$\theta = 2.6\text{--}27^\circ$

$\mu = 0.10 \text{ mm}^{-1}$

$T = 100 \text{ K}$

Plate, colourless

$0.23 \times 0.19 \times 0.09 \text{ mm}$

### Data collection

Stoe IPDS 2T  
diffractometer

1362 independent reflections

Radiation source: fine-focus sealed tube graphite	1065 reflections with $I > 2\sigma(I)$
Detector resolution: 6.67 pixels $\text{mm}^{-1}$	$R_{\text{int}} = 0.049$
rotation method scans	$\theta_{\text{max}} = 26.8^\circ$ , $\theta_{\text{min}} = 2.6^\circ$
Absorption correction: integration ( <i>X-RED</i> ; Stoe & Cie, 2006)	$h = -20 \rightarrow 17$
$T_{\text{min}} = 0.991$ , $T_{\text{max}} = 0.997$	$k = -6 \rightarrow 6$
6001 measured reflections	$l = -10 \rightarrow 10$

### Refinement

Refinement on $F^2$	Secondary atom site location: difference Fourier map
Least-squares matrix: full	Hydrogen site location: difference Fourier map
$R[F^2 > 2\sigma(F^2)] = 0.032$	All H-atom parameters refined
$wR(F^2) = 0.085$	$w = 1/[\sigma^2(F_o^2) + (0.0548P)^2]$
$S = 0.97$	where $P = (F_o^2 + 2F_c^2)/3$
1362 reflections	$(\Delta/\sigma)_{\text{max}} < 0.001$
115 parameters	$\Delta\rho_{\text{max}} = 0.18 \text{ e } \text{\AA}^{-3}$
0 restraints	$\Delta\rho_{\text{min}} = -0.15 \text{ e } \text{\AA}^{-3}$
Primary atom site location: structure-invariant direct methods	Extinction correction: <i>SHELXL97</i> (Sheldrick, 2008), $F_c^* = kFc[1 + 0.001xFc^2\lambda^3/\sin(2\theta)]^{-1/4}$
	Extinction coefficient: 0.032 (7)

### Special details

**Experimental.** DSC (rate of heating = 10 K  $\text{min}^{-1}$ ):  $T_m = 143^\circ\text{C}$ . IR (ATR):  $\nu = 3380$  (m, NH), 3312 (s, NH), 3187 (m, NH), 1652 (vs, C=O), 1621 (vs, C=O), 1551 (vs, NH)  $\text{cm}^{-1}$ .  $^1\text{H}$  NMR (300 MHz,  $\text{D}_2\text{O}$ ):  $\delta = 3.93$  (s, 2H, N- $\text{CH}_2$ - $\text{CONH}_2$ ), 5.77 [dd, J(doublet 1) = 2.0 Hz, J(doublet 2) = 9.5 Hz, 1H,  $\text{H}_{\text{olef}}$ ], 6.20 [dd, J(doublet 1) = 2.0 Hz, J(doublet 2) = 17.1 Hz, 1H,  $\text{H}_{\text{olef}}$ ], 6.29 [dd, J(doublet 1) = 9.5 Hz, J(doublet 2) = 17.2 Hz, 1H,  $\text{H}_{\text{olef}}$ ].  $^{13}\text{C}$  NMR (75 MHz,  $\text{D}_2\text{O}$ ):  $\delta = 42.7$  (-N- $\text{CH}_2$ -), 128.8 ( $\text{C}_{\text{olef}}$ ), 130.0 ( $\text{C}_{\text{olef}}$ ), 169.6 (-CO-), 174.8 (CO-). Flame emission spectroscopy: potassium content 5 p.p.m.

**Geometry.** All s.u.'s (except the s.u. in the dihedral angle between two l.s. planes) are estimated using the full covariance matrix. The cell s.u.'s are taken into account individually in the estimation of s.u.'s in distances, angles and torsion angles; correlations between s.u.'s in cell parameters are only used when they are defined by crystal symmetry. An approximate (isotropic) treatment of cell s.u.'s is used for estimating s.u.'s involving l.s. planes.

**Refinement.** Refinement of  $F^2$  against ALL reflections. The weighted  $R$ -factor  $wR$  and goodness of fit  $S$  are based on  $F^2$ , conventional  $R$ -factors  $R$  are based on  $F$ , with  $F$  set to zero for negative  $F^2$ . The threshold expression of  $F^2 > 2\sigma(F^2)$  is used only for calculating  $R$ -factors(gt) *etc.* and is not relevant to the choice of reflections for refinement.  $R$ -factors based on  $F^2$  are statistically about twice as large as those based on  $F$ , and  $R$ -factors based on ALL data will be even larger.

### Fractional atomic coordinates and isotropic or equivalent isotropic displacement parameters ( $\text{\AA}^2$ )

	<i>x</i>	<i>y</i>	<i>z</i>	$U_{\text{iso}}^*/U_{\text{eq}}$
C1	0.91738 (9)	0.4644 (3)	0.66968 (16)	0.0334 (3)
C2	0.87077 (8)	0.6065 (3)	0.75755 (15)	0.0269 (3)

C3	0.80276 (7)	0.4732 (3)	0.83438 (13)	0.0218 (3)
C6	0.68733 (7)	0.5421 (3)	0.98560 (13)	0.0229 (3)
C7	0.61296 (7)	0.4355 (3)	0.86952 (13)	0.0209 (3)
N5	0.75513 (6)	0.6473 (2)	0.90665 (12)	0.0221 (3)
N8	0.56460 (7)	0.2477 (2)	0.92691 (12)	0.0271 (3)
O4	0.79110 (6)	0.21891 (18)	0.83202 (10)	0.0280 (2)
O9	0.59828 (5)	0.52628 (19)	0.73164 (9)	0.0248 (2)
H1A	0.9069 (10)	0.273 (4)	0.6562 (19)	0.038 (4)*
H1B	0.9623 (10)	0.553 (4)	0.620 (2)	0.041 (4)*
H2	0.8770 (10)	0.802 (4)	0.7774 (18)	0.036 (4)*
H5	0.7628 (10)	0.822 (4)	0.8996 (19)	0.034 (4)*
H6A	0.7081 (8)	0.395 (3)	1.0551 (17)	0.023 (3)*
H6B	0.6661 (9)	0.697 (3)	1.0471 (17)	0.025 (3)*
H8A	0.5799 (10)	0.181 (4)	1.029 (2)	0.042 (4)*
H8B	0.5176 (11)	0.194 (4)	0.867 (2)	0.040 (4)*

*Atomic displacement parameters ( $\text{\AA}^2$ )*

	$U^{11}$	$U^{22}$	$U^{33}$	$U^{12}$	$U^{13}$	$U^{23}$
C1	0.0316 (7)	0.0359 (8)	0.0336 (7)	0.0022 (6)	0.0078 (5)	0.0017 (6)
C2	0.0260 (6)	0.0247 (7)	0.0300 (6)	-0.0003 (5)	0.0039 (5)	0.0015 (5)
C3	0.0246 (6)	0.0198 (6)	0.0201 (5)	0.0000 (5)	0.0001 (4)	0.0001 (4)
C6	0.0261 (6)	0.0237 (6)	0.0189 (6)	-0.0002 (5)	0.0028 (4)	-0.0010 (5)
C7	0.0231 (6)	0.0211 (6)	0.0193 (5)	0.0030 (5)	0.0058 (4)	-0.0008 (4)
N5	0.0244 (5)	0.0177 (6)	0.0246 (5)	-0.0012 (4)	0.0040 (4)	-0.0010 (4)
N8	0.0286 (5)	0.0318 (7)	0.0204 (5)	-0.0076 (4)	0.0020 (4)	0.0030 (4)
O4	0.0361 (5)	0.0180 (5)	0.0304 (5)	-0.0008 (4)	0.0065 (4)	-0.0011 (4)
O9	0.0273 (4)	0.0291 (5)	0.0178 (4)	0.0006 (4)	0.0028 (3)	0.0025 (3)

*Geometric parameters ( $\text{\AA}$ ,  $^\circ$ )*

C1—C2	1.3160 (19)	C6—C7	1.5198 (16)
C1—H1A	0.937 (18)	C6—H6A	0.950 (15)
C1—H1B	0.981 (18)	C6—H6B	0.994 (15)
C2—C3	1.4867 (17)	C7—O9	1.2405 (13)
C2—H2	0.956 (18)	C7—N8	1.3235 (16)
C3—O4	1.2360 (15)	N5—H5	0.850 (19)
C3—N5	1.3356 (16)	N8—H8A	0.927 (18)
C6—N5	1.4412 (15)	N8—H8B	0.881 (17)
C2—C1—H1A	118.2 (10)	N5—C6—H6B	108.4 (8)
C2—C1—H1B	121.6 (10)	C7—C6—H6B	107.4 (8)
H1A—C1—H1B	120.2 (15)	H6A—C6—H6B	110.1 (11)
C1—C2—C3	122.01 (13)	O9—C7—N8	123.05 (11)
C1—C2—H2	123.8 (10)	O9—C7—C6	121.30 (11)
C3—C2—H2	114.2 (10)	N8—C7—C6	115.62 (10)
O4—C3—N5	122.19 (11)	C3—N5—C6	120.42 (11)
O4—C3—C2	122.42 (11)	C3—N5—H5	119.2 (11)
N5—C3—C2	115.39 (11)	C6—N5—H5	120.2 (11)

N5—C6—C7	112.57 (9)	C7—N8—H8A	119.6 (11)
N5—C6—H6A	109.3 (8)	C7—N8—H8B	118.6 (11)
C7—C6—H6A	108.9 (8)	H8A—N8—H8B	121.8 (15)
C1—C2—C3—O4	6.58 (19)	O4—C3—N5—C6	-0.03 (16)
C1—C2—C3—N5	-173.59 (12)	C2—C3—N5—C6	-179.87 (10)
N5—C6—C7—O9	-26.19 (17)	C7—C6—N5—C3	-70.81 (14)
N5—C6—C7—N8	155.59 (11)		

*Hydrogen-bond geometry (Å, °)*

<i>D</i> —H $\cdots$ <i>A</i>	<i>D</i> —H	H $\cdots$ <i>A</i>	<i>D</i> $\cdots$ <i>A</i>	<i>D</i> —H $\cdots$ <i>A</i>
N5—H5 $\cdots$ O4 <sup>i</sup>	0.850 (19)	2.062 (19)	2.8946 (14)	166.3 (15)
N8—H8B $\cdots$ O9 <sup>ii</sup>	0.881 (17)	2.081 (17)	2.9494 (14)	168.2 (15)
N8—H8A $\cdots$ O9 <sup>iii</sup>	0.927 (18)	1.971 (18)	2.8855 (14)	168.6 (16)

Symmetry codes: (i)  $x, y+1, z$ ; (ii)  $-x+1, y-1/2, -z+3/2$ ; (iii)  $x, -y+1/2, z+1/2$ .

Fig. 1

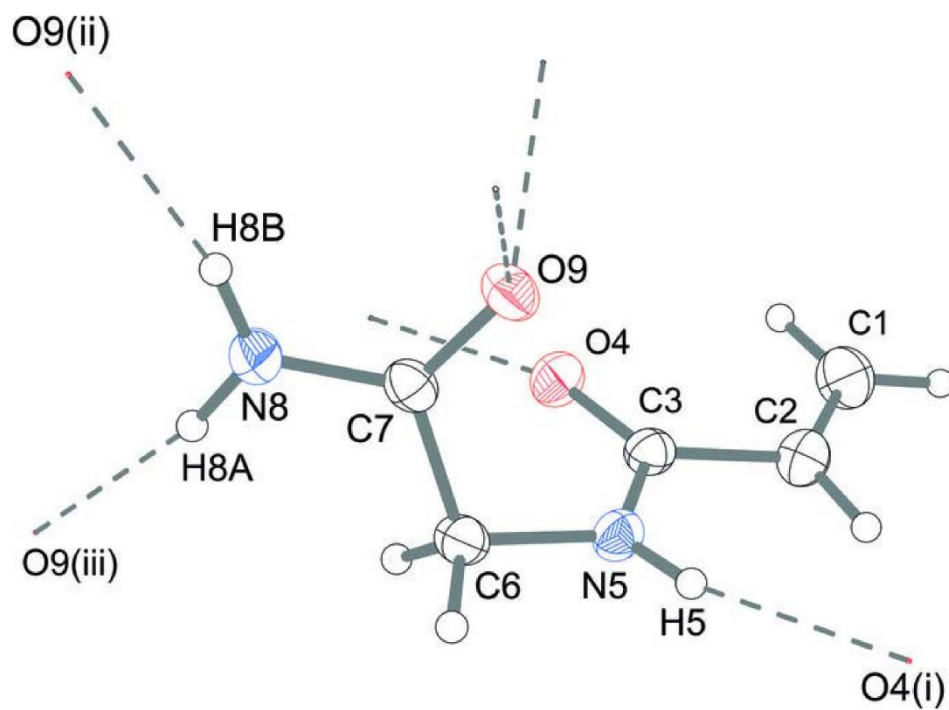
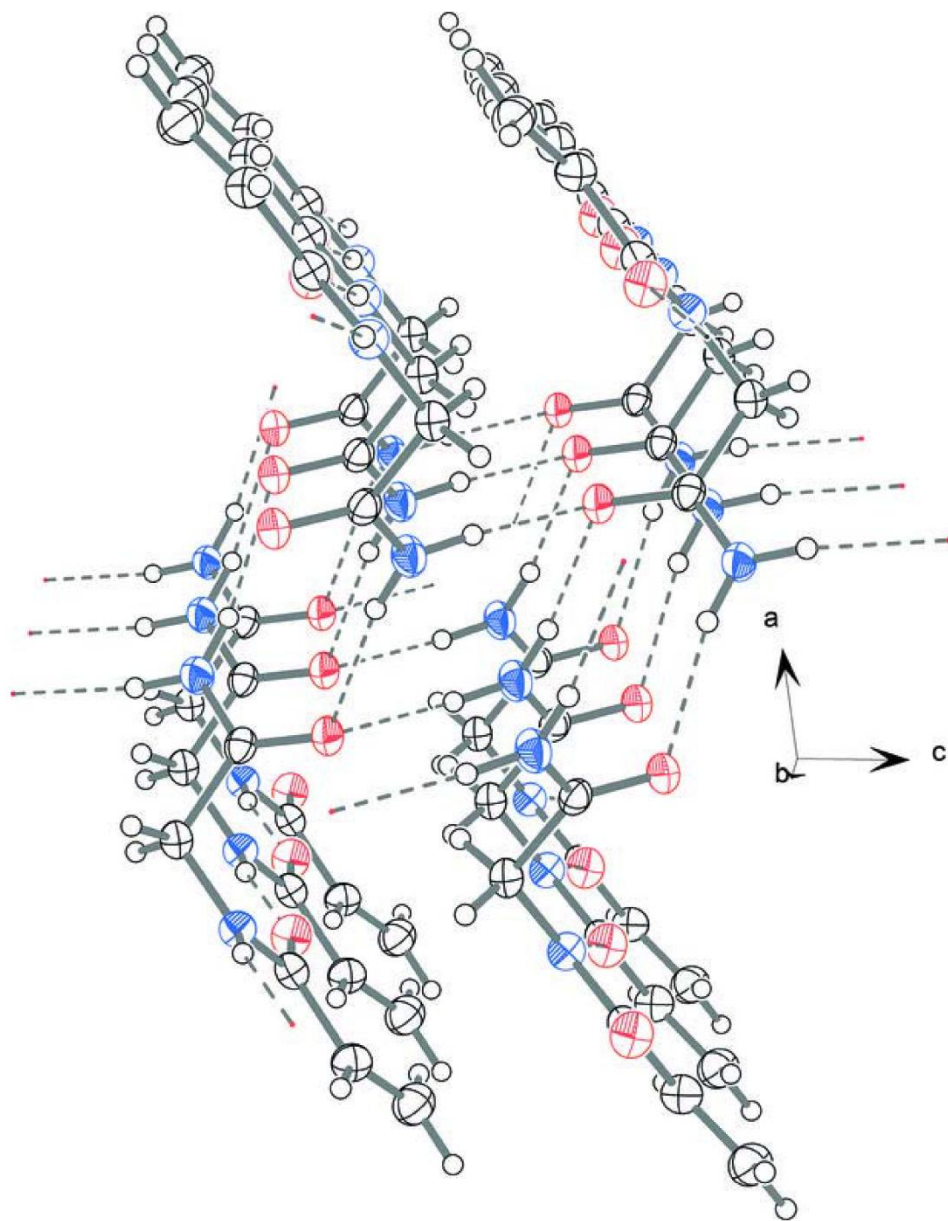


Fig. 2





## Publication 4

### **First Example of a Universal and Cost-Effective Approach: Polymers with Tunable Upper Critical Solution Temperature in Water and Electrolyte Solution**

Jan Seuring, Seema Agarwal, *Macromolecules* **2012**, *45*, 3910-3918.

doi: 10.1021/ma300355k

#### **Author contributions**

Experimental work and writing of the manuscript was done by Jan Seuring. Prof. Seema Agarwal was responsible for supervision and correction of the manuscript.

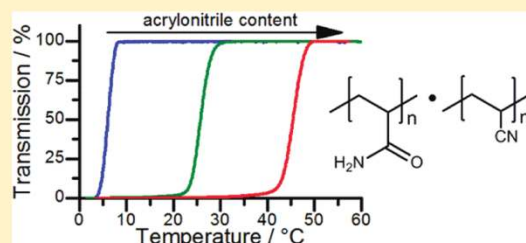
# First Example of a Universal and Cost-Effective Approach: Polymers with Tunable Upper Critical Solution Temperature in Water and Electrolyte Solution

Jan Seuring and Seema Agarwal\*

Department of Chemistry and Scientific Center for Materials Science, Philipps-Universität Marburg, Hans-Meerwein Straße, D-35032 Marburg, Germany

**S** Supporting Information

**ABSTRACT:** We present a powerful universal and versatile approach for the synthesis of polymers that show a UCST in water. Up to now only a few polymers were known that show an upper critical solution temperature (UCST) in water. This study establishes general requirements to obtain polymers with a UCST in water as well as electrolyte solution. It is demonstrated that old homo- and copolymer systems like poly(methacrylamide) and poly(acrylamide-*co*-acrylonitrile) can exhibit a UCST in water and how polymers with a tunable UCST can be synthesized by copolymerization of acrylamide and acrylonitrile, monomers that are industrially produced on large scales. Controlled increase of the UCST by copolymerization of acrylamide with varying amounts of acrylonitrile was shown, and it could be varied between 6 and 60 °C. The hysteresis between the cloud point upon cooling and heating was very small with only 1–2 °C in most cases. The cloud points in pure water were similar to the cloud points measured in phosphate buffered saline. Also, it is possible to prepare highly concentrated thermoresponsive polymer solutions without gel formation.



## 1. INTRODUCTION

Water-soluble thermoresponsive polymers have been subject to extensive research in academic and applied polymer science over the past decades. Because of their drastic property changes (commonly change of hydrophilicity) upon small changes of temperature, numerous so-called “smart” applications have been proposed and demonstrated. Among them are switchable hydrophilic–hydrophobic surfaces,<sup>1</sup> chromatography,<sup>2</sup> temperature-triggered drug release,<sup>3</sup> thermally switchable optical devices,<sup>4</sup> or bioseparation.<sup>5</sup> However, due to the need of special monomers, commercial applications remained restricted to small-scale applications like coatings for cell-culture dishes.

For all applications mentioned above poly(*N*-isopropylacrylamide) (PNiPAAm) was used. This polymer exhibits a lower critical solution temperature (LCST). Although the term water-soluble “thermoresponsive polymer” is often used in a general manner, it is synonym for polymers with LCST since no examples are presented for polymers with an upper critical solution temperature (UCST) in water, a fact supported by a 2010 review and survey on water-soluble thermoresponsive polymers.<sup>6</sup> In order to extend the range of applications, the development of polymers that show a sharp UCST in water is highly desirable.

Very few polymers are known that exhibit a UCST in water under practically relevant conditions, i.e., with phase transitions between 0 and 100 °C at atmospheric pressure (Chart 1). The UCST of all known examples is based on either coulomb interactions or thermally reversible hydrogen bonding. The first

is the case for some zwitterionic polymers like poly(betaines) (1).<sup>7,8</sup>

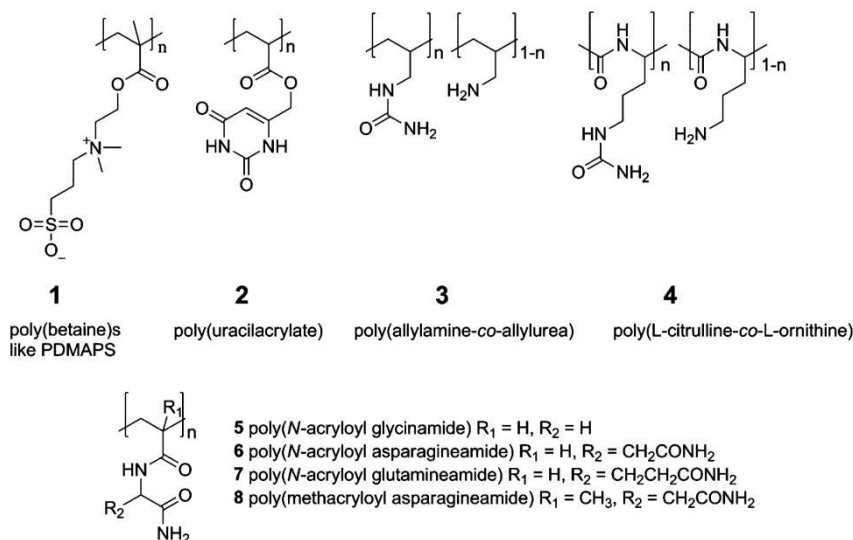
However, coulomb interactions are disturbed in the presence of electrolytes. The very strong sensitivity of the phase transition temperature ( $T_p$ ) to electrolyte concentration and polymer concentration makes them unsuitable for most applications. If the UCST relies on hydrogen bonding, the phase transition temperature is less sensitive to both electrolytes (except specifically hydrogen bond breaking agents like thiocyanates) and polymer concentration. This makes them promising candidates for many fields of applications. All known examples are poly(uracil acrylate) (2),<sup>9</sup> urea-modified polymers (3, 4),<sup>10</sup> and derivatives of poly(*N*-acryloylglycinamide) (poly(NAGA)) (6, 7, 8).<sup>11,12</sup> The UCST transition of poly(uracil acrylate), however, cannot be reversible due to the significant hydrolysis of the ester bond. The resulting carboxyl groups gradually reduce the phase transition temperature until phase separation is completely suppressed. Very recently, Shimada et al. synthesized ureido-modified polymers by a polymer analogue approach which represents an interesting alternative to the vinyl based strategy in our work.<sup>10</sup> The phase transition temperature can be tuned by the degree of ureido functionalization. The residual amine groups are partially protonated at neutral and acidic pH. Toward lower degrees of functionalization the cloud points of these polymers

**Received:** February 22, 2012

**Revised:** April 13, 2012

**Published:** April 26, 2012

Chart 1. All Known Examples of Polymers with a UCST-Type Phase Transition in Water and/or Electrolyte Solution under Practically Relevant Conditions



were increasingly dependent on pH and electrolyte concentration.

Interestingly, poly(NAGA) (5) is known for decades, but the UCST behavior had not been reported. Poly(NAGA) was first synthesized by Haas and Schuler in 1964.<sup>13</sup> They observed a gelatin-like thermoreversible gelation of concentrated aqueous solutions. In further studies they concluded that the gelation is based on physical cross-linking by hydrogen bonding.<sup>14–18</sup> These conclusions were later confirmed by others using Raman spectroscopy and light scattering.<sup>19,20</sup> However, in the aforementioned publications no UCST behavior was reported until we reported in 2010.<sup>21</sup> It has been failed to notice the UCST in the past because ionic groups have been introduced unintentionally by either acrylate impurities in the monomer, hydrolysis of the polymer side chains, and/or usage of ionic initiators or chain transfer agents. Proof for these conclusions along with a procedure to obtain stable aqueous solutions of nonionic poly(NAGA) so that the UCST behavior can be exploited in pure water as well as in physiological milieu was recently published by us.<sup>22</sup> This report also included a basic study of the phase separation by turbidity measurements and preliminary results of ultrasensitive differential scanning calorimetry and light scattering. The phase transition temperature of a 1 wt % aqueous solution of poly(NAGA) is about 22 °C. For many applications a higher phase transition temperature is needed, e.g., around 37 °C for biomedical applications. Thus, it is desirable to gain control over the phase transition temperature so it can be tailored to suit a given application. In the present study it is shown how the phase transition temperature can be increased in a controlled manner by copolymerization with hydrophobic comonomers. This possibility was briefly mentioned in a patent of Ohnishi et al.<sup>23</sup> although no examples have been shown so far. The hypothesis that  $T_p$  can be increased by copolymerization with hydrophobic comonomers was based on the following assumption. Polymers dissolve in a solvent when the Gibbs energy of dissolution ( $\Delta G$ ) is negative. Polymer solutions show a UCST when both the enthalpy of dissolution ( $\Delta H$ ) and entropy of dissolution ( $\Delta S$ ) are positive. At the phase transition temperature ( $T_p$ ) dissolution and phase separation are in equilibrium; i.e.,  $\Delta G$  is zero and, therefore,  $T_p = \Delta H/\Delta S$ . Thus,  $T_p$  can be increased by

increasing the ratio  $\Delta H/\Delta S$  which can be achieved by either increasing  $\Delta H$  or decreasing  $\Delta S$ . In the case of UCST polymers that rely on reversible hydrogen bonding  $\Delta H$  is governed by the positive contribution of polymer–polymer hydrogen bonds. We would expect that the value of  $\Delta H$  is not greatly influenced by the copolymerization with minor quantities of hydrophobic comonomers. Few polymer–polymer hydrogen bonds would be sacrificed; some additional polymer–polymer van der Waals interactions would be added. Crucial influence is expected on  $\Delta S$  because of the strong hydrophobic effect. The hydration shell of hydrophobic polymer segments is highly ordered because the lack of options for hydrogen bonds to the polymer decreases the number of orientations water molecules can occupy. This represents a strong negative contribution to the entropy of dissolution and diminishes the overall value of  $\Delta S$ , which leads to an increase of the  $\Delta H/\Delta S$  ratio, hence  $T_p$ .

The concept was demonstrated using butyl acrylate (BA) or styrene (St) as comonomers. However, both monomers had disadvantages. BA is hydrolytically unstable, and styrene shows adverse copolymerization behavior with acrylamides. For this reasons acrylonitrile (AN) was chosen as a third comonomer and copolymerized with commercially available acrylamide (AAm). For polyacrylamide we assumed a theoretical UCST below 0 °C. Thus, it could be shown that the concept how to increase the UCST in a controlled manner can be transferred to completely new copolymer systems. By combining these and former results, it was possible to establish general requirements that must be fulfilled to obtain polymers with a tunable UCST in water as well as electrolyte solution. The synthesis of thermoresponsive poly(methacrylamide) (PMAAm) gave further support to this theory. The resulting polymers were analyzed by NMR, gel permeation chromatography, and differential scanning calorimetry. The phase transition behavior was studied by turbidimetry. In this study the development of a versatile and cost-effective approach for the synthesis of water-soluble thermoresponsive polymers was also one of the key issues.

## 2. EXPERIMENTAL SECTION

**2.1. Materials.** Azobis(isobutyronitrile) (Fluka) was recrystallized from ethanol. Acrylamide (Fisher Scientific,  $\geq 99.9\%$ , electrophoresis

grade,  $\leq 0.002\%$  acrylic acid), acrylonitrile (Acros,  $>99\%$ ), butyl acrylate (Aldrich,  $>99\%$ ), and methacrylamide (Aldrich,  $98\%$ ) were used as received. Acrylate free *N*-acryloyl glycinamide ( $T_m(\text{DSC}) = 143\text{ }^\circ\text{C}$ , residual potassium  $<5\text{ ppm}$ ) was synthesized according to a recently published procedure.<sup>22</sup> Styrene (BASF) and solvents were distilled prior to use. Ultrapure water was obtained from a TKA Micro UV system model 08.1005 (conductivity =  $0.06\text{ }\mu\text{S/cm}$ , filtered through  $200\text{ nm}$  filter, UV treated). Phosphate buffered saline was prepared using precalibrated tablets (Aldrich).

**2.2. Analytical Techniques.**  $^1\text{H}$  spectra were recorded on a Bruker Avance DRX-500 (500 MHz) either in  $\text{D}_2\text{O}$  at  $80\text{ }^\circ\text{C}$  or  $\text{DMSO-}d_6$  at  $100\text{ }^\circ\text{C}$ .

For thermal characterization Mettler thermal analyzers having 851 TG and 821 DSC modules were utilized. Indium and zinc standards were used for temperature and enthalpy calibration of the 821 DSC module. Differential scanning calorimetric (DSC) scans were recorded in nitrogen atmosphere (flow rate =  $80\text{ mL/min}$ ) at a heating rate of  $10\text{ }^\circ\text{C/min}$ . The glass transition temperature ( $T_g$ ) was taken as the inflection point of the observed shift in the baseline of the second heating cycle of a DSC scan. Thermal stability was determined by thermogravimetric analysis (TGA) in nitrogen atmosphere (flow rate =  $50\text{ mL/min}$ ) using powdered samples. A heating rate of  $10\text{ }^\circ\text{C/min}$  and a sample size of  $5\text{--}20\text{ mg}$  were used in each experiment.

Turbidity measurements were performed on a custom-modified Tepper turbidity photometer TP1-D at a wavelength of  $670\text{ nm}$ , a cell path length of  $10\text{ mm}$ , and magnetic stirring. The heating program started at high temperature, and it was cooled to  $3.5\text{ }^\circ\text{C}$  at a constant cooling rate of  $1.0\text{ }^\circ\text{C/min}$  followed by heating back to the starting temperature at the same rate. The inflection point of the transmittance curve was considered as cloud point. It was graphically determined by the maximum of the first derivative of the heating or cooling curve, respectively. For sample preparation the polymers were weighed into  $2\text{ mL}$  polypropylene tubes. The dissolution parameters for poly(BA-*co*-NAGA) and poly(NAGA-*co*-St) were  $c = 1.0\text{ wt } \%$  in phosphate buffered saline (PBS, pH 7.4),  $T = 70\text{ }^\circ\text{C}$  inside the tubes,  $t = 20\text{ min}$ , sonication. The dissolution parameters for poly(AAm-*co*-AN) were  $c = 1.0\text{ wt } \%$  in either phosphate buffered saline (pH 7.4) or pure water,  $T = 70\text{ }^\circ\text{C}$  inside the tubes,  $t = 5\text{ min}$ , no sonication. The dissolution parameters for poly(methacrylamide) were  $c = 1.0\text{ wt } \%$  in pure water,  $T = 70\text{ }^\circ\text{C}$  inside the tubes,  $t = 15\text{ min}$ , sonication. The hot samples were quickly filtered through a preheated  $1.2\text{ }\mu\text{m}$  PET filter into the cuvette.

For sonication a heated Bandelin Sonorex RK 102 H ultrasound device (HF power =  $120\text{ W}$ , HF peak performance =  $480\text{ W}$ , HF frequency =  $35\text{ kHz}$ ) was used.

IR spectroscopy was performed on a Digilab Excalibur Series FTS 3000 spectrometer by the attenuated total reflection technique employing a ZnSe crystal. The spectra were analyzed using the software Win-IR Pro 3.3. The copolymer composition for poly(AAm-*co*-AN)s was determined by IR spectroscopy using a calibration curve (Supporting Information). Standards were thoroughly mixed using very fine powders of polyacrylamide and polyacrylonitrile homopolymers. Both samples and calibration standards were measured nine times with 32 scans per measurement. The error bars display the standard deviation of the determined peak ratios.

To detect possible micelle formation, dynamic light scattering was performed on a Beckman Coulter DelsaNano C particle analyzer at a scattering angle of  $165^\circ$ . The cuvette was rinsed with filtered water ( $200\text{ nm}$  pore size), and the warm and clear sample was filtered through a warm  $1.2\text{ }\mu\text{m}$  PET syringe filter into the cuvette. The autocorrelation function was averaged over 120 runs of  $3\text{ s}$  each.

Molecular weights and molecular weight distributions of the polymers were determined by gel permeation chromatography (GPC) with dimethyl sulfoxide as eluent. Two PLGel Mixed-D columns (particle size  $5\text{ }\mu\text{m}$ , dimension  $7.5\text{ mm} \times 300\text{ mm}$ ) calibrated with narrow Pullulan standards and a differential refractive index detector were employed. The flow rate was  $1.0\text{ mL/min}$ . The molecular weight distributions were calculated using the software Cirrus 3.3.

**2.3. Syntheses.** **2.3. General Procedure for the Purification and Isolation of Polymers.** The reaction mixture was quickly cooled to room temperature in an ice bath, and the polymer was precipitated in 10-fold excess volume of methanol. It was centrifuged ( $10\text{ min}$ ,  $8000\text{ rpm}$ ), and after decantation the sediment was thoroughly slurried with methanol using a glass rod. The centrifugation–wash cycles were repeated three times. Subsequently, the polymer was dried in the vacuum oven at  $70\text{ }^\circ\text{C}$  for  $24\text{ h}$ . The brittle pellet was grinded to a powder using a glass rod and further dried for another  $24\text{ h}$  to obtain a powdery white polymer. For some copolymers that precipitated in more compact particles, e.g., poly(AAm-*co*-AN), other isolation techniques like filtration may be more convenient, but for comparability reasons it was considered better to use the same workup procedure for all polymers in this study.

**Synthesis of Poly(BA-*co*-NAGA) of Various Compositions.** Example for a butyl acrylate feed content of  $9.0\text{ mol } \%$ .  $22.6\text{ mg}$  ( $0.18\text{ mmol}$ ) of butyl acrylate was weighed into a  $25\text{ mL}$  nitrogen flask and dissolved in  $8.9\text{ mL}$  of distilled DMSO. In order to obtain the desired butyl acrylate feed content of  $9.0\text{ mol } \%$ ,  $228\text{ mg}$  of *N*-acryloyl glycinamide ( $1.78\text{ mmol}$ ) was added. The solution was degassed by three freeze–pump–thaw cycles. Then  $100\text{ }\mu\text{L}$  of a separately degassed initiator solution containing  $1.6\text{ mg}$  of AIBN ( $9.8\text{ }\mu\text{mol}$ ) was added, and the flask was placed into an oil bath preheated to  $70\text{ }^\circ\text{C}$ . It was polymerized for  $19\text{ h}$ . The total monomer concentration was  $0.22\text{ M}$  and the total volume  $9.0\text{ mL}$  for all reactions. The yield was between  $87$  and  $93\%$  for all reactions. Further

**Table 1. Controlled Increase of the Cloud Points by Copolymerization of NAGA with Varying Amounts of BA<sup>a</sup>**

entry	BA in feed/ mol %	BA in polymer <sup>b</sup> / mol %	$T_g/^\circ\text{C}$	cloud point/ $^\circ\text{C}$	
				cooling	heating
1	0	0	186	10.2	21.3
2	3.0	3.4	182	9.1	19.5
3	6.0	6.2	179	7.0	18.2
4	9.0	10.0	170	6.5	17.8
5	10.0	12.0	167	8.2 (8.8)	19.8 (18.1)
6	12.5	14.1	166	14.5 (15.0)	27.4 (26.3)
7	13.3	14.4	167	17.5	30.3
8	14.2	16.0	165	27.5	41.3
9	15.0	17.7	164	45.9 <sup>c</sup>	n.d. <sup>c</sup>
10	17.5	18.5	162	55.9 <sup>c</sup>	n.d. <sup>c</sup>
11	20.0	21.2	155	57.5 <sup>c</sup>	n.d. <sup>c</sup>

<sup>a</sup>The cloud points were measured at polymer concentrations of  $1.0\text{ wt } \%$  in PBS or water (values in parentheses). <sup>b</sup>Calculated from NMR spectra; error margin =  $\pm 0.5\%$ . <sup>c</sup>Because of the high cloud points of these samples, the turbidity measurements were started at  $75\text{ }^\circ\text{C}$ . The samples flocculated very fast instead of forming milky dispersions. Therefore, the cloud point upon cooling was defined as the temperature where the transmission had fallen to  $80\%$ . For the same reasons the cloud point upon heating could not be determined. Also, it should be noted that the repeatability of these turbidity measurements was not good because of the significant hydrolysis of butyl acrylate at temperatures  $>50\text{ }^\circ\text{C}$ .

details are given in Table 1.  $^1\text{H}$  NMR ( $500\text{ MHz}$ ,  $\text{D}_2\text{O}$ ,  $T = 80\text{ }^\circ\text{C}$ , the residual solvent peak was calibrated to  $\delta = 4.20$ )  $\delta/\text{ppm} = 0.82$  ( $-\text{CH}_3$ ),  $1.26$  ( $-\text{CH}_2-\text{CH}_3$ ),  $1.3\text{--}1.9$  (polymer backbone,  $-\text{CH}_2-$ ;  $\text{O}-\text{CH}_2-\text{CH}_2-$ ),  $1.9\text{--}2.4$  (polymer backbone,  $-\text{CH}-$ ),  $3.6\text{--}4.05$  ( $\text{NH}-\text{CH}_2-\text{CONH}_2$ ;  $\text{O}-\text{CH}_2-$ ). TGA for sample with BA content of  $21.3\text{ mol } \%$  (rate of heating =  $10\text{ K/min}$ );  $T(5\%) = 289\text{ }^\circ\text{C}$ .

**Synthesis of Poly(NAGA-*co*-St) of Various Compositions.** Example for a styrene feed content of  $9.0\text{ mol } \%$ .  $18.9\text{ mg}$  ( $0.18\text{ mmol}$ ) of styrene was weighed into a  $10\text{ mL}$  Schlenk flask and dissolved in  $1.9$

Table 2. Increase of the Cloud Points by Copolymerization of NAGA with Varying Amounts of Styrene<sup>a</sup>

entry	St in feed/mol %	St in polymer <sup>b</sup> /mol %	c(total monomer)/M	time/h	yield/%	M <sub>n</sub> /Da	PDI	T <sub>g</sub> /°C	cloud point/°C	
									cooling	heating
1	0	0	0.22	2	86	34700 <sup>f</sup>	2.03 <sup>f</sup>	186	10.2	21.3
2	5.0	5.0	1.0	19	90	31 500	3.82 <sup>g</sup>	183	12	23
3	10.0 <sup>c</sup>	10.7	2.0	20.5	95	37 300	4.53 <sup>g</sup>	180	18	30
4	10.0	12.0	2.0	8.0	75	40 900	2.80 <sup>g</sup>	182	20 <sup>d</sup>	31 <sup>d</sup>
5	10.0	13.5	2.0	6.5	64	37 700	2.77	180	56 <sup>d</sup>	61 <sup>d</sup>
6	10.0	14.3	2.0	5.5	51	40 500	2.36	179	62 <sup>d</sup>	63 <sup>d</sup>
7	10.0	17.8	2.0	4.0	39	39 300	2.04	179	65	65
8	10.0	20.6	2.0	1.0	17	46 700	2.07	179	85 ± 5 <sup>e</sup>	85 ± 5 <sup>e</sup>
9	10.0	23.7	2.0	0.5	8	n.d.	n.d.	n.d.	insoluble	insoluble
10	11.7	17.4	1.0	19	50	22 400	2.01	181	55.5	58
11	13.3	18.7	1.0	19	49	21 600	1.91	178	70.1	70
12	15.0	16.2	2.0	19	88	29 900	2.28	179	85 ± 5 <sup>e</sup>	85 ± 5 <sup>e</sup>
13	17.5	26.8	1.0	19	34	18 700	1.90	174	insoluble	insoluble

<sup>a</sup>The cloud points were measured at polymer concentrations of 1.0 wt % in PBS. <sup>b</sup>Calculated from NMR spectra; error margin = ±0.5%. <sup>c</sup>This sample formed gel during polymerization. <sup>d</sup>Very broad transition (see Figure 5). <sup>e</sup>This cloud point was determined visually because it was beyond the heating limit of the turbidity photometer. <sup>f</sup>After 30 min of sonication at 60 °C in DMSO with 0.1 M KSCN as eluent (see Supporting Information). <sup>g</sup>Bimodal molecular weight distribution.

Table 3. Controlled Increase of the Cloud Points by Copolymerization of Acryamide with Varying Amounts of Acrylonitrile<sup>a</sup>

entry	AN in feed/mol %	AN in polymer <sup>b</sup> /mol %	yield/%	M <sub>n</sub> /Da	PDI	T <sub>g</sub> /°C	cloud point/°C	
							cooling	heating
1	0	0	49	38 600	3.32	193	soluble	soluble
2	11.8	7.6 ± 1.3	48	39 900	2.49	172	6.4	7.4
3	12.1	8.1 ± 1.4	49	43 900	2.33	172	16.4	20.6
4	13.4	10.4 ± 1.0	50	40 700	2.19	169	19.6	21.3
5	15.0	12.6 ± 1.2	51	35 200	2.69	168	25.4 (28.9)	28.3 (32.5)
6	15.7	13.5 ± 1.4	45	33 900	2.84	167	30.9 (32.9)	33.2 (35.1)
7	16.6	14.3 ± 1.1	62	32 800	2.88	161	45.4	47.6
8	18.4	15.6 ± 1.4	50	35 900	2.75	160	51.0	52.4
9	22.0	16.9 ± 1.1	44	37 200	2.92	158	56.7	57
10	30.0	19.7 ± 1.3	42	32 100	2.83	150	insoluble	insoluble

<sup>a</sup>The cloud points were measured at polymer concentrations of 1.0 wt % in PBS or water (values in parentheses). <sup>b</sup>Determined by IR spectroscopy using a calibration curve.

mL of distilled DMSO. In order to obtain the desired styrene feed content of 9.0 mol %, 235 mg of *N*-acryloylglycinamide (1.83 mmol) was added. The solution was degassed by three freeze–pump–thaw cycles. Then 100 μL of a separately degassed initiator solution containing 1.7 mg of AIBN (10 μmol) was added, and the flask was placed into an oil bath preheated to 70 °C. The total monomer concentration was either 1.0 or 2.0 M with total volumes of 2.0 or 1.0 mL, respectively. Further details are given in Table 2. <sup>1</sup>H NMR (500 MHz, D<sub>2</sub>O, T = 80 °C, the residual solvent peak was calibrated to δ = 4.20) δ/ppm = 1.1–1.9 (polymer backbone, –CH<sub>2</sub>–), 1.9–2.6 (polymer backbone, –CH–), 3.33–4.1 (NH–CH<sub>2</sub>–CONH<sub>2</sub>), 6.7–7.5 (phenylic protons, –C<sub>6</sub>H<sub>5</sub>). TGA for polymer with a styrene content of 26.8 mol % (rate of heating = 10 K/min); T(5%) = 310 °C.

**Synthesis of Poly(AAm-co-AN) of Various Compositions.** Example for an acrylonitrile feed content of 15 mol %. 48 mg (0.9 mmol) of acrylonitrile was weighed into a 10 mL nitrogen flask and dissolved in 5.5 mL of distilled DMSO. In order to obtain the desired acrylonitrile feed content of 15 mol % 363 mg of acrylamide (5.1 mmol) was added. The solution was degassed by three freeze–pump–thaw cycles. Then 500 μL of a separately degassed initiator solution containing 4.9 mg of AIBN (0.03 mmol) was added, and the flask was placed into an oil bath preheated to 60 °C. It was polymerized for 5.5 h. The total monomer concentration was 1.0 M and the total volume 6.0 mL for all reactions. Further details are given in Table 3. <sup>1</sup>H NMR (500 MHz, DMSO-*d*<sub>6</sub>, T = 100 °C, the solvent signal was calibrated to 2.50 ppm) δ/ppm = 1.2–2.0 (polymer backbone, –CH<sub>2</sub>–), 2.0–2.7 (polymer backbone, –CH–CONH<sub>2</sub>), 2.3–3.1 (polymer backbone, –CH–CN),

6.7 (–NH<sub>2</sub>). IR (FT-ATR): ν = 3650–3050 (mb, NH), 3000–2850 (w, CH), 2242 (w, CN), 1659 (vs, CO), 1450 (m), 1413 (m), 1348 (m), 1312 (m), 1118 (w) cm<sup>–1</sup>. TGA for a polymer with a acrylonitrile content of 19.7 ± 1.3 mol % (rate of heating = 10 K/min); T(5%) = 274 °C.

**Synthesis of Poly(methacrylamide).** In a 10 mL nitrogen flask 510 mg (6.0 mmol) of methacrylamide was dissolved in 5.5 mL of distilled DMSO. The solution was degassed by three freeze–pump–thaw cycles. Then 500 μL of a separately degassed initiator solution containing 4.92 mg of AIBN (0.03 mmol) was added, and the flask was placed into an oil bath preheated to 60 °C. After about 30 min the solution became turbid. It was polymerized for 5.5 h to yield 143 mg (28%) of polymer. After workup the polymer could not be redissolved in DMSO for GPC analysis. TGA (rate of heating = 10 K/min); T(5%) = 291 °C. DSC (rate of heating = 10 K/min) no transitions from 25 to 255 °C.

### 3. RESULTS AND DISCUSSION

**3.1. Copolymers of NAGA and Butyl Acrylate.** Free radical copolymerization of *N*-acryloylglycinamide and butyl acrylate has been performed with different feed ratios (Table 1). The amount of butyl acrylate repeating units in the purified polymer was determined by NMR spectroscopy in D<sub>2</sub>O at 80 °C (Figure S1, Supporting Information). As expected, the acrylate content in the polymer increased with increasing feed

content. Determination of the molecular weight by GPC was not trivial because of aggregate formation (described in detail in Supporting Information). However, one can state that the number-average molecular weight is greater than 10 kDa for all copolymers. The dependence of the phase transition temperature from the BA content is a complex function (Table 1 and Figure 1).

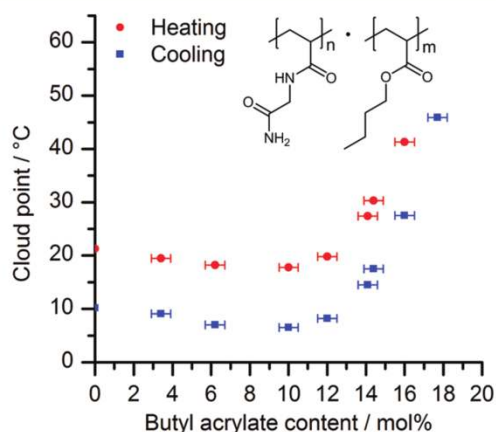


Figure 1. Cloud points of 1.0 wt % solutions of poly(BA-co-NAGA)s as a function of butyl acrylate content.

Interestingly, copolymers with BA contents lower than 11 mol % showed lower cloud points than the poly(NAGA) homopolymer with a local minimum at 9 mol % BA. From 11 mol % upward the cloud points increased rapidly. The cloud points between 6 and about 60 °C could be achieved just by changing the amount of BA in copolymers. It is worth noticing that all of these copolymers dissolved much faster than the poly(NAGA) homopolymer. Also, samples with a higher BA content flocculated very fast upon cooling. The particle sizes increased rapidly to millimeter-sized flakes which heavily affected the turbidity measurement. When the speed of particle growth is high compared to the increase of particle numbers, the turbidity curve becomes broad and noisy (even decreasing turbidity upon cooling can occur) despite a probably sharp UCST transition (Figure 2).

Unfortunately, the repeatability of these turbidity measurements was not good because of the hydrolysis of butyl acrylate

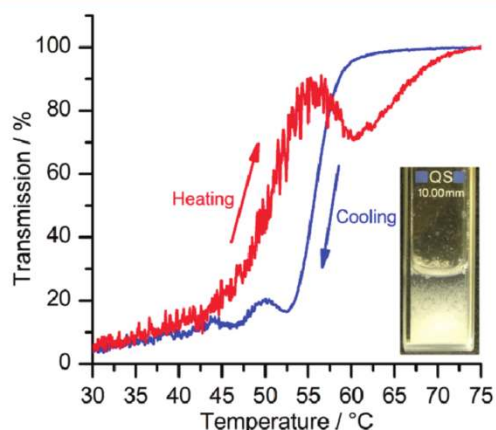


Figure 2. Turbidity curve of a 1.0 wt % solution of poly(BA-co-NAGA) in phosphate buffered saline. The polymer contains 21 mol % butyl acrylate.

at temperatures >50 °C. At temperatures higher than 50 °C hydrolysis of BA caused a gradual decrease of the cloud point from one turbidity measurement to the next (Figure 3).

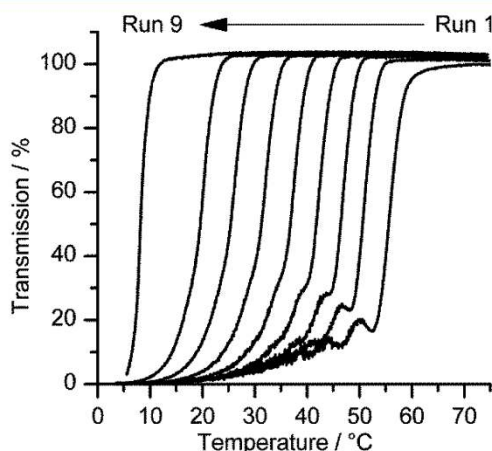


Figure 3. Nine consecutive turbidity cooling curves of poly(BA-co-NAGA) with a butyl acrylate content of 21 mol %. It was measured in PBS. The measurement range was 75–3.5 °C, and the heating rate was 1.0 °C/min.

Recently, it has been shown by us for the poly(NAGA) homopolymer that prolonged heating at high temperatures causes a gradual decrease of the cloud point.<sup>22</sup> This is due to the ionic nature of acrylic acid units in the polymer backbone that are a consequence of the hydrolysis of amide bonds of the NAGA units. Since esters are more susceptible to hydrolysis than amides, the reversibility of the UCST transition of poly(BA-co-NAGA)s was not good. The fact that the cloud point was affected even in phosphate buffered saline shows that the amount of carboxyl groups must exceed 1 mol %, thus affecting the hydrophilic–lipophilic balance. The occurrence of hydrolysis was confirmed by the detection of *n*-butanol by GCMS (as trimethylsilyl derivative with  $m/z = 146$ ).

**3.2. Copolymers of NAGA and Styrene.** In order to obtain polymers that are more stable to hydrolysis, styrene was chosen as a nonhydrolyzable hydrophobic comonomer. Free radical polymerization of NAGA with styrene has been performed with different feed ratios (Table 2). The yield decreased with increasing styrene in the feed. To obtain good yields with higher styrene contents, the monomer concentration had to be increased. The amount of styrene repeating units in the purified polymer was determined by NMR spectroscopy in D<sub>2</sub>O at 80 °C or DMSO-*d*<sub>6</sub> at 100 °C for higher styrene contents (Figures S2 and S3, Supporting Information). As anticipated, these copolymers showed an increased phase transition temperature with good repeatability (Figure 4). The cloud point increased with increase in the amount of styrene in the copolymers until about 15 mol %; further increase in the amount of styrene in copolymers led to water insoluble polymers.

However, with batchwise conventional free radical copolymerization it was more difficult to target a specific cloud point value, and it depended upon conversion (entries 3–9, Table 2). The turbidity curves became very broad at high conversions, making it difficult to determine a distinct cloud point (Figure 5).

In a set of experiments the styrene feed content was 10.0 mol %, and the polymerization was stopped at different conversions.

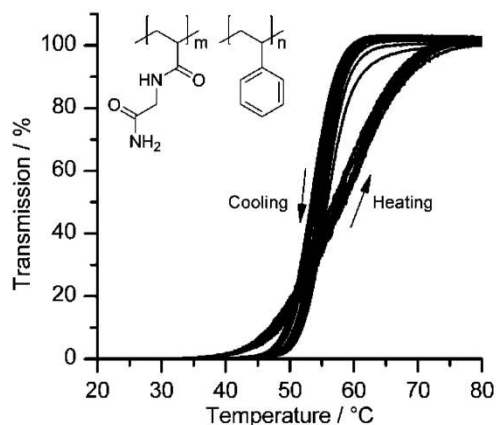


**Figure 4.** Nine consecutive turbidity curves of a 1.0 wt % solution of poly(NAGA-co-St) in PBS with a styrene content of 17.4 mol % in the polymer.

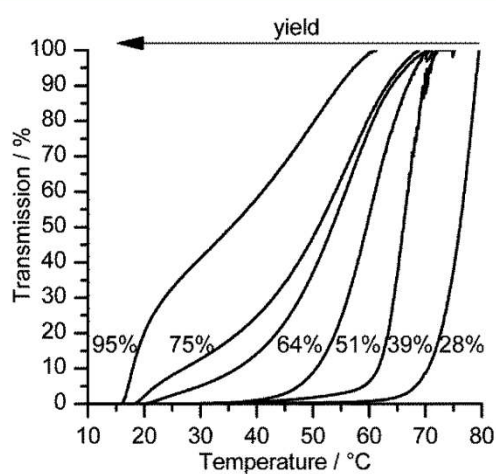


**Figure 5.** Turbidity cooling curves of 1.0 wt % solutions of poly(NAGA-co-St) in PBS. The polymers were polymerized to different conversions while using the same styrene feed content of 10.0 mol %.

At low conversions the styrene content in the polymer was much higher than in the feed content, e.g., 23.7 mol % at 8% yield, and the resulting polymer was not soluble in water or phosphate buffer at any temperature. This must be attributed to a considerable difference in copolymerization parameters under the reaction conditions used in this work. A determination of the parameters for this particular system would be beyond the scope of this work and of limited use since it has been shown for acrylamides that the copolymerization parameters depend strongly on the copolymerization conditions.<sup>24</sup> The polymers obtained at higher yields (17–95%) showed not only temperature-dependent solubility (cloud point) but a systematic trend. The cloud point decreased with increase in conversion (entries 3–9, Table 2). This was correlated to the increased amount of NAGA in the copolymers with increase in yield; at 95% yield the NAGA:styrene ratio was around 89:11 as compared to NAGA:styrene ratio of around 79:21 for 17% yield. Free radical polymerization of such systems leads to a heterogeneous mixture of polymer compositions at high yields, each individual composition having a different cloud point. This explains why the turbidity curves became broad at high yields. It is also apparent that the polydispersity index determined by GPC increased with polymerization yield. This may be

explained by the changing kinetics during polymerization due to the constantly changing feed composition and by the fact that different copolymer compositions may show different hydrodynamic diameters despite having the same molecular weight.

**3.3. Copolymers of Acrylamide and Acrylonitrile.** By combination of previous and the present results, it was possible to develop a universal approach for the synthesis of polymers with a tunable UCST in water and electrolyte solution. Such polymers are obtained when the following requirements are fulfilled:

1. The polymer must contain groups that are capable of forming reversible hydrogen bonds. Poly(uracil acrylate) (Chart 1) possesses the DNA base uracil which is the obvious standard example for reversible hydrogen bonding. The eye-catching similarity of all other known UCST polymers was that they all featured primary amide groups (Chart 1; the primary amide group can be considered to be a part of the ureido group). Thus, the primary amide group appears to be the key functionality for the reversible hydrogen bonding.

2. The content of ionic groups must be as low as possible. Previous studies revealed that the content of ionic groups must be kept to a minimum.<sup>22</sup> This is achieved by the use of monomers that are free of acrylic acid or acrylate and by avoiding ionic initiators as well as ionic chain transfer agents. During processing and application no hydrolysis of amide or ester bonds must occur because it will result in carboxyl groups which are in equilibrium with negatively charged carboxylate. Hence, the monomers used should be of high hydrolytic stability.

3. The hydrophilic–lipophilic balance of the polymer has to be tuned so that the phase transition temperature is in the desired temperature range. In the present study it was proven that copolymerization of NAGA with the hydrophobic comonomers butyl acrylate and styrene is a method to increase the phase transition temperature. In order to obtain a reversible and sharp phase transition, the comonomer should be hydrolytically stable and the copolymerization should proceed in a way that provides a narrow distribution of copolymer compositions.

To test this hypothesis, copolymers from acrylamide and acrylonitrile have been synthesized in various compositions (Table 3). A nonionic copolymer from those comonomers should fulfill all of the above requirements. Acrylamide is the simplest monomer that features a primary amide group. Interpenetrating networks of polyacrylamide and poly(acrylic acid) and cross-linked gels of copolymers from acrylamide and acrylic acid have been shown to exhibit a thermoresponsive volume phase transition,<sup>25,26</sup> but non-cross-linked copolymers have not been reported to show a UCST. The fact that polyacrylamide can form intra- and intermolecular hydrogen bonds is long known<sup>27–29</sup> so it should fulfill the first requirement. The polymerization was performed in dimethyl sulfoxide with the nonionic initiator AIBN. The obtained polymers were nonionic and fulfill the second requirement. The homopolymer, however, did not show a UCST because it is too hydrophilic. For adjusting the hydrophilic–lipophilic balance acrylonitrile was chosen as a comonomer because it is hydrophobic, hydrolytically stable and has got similar *Q* and *e* values like acrylamide allowing a statistical free radical copolymerization (third requirement). Different copolymers were made by changing molar ratio of the two comonomers in the feed and structural characterization was carried out using

$^1\text{H}$  NMR (Figure S4, Supporting Information). A sharp UCST-type phase transition could be observed for the copolymers. The phase transition temperature could be tuned as a function of copolymer composition (Table 3 and Figure 6).

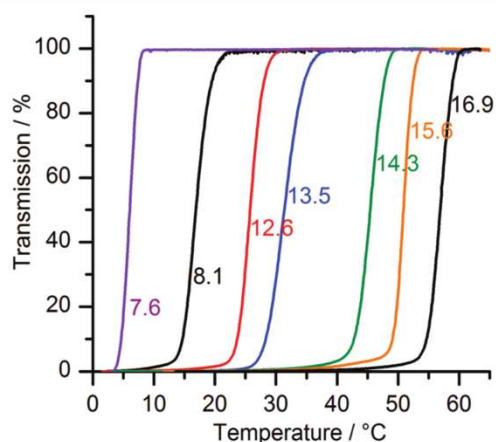


**Figure 6.** Turbidity cooling curves of poly(AAm-co-AN)s with different copolymer compositions. The numbers state the acrylonitrile content in mol % (error 1.0–1.4 mol %).

Compared to the homo- and copolymers using NAGA, the initial dissolution of the dry polymers was very fast. All samples could be dissolved at 70 °C within 5 min without sonication. Also, at a heating rate of 1.0 °C/min the hysteresis between the cloud point upon cooling and heating was very small with only 1–2 °C in most cases (Figure 7). Above the phase transition

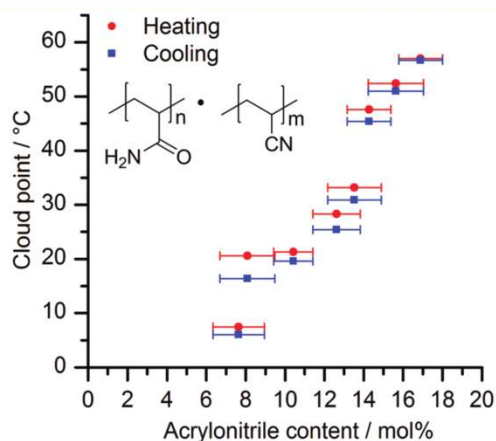


**Figure 7.** Cloud points of 1.0 wt % solutions in PBS of poly(AAm-co-AN)s as a function of acrylonitrile content.

temperature the solutions were optically transparent and did not self-organize to micelles or other well-defined supra-molecular structures. This was proven by the insufficient scattering of light. Dynamic light scattering was performed at 50 °C on a 2 mg/mL aqueous solution of sample 4 of Table 3. The scattering intensity at full laser power (30 mW) and a scattering angle of 165° was too low for a meaningful data analysis.

The hydrolytic stability was excellent. Nine consecutive turbidity measurements exactly coincided (Figure 8). The cloud points in pure water were similar to the cloud points measured in PBS, i.e., only 2–3 °C higher. Also, it was possible to prepare highly concentrated thermoresponsive polymer solutions with-

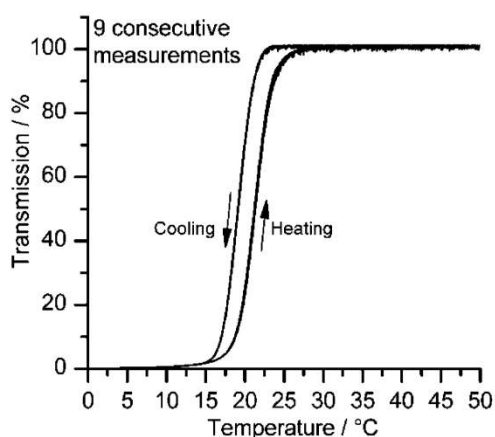


**Figure 8.** Nine consecutive turbidity curves of a 1.0 wt % solution of poly(AAm-co-AN) in PBS with acrylonitrile content of 10.4 mol % in the polymer.

out gel formation. Figure 9 shows how the cloud points of poly(AAm-co-AN) with an acrylonitrile content of 7.6 mol %

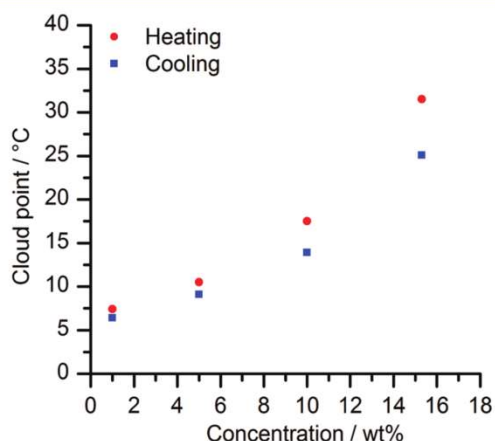


**Figure 9.** Cloud points of poly(AAm-co-AN) solutions in PBS as a function of polymer concentration. The acrylonitrile content of the polymer was 7.6 ± 1.3 mol %.

(Table 3, entry 2) increased with concentration up to 15.3 wt %. The curvature of this partial cloud point curve is opposite than observed for most UCST-type phase separations. We cannot yet explain this observation but point out that deviations from the typical curvature can be caused by the molecular weight distribution<sup>30</sup> or the concentration dependence of the interaction parameter.<sup>31</sup> The combination of intra- and interpolymer hydrogen bonding in competition to water certainly causes a complex concentration dependence of the interaction parameter.

**3.4. Synthesis of Thermoresponsive Poly-(methacrylamide).** In 1957, Silberberg et al. conducted temperature-dependent light scattering experiments on dilute aqueous poly(methacrylamide) (PMAAm) solutions.<sup>32</sup> These results indicated a theta point in water at 6 °C and suggested the presence of intra- and intermolecular hydrogen bonds. Viscosity studies of Eliassaf gave further support for the formation of hydrogen bonds.<sup>33</sup> Despite these hints, PMAAm has never been shown to exhibit a UCST-type phase separation. It is important to note that Silberberg and Eliassaf used potassium persulfate as an ionic initiator. It is very likely that



this was one of the causes that prevented them to observe phase separation upon cooling. Judging PMAAm according to the requirements for the synthesis of UCST polymers that were established in section 3.2 revealed: First, its primary amide group should provide for reversible hydrogen bonding. Second, the additional methyl group at the polymer backbone makes PMAAm more hydrophobic than polyacrylamide so the hydrophilic–lipophilic balance may already be suitable for a phase transition temperature between 0 and 100 °C. Third, the polymer may exhibit a UCST when it is nonionic. These assumptions proved to be correct. PMAAm showed indeed a UCST in water when the nonionic initiator AIBN was used for polymerization in DMSO. At a concentration of 1.0 wt % it showed a phase transition temperature of about 40.5 °C upon cooling and 57 °C upon heating in pure water (Figure 10). The phase transition was very slow causing a strong hysteresis of the turbidity curve.

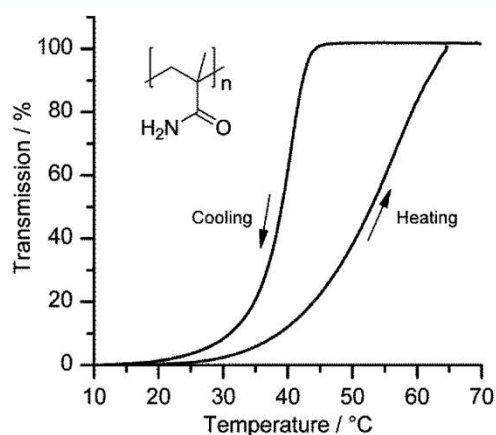


**Figure 10.** Turbidity curve of a 1.0 wt % aqueous solution of poly(methacrylamide). The heating rate was 1.0 °C/min.

**3.5. Hysteresis.** From the sum of all cloud point measurements it can be concluded that the hysteresis depends mainly on four factors: (1) the chain mobility originating from the specific polymer structure, (2) the chain mobility at the phase transition temperature, (3) aging below the phase transition temperature in the case of UCST-type phase transitions, and (4) the polymer concentration. Concerning the first point, a similar observation has been made for the LCST polymers PNiPAAm and PNiPMAAm.<sup>34</sup> PNiPAAm shows almost no hysteresis, whereas PNiPMAAm shows a pronounced one. This can be explained by the lower chain mobility caused by the methyl group in the polymer backbone. The glass transition temperature of the dry polymer is a good measure for the chain mobility. In analogy to PNiPAAm ( $T_g = 130\text{--}140\text{ °C}$ )<sup>35,36</sup> and PNiPMAAm ( $T_g = 176\text{ °C}$ )<sup>37</sup> the glass transition temperatures of PAAm and its copolymers with acrylonitrile are much lower than the  $T_g$  of PMAAm. The  $T_g$  of PMMAm was determined to be higher than 255 °C (decomposition at higher temperatures), whereas the  $T_g$ s of PAAm and its copolymers are 193 °C and lower (Table 3). This explains why the cloud point hysteresis of polymers with similar phase transition temperature increases in the order PNiPAAm < poly(AAm-*co*-AN) < poly(NAGA-*co*-styrene)  $\approx$  PNiPMAAm < PMAAm. Of course, the speed of equilibration is strongly dependent on the temperature. Hence, it is a general trend that hysteresis increases with decreasing phase transition

temperature (Table 2). There may be exceptions from this trend (e.g., entries 2 and 3 from Table 3). This is due to the fact that at a heating/cooling rate of 1.0 °C/min a polymer with a very low cloud point has very little time to age below its phase transition temperature during the measurement cycle. The influence of aging on the hysteresis has been demonstrated before.<sup>22</sup>

#### 4. CONCLUSION

This study presented a powerful universal and versatile approach for the synthesis of polymers that show a UCST in water. It was demonstrated that old homo- and copolymer systems like poly(methacrylamide) and poly(acrylamide-*co*-acrylonitrile) can exhibit a UCST in water and how polymers with a tunable UCST can be synthesized by copolymerization of acrylamide and acrylonitrile, monomers that are industrially produced on large scales. The fact that the transition can be exploited from dilute to concentrated solutions and in the presence of electrolytes promises a broad applicability. Those polymers can be designed from scratch by obeying the following rules: (1) The polymer must contain groups that are capable of forming reversible hydrogen bonds. (2) The content of ionic groups must be as low as possible. (3) The hydrophilic–lipophilic balance of the polymer has to be tuned so that the phase transition temperature is in the desired temperature range.

Adhering to these basic principles makes the use of special monomers unnecessary. It was demonstrated how polymers with a tunable UCST can be synthesized by copolymerization of acrylamide and acrylonitrile, monomers that are industrially produced on large scales. For the first time the cost-effective synthesis would allow large-scale applications of thermoresponsive polymers like in wastewater treatment or similar applications.

#### ■ ASSOCIATED CONTENT

##### 📄 Supporting Information

Spectroscopic data, additional figures, and discussion of molecular weight determination by GPC. This material is available free of charge via the Internet at <http://pubs.acs.org>.

#### ■ AUTHOR INFORMATION

##### Corresponding Author

\*E-mail: [agarwal@staff.uni-marburg.de](mailto:agarwal@staff.uni-marburg.de).

##### Notes

The authors declare no competing financial interest.

#### ■ ACKNOWLEDGMENTS

The authors thank the Philipps-University of Marburg for financial support and Ziyin Fan for carrying out few reactions during the work.

#### ■ ABBREVIATIONS

AAm, acrylamide; AN, acrylonitrile; BA, butyl acrylate; DSC, differential scanning calorimetry; LCST, lower critical solution temperature; NAGA, *N*-acryloylglycinamide; PBS, phosphate buffered saline; PMAAm, poly(methacrylamide); PNiPAAm, poly(*N*-isopropylacrylamide); PNiPMAAm, poly(*N*-isopropylmethacrylamide); St, styrene; TGA, thermal gravimetric analysis; UCST, upper critical solution temperature.

■ REFERENCES

- (1) Yamada, N.; Okano, T.; Sakai, H.; Karikusa, F.; Sawasaki, Y.; Sakurai, Y. *Macromol. Rapid Commun.* **1990**, *11*, 571–576.
- (2) Kanazawa, H.; Yamamoto, K.; Matsushima, Y. *Anal. Chem.* **1996**, *68*, 100–105.
- (3) Bae, Y. H.; Okano, T.; Hsu, R.; Kim, S. W. *Macromol. Rapid Commun.* **1987**, *8*, 481–485.
- (4) Asher, S. A.; Weissman, J. M.; Sunkura, H. B. Thermally switchable optical devices, U.S. Patent 6,165,389, March 10, 2000.
- (5) Chen, J. P.; Hoffman, A. S. *Biomaterials.* **1990**, *11*, 631–634.
- (6) Aseyev, V.; Tenhu, H.; Winnik, F. M. *Adv. Polym. Sci.* **2010**, *242*, 29–89.
- (7) Kudaibergenov, S.; Jaeger, W.; Laschewsky, A. *Adv. Polym. Sci.* **2006**, *201*, 157–224.
- (8) Chen, L.; Honma, Y.; Mizutani, T.; Liaw, D.; Gong, J. P.; Osada, Y. *Polymer* **2000**, *41*, 141–147.
- (9) Aoki, T.; Nakamura, K.; Sanui, K.; Ogata, N.; Kikuchi, A.; Okano, T.; Sakurai, Y. *Proc. Int. Symp. Controlled Release Bioact. Mater.* **1996**, *23*, 767.
- (10) Shimada, N.; Ino, H.; Maie, K.; Nakayama, M.; Kano, A.; Maruyama, A. *Biomacromolecules* **2011**, *12*, 3418–3422.
- (11) Nagaoka, H.; Ohnishi, N.; Eguchi, M. Thermoresponsive Polymer and Production Method Thereof. U.S. Patent 2007/0203313 A1, Aug 30, 2007.
- (12) Glatzel, S.; Laschewsky, A.; Lutz, J. *Macromolecules* **2011**, *44*, 413–415.
- (13) Haas, H. C.; Schuler, N. W. *Polym. Lett.* **1964**, *2*, 1095–1096.
- (14) Haas, H. C.; Moreau, R. D.; Schuler, N. W. *J. Polym. Sci., Part A-2: Polym. Phys.* **1967**, *5*, 915–927.
- (15) Haas, H. C.; Chiklis, C. K.; Moreau, R. D. *J. Polym. Sci., Part A-1: Polym. Chem.* **1970**, *8*, 1131–1145.
- (16) Haas, H. C.; MacDonald, R. L.; Schuler, A. N. *J. Polym. Sci., Part A-1: Polym. Chem.* **1970**, *8*, 1213–1226.
- (17) Haas, H. C.; Manning, M. J.; Mach, M. H. *J. Polym. Sci., Part A-1: Polym. Chem.* **1970**, *8*, 1725–1730.
- (18) Haas, H. C.; MacDonald, R. L.; Schuler, A. N. *J. Polym. Sci., Part A-1: Polym. Chem.* **1970**, *8*, 3405–3415.
- (19) Marstokk, O.; Nyström, B.; Roots, J. *Macromolecules* **1998**, *31*, 4205–4212.
- (20) Ostrovskii, D.; Jacobsson, P.; Nyström, B.; Marstokk, O.; Kopperud, H. B. M. *Macromolecules* **1999**, *32*, 5552–5560.
- (21) Seuring, J.; Agarwal, S. *Macromol. Chem. Phys.* **2010**, *211*, 2109–2117.
- (22) Seuring, J.; Frank, F. M.; Huber, K.; Agarwal, S. *Macromolecules* **2012**, *45*, 374–384.
- (23) Ohnishi, N.; Furukawa, H.; Kataoka, K.; Ueno, K. Polymer Having An Upper Critical Solution Temperature. U.S. Patent 7,195,925 B2, March 27, 2007.
- (24) Saini, G.; Leoni, A.; Franco, S. *Makromol. Chem.* **1971**, *144*, 235–244.
- (25) Katano, H.; Maruyama, A.; Sanui, K.; Ogata, N.; Okano, T.; Sakurai, Y. *J. Controlled Release* **1991**, *16*, 215–228.
- (26) Bouillot, P.; Vincent, B. *Colloid Polym. Sci.* **2000**, *278*, 74–79.
- (27) Bovey, F. A.; Tiers, G. V. D. *J. Polym. Sci., Part A* **1963**, *1*, 849–861.
- (28) Kulicke, W.; Kniewske, R.; Klein, J. *Prog. Polym. Sci.* **1982**, *8*, 373–468.
- (29) Tanaka, N.; Ito, K.; Kitano, H. *Macromolecules* **1994**, *27*, 540–544.
- (30) Koningsveld, R. *Adv. Colloid Interface Sci.* **1968**, *2*, 151–215.
- (31) Rebelo, L. P.; Van Hook, W. A. *J. Polym. Sci., Part B: Polym. Phys.* **1993**, *31*, 895–897.
- (32) Silberberg, A.; Eliassaf, J.; Katchalsky, A. *J. Polym. Sci.* **1957**, *23*, 259–284.
- (33) Eliassaf, J. *J. Appl. Polym. Sci.* **1960**, *3*, 372.
- (34) Netopilik, M.; Bohdanecky, M.; Chytry, V.; Ulbrich, K. *Macromol. Rapid Commun.* **1997**, *18*, 107–111.
- (35) Brandrup, J.; Immergut, E. H.; Grulke, E. A. *CRC Polymer Handbook*; Wiley: New York, 1999.
- (36) Van Durme, K.; Assche, G. V.; Van Mele, B. *Macromolecules* **2004**, *37*, 9596–9605.
- (37) Sanchez, M. S.; Hanykova, L.; Ilavsky, M.; Pradas, M. M. *Polymer* **2004**, *45*, 4087–4094.

## Supporting Information

# A Universal and Cost-Effective Approach: Polymers with Tunable Upper Critical Solution Temperature in Water and Electrolyte Solution

Jan Seuring and Seema Agarwal\*

Philipps-Universität Marburg, Fachbereich Chemie, Hans-Meerwein Straße, D-35032

Marburg, Germany

E-mail: agarwal@staff.uni-marburg.de

## A. Spectroscopic data

### A.1. NMR spectroscopy of poly(BA-co-NAGA)

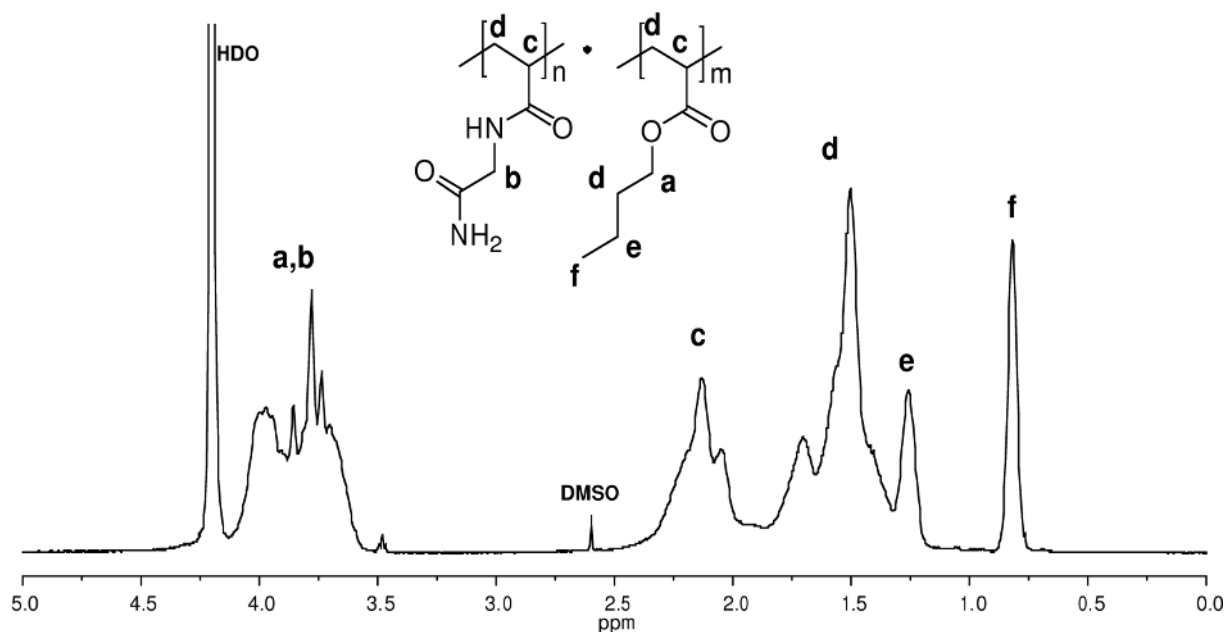
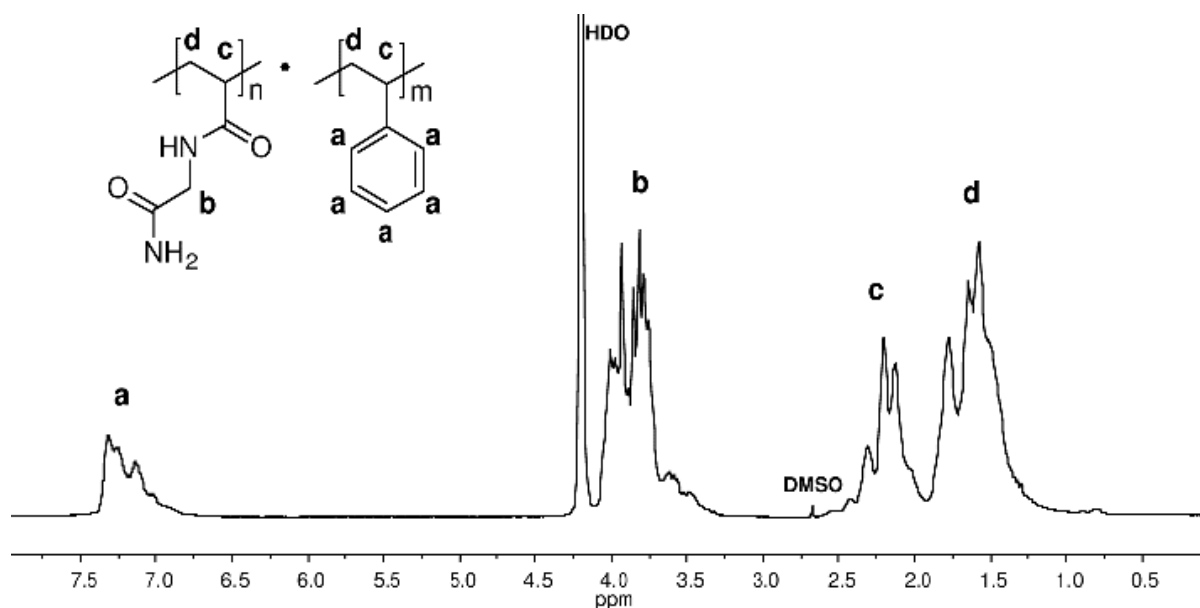


**Figure S1.** 500 MHz  $^1\text{H}$  NMR spectrum of poly(BA-co-NAGA) with an butyl acrylate content of 21.2 mol% recorded in  $\text{D}_2\text{O}$  at 80 °C.

$^1\text{H-NMR}$  (500 MHz,  $\text{D}_2\text{O}$ ,  $T = 80\text{ }^\circ\text{C}$ , the residual solvent peak was calibrated to  $\delta = 4.20$ )  
 $\delta = 0.82$  ( $-\text{CH}_3$ ),  $1.26$  ( $-\text{CH}_2-\text{CH}_3$ ),  $1.3-1.9$  (polymer backbone,  $-\text{CH}_2-$ ;  $\text{O}-\text{CH}_2-\text{CH}_2-$ ),  $1.9-2.4$   
 (polymer backbone,  $-\text{CH}-$ ),  $3.6-4.05$  ( $\text{NH}-\text{CH}_2-\text{CONH}_2$ ;  $\text{O}-\text{CH}_2-$ ).

The butyl acrylate content in the polymers was calculated by comparing the integral of the methyl group **f** of butyl acrylate at  $0.82$  ppm to the integral of the methylene groups **a** and **b** that are adjacent to heteroatoms at  $3.6-4.1$  ppm (Figure S1).

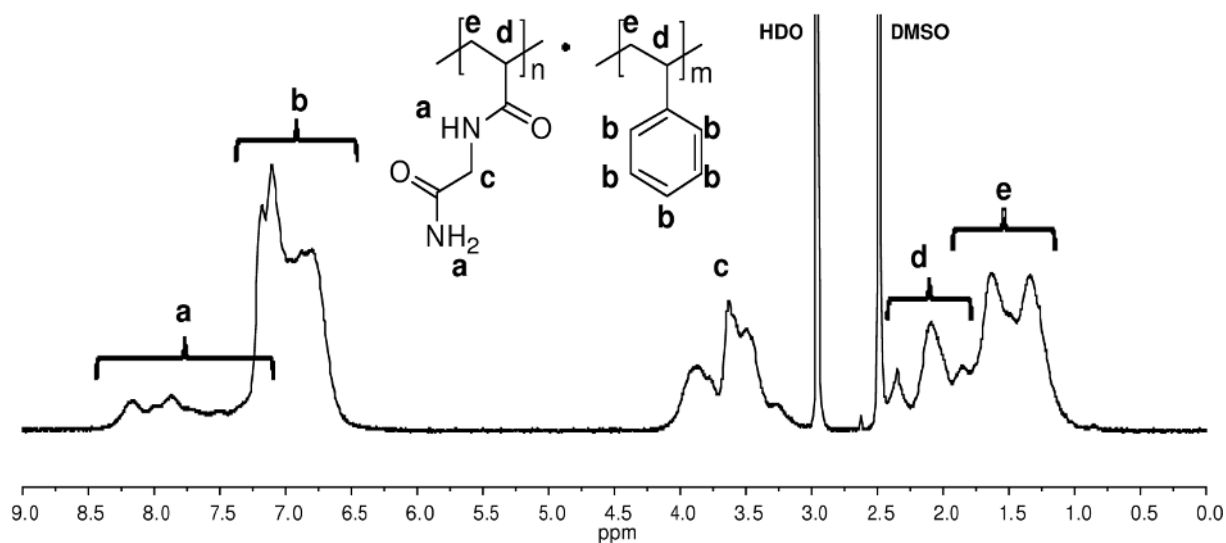
### A.2. NMR spectroscopy of poly(NAGA-co-St) in $\text{D}_2\text{O}$



**Figure S2.** 500 MHz  $^1\text{H}$  NMR spectrum of poly(NAGA-co-St) with an styrene content of 10.2 mol% recorded in  $\text{D}_2\text{O}$  at  $80\text{ }^\circ\text{C}$ .

$^1\text{H-NMR}$  (500 MHz,  $\text{D}_2\text{O}$ ,  $T = 80\text{ }^\circ\text{C}$ , the residual solvent peak was calibrated to  $\delta = 4.20$ )  
 $\delta = 1.1-1.9$  (polymer backbone,  $-\text{CH}_2-$ ),  $1.9-2.6$  (polymer backbone,  $-\text{CH}-$ ),  $3.33-4.1$  ( $\text{NH}-\text{CH}_2-\text{CONH}_2$ ),  $6.7-7.5$  (phenylic protons,  $-\text{C}_6\text{H}_5$ ).

The styrene content in the polymers was calculated by comparing the integral of the aromatic protons **a** of styrene at  $6.7-7.5$  ppm to the integral of the methylene group **b** that is adjacent to nitrogen at  $3.33-4.1$  ppm (Figure S2).

A.3. NMR spectroscopy of poly(NAGA-co-St) in DMSO-*d*6

**Figure S3.** 500 MHz <sup>1</sup>H NMR spectrum of poly(NAGA-co-St) with an styrene content of 26.8 mol% recorded in DMSO-*d*6 at 100 °C.

<sup>1</sup>H-NMR (500 MHz, DMSO-*d*6, T = 100 °C, the residual solvent peak was calibrated to  $\delta = 2.50$ )  $\delta = 1.0$ - $1.9$  (polymer backbone, -CH<sub>2</sub>-),  $1.8$ - $2.5$  (polymer backbone, -CH-),  $3.1$ - $4.2$  (NH-CH<sub>2</sub>-CONH<sub>2</sub>),  $6.6$ - $7.4$  (phenylic protons, -C<sub>6</sub>H<sub>5</sub>),  $7.1$ - $8.4$  (NH, NH<sub>2</sub>).

The styrene content in the polymers was calculated by comparing the integral of the methylene group **b** that is adjacent to nitrogen at 3.1-4.2 ppm to the sum of the backbone protons **d** and **e** at 1.0 to 2.5 ppm (Figure S3).

## A.4. NMR spectroscopy of poly(AAm-co-AN)

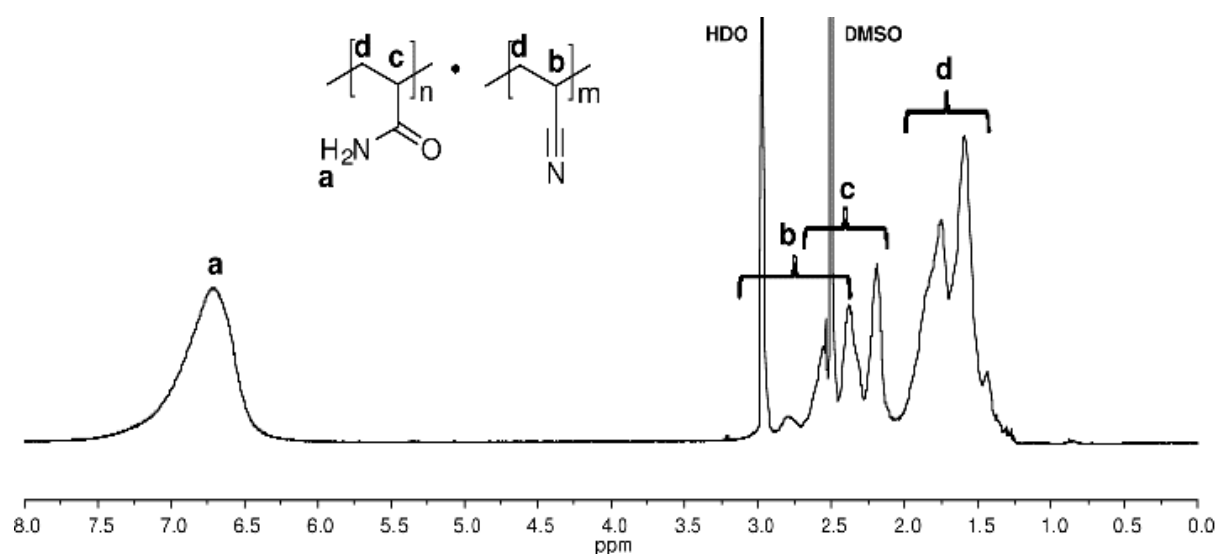


**Figure S4.** 500 MHz  $^1\text{H}$  NMR spectrum of poly(AAm-co-AN) with an acrylonitrile content of  $7.6 \pm 1.3$  mol% recorded in DMSO- $d_6$  at 100 °C.

$^1\text{H-NMR}$  (500 MHz, DMSO- $d_6$ , T = 100 °C, the solvent signal was calibrated to 2.50 ppm)  $\delta = 1.2\text{-}2.0$  (polymer backbone,  $-\text{CH}_2-$ ),  $2.0\text{-}2.7$  (polymer backbone,  $-\text{CH-CONH}_2$ ),  $2.3\text{-}3.1$  (polymer backbone,  $-\text{CH-CN}$ ),  $6.7$  ( $-\text{NH}_2$ ).

## A.5. IR-spectroscopic determination of the copolymer composition of poly(AAm-co-AN)s

Due to overlapping signals and partial deuterium exchange of the NH-protons the  $^1\text{H}$  NMR spectrum could not be used to calculate the polymer composition. Instead, the integral ratios of the infrared vibrational bands of the carbonyl and nitrile group were determined (Figure S5). IR spectroscopy was performed on a Digilab Excalibur Series FTS 3000 spectrometer by the attenuated total reflection technique employing a ZnSe crystal. The spectra were analyzed using the software Win-IR Pro 3.3. For determination of the copolymer compositions of poly(AAm-co-AN)s a calibration curve was recorded (Figure S6). Standards were thoroughly mixed using very fine powders of polyacrylamide and polyacrylonitrile homopolymers. Both samples and calibration standards were measured nine times with 32 scans per measurement. The error bars display the standard deviation of the determined peak ratios.

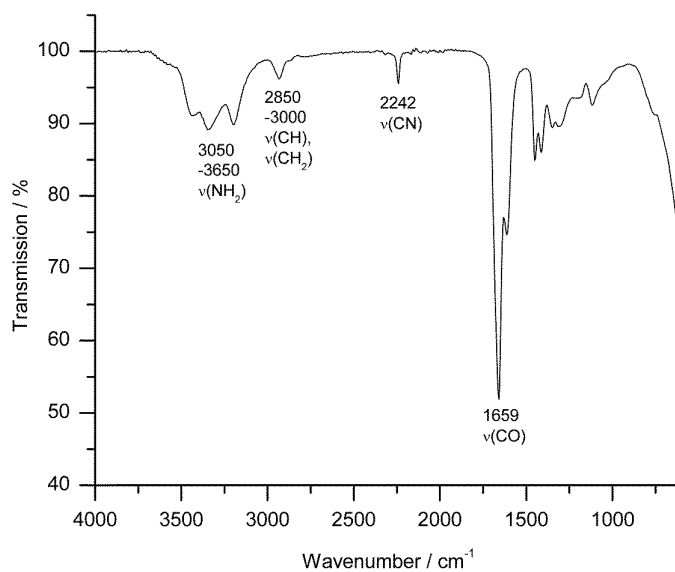


**Figure S5.** Infrared spectrum of poly(AAm-co-AN) with a acrylonitrile content of  $19.7 \pm 1.3$  mol%.

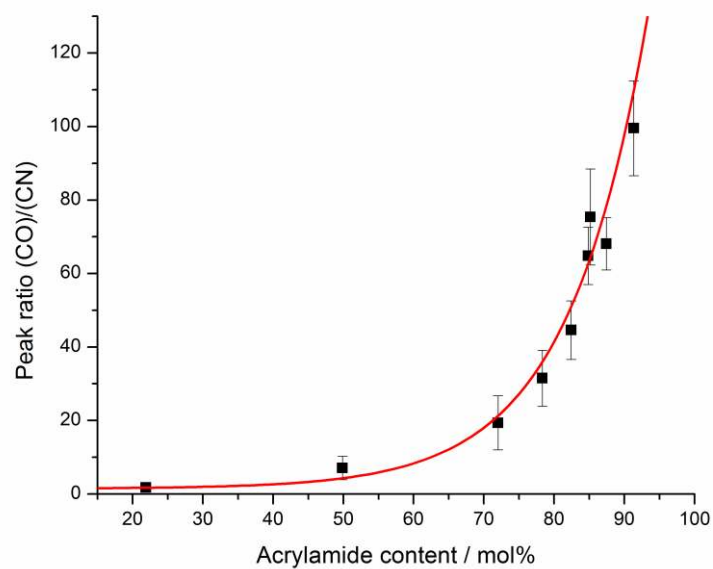


**Figure S6.** Calibration curve used for the determination of the copolymer compositions of poly(AAm-co-AN)s.

## B. Further Results and Discussion

### B.1. Relative molecular weight determination by GPC

Molecular weight determination of the polymers that form intermolecular hydrogen bonds is not trivial due to their strong tendency to aggregate. For poly(NAGA) it is particularly difficult because only water above the phase transition temperature and dimethyl sulfoxide are known to be suitable solvents and even in those there is always a fraction of aggregated polymer.<sup>1,2</sup> Molecular dispersion has been achieved in 2 M aqueous sodium thiocyanate solution but GPC does not tolerate such a high concentration of salt. It was possible to obtain aggregate free molecular weight distributions (MWDs) in 0.3 M aqueous formic acid solution.<sup>3</sup> Under these acidic conditions, however, poly(acrylamide)s could partially hydrolyze. In order to analyze copolymers of poly(NAGA) with increased hydrophobicity dimethylsulfoxide was considered the best eluent of the available options. The poly(NAGA) homopolymer and copolymers with BA showed very broad MWDs (Figure S7).

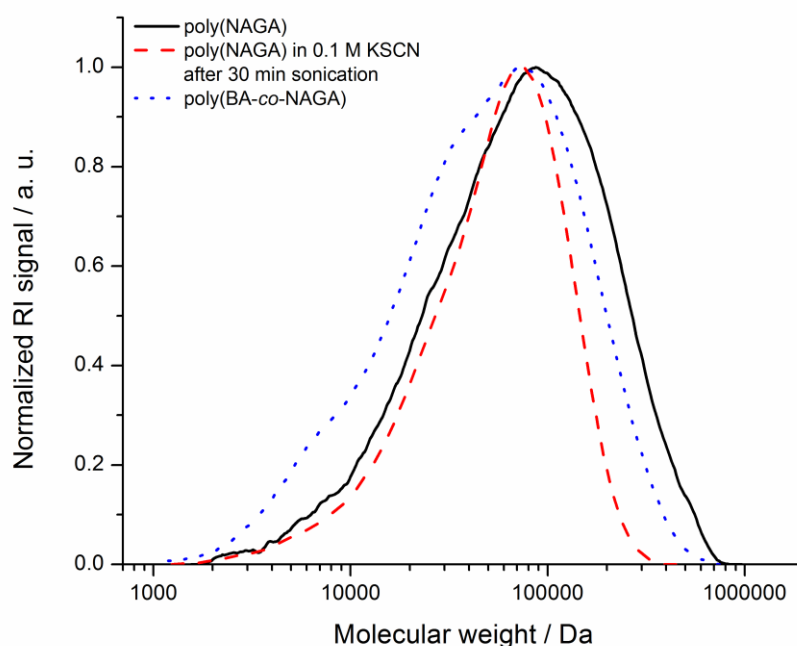


**Figure S7.** GPC of poly(NAGA) and poly(BA-co-NAGA) in pure DMSO or 0.1 M KSCN solution.

When poly(NAGA) was measured in DMSO containing 0.1 M potassium thiocyanate with 30 min sonication at 60 °C prior to measurement the high molecular weight fraction disappeared



and the polydispersity and shape of the MWD became as expected for a free radical polymerization ( $M_n = 34700$ ,  $PDI = 2.0$ ). Hence, it is likely that the broad MWD in pure DMSO is a superposition of a MWD of aggregates and a single chain MWD. Only by the combination of potassium thiocyanate additive and sonication it was possible to break the aggregates. The same method could not break the aggregates in the case of copolymers with BA. Prolonged heating prior to measurement, using lithium bromide as additive or taking the samples directly from the reaction mixture without workup had no or adverse effect. At least it is possible to conclude that the  $M_n$ -values of poly(NAGA-*co*-BA)s are greater than 10 kDa. Interestingly, poly(NAGA-*co*-styrene)s and poly(AAm-*co*-AN)s showed aggregate free, unimodal distributions (Figure S8). The number average molecular weights were all in the range of 15 to 50 kDa. This further supports the conclusion that the signal observed after sonication of the poly(NAGA) homopolymer in 0.1 M KSCN solution originates from single chains. The molecular weights observed are typical for solution polymerization of polyacrylamides in DMSO.<sup>4</sup> The MWs obtained from polymerization in DMSO are lower than in water because the  $k_p k_0^{0.5}$  ratio of acrylamide polymerization is 12 times lower in DMSO. It is also worth mentioning that poly(NAGA) needs several hours to dissolve in DMSO whereas poly(NAGA-*co*-styrene)s and poly(AAm-*co*-AN)s need only 5-30 min.

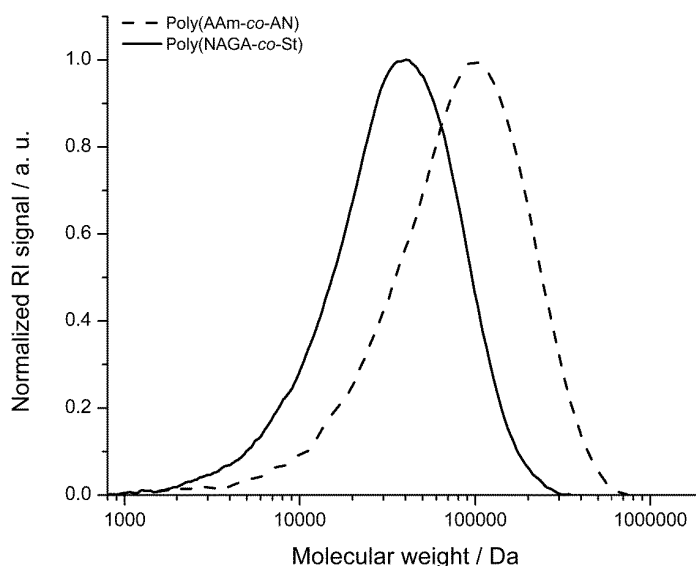


**Figure S8.** Representative GPC curves of poly(AAm-*co*-AN) and poly(NAGA-*co*-St) in pure DMSO as eluent.

## References

- (1) Marstokk, O.; Nyström, B.; Roots, J. *Macromolecules* **1998**, *31*, 4205-4212.
- (2) Glatzel, S.; Laschewsky, A.; Lutz, J. *Macromolecules* **2011**, *44*, 413-415.
- (3) Seuring, J.; Agarwal, S. *Macromol. Chem. Phys.* **2010**, *211*, 2109-2117.
- (4) Kurenkov, V. F.; Abramova, L. I. *Polym.-Plast. Tech. Eng.* **1992**, *31*, 659-704.

## Publication 5

### Controlled Radical Polymerization of *N*-Acryloylglycinamide and UCST-type Phase Transition of the Polymers

Fangyao Liu, Jan Seuring, Seema Agarwal,

*Journal of Polymer Science, Part A: Polymer Chemistry* **2012**.

DOI: 10.1002/pola.26322

#### **Author contributions**

Fangyao Liu and Jan Seuring contributed equally to this work. Kinetic experiments, turbidity measurements and chain extension were conducted by Fangyao Liu. Preliminary experiments, development of the polymerization conditions and writing of the manuscript was done by Jan Seuring. Prof. Seema Agarwal was responsible for supervision and correction of the manuscript.

# Controlled Radical Polymerization of *N*-Acryloylglycinamide and UCST-Type Phase Transition of the Polymers

Fangyao Liu, Jan Seuring, Seema Agarwal

Department of Chemistry, Scientific Center for Materials Science, Philipps-Universität Marburg, Hans-Meerwein Strasse, D-35032 Marburg, Germany

Correspondence to: S. Agarwal (E-mail: agarwal@staff.uni-marburg.de)

Received 18 May 2012; accepted 28 July 2012; published online

DOI: 10.1002/pola.26322

**ABSTRACT:** *N*-Acryloylglycinamide was polymerized via the reversible addition fragmentation transfer process without sacrificing its key property, the upper critical solution temperature in water. This could be achieved by choosing an appropriate non-ionic initiator [2,2'-azobis(4-methoxy-2,4-dimethyl valeronitrile) (V-70)] and nonionic chain-transfer agent (cyanomethyl dodecyl trithiocarbonate). A good molar mass control was accomplished as proved by the linear increase of molar mass with conversion, a chain extension experiment, and low dispersity. The influence

of molar mass, polymer end groups, or salt concentration on the cloud point was analyzed by turbidimetry. Polymer end groups exerted a distinct effect on the cloud points, whereas the influence increased with decreasing molar masses. © 2012 Wiley Periodicals, Inc. *J Polym Sci Part A: Polym Chem* 000: 000–000, 2012

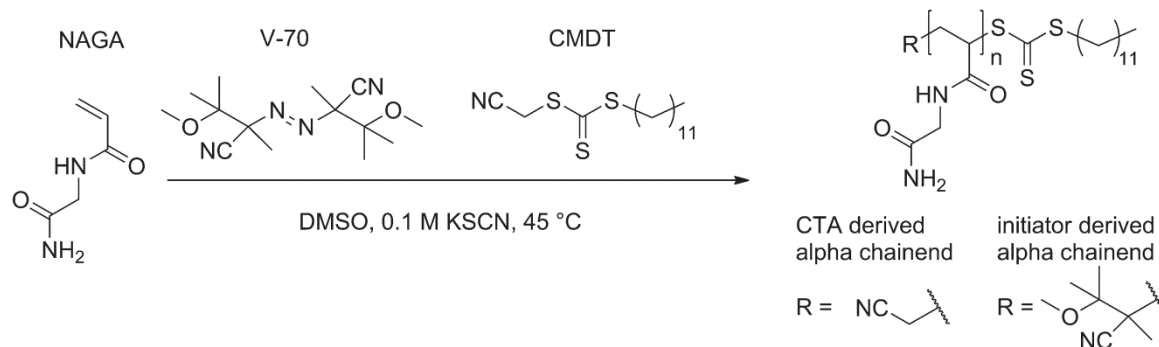
**KEYWORDS:** *N*-acryloylglycinamide; RAFT; smart polymers; thermoresponsive polymers; upper critical solution temperature

**INTRODUCTION** Although the general term water-soluble “thermoreponsive polymer” is frequently applied, it actually represents a synonym for polymers with lower critical solution temperature (LCST), as only very few examples of polymers with an upper critical solution temperature (UCST) in water under practically relevant conditions were reported, that is, with phase transitions between 0 and 100 °C, atmospheric pressure, and relevant ionic strength (from pure water to physiological milieu). This is supported by a 2010 review and survey on nonionic water-soluble thermoresponsive polymers.<sup>1</sup> The UCST of all known examples is based either on Coulomb interactions or on thermally reversible hydrogen bonding. The first applies for some zwitterionic polymers like poly(betaine)s.<sup>2–6</sup> However, Coulomb interactions are disturbed in the presence of electrolytes. The very strong sensitivity of the phase transition temperature to electrolyte concentration and polymer concentration makes them unsuitable for most applications. If the polymers are non-ionic and the UCST is due to hydrogen bonding, the phase transition temperature is less sensitive to both electrolytes (except for specifically hydrogen bond-breaking agents like thiocyanates) and polymer concentration, and therefore, they represent promising candidates for many fields of applications. Yet, very few examples of nonionic, hydrogen-bonding UCST polymers were reported.<sup>7–9</sup> Poly(*N*-acryloylglycinamide) [poly(NAGA)] is one of these polymers. For the first time, it was synthesized by Haas and Schuler in 1964.<sup>10(a)</sup>

They found that poly(NAGA) can form thermoreversible gels in concentrated aqueous solutions.<sup>10(a–f)</sup> Haas and Schuler furthermore reported that hydrogen bond-interrupting agents like thiocyanate or urea can prevent the gel formation.<sup>10(b)</sup> Poly(NAGA) also does not exhibit thermoreversible gelation behavior in dilute solutions; however, it contains polymer aggregates despite of its transparent and homogeneous appearance. This was initially evidenced by a nonlinear dependency among reduced viscosity and polymer concentration in pure water, along with the fact that the viscosity dropped significantly on addition of sodium thiocyanate.<sup>10(b)</sup> Later, the conclusions of Haas and Schuler were confirmed by light scattering and Raman spectroscopy.<sup>11,12</sup> We would like to emphasize in this context that although both thermoreversible gelation and aggregate formation in dilute solution are due to hydrogen bonding, these phenomena differ considerably from a UCST-type phase separation. For UCST behavior, the occurrence of phase separation is a stringent requirement.<sup>13</sup> In contrast, in the thermoreversible gelation of concentrated poly(NAGA) solutions, no phase separation takes place as the gel is only in one phase with homogenous properties. The formation of aggregates in dilute solution can be regarded as a form of microphase separation. However, a preliminary temperature-dependent light scattering study of poly(NAGA) suggested that these aggregates are thermodynamically stable above the phase transition temperature and no macrophase separation sets in.<sup>14</sup> It is yet

Fangyao Liu and Jan Seuring have contributed equally to the experimental part.

© 2012 Wiley Periodicals, Inc.



**SCHEME 1** Schematic representation of the optimum conditions developed in this work for the RAFT polymerization of *N*-acryloylglycinamide while retaining the UCST of the resulting polymers in water.

unclear whether there is a distinct temperature where aggregates form/break; however, most likely these aggregates are just thermosensitive rather than thermoresponsive. Based on this, a behavior comparable with micelles that comprise a gradual decrease of the aggregation number with temperature would be most likely. Thus, despite numerous contributions focused on the thermoreversible gelation of poly(NAGA), a UCST-type phase separation has not been reported in the publications mentioned above. We recently revealed the reason for this:<sup>14</sup> it has been failed to notice the UCST in the past because ionic groups were introduced unintentionally either by acrylate impurities in the monomer, hydrolysis of the polymer side chains, and/or usage of ionic initiators or chain-transfer agents (CTAs). Ionic groups in polymers contribute strongly exothermic to the enthalpy of mixing.<sup>15,16</sup> The effect on the UCST of poly(NAGA) is extreme because the enthalpy change of the phase transition is already two magnitudes smaller than for most LCST polymers such as PNiPAAm.<sup>17–19</sup> The proof for these conclusions along with a procedure to obtain stable aqueous solutions of nonionic poly(NAGA) that allows exploitation of UCST in pure water as well as physiological milieu was published.<sup>14</sup> Most recently, the synthesis of thermoresponsive poly(acrylamide-co-acrylonitrile)s and poly(methacrylamide) indicated that the knowledge gained for poly(NAGA) is valid for the whole polymer class of nonionic hydrogen-bonding UCST polymers.<sup>20</sup>

Recent work of Lutz and coworkers<sup>21</sup> regarding the controlled radical polymerization of NAGA by reversible addition fragmentation transfer (RAFT) polymerization gave additional support to our findings. The fact that poly(NAGA) prepared via RAFT polymerization did not comprise a cloud point in water can most likely be deduced to the usage of an ionic radical initiator (VA-044) and an ionic CTA [sodium 3-(((benzylthio)-carbonothioyl)thio)propane-1-sulfonate]. The cloud point suppressing effect of the ionic end groups could be compensated by the addition of electrolytes; however, it is preferable to obtain polymers that exhibit the desired functionality in pure water as well and are not strongly influenced by the electrolyte concentration.

This work was carried out with the aim to provide controlled radical polymerization of NAGA by the RAFT process

without sacrificing the most interesting property of the polymers, the UCST in water. The underlying concept of this work was to use nonionic radical initiators and nonionic CTAs to achieve molar mass control and well-defined chain ends without sacrificing the thermoresponsivity in water (Scheme 1). Although this concept has been developed in our previous work, we could not achieve good molar mass control ( $D > 2$ ), and therefore, an appropriate correlation of properties with the molar mass distribution was not possible. There were two motivations for this study: on one hand, the determination of molar mass dependence of the phase transition required control over the molar mass—this can be achieved by RAFT; and on the other hand, RAFT represents an excellent method for a precise functionalization of polymer end groups. Besides allowing both grafting from and grafting onto various substrates, it enables straightforward preparation of complex macromolecular architectures such as (multi)block copolymers, dendrimers, star polymers, comb polymers, and so forth.<sup>22</sup> This will be important for the development of smart materials with UCST-type thermoresponsivity of poly(NAGA) in the future.

## EXPERIMENTAL

### Materials

Azobisisobutyronitrile (Fluka) was recrystallized from ethanol. Acrylate-free *N*-acryloylglycinamide [NAGA;  $m_p(\text{DSC}) = 143$  °C, residual potassium < 5 ppm] was synthesized according to a recently published procedure.<sup>14</sup> 3-(((Benzylthio)carbonothioyl)thio)propane-1-sulfonate (BCPS) and dibenzyltrithiocarbonate (DBTC) were synthesized according to the literature.<sup>21,23</sup> 2,2'-Azobis(4-methoxy-2,4-dimethyl valeronitrile) (V-70; Wako), cyanomethyl dodecyl trithiocarbonate (CMDT, 98%; Aldrich), and potassium thiocyanate (99%, p.a.; Grüssing) were used as received. Solvents were distilled before use. Ultrapure water was obtained from a TKA Micro UV system model 08.1005 (conductivity = 0.06  $\mu\text{S/cm}$ , filtered through 200 nm filter, UV treated). Phosphate buffered saline (PBS) was prepared using precalibrated tablets (Aldrich).

### Analytical Techniques

<sup>1</sup>H spectra were recorded on a Bruker Avance DRX-500 (500 MHz) either in D<sub>2</sub>O at 80 °C or DMSO-*d*<sub>6</sub> at 100 °C.

**TABLE 1** RAFT Polymerization of NAGA with AIBN as Initiator and Dibenzyltrithiocarbonate (DBTC) as CTA

Entry	Time (min)	Yield (%)	$M_{n, \text{theo}}$ (g/mol)	$M_n$ (g/mol)	D	Cloud point in PBS <sup>a</sup> (°C)	
						Cooling	Heating
1	200	19	15,100	7,260	3.0	18.8	30.1
2	230	32	25,200	9,450	2.9	17.3	28.1
3	300	51	39,300	12,600	2.7	17.3	29.1
4	635	48	37,500	12,600	3.0	16.9	28.8

The Mono:CTA:In ratio was 600:1:0.2 with a monomer concentration of 0.59 M.

<sup>a</sup>  $c = 0.2$  wt %; heating rate = 1.0 °C/min.

Turbidity measurements were performed on a custom-modified Tepper turbidity photometer TP1-D at a wavelength of 670 nm, a cell path length of 10 mm, and magnetic stirrer. The polymer solutions (above phase transition temperature) were filtered through a warm 1.2- $\mu\text{m}$  PET syringe filter before measurement. The heating program started at 60 °C and proceeded via cooling to 3.5 °C at a constant rate of 1.0 °C/min followed by reheating to the starting temperature with the same rate. The inflection point of the transmittance curve was considered as cloud point. It was graphically determined by the maximum of the first derivative of the heating or cooling curve, respectively. For sample preparation, the polymers were weighed into 2-mL polypropylene tubes. The dissolution parameters for poly(NAGA) in PBS (pH 7.4) and salt solutions were as follows:  $c = 1.0$  wt %,  $T = 70$  °C inside the tubes, and  $t = 90$  min without sonication. The parameters in pure water were as follows:  $c = 1.0$  wt %,  $T = 70$  °C inside the tubes, and  $t = 60$  min with sonication. For sonication, a heated Bandelin Sonorex RK 102 H ultrasound device (HF power = 120 W, HF peak performance = 480 W, HF frequency = 35 kHz) was used. The samples were diluted to 0.2 wt %, and the hot samples were quickly filtered through a preheated 1.2- $\mu\text{m}$  PET-filter into the cuvette.

Molar masses and molar mass distributions of the polymers were determined by gel permeation chromatography (GPC) with dimethyl sulfoxide as eluent. Two PL-Gel Mixed-D columns (particle size 5  $\mu\text{m}$ , dimension 7.5 mm  $\times$  300 mm) calibrated with narrow Pullulan standards and a differential refractive index detector were used. The flow rate was 1.0 mL/min. The molar mass distributions were calculated using the software Cirrus 3.3. The theoretical number-average molar mass  $M_{n, \text{theo}}$  was calculated using the following equation:

$$M_{n, \text{theo}} = [c_0(\text{monomer})/c_0(\text{CTA})] \times x_p \times M_{\text{NAGA}} + M_{\text{CTA}} \quad (1)$$

where  $c_0(\text{monomer})$  and  $c_0(\text{CTA})$  refer to the initial concentrations of monomer and RAFT CTA, respectively;  $x_p$  denotes monomer conversion; and  $M_{\text{NAGA}}$  and  $M_{\text{CTA}}$  are the molar masses of the monomer and CTA.

## Syntheses

### General Procedure for the Purification and Isolation of Polymers

The reactions were stopped by air contact. Thereafter, the polymers were precipitated from the 10-fold excess volume of methanol. Subsequent to centrifugation (10 min, 8000 rpm) and decantation, the sediment was thoroughly slurried with methanol using a glass rod. The centrifugation-wash cycles were repeated three times. Subsequently, the polymer was dried in the vacuum oven at 70 °C for 24 h. The brittle pellet was grinded to a powder using a glass rod and further dried for another 24 h to obtain a powdery white polymer.

### Example of RAFT Polymerization of NAGA with DBTC as CTA

In a 25-mL nitrogen flask, 1 g NAGA (200 equiv) and 11.3 mg DBTC (1 equiv) were dissolved in 11.2 mL distilled DMSO. The solution was degassed by three freeze-pump-thaw cycles. One hundred microliters of a separately degassed DMSO solution containing 1.3 mg of AIBN (0.2 equiv) was added, and the flask was placed into an oil bath that was preheated to 70 °C. Further details are given in Table 1.

<sup>1</sup>H NMR (500 MHz, D<sub>2</sub>O,  $T = 80$  °C; the HDO peak was calibrated to  $\delta = 4.20$  ppm): 1.3–1.8 (polymer backbone,  $-\text{CH}_2-$ ), 2.0–2.3 (polymer backbone,  $-\text{CH}-$ ), 2.5 (S- $\text{CH}_2$ -Ph), 3.6–4.05 (NH- $\text{CH}_2$ -CONH<sub>2</sub>), 7.05–7.3 (Ar-H).

### Example of RAFT Polymerization of NAGA with CMDT as CTA

In a 50-mL nitrogen flask, 2 g NAGA (200 equiv) was dissolved in 24.7 mL distilled DMSO containing 0.1 M KSCN. One milliliter of a CTA-stock solution in the same solvent containing 24.8 mg CMDT (1 equiv) was added. This solution was degassed by three freeze-pump-thaw cycles. A V-70 stock solution was prepared by dissolving V-70 in separately degassed DMSO with 0.1 M KSCN. From this stock solution, 800  $\mu\text{L}$  solution containing 1.93 mg of V-70 (0.08 equiv) was quickly added to the reaction mixture. The mixture was placed into a preheated oil bath and stirred for 4 h at 45 °C. Further details are given in Table 3.

<sup>1</sup>H NMR (500 MHz, DMSO- $d_6$ ,  $T = 100$  °C; the DMSO peak was calibrated to  $\delta = 2.50$  ppm): 0.87 (alkyl- $\text{CH}_3$ ), 1.27

**TABLE 2** RAFT Polymerization of NAGA with AIBN as Initiator and CMDT as CTA

Entry	Time (min)	Yield (%)	$M_{n, \text{theo}}$ (g/mol)	$M_n$ (g/mol)	$D$
1	25	5	4,110	4,450	1.69
2	65	12	9,670	8,610	1.69
3	140	28	21,300	12,600	1.95

The Mono:CTA:In ratio was 600:1:0.2 with a monomer concentration of 0.59 M.

(alkyl), 1.3–1.8 (polymer backbone,  $-\text{CH}_2-$ ), 1.9–2.3 (polymer backbone,  $-\text{CH}-$ ), 2.3–2.4 ( $\text{S}-\text{CH}_2$ -alkyl), 3.35 ( $\text{S}-\text{CH}_2-\text{CN}$ ), 3.4–4.05 ( $\text{NH}-\text{CH}_2-\text{CONH}_2$ ), 6.5–7.3 ( $\text{CONH}_2$ ), 7.3–7.4 ( $\text{CONH}-$ ).

#### Chain Extension of the RAFT Polymer

Poly(NAGA) (79 mg; synthesized by RAFT polymerization, 1 equiv based on  $M_{n, \text{theo}} = 6524$  g/mol) was dissolved at 75 °C in 2 mL distilled DMSO solution containing 0.1 M KSCN in a 10-mL nitrogen flask. After cooling to room temperature, 151 mg NAGA (100 equiv) was added. The solution was degassed by three freeze-pump-thaw cycles. A V-70 stock solution was prepared by dissolving V-70 in separately degassed 0.1 M KSCN containing DMSO. From this stock solution, 200  $\mu\text{L}$  solution containing 0.29 mg of V-70 (0.08 equiv) was quickly added to the reaction mixture. The mixture was placed into a preheated oil bath and stirred for 4 h at 45 °C. The chain extension was followed by  $^1\text{H}$  NMR and GPC (Figs. 5 and 6).

## RESULTS AND DISCUSSION

### RAFT Polymerization of NAGA

It has been previously shown that even trace amounts of ionic groups in the polymer repeating units or at the chain ends of poly(NAGA) cause an extreme depression of the cloud point until the phase separation is completely suppressed.<sup>14</sup> At least up to a  $P_n$  of 200, polymers with  $\alpha$ -chain ends—derived from the initiator 2,2'-azobis[2-(2-imidazolin-2-yl)propane]dihydrochloride (VA-044)—or polymers with a sulfonate group at the  $\omega$ -chain ends, based on the CTA sodium BCPS, did not exhibit a cloud point in dilute aqueous solution. In this work, nonionic initiators and CTAs were used to obtain poly(NAGA) with thermoresponsivity. Most of these nonionic reagents are insoluble in water, and therefore, dimethyl sulfoxide was chosen as polymerization medium. First attempts were carried out using nonionic DBTC as CTA and AIBN as nonionic radical initiator, and indeed, the resulting polymer showed a cloud point (Table 1). However, at a reaction temperature of 70 °C, an inhibition period of about 150 min was observed besides an insufficient molar mass control with broad dispersities (Table 1). The occurrence of an inhibition period during the RAFT process indicates a slow re-initiation by the R-group.<sup>22</sup> In the case of DBTC, the benzyl radical is too stable for a fast re-initiation.

These results suggested a change of the R-group of the CTA. Cyanomethyl dodecyl trithiocarbonate (CMDT) was chosen as

new CTA, and polymerization of NAGA was carried out using the same conditions (Table 2). In this case, no inhibition was observed but the dispersities were relatively high, i.e. about 1.7. In general, free radical polymerization of water-soluble acrylamides in organic solvents such as DMSO does not yield very high molar masses. For instance, the  $k_p k_0^{0.5}$  ratio of acrylamide in DMSO is 12 times lower than in water.<sup>24</sup> When NAGA is polymerized with AIBN as initiator at 70 °C for 2 h and a monomer concentration of 0.59 M, the molar mass is  $M_n = 64,300$  g/mol. It is not possible to conduct a well-controlled radical polymerization beyond the molar mass that is achieved by free radical polymerization under the same conditions. Therefore, the focus was changed to optimize the conditions for free radical polymerization. For acrylamide, it has been observed that the molar mass increases with decreasing reaction temperature.<sup>24,25</sup> The same was found for the free radical polymerization of NAGA. By using the nonionic radical initiator V-70 with a half life decomposition temperature of 30 °C, the reaction temperature could be decreased from 70 to 45 °C. The obtained molar mass was significantly higher with a number-averaged molecular weight of 88,200 g/mol. Therefore, further RAFT polymerizations were carried out using V-70 as radical initiator. At 45 °C with V-70 as initiator and CMDT as CTA, RAFT polymerization of NAGA led to improved polydispersities of about 1.4 for the main peak of the elugram. However, the GPC elugrams comprised shoulders in the region of 64,300 g/mol where free radically polymerized polymer is expected (Fig. 1).

It is known that poly(NAGA) can form physical aggregates in DMSO,<sup>21</sup> and therefore, aggregation might have interfered during the RAFT polymerization. Shoulders from high molar mass impurities were previously observed for the RAFT polymerization of NiPAAm;<sup>26</sup> however, the reasons are unclear. Although no physical aggregates were observed in the GPC ( $c = 2$  mg/mL), one could assume that an insufficient

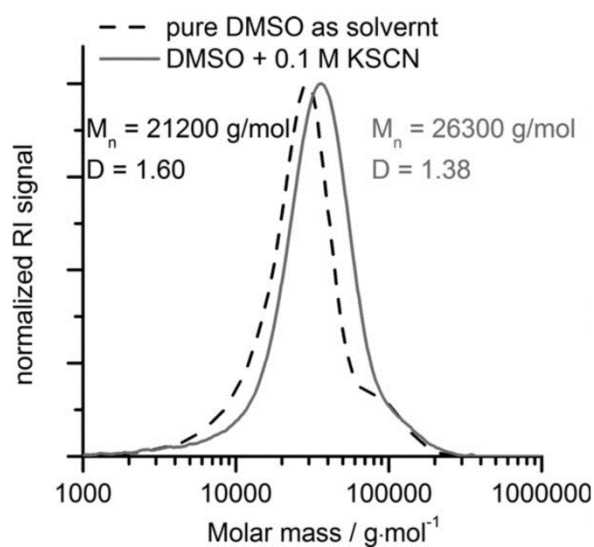


**FIGURE 1** Influence of potassium thiocyanate additive in the polymerization medium on the molar mass distribution of poly(NAGA) synthesized by RAFT.

**TABLE 3** RAFT Polymerization of NAGA with V-70 as Initiator and CMDT as CTA

Entry	Mono:CTA:In	$t$ (h)	Yield (%)	$M_{n, \text{theo}}$ (g/mol)	$M_n$ (g/mol)	$D$	Cloud points in PBS <sup>a</sup> (°C)	
							Cooling	Heating
1	50:1:0.1	20	68	4,674	3,670	1.18	22	n.d. <sup>b</sup>
2	100:1:0.04	0.67	37	5,015	3,340	1.41	n.d. <sup>b</sup>	n.d. <sup>b</sup>
3		0.83	39	5,330	4,470	1.32	n.d. <sup>b</sup>	n.d.
4		1	49	6,527	5,060	1.39	23	n.d. <sup>b</sup>
5		1.5	58	7,690	6,440	1.35	14.1	43
6		2	63	8,332	7,030	1.32	12.6	38
7		3	68	8,965	7,100	1.36	13.0	37
8		6	78	10,246	7,290	1.37	11.9	36
9	200:1:0.08	0.33	27	7,224	4,960	1.53	26	n.d. <sup>b</sup>
10		0.5	38	10,055	8,270	1.31	12.9	38
11		0.75	51	13,452	11,000	1.31	10.5	32
12		1	61	15,978	12,200	1.32	9.3	30.9
13		1.5	72	18,806	13,700	1.27	9.7	31.0
14		3	79	20,600	15,700	1.41	8.5	28.3
15		5.33	88	22,762	15,700	1.33	8.7	26.2
16	500:1:0.2	1	62	39,915	29,400	1.38	8.4	24.7
17		1.5	76	49,202	29,700	1.43	9.1	23.9
18		2	80	51,699	30,900	1.47	8.8	24.5
19		3	87	56,307	33,500	1.43	9.0	24.8
20		5	92	59,584	32,700	1.65	9.1	25.2
21		6	95	61,000	34,300	1.50	9.4	25.5

The monomer concentration was 0.59 M. The V-70 concentration was 0.24 mM except for the first entry where it was 1.2 mM.

<sup>a</sup> Polymer concentration was 0.2 wt %.

<sup>b</sup> Cloud point not determined due to very broad transition.

solubilization in the concentrated reaction mixture (75 mg/mL) leads to hindered accessibility of the growing chain ends, and therefore, hindered chain equilibration and inevitably resulted in less control. Based on this hypothesis, 0.1 M potassium thiocyanate was added to the polymerization medium to break intramolecular and intermolecular hydrogen bonds. Using this additive, the shoulder in the GPC elugrams disappeared, and a controlled RAFT polymerization of NAGA could be achieved (Fig. 1). Kinetic studies were conducted with monomer:CTA ratios of 100:1, 200:1, and 500:1 (Table 3). The absolute monomer and initiator concentrations were held constant at 0.59 M and 0.24 mM, respectively. Constant concentration of the growing polymer chains was supported by the first-order kinetic plots (Fig. 2). A slight retardation was observed at higher CTA concentrations, which resulted in lower conversions. In a single experiment with a monomer:CTA ratio of 50, the initiator concentration was increased to 1.2 mM.

Molar masses increased linearly depending on the conversion (Figs. 3 and 4); the dispersity was 1.3–1.4. Number-averaged molar masses  $M_n$  were always lower when compared with the theoretical molar masses  $M_{n, \text{theo}}$ . Pullulan was used as standard for GPC calibration, and the molar masses determined were not absolute. Therefore, a deviation

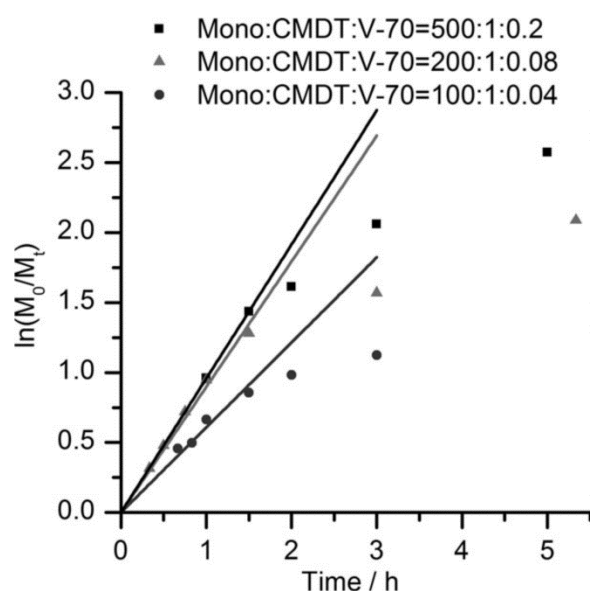


**FIGURE 2** First-order kinetic plots of the RAFT polymerization of NAGA with different monomer:CTA ratios. The monomer concentration was 0.59 M, and the initiator concentration was 0.24 mM.



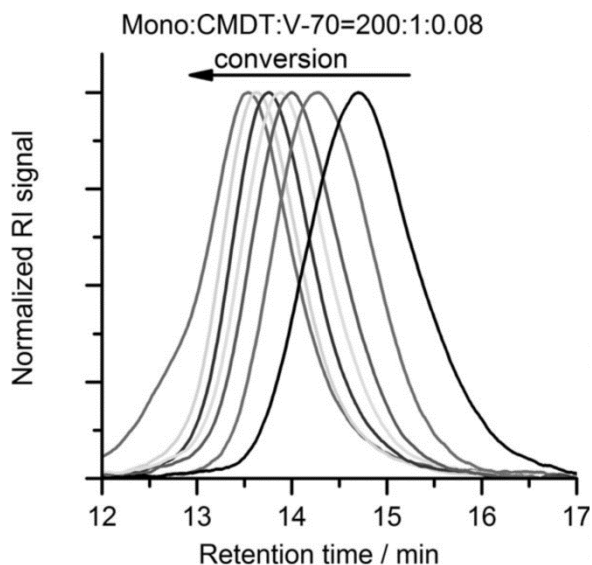


**FIGURE 3** GPC elograms of poly(NAGA) synthesized by RAFT using Mono:CMDT:V-70 in the ratio 200:1:0.08. Conversion from right to the left: 27, 38, 51, 61, 72, 79, and 88%.

of  $M_n$  from  $M_{n, \text{theo}}$  is not unusual. At higher Mono:CTA:In ratios (500:1:0.08), the deviation from  $M_{n, \text{theo}}$  increased, despite of the proceeding increase of molar mass with conversion. Nearly quantitative functionalization of the polymer chain ends by the RAFT agent could be demonstrated by a chain extension experiment (Fig. 5). Here, a polymer with  $M_n = 5060 \text{ g/mol}$  (Table 3, entry 4) was prepared by RAFT. This polymer was subsequently used as macroinitiator for the polymerization of new NAGA monomer to obtain a chain-extended polymer of  $M_n = 13,400 \text{ g/mol}$ . Disappearance of the macroinitiator was evident from the corresponding GPC elugram, thereby almost quantitative end-group functionalization via the RAFT process was proven. More-

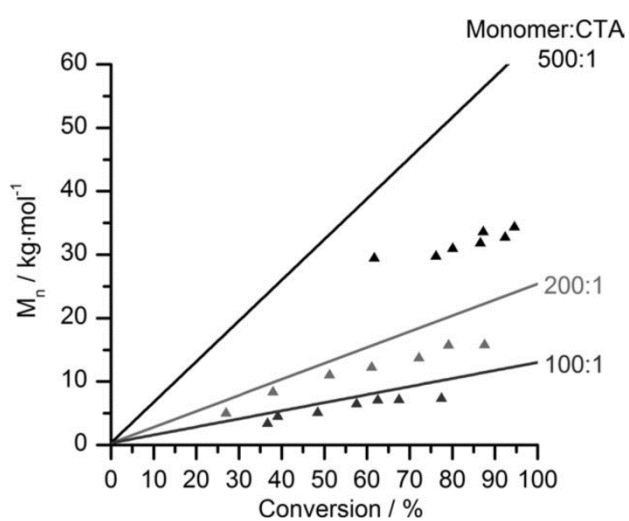


**FIGURE 4** Molar masses determined by GPC as a function of conversion for different monomer:CTA ratios. Lines =  $M_{n, \text{theo}}$ ; triangles =  $M_n$ .

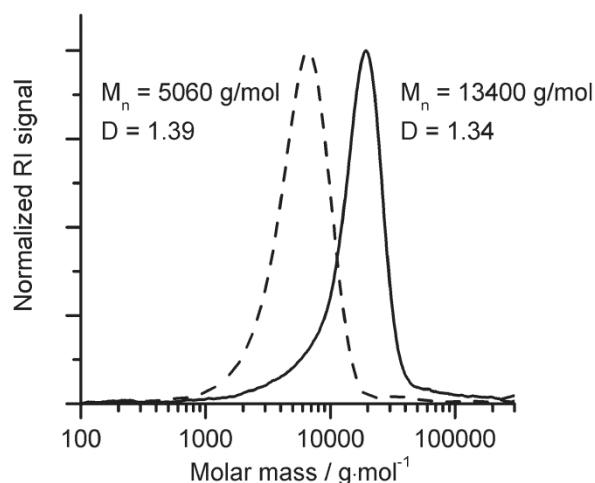


**FIGURE 5** GPC traces illustrating the successful chain extension of poly(NAGA) synthesized by RAFT. Dotted line: polymer before chain extension; solid line: polymer after chain extension.

over, this is in agreement with the decreasing end-group signals in the  $^1\text{H}$  NMR spectra (Fig. 6).

#### Molar Mass and End-Group Dependence of the Cloud Points of Poly(NAGA)

Polymers synthesized by controlled radical polymerization were used to prepare 0.2 wt % solutions in either pure water or PBS. The advantage of the RAFT system developed in this work is that the polymers show a UCST in pure water, media with low ionic strength, and media with higher ionic strength like PBS. For instance, the sample with  $M_n = 29,400 \text{ g/mol}$  (Table 3, entry 16) displayed cloud points in pure water of  $11.8 \text{ }^\circ\text{C}$  on cooling and  $28.8 \text{ }^\circ\text{C}$  on heating, respectively. In PBS, the cloud points were  $8.4 \text{ }^\circ\text{C}$  on cooling and  $24.7 \text{ }^\circ\text{C}$  on heating. A more detailed discussion concerning salt effects is given in "Influence of Electrolytes on the Cloud Point of Poly(NAGA) Synthesized by RAFT" section. Figure 7 depicts nine consecutive turbidity measurements of a representative sample with  $M_n = 29,400 \text{ g/mol}$  (Table 3, entry 16); reversibility of the phase transitions was excellent. To analyze the dependence of cloud points on the molar mass, PBS was adopted as solvent. This choice was based on the fact that sonication was required to dissolve nonionic poly(NAGA) in pure water; however, as this procedure bears the risk of molar mass degradation, it should be avoided. This appears to be a particular drawback of the long dodecyl chain of CMDT and could be overcome in the future by using derivatives with shorter alkyl chains instead. All samples could be dissolved in PBS by heating to  $70 \text{ }^\circ\text{C}$  for 90 min. Subsequently, the cloud points of these solutions were determined by turbidimetry and plotted as a function of the molar mass (Fig. 8). At molar masses from  $M_n = 15\text{--}35 \text{ kg/mol}$ , cloud points were independent of the molar mass. However, below  $M_n = 15 \text{ kg/mol}$ , the influence of the polymer end group was significant. In the case of RAFT polymerization with CMDT as CTA, the dodecyl end groups are hydrophobic, which gives a reason for the observed increasing

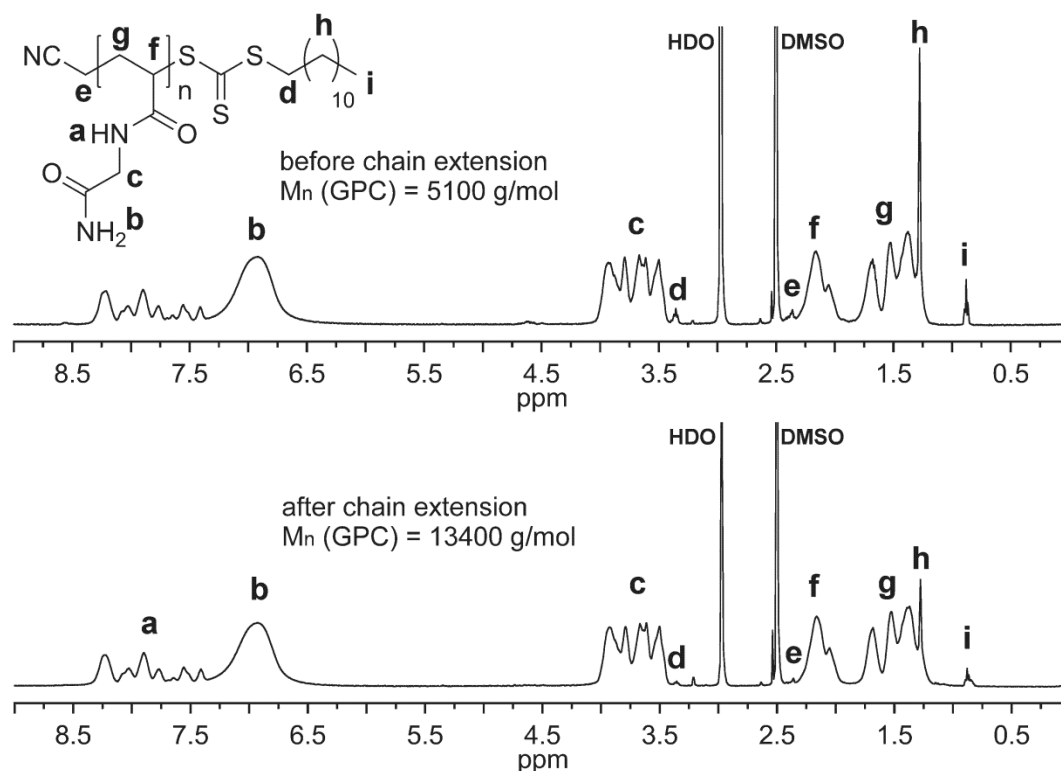


**FIGURE 6** <sup>1</sup>H NMR spectra of poly(NAGA) synthesized by RAFT before and after chain extension. The spectra were measured in DMSO-*d*<sub>6</sub> at 100 °C.

cloud points toward lower molar masses. The cloud points on cooling increased steadily from  $T_c = 9$  °C at  $M_n = 15,700$  g/mol to  $T_c = 22$  °C at  $M_n = 3670$  g/mol.

From the molar mass dependence, it can be deduced that the broadness of the molar mass distribution (represented by dispersity *D*) does not exert any influence on the cloud points as long as the low molar mass region is not reached. However, if molar masses cover this range, a mixture of polymers with different cloud points is present and consequently results in a broadening of the phase transition zone. Furthermore, this conclusion

is supported by the fact that the phase transitions become broader at lower molar masses when compared with polymers exhibiting similar *D*-values (samples with  $M_n = 8270$ , 13,700, and 29,400 g/mol in Fig. 9). The temperature intervals in which the transmission dropped from 90% to 10% during cooling and increased from 10% to 90% during heating were taken as a measure of the sharpness of transition. For poly(NAGA) synthesized by RAFT with  $M_n = 29,400$  g/mol and a *D* value of 1.38, the intervals were 2.1 °C on cooling and 6.6 °C on heating. Toward decreasing molar masses of  $M_n = 13,700$  and 8270 g/mol with *D*-values of 1.27 and 1.31, the corresponding intervals increased

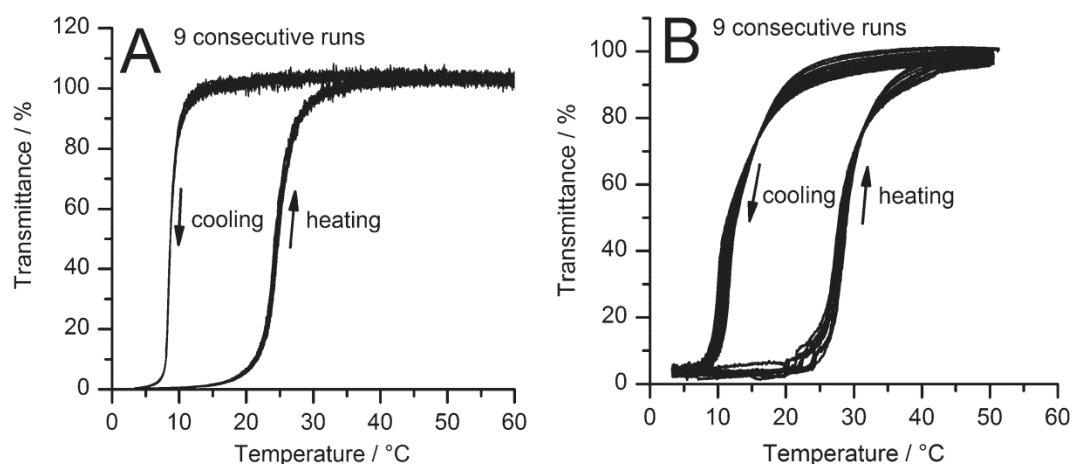


**FIGURE 7** Nine consecutive turbidity measurements of poly(NAGA) synthesized by RAFT with a molar mass of  $M_n = 29,400$  g/mol. The concentration was 0.2 wt % in (A) PBS and (B) pure water.

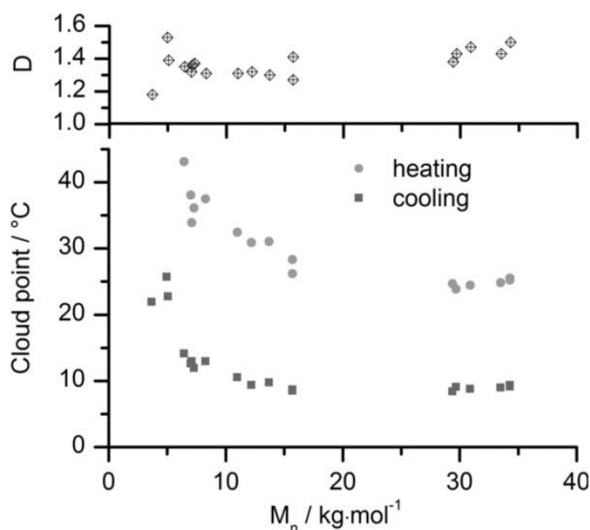


**FIGURE 8** Cloud points of poly(NAGA) synthesized by RAFT using CMDT as CTA as a function of molar mass.

to 4.5 and 8.8 °C on cooling and 11.9 and 18.1 °C on heating, respectively. Below  $M_n = 5000$  g/mol, the transitions became very broad and were not fully reversible in the time frame of one measurement cycle. To fully redissolve, they required further heating to 70 °C for a couple of minutes. Apparent deviations from the cloud point trend in the lower molar mass region, for instance, entries 1 and 9 of Table 3, can also be explained by dispersity effects. All effects discussed above should be less pronounced when CTAs with shorter alkyl groups are used, for example, cyanomethyl ethyltrithiocarbonate.

In analogy with our observations, the inverse influence of the end-group polarity was reported for polymers with LCST. Huber et al.<sup>27</sup> showed for poly(2-isopropyl-2-oxazoline) with a molar mass of about 3000 g/mol that a change of the terminal groups from a methyl to a nonyl moiety decreased the cloud point by 19 °C from 47 °C for PiPrOx<sub>25</sub> to 28 °C for Non-PiPrOx<sub>25</sub>. Xia et al.<sup>28</sup> performed ATRP of NiPAAm using the hydrophilic initiator chloropropionamide (CP). The cloud

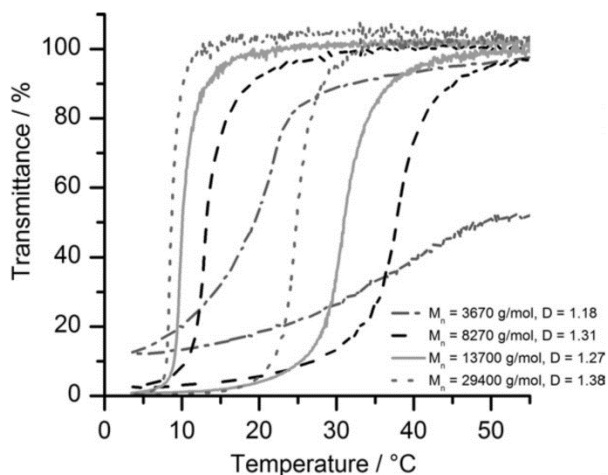


**FIGURE 9** Influence of the molar mass distribution on the turbidity curve of poly(NAGA) with hydrophobic end groups.

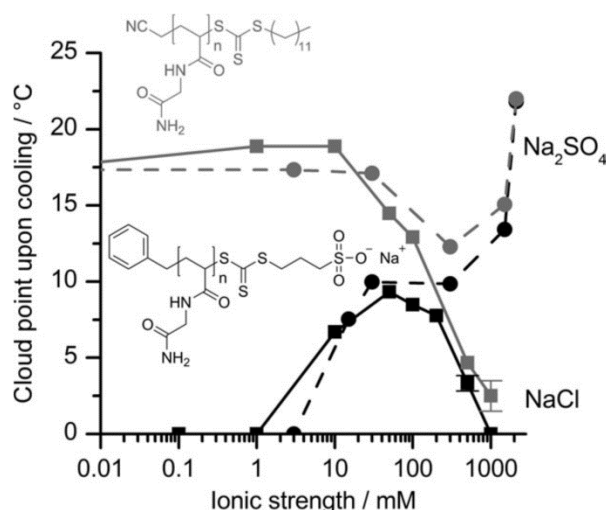


**FIGURE 10** Cloud points of poly(NAGA) with ionic or nonionic end groups as a function of ionic strength. Here, cloud point of zero means that the polymer was water soluble at 0 °C.

point (50%T) of PNiPAAm-CP polymers thereby dropped from 45.3 to 34.4 °C as the  $M_{n, \text{theo}}$  increased from 3000 to 16,300 g/mol. As expected, the end-group effect was most significant for the low molar mass samples and considerably less remarkable for longer chains.

#### Influence of Electrolytes on the Cloud Point of Poly(NAGA) Synthesized by RAFT

In a recent contribution, we showed that RAFT polymerization with an ionic CTA led to a polymer that does not exhibit a UCST in pure water but in PBS.<sup>14</sup> However, RAFT polymerization with a nonionic CTA resulted in a polymer that exhibited a UCST in both media. In this work, the influence of salt additives on both types of polymers is analyzed in detail. Two samples were synthesized using different CTA/initiator systems: poly(NAGA) with a sulfonate omega end group was synthesized according to Lutz and coworkers<sup>21</sup> using BCPS as CTA and V-044 as initiator, and on the contrary, nonionic poly(NAGA) was prepared with CMDT as CTA and V-70 as initiator. In both cases, a monomer:CTA ratio of 200:1 was used. Figure 10 displays the cloud points on cooling as a function of salt concentration. In pure water, the nonionic polymer with dodecyl omega end group showed a cloud point on cooling of 17.4 °C and a cloud point on heating of 34.6 °C. For the poly(NAGA) with a sulfonate (ionic) omega end group, no cloud point could be detected in pure water. However, cloud points were observed at sodium chloride concentrations above 1 mM and increased considerably with NaCl concentration as the end group got shielded by sodium cations. A further increase in NaCl concentration caused a steady decrease of the cloud points until they disappeared at around 1000 mM NaCl. At high concentrations of NaCl, the same trend was observed for nonionic poly(NAGA). This is an effect specific to sodium chloride; the influence of sodium sulfate was more complex. In case of nonionic poly(NAGA), there was a local minimum of the cloud points at around 100 mM sodium sulfate, which is even lower than the cloud point in

pure water. Beyond this concentration, the cloud points steadily increased for both polymers. This increase is in agreement with the Hofmeister series of ions, which was established to describe the effect of ions on the solubility of proteins.<sup>29</sup> Such correlations according to the Hofmeister series were also reported for LCST polymers like PNiPAAm. Here, the effect of salts was thoroughly investigated and even contributed to revision of the underlying mechanism of the Hofmeister series.<sup>30,31</sup> Now it is unambiguous that ions act via polarization effects, surface tension, as well as direct ion binding and therefore could affect thermoresponsivity in a different manner. Real biological fluids are complex and contain both chaotropic and kosmotropic agents, and hence, the UCST behavior is very difficult to predict. However, it was previously shown that poly(NAGA) retains its UCST in human blood serum.<sup>14</sup>

## CONCLUSIONS

NAGA was polymerized by a controlled radical polymerization with good molar mass control, as demonstrated by the linear increase of molar mass with conversion and a chain-extension experiment. This was achieved without sacrificing its key property, the UCST in water. Because of the molar mass control, it was possible to analyze the molar mass dependence of the cloud points. In analogy to LCST-polymers, it was detected that polymer end groups exerted a strong effect on the cloud points with increasing influence toward lower molar masses. The hydrophobic dodecyl end groups derived from the CTA caused an increase in the cloud points. Furthermore, with RAFT a well-established method of controlled polymerization enables precise end-group functionalization, grafting reactions, and synthesis of block copolymers. This allows the design of smart materials with UCST-type thermoresponsivity, a class of materials that is largely underrepresented because of the limited number of available materials with such behavior.

## ACKNOWLEDGMENTS

The authors thank the Philipps-Universität Marburg for financial support, the group of Prof. Barner-Kowollik (KIT) for the provision of dibenzyltrithiocarbonate, and Anna Fichtner for assisting with preliminary experiments for the RAFT polymerization.

## REFERENCES AND NOTES

- Aseyev, V.; Tenhu, H.; Winnik, F. M. *Adv. Polym. Sci.* **2010**, *242*, 29–89.
- Schulz, D. N.; Pfeiffer, D. G.; Agarwal, P. K.; Larabee, J.; Kaladas, J. J.; Soni, L.; Handwerker, B.; Garner, R. T. *Polymer* **1986**, *27*, 1734–1742.
- Huglin, M. B.; Radwan, M. A. *Polym. Int.* **1991**, *26*, 97–104.
- Chen, L.; Honma, Y.; Mizutani, T.; Liaw, D.; Gong, J. P.; Osada, Y. *Polymer* **2000**, *41*, 141–147.
- Arotcarena, M.; Heise, B.; Ishaya, S.; Laschewsky, A. *J. Am. Chem. Soc.* **2002**, *124*, 3787–3793.
- Virtanen, J.; Arotcarena, M.; Heise, B.; Ishaya, S.; Laschewsky, A.; Tenhu, H. *Langmuir* **2002**, *18*, 5360–5365.
- Aoki, T.; Nakamura, K.; Sanui, K.; Ogata, N.; Kikuchi, A.; Okano, T.; Sakurai, Y. *Proc. Int. Symp. Controlled Release Bioactive Mater.* **1996**, *23*, 767.
- Nagaoka, H.; Ohnishi, N.; Eguchi, M. Thermoresponsive Polymer and Production Method Thereof. U.S. Patent 2007/0203313-A1, August 30, **2007**.
- Shimada, N.; Ino, H.; Maie, K.; Nakayama, M.; Kano, A.; Maruyama, A. *Biomacromolecules* **2011**, *12*, 3418–3422.
- (a) Haas, H. C.; Schuler, N. W. *Polym. Lett.* **1964**, *2*, 1095–1096; (b) Haas, H. C.; Moreau, R. D.; Schuler, N. W. *J. Polym. Sci. Part A-2: Polym. Phys.* **1967**, *5*, 915–927; (c) Haas, H. C.; Chiklis, C. K.; Moreau, R. D. *J. Polym. Sci. Part A-1: Polym. Chem.* **1970**, *8*, 1131–1145; (d) Haas, H. C.; MacDonald, R. L.; Schuler, A. N. *J. Polym. Sci. Part A-1: Polym. Chem.* **1970**, *8*, 1213–1226; (e) Haas, H. C.; Manning, M. J.; Mach, M. H. *J. Polym. Sci. Part A-1: Polym. Chem.* **1970**, *8*, 1725–1730; (f) Haas, H. C.; MacDonald, R. L.; Schuler, A. N. *J. Polym. Sci. Part A-1: Polym. Chem.* **1970**, *8*, 3405–3415.
- Marstokk, O.; Nyström, B.; Roots, J. *Macromolecules* **1998**, *31*, 4205–4212.
- Ostrovskii, D.; Jacobsson, P.; Nyström, B.; Marstokk, O.; Kopperud, H. B. M. *Macromolecules* **1999**, *32*, 5552–5560.
- IUPAC. In Compendium of Chemical Terminology, 2nd ed. (the "Gold Book"; compiled by A. D. McNaught and A. Wilkinson); Blackwell Scientific Publications: Oxford, **1997**. XML online corrected version: <http://goldbook.iupac.org> (2006) created by M. Nic, J. Jirat, and B. Kosata; updates compiled by A. Jenkins. ISBN 0-9678550-9-8; doi:10.1351/goldbook.
- Seuring, J.; Frank, F. M.; Huber, K.; Agarwal, S. *Macromolecules* **2012**, *45*, 374–384.
- Feil, H.; Bae, Y. H.; Feijen, J.; Kim, S. W. *Macromolecules* **1993**, *26*, 2496–2500.
- Kunugi, S.; Tada, T.; Yamazaki, Y. *Langmuir* **2000**, *16*, 2042–2044.
- Schild, H. G.; Tirrell, D. A. *J. Phys. Chem.* **1990**, *94*, 4353–4356.
- Mumick, P. S.; McCormick, C. L. *Polym. Eng. Sci.* **1994**, *34*, 1419–1428.
- Ding, Y.; Ye, X.; Zhang, G. *Macromolecules* **2005**, *38*, 904–908.
- Seuring, J.; Agarwal, S. *Macromolecules* **2012**, *45*, 3910–3918.
- Glatzel, S.; Badi, N.; Päch, M.; Laschewsky, A.; Lutz, J. *Chem. Commun.* **2010**, *46*, 4517–4519.
- Handbook of RAFT Polymerization; Barner-Kowollik, C., Ed.; Wiley-VCH: Weinheim, **2008**.
- Wood, M. R.; Duncalf, D. J.; Rannard, S. P.; Perrier, S. *Org. Lett.* **2006**, *8*, 553–556.
- Kurenkov, V. F.; Abramova, L. I. *Polym. Plast. Technol. Eng.* **1992**, *31*, 659–704.
- Wu, X.; Lu, C.; Wu, G.; Zhang, R.; Ling, L. *Fibers Polym.* **2005**, *6*, 103–107.
- Schilli, C.; Lanzendörfer, M. G.; Müller, A. H. E. *Macromolecules* **2002**, *35*, 6819–6827.
- Huber, S.; Hutter, N.; Jordan, R. *Colloid Polym. Sci.* **2008**, *286*, 1653–1661.
- Xia, Y.; Burke, N. A. D.; Stöver, H. D. H. *Macromolecules* **2006**, *39*, 2275–2283.
- Hofmeister, F. *Arch. Exp. Pathol. Pharmacol.* **1888**, *24*, 247–260.
- Zhang, Y.; Furyk, S.; Bergbreiter, D. E.; Cremer, P. S. *J. Am. Chem. Soc.* **2005**, *127*, 14505–14510.
- Zhang, Y.; Cremer, P. S. *Curr. Opin. Chem. Biol.* **2006**, *10*, 658–663.

## Publication 6

### **A Review Article: Polymers with Upper Critical Solution Temperature in Aqueous Solution**

Jan Seuring, Seema Agarwal, *Macromolecular Rapid Communications* **2012**.

DOI: 10.1002/marc.201200433

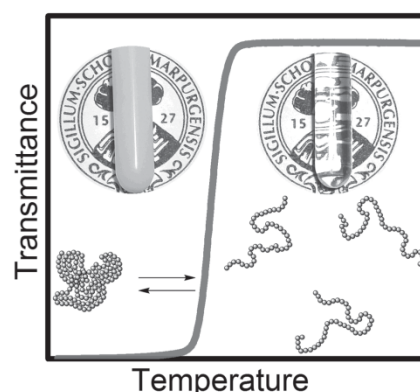
#### **Author contributions**

Literature research and writing of the manuscript was done by Jan Seuring. Prof. Seema Agarwal was responsible for supervision, discussion of the content and correction of the manuscript.

# Polymers with Upper Critical Solution Temperature in Aqueous Solution

Jan Seuring, Seema Agarwal\*

This review focuses on polymers with upper critical solution temperature (UCST) in water or electrolyte solution and provides a detailed survey of the yet few existing examples. A guide for synthetic chemists for the design of novel UCST polymers is presented and possible handles to tune the phase transition temperature, sharpness of transition, hysteresis, and effectiveness of phase separation are discussed. This review tries to answer the question why polymers with UCST remained largely underrepresented in academic as well as applied research and what requirements have to be fulfilled to make these polymers suitable for the development of smart materials with a positive thermoresponse.



## 1. Introduction

Thermoresponsive polymers have been subject to extensive research in academic and applied polymer science over the last decades. A thermoresponsive polymer undergoes drastic property changes upon small changes of temperature. Among them, water-soluble thermoresponsive polymers are of special interest because water is the cheapest and safest solvent as well as the solvent of living systems allowing application in the huge field of biochemistry and medicine. Although other property changes are conceivable (e.g., thermochrome polymers), the vast majority exhibits a change of hydrophilicity with temperature. This group of polymers is divided into polymers that phase separate from solution upon heating and those that phase separate upon cooling. The first display a lower critical solution temperature (LCST) in their phase

diagram the latter an upper critical solution temperature (UCST). The motivation behind research in this field is the development of so-called “smart” applications that exploit this kind of responsivity. Examples are switchable hydrophilic–hydrophobic surfaces,<sup>[1–3]</sup> chromatography,<sup>[4]</sup> temperature-triggered drug release,<sup>[5,6]</sup> targeted drug delivery,<sup>[7]</sup> gene therapy,<sup>[8,9]</sup> thermally switchable optical devices,<sup>[10]</sup> or bioseparation.<sup>[11–13]</sup> However, with few exceptions applications were demonstrated only for LCST polymers and due to the need of special monomers commercial applications remained restricted to small scales like coatings for cell-culture dishes<sup>[14–16]</sup> or bioseparation.<sup>[17]</sup>

Reviews on water-soluble thermoresponsive polymers are numerous. We like to refer to an excellent recent review of Aseyev et al.<sup>[18]</sup> As they have already pointed out there are about 60 reviews on “stimuli-responsive polymers” or “thermoresponsive polymers” each year (Scifinder scholar, word search, 2005–2010). It is suspicious, however, that the reviews deal almost exclusively with polymers that show an LCST in water and the few examples of UCST polymers are merely a side note, if at all. Between 2005–2010, about 330 publications per year

Dipl. Chem. J. Seuring, Prof. S. Agarwal  
Philipps-Universität Marburg, Department of Chemistry and  
Scientific Center for Materials Science, Hans-Meerwein Straße,  
35032, Marburg, Germany  
E-mail: agarwal@staff.uni-marburg.de

were on “LCST” in contrast to only 44 on “UCST” of which just one per year dealt with UCST behavior in water. A second misbalance is apparent within the class of LCST polymers where the vast majority of publications deal with PNiPAAm (average of 460 per year, 2005–2010). Other LCST polymers like poly(oligo(ethylene glycol)methacrylate) or the structural isomer poly(2-isopropyl-2-oxazoline) account for just 21 or six publications per year, respectively.

This is the first review dealing exclusively with polymers that exhibit a UCST in aqueous solution. It is a unique situation for a review that the number of publications concerning water-soluble UCST polymers is so small that each can be discussed in quite detail. It is not only the scope of this review to present a comprehensive collection of all known UCST polymers but also to answer the question why the thermoresponsivity of these polymers could not get the attention of polymer chemists. The authors feel that applied polymer chemists underestimate the importance of the polymer phase diagram and focus too much on merely tuning the phase transition temperature in dilute solution. Apart from its commercial availability, the hegemony of PNiPAAm in the realm of LCST polymers can be explained by its particular phase diagram. For this reason, the physical basis of the UCST transition as well as synthesis and characterization will be equally discussed. Finally, we try to conclude apparent structure–property correlations from the available data, direct basic research, and suggest strategies for the development of UCST polymers that can compete to the broad applicability of PNiPAAm.

Not included in this review are interpolymer complexes showing UCST behavior or polymers that show a UCST in water–organic solvent mixtures because the underlying theory is even more complex, and we consider them less promising candidates for application. From our point of view, the systems with the fewest components and simplest structures are the most valuable as they simplify the deduction of structure–property relationships. Furthermore, their property of interest (here UCST) is usually dependent on fewer variables allowing a broader application.

### 1.1. The Physical Basis

The aim of this section is to briefly review the classic approach for the explanation of polymer phase diagrams, show its limitations regarding aqueous polymer solutions, and point out where recent discoveries in the field of UCST polymers could help to refine our understanding of aqueous polymer solutions. For a more general and comprehensive understanding of the equilibrium thermodynamics of polymer phase diagrams, the reader is encouraged to consult the monograph “Polymer Phase Diagrams” of Koningsvald, Stockmayer, and Nies.<sup>[19]</sup>



**Jan Seuring** received a Diploma in Chemistry from the University of Marburg in 2009 with a thesis on polymerizable surfactants. During his undergraduate studies, he made a half year research internship in Prof. Peter Lay’s group at the University of Sydney working on potential anti-diabetic molybdenum complexes. He is currently working on his Ph.D. in the group of Prof. Seema Agarwal on polymers with upper critical solution temperature in water. His research interests are water-soluble polymers, stimuli-responsive polymers, and colloid and interface science.



**Seema Agarwal** is an apl professor at Philipps-Universität Marburg, Germany. She did double masters in chemistry and polymers science and technology and later obtained her Ph.D. from the Indian Institute of technology, Delhi, India. She was a Humboldt Fellow from 1997–1999 in the laboratory of Prof. Andreas Greiner, Germany. She accomplished her habilitation for macromolecular chemistry in 2007 at the University of Marburg. She is a recipient of Hermann-Schnell award. She has more than 100 scientific publications in different journals and coauthored a book on electrospinning. Her research interests are responsive polymers, biodegradable polymers and bio materials, controlled polymerizations, and electrospinning.

### 1.2. The Phase Behavior of Polymer Solutions

Above the UCST and below the LCST, a solute is miscible with a solvent in all proportions.<sup>[20]</sup> This definition implies that below the UCST and above the LCST there is a miscibility gap over a certain range of compositions in which phase separation occurs.<sup>[21]</sup> The phase behavior is conveniently displayed by isobaric phase diagrams where temperature is plotted versus the solute concentration as shown schematically for UCST behavior in Figure 1.

Coming from the one-phase region (homogeneous solution), the binodal curve denotes the temperature–composition pairs where phase separation into a solute rich and solute poor phase sets in. The composition of the two phases can be determined by drawing a tie-line that connects the two branches of the binodal at a given temperature. Assuming a mixture of two compounds A and B with the mole fraction  $c_{1a}$ , the compounds are miscible at the temperature  $T_1$ . When decreasing the temperature to the phase-separation temperature  $T_p$  (here  $T_2$ ), phase separation sets in with a second phase of composition  $c_{1b}$  on the verge of appearing. Further decreasing the

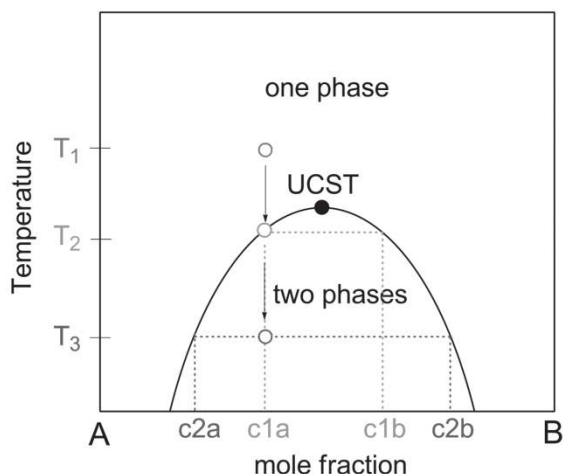


**Figure 1.** Idealized phase diagram of a strictly binary mixture with UCST miscibility gap. The composition of the coexisting phases can be determined by drawing tie-lines in between the two branches of the binodal (coexistence curve).

temperature to  $T_3$  favors the separation of A from B and the composition of the coexisting phases change to  $c_{2a}$  and  $c_{2b}$ . In strictly binary mixtures, the UCST is defined as the maximum of the binodal. These fundamentals are true for all kinds of mixtures including low molar mass compounds, polymer solutions as well as polymer blends, and the shape of the phase diagram decides how effective phase separation occurs. This is directly related to how drastic the hydrophilic–lipophilic switch of, for example, a modified surface will be and it becomes clear that not only tuning of the UCST is of importance but tuning the shape of the whole phase diagram.

To construct the phase diagram, one has to compare the Gibbs energy of the homogeneous solution with the Gibbs energy of two coexisting phases. In equilibrium, the system will favor the state of lower Gibbs energy. The Gibbs energy of mixing  $\Delta G$  can be described by an equation independently derived by Staverman and Van Santen, by Huggins and by Flory (FHS model, Equation 1).<sup>[22–27]</sup>

$$\frac{\Delta G}{NRT} = \left(\frac{\phi_1}{m_1}\right) \ln(\phi_1) + \left(\frac{\phi_2}{m_2}\right) \ln(\phi_2) + g\phi_1\phi_2 \quad (1)$$

The first two terms in Equation 1 represent the ideal or combinatorial part of the entropy of mixing. The combinatorial entropy of mixing for polymers is based on a lattice model where an arbitrary lattice site volume is defined and  $m$  denotes the number of lattice sites that are occupied by a molecule. In case of polymer solutions,  $m_2$  is far greater than  $m_1$ . Using this model, it turned out to be handier to describe the composition in terms of the volume fraction  $\phi_2$ . The FHS model shows that the combinatorial entropy of mixing is much smaller for polymers than for low molar mass compounds. Therefore, even

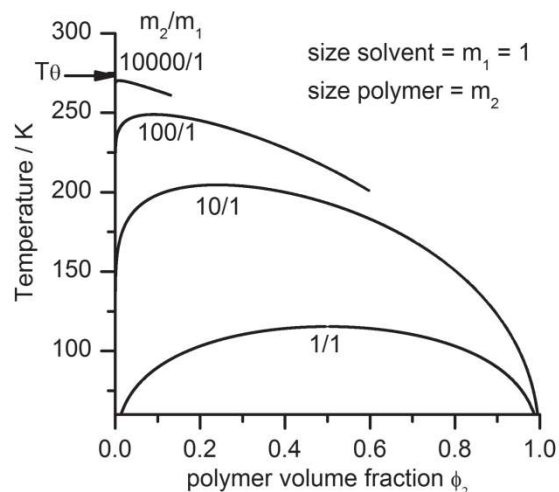


**Figure 2.** Binodals calculated on the basis of Equation 1 with varying values of  $m_1$  and  $m_2$ .

little interaction can cause miscibility gaps. For modeling phase diagrams, it is common practice to introduce the interaction parameter  $g$ . Assuming simple van der Waals forces, Figure 2 shows the influence of molar mass represented by the  $m_2/m_1$  ratio on the phase diagram.

The UCST increases with increasing chain length due to the decreasing entropy of mixing. Disparity in size causes the critical composition to shift into the solvent-rich region. This is in agreement with the observation that mixtures of low molar mass compounds like n-hexane/aniline show a symmetric miscibility gap with a critical volume fraction of about 0.5,<sup>[28]</sup> while the phase diagram of poly(ethylene) in diphenylether is highly asymmetric.<sup>[29,30]</sup> Figure 2 illustrates the  $\theta$  temperature, which corresponds to the UCST for  $m \rightarrow \infty$  and  $\phi_2 \rightarrow 0$ . In other words, the  $\theta$  temperature is the extrapolated upper critical solution temperature of a polymer solution with infinite molar mass and a concentration of zero. The asymmetry is not always as large as shown for the system polystyrene in cyclohexane.<sup>[31,32]</sup> Here, the top around the UCST is flattened and extends in the high concentration region. This behavior is attributed to the concentration dependence of the interaction parameter  $g$ , which normally increases monotonically in non-polar systems. Among the causes are the change in chain connectivity and variability with concentration.<sup>[33–35]</sup> Hence, the concentration dependence differs with molar mass. Strong concentration dependence can also explain the flat phase diagram of poly(ethyl acrylate) in isopropanol<sup>[36]</sup> or bimodal phase diagrams as for polystyrene in acetone.<sup>[37]</sup> That polymers can show an LCST or even both UCST and LCST are due to complex temperature dependencies of the interaction parameter  $g$  (Figure 3).

The interaction parameter can be modified to account for both concentration and temperature dependence



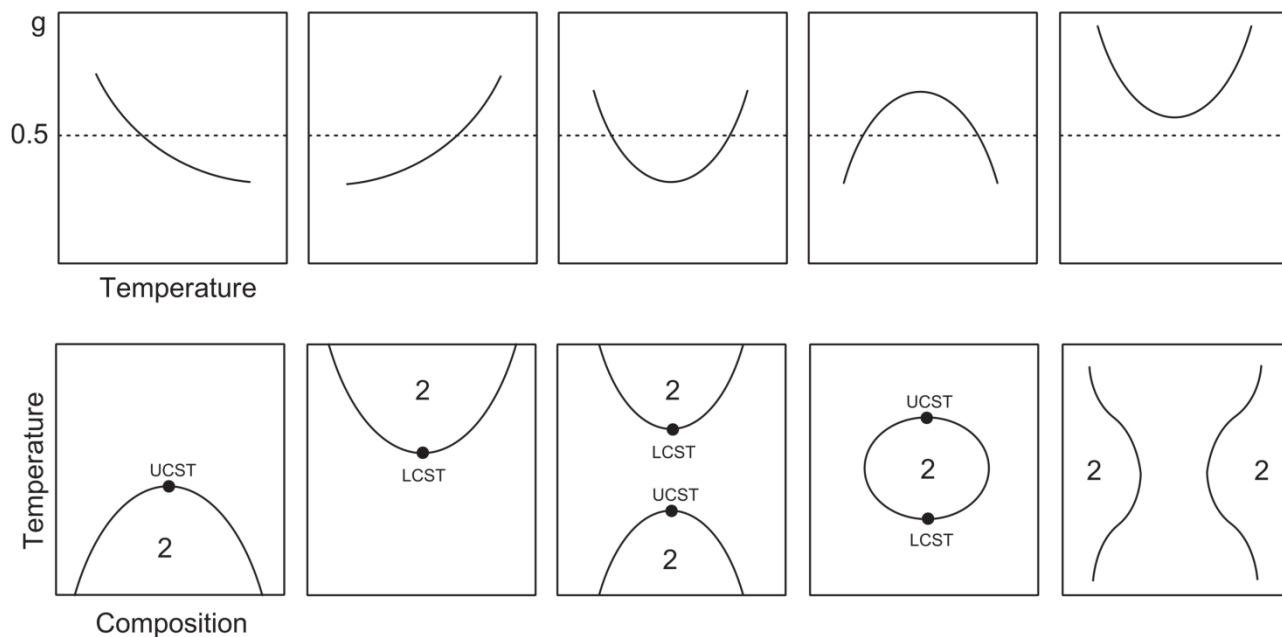


Figure 3. Correlation between the temperature dependence of the interaction parameter  $g$  and the type of miscibility gap. “2” denotes the two-phase region.

using a polynomial in  $\phi_2$  (Equation 2) where each  $g_k$  may depend on temperature like, for example, Equation 10.

$$g = \sum_{k=0}^n g_k \phi_2^k \quad k = 0, 1, 2, 3, \dots, n \quad (2)$$

$$g_k = g_{k0} + \frac{g_{k1}}{T} + g_{k2}T \quad g_{k0}, g_{k1}, g_{k2} = \text{const.} \quad (3)$$

Another important feature of polymer solutions with high melting polymers is that a solid–liquid phase equilibrium will appear at high polymer concentrations.<sup>[38]</sup> For polymers with high  $T_g$ , a similar observation is made and it is convenient to add this data to the phase diagram although it is no real equilibrium.<sup>[39]</sup> This is schematically shown in Figure 4 and can severely affect the phase-separation process. The  $T_g$  of a polymer drops with increasing solvent content. The intersection of the  $T_g$  composition curve with the binodal is called Berghmans point. Phase separation above the Berghmans point results in two liquid phases and the composition of the two coexisting phases can be determined by tie-lines according to Figure 1. However, when phase separation occurs below the Berghmans point, the polymer-rich phase will vitrify before it has reached its equilibrium composition defined by the binodal.

In the discussion above, it was assumed that the polymer solution is strictly binary. This is never true for polymer solutions. Even if a polymer can be synthesized in a narrow distribution, current methods do not

allow a perfectly uniform molar mass and a mixture of different chain lengths is obtained. For this reason, a polymer solution is only a quasi-binary mixture and the molar mass distribution has to be taken into account. One can measure the appearance of first cloudiness in such systems but the obtained cloud-point curve differs from a simple binodal. Phase separation is accompanied by fractionation and the composition of the coexisting phases cannot be visualized by tie-lines as shown in Figure 1. The critical point is not the maximum of the

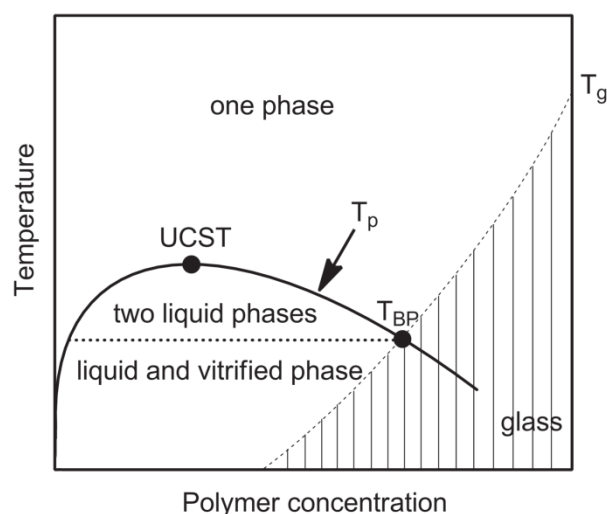


Figure 4. Possible phase diagram for a strictly binary polymer-solvent mixture with a high  $T_g$  polymer.

cloud-point curve and is found at higher polymer concentrations. In comparison to the strictly binary mixture, the maximum of the cloud-point curve is shifted in direction of the solvent-rich region and to higher temperatures. It is called the threshold temperature. The FHS model can be extended to account for dispersity.<sup>[40,41]</sup> Moreover, in quasi-binary mixtures, three-phase equilibria can appear. As a consequence, the curvature of the cloud-point curve changes sign and shoulders close to the critical point are observed.<sup>[42,43]</sup> These are general effects of the molar mass distribution, which are not related to end-group effects. For end-group effects,  $\overline{M}_w/\overline{M}_n$  is of importance as will be discussed separately for the individual cases. However, for simplicity, the terminology of strictly binary mixtures will be used throughout this review unless explanation of certain observations demands otherwise.

### 1.3. The Phase Behavior of Polymers in Water

Polymers that are water soluble need to contain polar groups that are able to interact with water by dipole–dipole interactions and hydrogen bonding (enthalpy) thereby avoiding the strong hydrophobic effect in water (entropy). These types of interactions exhibit a stronger and more complex (nonmonotonic) concentration and temperature dependence than simple van der Waals interactions in organic solvents. Although modification of the interaction parameter according to Equation 2 can result in fairly accurate fittings of the experimental data, it has no direct molecular basis and does not provide insight into the molecular origin of miscibility gaps. The strong concentration dependence of the interaction in aqueous polymer solutions can lead even to off-zero critical points for infinite molar masses.<sup>[44]</sup> Since this discovery, the phase behavior of polymers is divided into three classes. The classical type I where the critical point for infinite molar mass is found at zero concentration, type II with one stable critical point that is not influenced by molar mass, and type III with two critical points. In type III, one critical point is stable and the other shifts to zero for infinite molar masses. Examples are the LCST behavior of PNiPAAm (type II)<sup>[45]</sup> and poly(vinylmethylether) (type III).<sup>[46]</sup> As the phase behavior of aqueous polymer solutions is dominated by strong polar interactions tailored models need to be employed to consider these interactions. For instance, an accurate theoretical prediction of the bimodal LCST and adjacent UCST miscibility gaps of PVME has been achieved by Nies and Van Durme by mapping the thermodynamic perturbation theory of Wertheim for saturation interaction (e.g., hydrogen bonding) on the FHS model. They also predicted two separate UCSTs in the supercooled state, which were just recently verified by experiment.<sup>[47]</sup> The phase behavior of poly(ethylene oxide) (PEO) could be modeled by taking competitive PEO–water and water–water hydrogen bonding into account.<sup>[48]</sup> Experimentally

reported values were used for the enthalpy and entropy of hydrogen bonding. Later, the same model was improved by including the nature of the endgroups.<sup>[49]</sup> To explain the very flat phase diagram of PNiPAAm, the concept of cooperative hydration has been introduced.<sup>[50,51]</sup> For the nonionic polymers that will be presented in this review, data concerning phase diagrams is scarce. However, further studies regarding the complete phase diagrams including the glass transition temperatures in the high concentration region would be very rewarding. Much could be learned about the concentration and molar mass dependence of different types of interaction as well as the efficiency of phase separation in these novel systems.

### 1.4. Methods for Characterization of the Phase Transition

In principle, all methods developed to characterize the phase transition of LCST polymers can be applied to investigate the UCST-type phase transition. Measuring the cloud point using a turbidity meter is the easiest and therefore most common way to follow phase separation in polymer solutions. At this point, it is very important to emphasize the difference between UCST–LCST, phase-separation temperature, and cloud point. The UCST–LCST is found only at the maximum/minimum of the binodal, that is, at a distinct critical polymer concentration. The phase-separation temperature describes the phase boundary of the system in equilibrium and is concentration dependent. The cloud point upon cooling and heating denotes the temperature where the solution becomes turbid and clears, respectively. Because of kinetic hindrance and aging in the collapsed state, the cloud points upon cooling and heating measured by a turbidity meter do not coincide with the phase-separation temperature. Typically, heating–cooling rates of 1 K/min are employed and all cloud points given in this review were measured at this rate unless stated otherwise. The difference between the cloud point upon cooling and heating is called hysteresis. In applied polymer science, most literature on thermoresponsive polymers deals with PNiPAAm. In the special case of PNiPAAm, the LCST and phase-separation temperature are very close together over a wide range of concentrations and the phase transition is very fast resulting in a tiny hysteresis. On the one hand, this explains the ease of application and large success of PNiPAAm, on the other hand, it explains why sometimes the term LCST is mistakenly used where it is in fact only the phase-separation temperature or cloud point.

Comparing cloud points measured by different experimenters is difficult for a number of reasons. The definition of the cloud point varies. Some note the appearance of first cloudiness, for example, the drop from 100% to 90% transmittance, others take the temperature at 50% transmittance or the inflection point of the turbidity

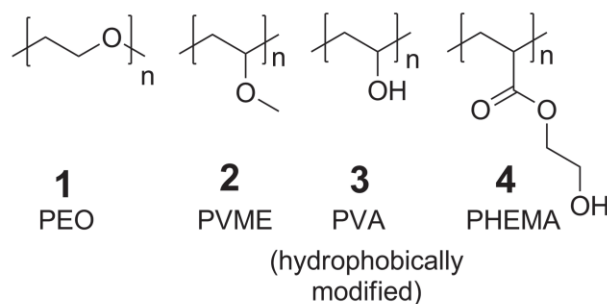
curve. Which method is most suitable depends on the actual shape of the turbidity curve. The cloud points depend on the heating–cooling rate and the transition from the two-phase to the one-phase region is influenced by the thermal history in the two-phase region. For reproducibility of cloud-point measurements, it is absolutely necessary to state the polymer concentration, the heating rate, and range as well as the definition of the cloud point. This is not restricted to turbidimetry and applies for all other methods of cloud-point determination. From the cloud points at different heating–cooling rates, one can extrapolate the phase transition temperature for zero heating rate. This can be done conveniently by using an automatic melting point apparatus.<sup>[52]</sup>

Differential scanning calorimetry is a powerful tool to analyze phase-separation processes because it allows separating enthalpic from entropic effects. However, first results for UCST polymers that rely on polymer–polymer hydrogen bonds show that the heat of transition is very small and ultrasensitive calorimeters have to be employed.<sup>[53]</sup> Static and dynamic light scattering was used to detect the coil-to-globule transition of single PNiPAAM chains in water or poly(styrene) in cyclohexane.<sup>[54,55]</sup> Due to disturbing aggregates, direct proof of the single-chain coil-to-globule transition of a UCST polymer in water could not yet be obtained although the collapse of aggregates was apparent.<sup>[53]</sup> Moreover, by light scattering, the second virial coefficient  $A_2$  and the  $\theta$  temperature can be determined, which gives important information regarding intermolecular interactions and the thermodynamic quality of the solvent. Hydrogen bonding and hydrophobic interaction between polymers and water can be investigated via NMR, IR, or fluorescence techniques.<sup>[56–59]</sup>

## 2. Polymers with UCST in Water Below 0 or Above 100 °C

Theoretically, most of the polymers show both an LCST and a UCST in a given solvent, which arises from the interaction parameter and its temperature dependence. The question is whether the phase transition takes place under conditions where the solvent is in its liquid state. Some well-established polymers are known to exhibit a UCST in water although under relatively extreme conditions (Scheme 1).

One example is poly(ethylene oxide) (PEO, **1**) that shows a loop-shaped miscibility gap with UCST > LCST.<sup>[60–62,48,49]</sup> The center of the loop is located at approximately 200 °C. At low molar masses < 3 kg mol<sup>-1</sup>, the critical volume fraction is about 0.2. As anticipated, the miscibility gap becomes larger, increasingly asymmetric and the critical points shift to the solvent-rich region as the molar mass increases. For instance, at  $\bar{M}_w = 15$  kg mol<sup>-1</sup>, the critical volume fraction is 0.1 with an LCST of 120 °C and a UCST



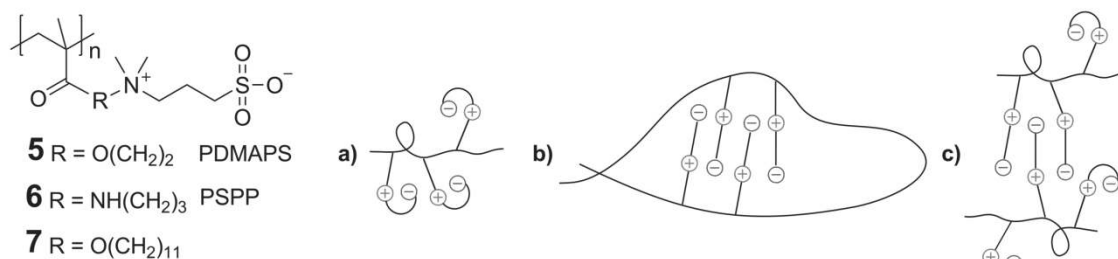
**Scheme 1.** Polymers with UCST in aqueous solution below 0 or above 100 °C.

of 296 °C.<sup>[62]</sup> A second UCST is expected in the supercooled state as indicated by the  $\theta$  temperature of  $-12 \pm 3$  °C.<sup>[18]</sup>

As mentioned previously, in addition to its bimodal LCST behavior, poly(vinyl methyl ether) (PVME, **2**) exhibits two UCST miscibility gaps in the low and high concentration region at about  $-15$  and  $-25$  °C, respectively.<sup>[46,47]</sup> UCST-type phase separation was proven by a combination of modulated temperature differential scanning calorimetry and wide angle x-ray diffraction.

Hydrophobically modified poly(vinyl alcohol)s (PVA, **3**) can show loop-shaped miscibility gaps with LCST < UCST. With few exceptions, the UCST is higher than 100 °C. One example is poly(ethylene-co-vinyl alcohol)s with ethylene contents greater than about 3 mol%. The critical volume fraction was about 0.025 and the gap decreased with decreasing ethylene content and molar mass until LCST and UCST merged at about 80 °C.<sup>[63]</sup> Other examples are partially butyl-functionalized PVAs.<sup>[64]</sup> Samples with butyl contents of 7.6 or 9.6 mol% and a molar mass of 134 kg mol<sup>-1</sup> showed a UCST of 103 or 108 °C, respectively, at a critical volume fraction of around 0.01. Although polymer complexes are beyond the scope of this review, it is worth mentioning at this place that there are mixtures of PVAs with a different degree of hydrolysis that display both UCST and LCST (UCST < LCST) while the single components are completely water-soluble or show only an LCST.<sup>[65]</sup>

Poly(hydroxyethylmethacrylate)s (PHEMA, **4**) with molar weights lower than 6 kg mol<sup>-1</sup> can show partial miscibility with water. For a sample with  $\bar{M}_n = 4$  kg mol<sup>-1</sup>, Longenecker et al.<sup>[66]</sup> showed a loop-shaped miscibility gap that is not so surprising when comparing the polymer structure of PHEMA to hydrophobically modified PVA. Both polymers have a well-balanced hydrophilicity–hydrophobicity and possess an alcohol functionality. The cloud points were measured as a function of polymer concentration. At a concentration of 0.1 wt%, the polymer was soluble over the whole temperature range. The cloud point increased from 80 to >90 °C with increasing the concentrations from 0.2 to 0.5 wt% suggesting a UCST above



**Scheme 2.** The UCST of zwitterionic polymers relies on intra- and intermolecular coulomb interaction: a) intragroup, b) intrachain, c) interchain.

100 °C. When HEMA was copolymerized with the cationic comonomer 3-(methacryloylamino)propyl]trimethylammonium chloride (MAPTAC), the miscibility gap disappeared but reappeared upon screening the charges with NaCl.

### 3. Polymers with UCST in Water within the 0–100 °C Range

#### 3.1. Zwitterionic Polymers

The rheological properties and self-assembly of zwitterionic polymers in solution have been studied extensively but research focused mainly on the interaction with low molar mass or polymeric electrolytes.<sup>[67–69]</sup> Although it appears to be a common feature of zwitterionic polymers, few studies were devoted to thermoresponsivity. The crucial differences in comparison to cationic and anionic polyelectrolytes are the different forms of self-association as shown in Scheme 2. These are responsible for the antipolyelectrolyte behavior, salt-dependent solubility, and thermoresponsivity.

To the best of our knowledge, the only compounds where turbidity curves and a partial phase diagrams of the homopolymers are available are poly-3-dimethyl(methacryloyloxyethyl) ammonium propane sulfonate (PDMAPS, **5**)<sup>[70,71]</sup> and poly(3-[N-(3-methacrylamidopropyl)-N,N-dimethyl]ammonio propane sulfonate (PSPP, **6**).<sup>[72]</sup>

The phase diagrams show an unusual dumbbell shape. Figure 5 depicts the partial phase diagram of PDMAPS with a UCST of 32 °C at 0.1 wt% and a minimum of 15 °C at 8 wt%.<sup>[70]</sup> The phase diagram is heavily affected by the molar mass. As expected, the miscibility gap narrows with decreasing molar mass but experiments are inconsistent on whether the critical point shifts into the solvent-rich region<sup>[71]</sup> according to the FHS model or remains independent of molar mass.<sup>[72]</sup> Salts disturb intra- and intermolecular association of the zwitterions by decreasing

the Debye length  $l_D = (4\pi \cdot l_B \cdot c_s)^{-0.5}$ , where  $l_B$  is the Bjerrum length in pure water and  $c_s$  is the concentration of added salt. The Debye length represents the distance at which opposite charges sense each other, hence, salt addition enhances the solubility of polyelectrolytes and lowers the UCST. For instance, a 0.1 wt% solution of PDMAPS with  $\bar{M}_w = 7.1 \times 10^5 \text{ g mol}^{-1}$  showed a cloud point upon cooling of about 55 °C in pure water.<sup>[70]</sup> Upon increasing the NaCl concentration from 0.05, over 0.1 to 0.3 wt%, the cloud point dropped to 45, over 39 to 18 °C.

Solubility promotion is even stronger for NaBr and NaI, which is explained by the stronger binding to ammonium ions. However, Mary et al.<sup>[72]</sup> found that solubility promotion does not start before reaching a crossover concentration, which was determined to be in the region of  $1 \times 10^{-3} \text{ M}$ . They calculated that when the salt concentration exceeds the crossover concentration, the Debye length falls below the average distance of opposite charges in the salt-free polymer coil, thus providing an argument for the onset of solubility promotion. Moreover, it was revealed

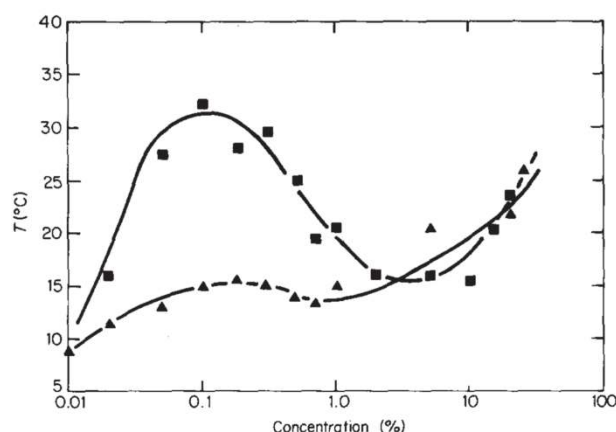


**Figure 5.** Effect of polymer concentration and salt on PDMAPS phase behavior.  $\bar{M}_w = 435 \text{ kg mol}^{-1}$ ; squares = cloud points upon cooling in pure water; triangles = cloud points in 0.3 wt% (0.05 M) NaCl. Reprinted with permission.<sup>[70]</sup> Copyright 1986, Elsevier.

that upon addition of very small amounts of NaCl, the cloud points of high molar mass PDMAPS and PSPP actually increased until reaching the crossover concentration. They explained this observation by charge asymmetries that were compensated by the addition of salt. This was supported by nonzero absolute values of the zeta-potential in pure water that decreased upon addition of salt. The negative zeta-potential of PDMAPS in pure water was rationalized by a substantial amount of hydrolysis (12%–15%), which occurs naturally during the synthesis and leads to negatively charged carboxylate groups. Yet, the positive zeta-potential of PSPP in pure water remained unexplained.

Chen et al.<sup>[73]</sup> have shown that solubility promotion is also observed when polymeric electrolytes like the polyanion poly(2-acrylamido-2-methyl-propane sulfonic acid) (PAMPS) are added. Statistical copolymers of DMAPS and NiPAAm showed both UCST and LCST behavior.<sup>[74]</sup> The cloud points varied with composition. For blockcopolymers consisting of a first block of PDMAPS and a second block of poly(*N,N*-diethylacrylamide)<sup>[75]</sup> or POEGMA,<sup>[76]</sup> the cloud points were in the same range as for the respective homopolymers. In contrast to the homopolymers or statistical copolymers, the blockcopolymers formed stable dispersions suggesting the formation of micelles where the blocks in core and corona can switch places depending on the temperature. Likewise, Arotcarena and co-workers<sup>[77,78]</sup> synthesized a blockcopolymer of PSPP and PNiPAAm.<sup>[77,78]</sup> Polymer **7** is a polysoap due to its undecyl linker between backbone and zwitterionic betaine group. At high molar masses of about 500 kg mol<sup>-1</sup>, it shows a cloud point of about 35 °C in dilute aqueous solution but similar to PDMAPS does not show a cloud point at physiological sodium chloride concentrations.<sup>[79]</sup> In addition to its thermoresponsive properties, polymer **7** exhibits surface activity as expected for polysoaps.

Although it is not a conventional polybetaine, Gonsior and Ritter<sup>[80]</sup> demonstrated that by noncovalent host-guest interactions of cyclodextrine-containing polyelectrolytes and adamantyl carboxylates, pseudo-betaine structures can form. These poly(pseudo-betaine)s display UCST behavior similar to the examples discussed above.

PDMAPS has already been employed in material science. The polymer was utilized for the synthesis of thermoresponsive hydrogels.<sup>[81,82]</sup> In analogy to its solution properties, a volume-phase transition was found in pure water, which disappeared at physiological NaCl concentrations. Furthermore, PDMAPS was successfully grafted onto nanoparticles of<sup>[60]</sup> fullerene, gold, and crosslinked polystyrene.<sup>[83–85]</sup> The particle shell was shown to reversibly swell and deswell at high and low temperature, respectively.

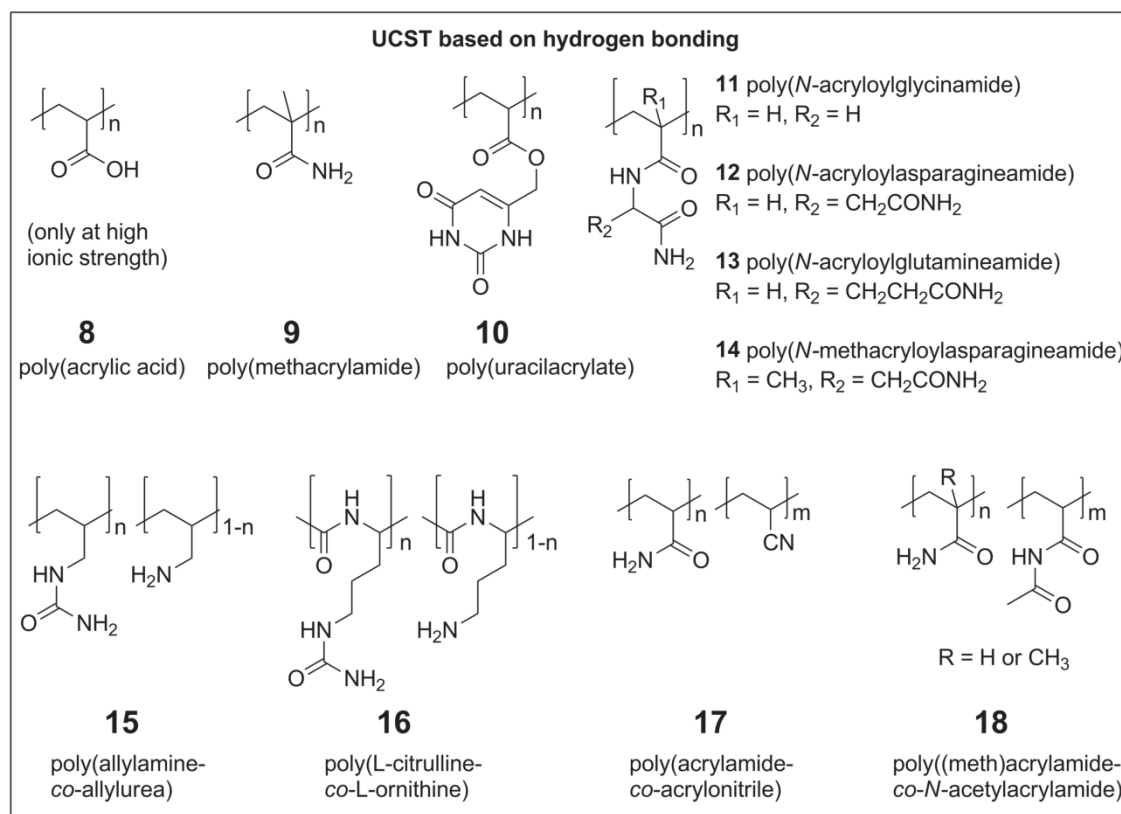
### 3.2. Polyelectrolytes in the Presence of Multivalent Counterions

It is known that like-charged polyelectrolytes—including important biopolymers like DNA—can undergo gelation as well as macroscopic phase separation in the presence of oppositely charged particles or multivalent ions.<sup>[86]</sup> Similar to polyzwitterions, most studies focused on critical additive concentrations and the type of additive but only few studies dealt with the temperature dependence of the phase separation. Jia et al.<sup>[87]</sup> synthesized a blockcopolymer consisting of PEO and poly(2-vinylpyridine) (P2VP). At low pH, the P2VP block is cationic due to protonation of the pyridine moiety and the polymer is water soluble. Addition of divalent peroxodisulfate ions below a critical temperature led to condensation of P2VPH<sup>+</sup> chains, forming the core of stable micelles. Above the critical temperature or upon reducing the peroxodisulfate ions to sulfate, dissociation of the micelles was observed. A similar finding was made by Plamper et al.<sup>[88]</sup> who added the trivalent anion [Co(CN)<sub>6</sub>]<sup>3-</sup> to poly(*N,N*-dimethylaminoethyl methacrylate) (PDMAEMA). At pH values > 9, PDMAEMA is uncharged and shows LCST behavior. Below pH 9, PDMAEMA behaves as a cationic polyelectrolyte and UCST-type phase separation could be observed upon cooling in the presence of [Co(CN)<sub>6</sub>]<sup>3-</sup>. Photoinduced ligand exchange to divalent [Co(CN)<sub>5</sub>H<sub>2</sub>O]<sup>2-</sup> weakened the bridging ability and, thus, reduced the cloud point. It is necessary to note that the above observations could only be made in buffer solution (ionic strength ≈ 0.1 M).

Judging by these reports, polyelectrolytes seem to possess an intrinsic ability for UCST behavior in the presence of multivalent counterions although a delicate balance of ionic strength, pH, and ion valency is required to observe it.

### 3.3. Carboxylic Polymers at Low pH or High Ionic Strength

In contrast to the pH-responsivity of poly(acrylic acid) (PAAc, **8**, Scheme 3), which has been studied in every detail and exploited in the field of smart materials, the UCST-type thermoresponsivity in aqueous solutions of high ionic strength is rarely mentioned. Although the UCST is also based on thermoreversible hydrogen bonding, the phase behavior is heavily influenced by the dissociation state and interaction with electrolytes. Flory and Osterheld<sup>[89]</sup> made the first cloud-point measurements of poly(acrylic acid) with a degree of neutralization of  $\alpha = 0.33$ . A comprehensive analysis of the cloud points as a function of sodium chloride concentration, degree of neutralization, molar mass, and polymer concentration in the dilute solutions was conducted by Buscall and Corner.<sup>[90]</sup> In pure water, there is no UCST behavior but cloud points



**Scheme 3.** Polymers with a UCST that is based on intra- and intermolecular hydrogen bonding. Copolymers are not included unless copolymerization is necessary to observe UCST behavior.

are observed for NaCl concentrations of  $400 \times 10^{-3} \text{ M}$  and above for unneutralized PAAc with  $\overline{M}_n > 20 \text{ kg mol}^{-1}$ . In most cases, the cloud-point curves are not strictly convex to the x-axis. As discussed previously, such shapes can be observed when the mixtures are not binary. Apart from the molar mass distribution, this is mainly due to the NaCl additive, which makes it, per definition, a ternary mixture. The cloud points increased linear with the square root of the molar mass and linear with NaCl concentration. The  $\theta$  temperatures were determined at various NaCl concentrations (0.4–2.16 M) for different degrees of neutralization (0–0.48).

Copolymers with AAC can also show a UCST. An enlightening example is the copolymers with 10, 17, and 29 mol% of NiPAAm that have been studied by Bokias et al.<sup>[91]</sup> With increasing NiPAAm content, they showed increased UCST, both UCST and LCST, and finally only LCST-type cloud points in aqueous NaCl solutions. In pure water, however, they did not show UCST behavior. Similar observations were made for copolymers of AAC and diethylacrylamide.<sup>[92]</sup>

Mori et al.<sup>[93]</sup> synthesized copolymers of AAC with vinylacetamide that exhibited both UCST and LCST behavior (apparently a closed loop miscibility gap) at,  $\overline{M}_w = 16 \text{ kg mol}^{-1}$ , pH < 3, and 0.5 M Na<sub>2</sub>SO<sub>4</sub>.

Of course, the carboxyl group that is responsible for the thermally reversible hydrogen bonding may be part of monomers other than acrylic acid. Similar to the observations reported by Mori<sup>[94]</sup> for poly(AAc-co-vinylacetamide), the blockcopolymer from *N*-acryloyl-L-proline methyl ester (A-Pro-OMe) and *N*-acryloyl-4-trans-hydroxy-L-proline (A-Hyp-OH) with a block unit ratio of 27:73 showed both UCST and LCST at, pH < 3 and 0.1 M NaCl.<sup>[94]</sup> Interestingly, the corresponding random copolymer did not show responsivity and was soluble over the whole temperature range. This may be attributed to a more efficient hydrogen bonding between two acid units compared to other possible pairings.

### 3.4. Poly(uracilacrylate)

Although poly(uracilacrylate) (PAU, **10**) has been synthesized earlier,<sup>[95]</sup> its thermoresponsivity was first recognized by Aoki et al.<sup>[96]</sup> who reported that “transmittance for purified homopolymer, poly(6-acryloyloxymethyluracil) (PAU), aqueous solution was 0% below 20 °C and 100% at higher temperatures”. Addition of urea decreased the cloud point, which was an indication that the UCST-behavior was based on thermoreversible hydrogen bonding. In the same report, they copolymerized uracilacrylate with

acrylamide and methylene-bis-acrylamide as crosslinker to receive a hydrogel that underwent swelling changes with temperature. From the data shown, it is impossible to say whether the degree of swelling was a continuous or discontinuous function of temperature (thermosensitivity or thermoresponsivity). In a succeeding publication, Aoki et al.<sup>[97]</sup> analyzed the influence for urea, adenosine, guanosine, and poly(adenylic acid) additives on the cloud point upon cooling of a 0.1 wt% aqueous PAU-solution. PAU was synthesized by free-radical polymerization in DMF using the nonionic initiator AIBN [the choice of solvent and initiator can have crucial influence on the UCST behavior as will be discussed for poly(*N*-acryloylglycinamide)]. In pure water, the cloud point was 60 °C. All additives caused a decrease of the cloud point by preventing the polymer from self-association. As expected, the effect was stronger for adenosine and poly(adenylic acid) as these compounds carried adenine allowing a more specific interaction with the complementary uracil moiety.

### 3.5. Poly(*N*-acryloylglycinamide) and Copolymers

Poly(*N*-acryloylglycinamide) (PNAGA, **11**) is currently the most studied polymer with a UCST based on thermally reversible hydrogen bonding. Conclusions made for PNAGA appear to be valid for all other polymers of this type, justifying a detailed review.

PNAGA was first synthesized in 1964 by Haas and Schuler.<sup>[98]</sup> They found that the polymer can form thermoreversible gels in concentrated aqueous solutions, similar to gelatin. Haas et al.<sup>[99]</sup> showed that hydrogen bond interrupting agents like thiocyanate or urea can prevent the formation of the gel and that the gel melting temperature increased with molar mass and concentration. Furthermore, they calculated that the average number of groups involved in a crosslink is too low to form crystallites.<sup>[100]</sup> This was supported by the very low heat of formation per crosslink. They estimated it to be  $-5$  to  $-12$  kcal mol<sup>-1</sup> of crosslinks.<sup>[101]</sup> They concluded that the crosslinking is based on randomly distributed hydrogen bonds. In dilute solutions, PNAGA does not show thermoreversible gelation. However, despite looking transparent and homogeneous, the solution contains polymer aggregates. This was first evidenced by a nonlinear dependency of the reduced viscosity from the polymer concentration in pure water and the fact that the viscosity dropped significantly upon addition of sodium thiocyanate.<sup>[99]</sup> About 30 years later, the presence of aggregates in dilute solution and their destruction by thiocyanate was confirmed by light scattering.<sup>[102]</sup> The fact that the physical crosslinking is based on thermoreversible hydrogen bonding was further evidenced by analyzing the shifts of the CO and NH-bands in the Raman spectrum.<sup>[103]</sup>

Haas and Schuler considered that free-radical polymerization of NAGA in water–alcohol mixture with

potassium peroxydisulfate as initiator were the most convenient reaction conditions. Hence, in all subsequent studies, these conditions were employed. Lutz and co-workers<sup>[104]</sup> reported controlled radical polymerization of NAGA by the RAFT process using sodium 3-(((benzylthio)carbonothioyl)thio)propane-1-sulfonate (BCPS) as CTA and 2,2'-Azobis[2-(2-imidazolin-2-yl)propane]dihydrochloride (VA-044) as initiator. The critical gelation concentration increased from  $>20$  wt% for  $\bar{M}_n = 16\,900$  g mol<sup>-1</sup> to  $\approx 4.5$  wt% for  $\bar{M}_n = 92\,500$  g mol<sup>-1</sup>.

Although studying the thermoreversible gelation of PNAGA, a UCST-type phase separation had not been reported. The thermoreversible gelation of concentrated PNAGA solutions involves no phase separation since the gel is only one phase with homogeneous properties. The formation of aggregates in dilute solution can be regarded as a form of microphase separation. However, a preliminary temperature depending light scattering study of PNAGA suggested that these aggregates are thermodynamically stable above the phase transition temperature and no macrophase separation sets in.<sup>[53]</sup> It is yet unclear whether there is a distinct temperature where aggregates form/break but most likely these aggregates are just thermosensitive rather than thermoresponsive. This means one would expect a behavior comparable to micelles that show a gradual decrease of the aggregation number with temperature. The first hint that the homopolymer of PNAGA might show UCST behavior was given by Ohnishi et al. They have shown UCST behavior for three derivatives of PNAGA<sup>[105]</sup> (see next section) and copolymers of NAGA with *N*-acetylacrylamide and biotin-functionalized methacrylamide.<sup>[106]</sup> Copolymers with NAGA were prepared by free-radical polymerization in DMSO using the nonionic initiator AIBN. The copolymers with biotin-functionalized methacrylamides were used for different bioseparation techniques. For instance, enzymes were bound to the biotin and could be recovered from solution after substrate conversion by phase separation upon cooling. Copolymers of NAGA and biotin-functionalized methacrylamide were also used for the development of magnetic nanoparticles called Thermamax.<sup>[107]</sup> The copolymer was immobilized at the surface of magnetite particles. Consequently, this system was used to separate substances with affinity to biotins, for example, avidin, from solution by flocculation below the cloud point and applying a magnetic field.

Despite the development of quite sophisticated biomedical applications, Ohnishi et al.<sup>[107]</sup> did not report the UCST of the PNAGA homopolymer or publish basic studies about the solution properties of its copolymers. Using the reaction conditions from the patents and a slightly altered monomer synthesis, the UCST-type phase transition of the PNAGA homopolymer was reported by us in 2010.<sup>[108]</sup> The cloud points from 0.03 to 5.4 wt% and gel melting points up to about 14 wt% of PNAGA in water are shown in Figure 6.

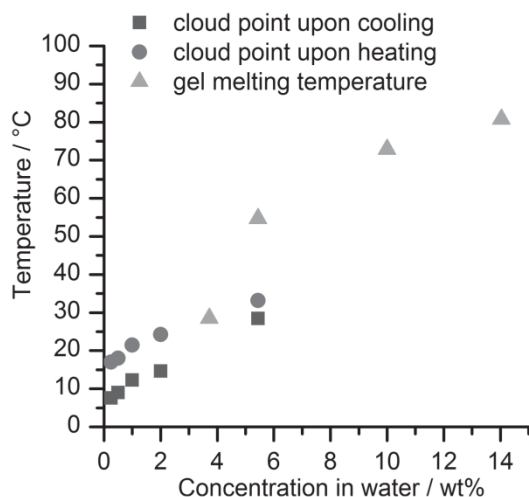


Figure 6. Cloud points of PNAGA in pure water as function of concentration. Data from [108].

However, at this time, it was not clear why Haas, Marstokk, Ostrovski, and Lutz could not observe the UCST of poly(NAGA) during their work and why the pioneering patents of Ohnishi did not get appropriate attention. It turned out that traces of ionic groups in the polymer dramatically suppress the UCST.<sup>[53]</sup> Ionic groups can be introduced intentionally or unintentionally in a multitude of ways (Scheme 4).

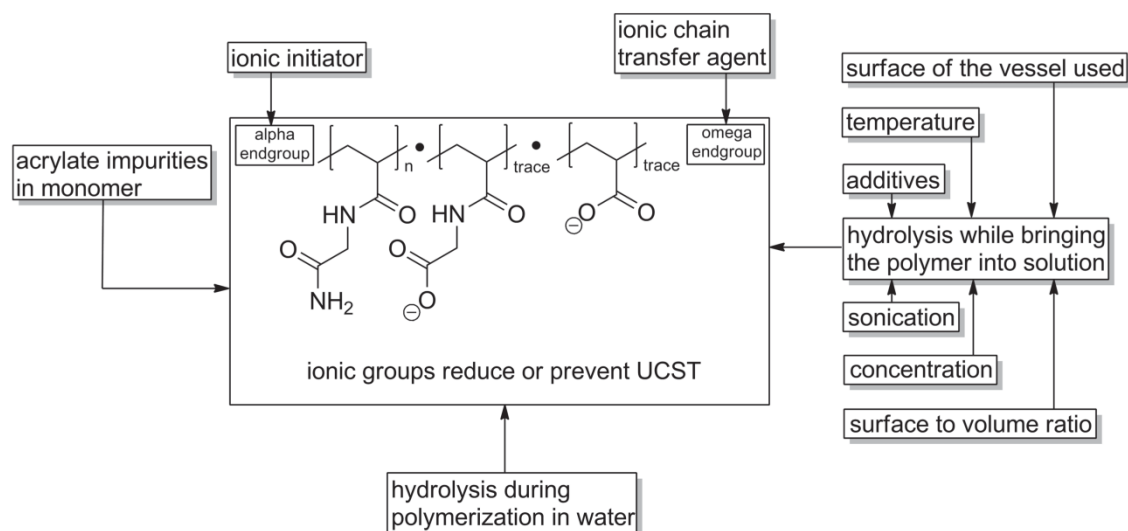
Acrylic acid or acrylate impurities in the monomer, hydrolysis during polymerization or processing introduces carboxyl groups into the polymer chain that dissociate at neutral pH. Amides are relatively stable against hydrolysis, especially at neutral pH. However, despite proceeding slowly hydrolysis does occur as shown for poly(acrylamide).<sup>[109,110]</sup> Since even trace amounts of ionic

groups significantly decrease the phase-separation temperature, hydrolysis must be taken into account and it is necessary to choose the dissolution conditions carefully. The influence of the temperature, time, and vessel material on the dissolution state and UCST behavior was investigated qualitatively for 1 wt% aqueous solutions.<sup>[53]</sup>

Accordingly, ionic radical initiators or ionic chain transfer agents strongly influence the cloud point. It was shown for poly(NAGA) synthesized by the RAFT process that at least up to a molar mass of  $25 \text{ kg mol}^{-1}$ , an ionic chain end prevents phase separation in pure water but the UCST suppressing effect can be counteracted by the addition of electrolytes.<sup>[53,111]</sup> Figure 7 demonstrates that added salts have two simultaneous effects.

First, they shield possible ionic groups. Second, they influence the cloud points according to the Hofmeister series of ions, which was established to describe the effect of ions on the solubility of proteins.<sup>[112]</sup> In the case of poly(NAGA) and copolymers NaSCN and NaCl act as chaotropes while  $\text{Na}_2\text{SO}_4$  acts as kosmotrope.<sup>[108,111,113]</sup> Such correlations according the Hofmeister series were also found for LCST polymers like PNiPAAm. Here, the effect of salts was thoroughly investigated and even helped to revise the underlying mechanism of the Hofmeister series.<sup>[114,115]</sup> It is now clear that ions act via polarization effects, surface tension, and direct ion binding and therefore could affect thermoresponsivity in a different manner. Real biological fluids are complex and contain both chaotropic and kosmotropic agents making the UCST behavior very difficult to predict. However, it was shown that PNAGA retains its UCST in human blood serum.<sup>[53]</sup>

The huge impact of ionic groups on the cloud point of PNAGA may be explained by its relatively low endothermic heat of transition (see “Section 4”). The heat of the LCST



Scheme 4. Pathways of (unintentional) introduction of charged groups into UCST polymers drawing on the example of PNAGA. Reprinted with permission.<sup>[53]</sup> Copyright 2012, American Chemical Society.



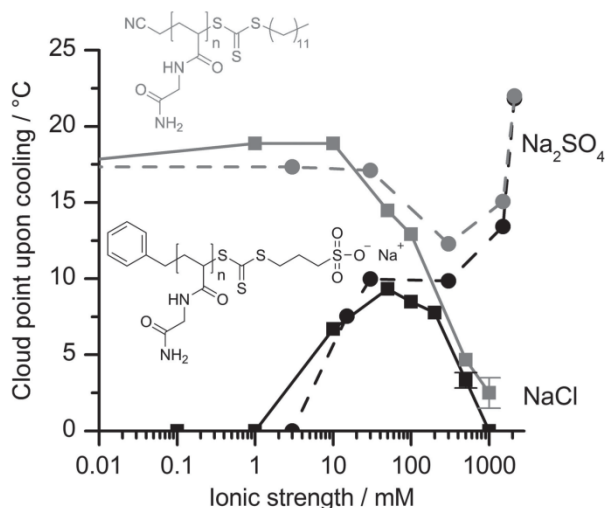


Figure 7. Cloud point of 0.2 wt% aqueous solutions of PNAGA with different chain ends as a function of ionic strength for different types of salt.<sup>[111]</sup>

transition of PNiPAAm is around  $42\text{--}76\text{ J g}^{-1}$ .<sup>[116–118]</sup> The heat of the UCST transition of PNAGA was only  $0.7 \pm 0.4\text{ kcal g}^{-1}$  and ultrasensitive DSC had to be employed to detect it.<sup>[53]</sup>

In order to investigate the effect of the molar mass distribution on the UCST behavior of PNAGA and lay the basis for grafting on substrates, controlled radical polymerization of NAGA via RAFT was performed using a nonionic initiator and a nonionic CTA.<sup>[121]</sup> PNAGA showed cloud points in pure water as well as electrolyte solution (Figure 7). The cloud points of nonionic poly(NAGA) were independent of molar mass from  $15\text{ to }35\text{ kg mol}^{-1}$ . Below  $15\text{ kg mol}^{-1}$ , the cloud points increased due to the hydrophobic dodecyl endgroup derived from the CTA. The turbidity curves became very broad below  $8\text{ kg mol}^{-1}$ . This could be explained by the dispersity of the molar mass distribution. Below  $8\text{ kg mol}^{-1}$ , the molar mass dependence of the cloud point becomes very strong, thus, the mixture of different chain lengths causes a broad turbidity curve. Following the same logic, the effect of dispersity is less pronounced at higher molar masses.

It is well known that the phase-separation temperature of LCST polymers increases by copolymerization with hydrophilic comonomers and decreases with hydrophobic comonomers and the same concept should apply to UCST polymers. For discussion of the thermodynamic reasons see “Section 4.” The hypothesis was confirmed by decreasing the cloud point of PNAGA by copolymerization with various amounts of the hydrophilic comonomer *N*-acetyl acrylamide<sup>[108]</sup> and increasing the cloud point by copolymerization with the hydrophobic comonomers butyl acrylate or styrene.<sup>[119]</sup> Although the concept worked as anticipated it turned out that for a reversible and sharp phase transition, the choice of monomer

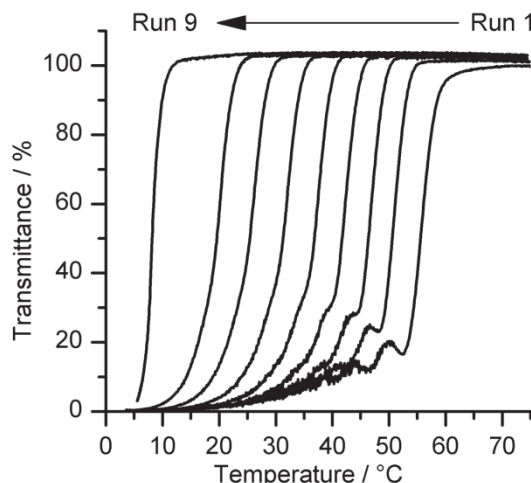


Figure 8. Gradual decrease of the cloud point of poly(BA-co-NAGA) caused by ester hydrolysis. Reprinted with permission.<sup>[119]</sup> Copyright 2012, American Chemical Society.

regarding hydrolytic stability and copolymerizability is crucial. Alkyl (meth)acrylates are considerably less stable to hydrolysis than alkyl acrylamides. Even in PBS where the salt should be able to compensate for small amounts of carboxylate groups, the cloud point of 1.0 wt% solution of poly(BA-co-NAGA) with 21 mol% BA in the polymer decreased from 60 to 5 °C within nine measurement cycles (Figure 8).

Styrene cannot hydrolyze but showed adverse copolymerization behavior with NAGA. The significant difference in the copolymerization parameters leads to an increasing heterogeneity of the copolymer compositions with conversion. Each copolymer composition shows a different cloud point, thus explaining the very broad transitions observed for high conversions (Figure 9).

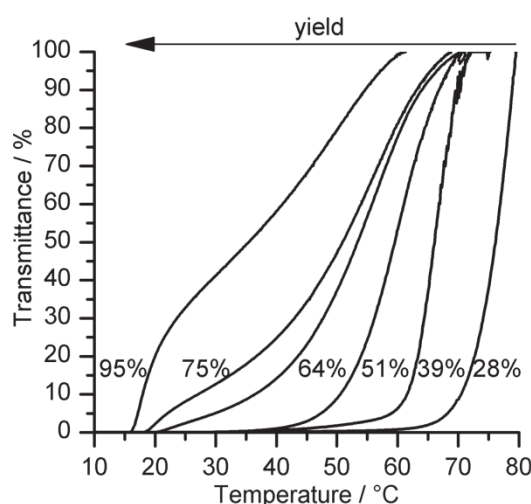


Figure 9. Copolymerization of NAGA with styrene. The UCST transition becomes broader with increasing conversion. Reprinted with permission.<sup>[119]</sup> Copyright 2012, American Chemical Society.

■ Table 1. Derivatives of PNAGA with UCST in water. Data from Ohnishi and co-workers.<sup>[105]</sup>

Polymer <sup>a)</sup>	$\bar{M}_n$ <sup>b)</sup> [kg mol <sup>-1</sup> ]	Cloud points <sup>c)</sup>
poly( <i>N</i> -acryloylasparagineamide) ( <b>12</b> )	16	22 °C in pure water 25 °C in 20 × 10 <sup>-3</sup> M Tris-HCl, pH 8
poly(methacryloylasparagineamide) ( <b>14</b> )	22	13 °C in pure water 33 °C (LCST type) in pure water 13 °C in PBS 30 °C (LCST type) in PBS
poly( <i>N</i> -acryloylglutamineamide) ( <b>13</b> )	17	2 °C in 40 × 10 <sup>-3</sup> M Tris-HCl, pH8 3 °C in 80 × 10 <sup>-3</sup> M Tris-HCl, pH8

<sup>a)</sup>ammonium peroxodisulfate was used as initiator; <sup>b)</sup>measured by GPC in 0.1 M NaNO<sub>3</sub> as eluent, calibration standard not given; <sup>c)</sup>c(polymer) = 0.2% (w/v), it was not specified whether it is the cloud point upon heating or cooling.

A hydrophobic monomer that shows both hydrolytic stability and better copolymerization behavior is acrylonitrile as demonstrated for copolymers with acrylamide.<sup>[119]</sup>

### 3.6. Derivatives of Poly(*N*-acryloylglutamineamide)

Ohnishi and co-workers<sup>[105]</sup> synthesized derivatives of NAGA using the same route as Haas and Schuler. Free-radical polymerization was performed in water using ammonium peroxodisulfate as a radical initiator. All characterization details available were summarized in Table 1.

*N*-acryloylasparagineamide (NAAAm, **12**) differs from NAGA by the substitution of a hydrogen atom of the side chain methylene group by a methylenecarbonyl group, hence introducing a second primary amide that is capable of forming additional hydrogen bonds. A 0.2% (w/v) solution of PNAAAm showed cloud points in pure water as well as 20 × 10<sup>-3</sup>M Tris-HCl buffer of 22 and 25 °C, respectively. The introduction of a methyl group to the polymer backbone in the case of PNMAAAm (**14**) led to a decrease of the UCST-type cloud point to 13 °C and the appearance of an LCST-type cloud point at 30 °C. By intuition one would expect an increase of the cloud point upon introduction of a hydrophobic methyl group but the opposite was the case. Similar observations have been made for the LCST polymer PNiPAAm and PMiPAAm.<sup>[120,121]</sup> The increase of LCST may be of enthalpic origin since the exothermic heat of mixing  $\Delta H_m$  increases with the introduction of an alpha methyl group.<sup>[122,123]</sup> However, the molecular cause of this increase is yet unclear. The cloud points of both PNAAAm and PNMAAAm synthesized by Ohnishi et al. did not change significantly upon addition of electrolytes.<sup>[105]</sup> This is an indication that the monomers were relatively free from acrylic acid and acrylate impurities. Despite their sulfate alpha chain end derived from

the charged initiator, the polymers show a cloud point in pure water. Two explanations are feasible. In contrast to PNAGA, PNAAAm, and PNMAAAm may exhibit stronger interpolymer hydrogen bonding due to the second primary amide group. Also, free-radical polymerization leads to a broad molar mass distribution. The relatively high cloud points observed by Ohnishi et al. were most likely caused by the high molar mass fractions, which are less influenced by the ionic chain end. This is supported by the fact that PNAAAm with a similar sulfonate endgroup, the same number-average molar mass, but narrow dispersity of 1.22 (later synthesized via RAFT) showed a much lower cloud point of only 4 °C.<sup>[124]</sup> Although the title of the corresponding publication suggests that the polymers are uncharged, the polymer chain ends are charged and their effect is strongly visible. The cloud point upon cooling decreased with molar mass (Figure 10A).  $T_c$  of a 1.0 wt% solution in pure water of a polymer with  $\bar{M}_n = 100$  kg mol<sup>-1</sup> was 26 °C, while  $T_c$  of sample with 17.3 kg mol<sup>-1</sup> was only 4 °C. That ionic chain ends decrease the cloud point, hydrophobic chain ends increase the cloud point, and that this effect gets stronger toward lower molar masses has been demonstrated for PNAGA. The fact that PNAAAm shows cloud points even at  $\bar{M}_n < 20$  kg mol<sup>-1</sup> where PNAGA with ionic chain ends does not may be attributed to stronger interpolymer hydrogen bonding due to the second primary amide group of the NAAAm repeating unit. As discussed in the theoretical part of this review, one should expect that a higher  $\Delta H$  value caused by increased interpolymer hydrogen bonding diminishes the negative impact of ionic groups. A partial phase diagram of PNAAAm of  $\bar{M}_n = 100$  kg mol<sup>-1</sup> and  $\bar{M}_n/\bar{M}_w = 1.22$  is shown in Figure 10B.

For Poly(*N*-acryloylglutamineamide) (**13**), no cloud point was given in pure water and the cloud points in 40 and 80 × 10<sup>-3</sup> M Tris-HCl buffer were very low with 2 and 3 °C,

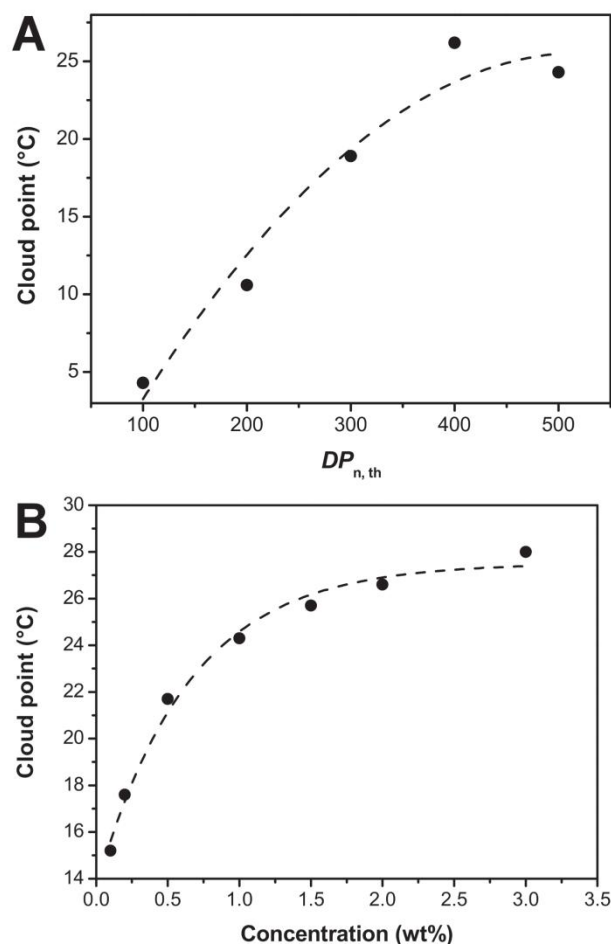
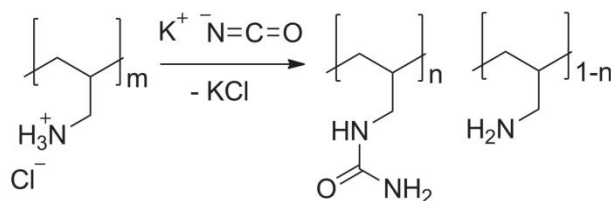


**Figure 10.** Cloud points of 1 wt% aqueous solutions of PNAAAm with sulfonate endgroups A: as function of molar mass; B: as a function of polymer concentration with  $\bar{M}_n = 100 \text{ kg mol}^{-1}$ . Reprinted with permission.<sup>[124]</sup> Copyright 2011, American Chemical Society.

respectively.<sup>[105]</sup> This is in contrast to the expectation that the more hydrophobic ethylenecarbamoyl substituent should lead to higher cloud points. It is not clear whether this is true or caused by impurities in the monomer.

### 3.7. Ureido-Modified Polymers

Shimada et al.<sup>[125]</sup> synthesized ureido-modified polymers by a polymer analogous approach (Scheme 5), which is an



**Scheme 5.** Synthesis of poly(allylamine-co-allylurea) by modification of poly(allylamine).

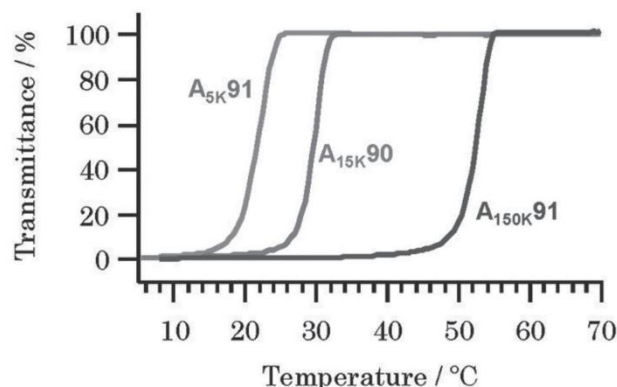


**Figure 11.** Transmittance curves of poly(allylamine-co-allylurea)s in electrolyte ( $150 \times 10^{-3} \text{ M NaCl}$ ,  $10 \times 10^{-3} \text{ M HEPES-NaOH}$  buffer, pH 7.5) with an allylurea content of about 91%. The indexes 5K, 15 K, and 150 K mean  $\bar{M}_w = 5, 15,$  and  $150 \text{ kg mol}^{-1}$ , respectively. Reprinted with permission.<sup>[125]</sup> Copyright 2011, American Chemical Society.

interesting alternative to the vinyl monomer-based UCST polymers. Commercially available poly(allylamine) hydrochlorides or poly(L-ornithine) hydrobromides of different molar masses were reacted with potassium cyanate to transform the amine groups into ureido groups.

The resulting poly(allylamine-co-allylurea)s (**15**) and poly(L-ornithine-co-L-citrulline)s (**16**) had a varying degree of functionalization. The UCST-type phase transition of 0.1 wt% solutions was studied as a function of molar mass and degree of functionalization. The cloud points were measured in  $10 \times 10^{-3} \text{ M HEPES-NaOH}$  buffer (pH 7.5) containing  $150 \times 10^{-3} \text{ M NaCl}$ . For instance, the  $T_c$  of poly(allylamine-co-allylurea)s with a degree of functionalization of around 91% increased with molar mass from 25 °C ( $\bar{M}_w = 5 \text{ kg mol}^{-1}$ ) over 32 °C ( $\bar{M}_w = 15 \text{ kg mol}^{-1}$ ) to 54 °C ( $\bar{M}_w = 150 \text{ kg mol}^{-1}$ ) (Figure 11).

Furthermore, at pH 7.5, the cloud points increased with the degree of functionalization, which is actually more related to a decrease of the residual amine content. For poly(L-ornithine-co-L-citrulline)s, the same trends were observed. At pH 7.5, amines ( $pK_a$  value around 9) are partially protonated, thus the polymers carry cationic charges. The UCST suppressing effect is the same as observed for anionic charges caused by carboxyl groups in PNAGA. Since the percentage of residual amine groups was higher than 1 mol%, the UCST lowering effect was strong and could not be fully compensated by the presence of  $150 \times 10^{-3} \text{ M NaCl}$ . These conclusions are supported by the fact that beyond pH 9, the cloud points were independent of the residual amine content. Additionally, the effect of different salts on the cloud points of poly(allylamine-co-allylurea) solutions was tested. Polymers with residual amine contents of 7% and higher had no cloud point in pure water. Upon addition of salt, the cationic charges got shielded and a cloud point appeared until a maximum

was reached between  $200$  and  $400 \times 10^{-3} \text{M}$  of salt. The further addition enhanced the solubility and decreased the cloud point (“salting in”). The magnitude of “salting in” depended on the type of salt and appeared to follow the Hofmeister series. The hysteresis was about  $3 \text{ }^\circ\text{C}$  for PAUs and not stated for POCs. A certainly important feature of POC with regard to possible biomedical applications is its biodegradability.

### 3.8. Copolymers Based on Acrylamide

The eye-catching similarity of most known H-bond-based UCST polymers was that they all featured primary amide groups (Scheme 3, the primary amide group can be considered to be a part of the ureido group). Thus, the primary amide group appears to be the key functionality for the reversible hydrogen bonding. Acrylamide is the simplest monomer that features a primary amide group. However, poly(acrylamide) is one of the oldest known synthetic polymers and a UCST had never been reported. We have shown that the UCST of poly(acrylamide) must be below  $0 \text{ }^\circ\text{C}$  but can be increased into the  $0$ – $100 \text{ }^\circ\text{C}$  range by copolymerization with a hydrophobic comonomer.<sup>[119]</sup> This was demonstrated by free-radical copolymerization of acrylamide (free of acrylic acid, commercially available as electrophoresis grade) with acrylonitrile in DMSO using the nonionic initiator AIBN. The cloud points were freely tunable by the amount of acrylonitrile in the copolymer (Figure 12A). The hysteresis of the cloud points was about  $2 \text{ }^\circ\text{C}$  and the repeatability of the turbidity measurements was excellent (heating up to  $60 \text{ }^\circ\text{C}$ ). The cloud-point curve in phosphate buffered saline was not convex to the concentration-axis (Figure 12B). Possible reasons are that the system is not binary due to the presence of salts and the molar mass distribution or because of a complex concentration dependence of the intra- and interpolymer hydrogen bonding.

Thorough study of the literature revealed that Ohnishi et al.<sup>[126]</sup> patented a copolymer of (meth)acrylamide and *N*-acetylacrylamide (**18**) that showed a UCST as early as 1999. It is not straightforward to explain why this system shows UCST behavior. It is known that the homopolymers poly(*N*-acetylacrylamide) and poly(acrylamide) show a UCST in water–alcohol mixtures but in pure water they are completely soluble.<sup>[127]</sup> Mixing of both influenced the UCST in water–alcohol systems indicating the formation of interpolymer complexes. The fact that copolymers of AAm and NAcAAm can show a UCST in water must originate from an increase in interpolymer interaction. Apparently, the interaction enhancement is found only for particular compositions. Ohnishi et al.<sup>[126]</sup> used three AAm:NAcAAm feed ratios, namely 1:12, 1:11, and 1:10. The cloud points of the resulting polymers decreased from 24 over 12 to  $4 \text{ }^\circ\text{C}$  indicating a maximum interaction

at very low NAcAAm contents. For the analogue MAAm:NAcAAm series, the cloud points increased from 21 over 45 to  $55 \text{ }^\circ\text{C}$ . Here, the maximum interaction is presumably at higher NAcAAm contents. At that time, it was unknown that the homopolymer poly(methacrylamide) can show a UCST itself. The low value of  $21 \text{ }^\circ\text{C}$  at the feed ratio 1:12 was likely due to methacrylic acid impurities in the monomer. The above early examples demonstrate that the general rule that hydrophilic comonomers decrease the UCST is not always applicable. This is because hydrophilic comonomers are likely to participate in the interpolymer hydrogen bonding. When the two monomers form stronger hydrogen bonds to each other than to themselves an increase of the cloud points may be observed.

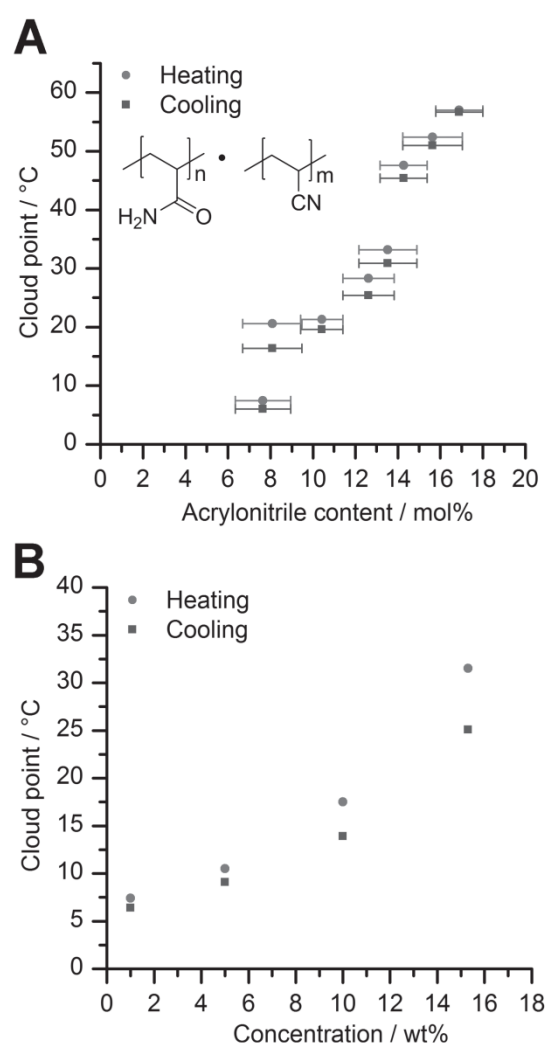


Figure 12. Cloud points of 1.0 wt% solutions in PBS of poly(AAm-co-AN)s A: as a function of acrylonitrile content; B: as a function of concentration. Reprinted with permission.<sup>[119]</sup> Copyright 2012, American Chemical Society.

### 3.9. Polymethacrylamide

Silberberg et al.<sup>[128]</sup> conducted temperature-dependent light scattering experiments on dilute aqueous poly(methacrylamide) (PMAAm, 9) solutions. These results indicated a  $\theta$  temperature in water at 6 °C and suggested the presence of intra- and intermolecular hydrogen bonds. Viscosity studies of Eliassaf<sup>[129]</sup> gave further support for the formation of hydrogen bonds. Despite these hints, PMAAm has never been shown to exhibit a UCST-type phase separation. It is important to note that Silberberg and Eliassaf used potassium persulfate as an ionic initiator. It is very likely that this was one of the causes that prevented them to observe phase separation upon cooling. We have synthesized poly(methacrylamide) by free-radical polymerization in DMSO using AIBN as an initiator.<sup>[119]</sup> Higher molar masses were not soluble in DMSO and the polymer precipitated during polymerization. The obtained polymer could be dissolved in pure water (70 °C and sonication) and a 1.0 wt% solution showed a  $T_c$  of 40.5 °C and a broad heating curve with  $T_h$  about 57 °C. The phase transition was very slow causing a strong hysteresis. It should be noted that so far no special characterization methods were employed to detect possible trace impurities of methacrylic acid in the monomer used (98%; Aldrich). Similar to poly(NAGA), the cloud points may vary with monomer purity.

The fact that PMAAm homopolymer shows a cloud point in the 0–100 °C range while PAAm homopolymer does not meet the expectation that an additional hydrophobic group should increase the UCST. However, it contradicts previous observations made for the pairs PNiPAAm/PiPMAAm and PNAAAm/PNMAAAm where an increase of LCST and a decrease of UCST have been observed, respectively. Although the difficult initial dissolution and strong hysteresis are drawbacks of this system, its simple molecular structure makes it very interesting for further studies.

### 3.10. Poly(*p*-dioxanone) Grafted onto PVA

The loop-shaped miscibility gaps of poly(ethylene-*co*-vinyl alcohol)s and butyl-functionalized PVAs have already been presented in the “Section 2.” Interestingly, Wu et al.<sup>[130]</sup> found that grafting poly(*p*-dioxanone) (PPDO) onto PVA can result in LCST or UCST behavior depending on the degree of polymerization ( $D_p$ ) of the PPDO side chains. UCST behavior was observed for  $D_p > 7$ . The cloud point of a 0.4 wt% solution in pure water could be tuned from 50 to 80 °C by adjusting the weight fraction of PPDO from 0.40 to 0.75. These results pose the question why hydrophobization with PPDO results in such a different phase behavior compared with poly(ethylene-*co*-vinyl alcohol)s and butyl-functionalized PVAs. A certainly significant difference is that PPDO provides additional hydrogen bond acceptor sites.

## 4. Tuning the Phase Transition Temperature: A Qualitative Approach

A qualitative concept is presented that enables the user to estimate and explain how the phase transition temperature  $T_p$  reacts to modification of a polymer. Additionally, it reveals one factor that influences the sharpness of the phase transition. The concept is applicable to both UCST and LCST polymers and could explain why  $T_p$  of water-soluble nonionic UCST polymers is more sensitive to introduction of ionic groups than  $T_p$  of LCST polymers. Furthermore, it may be a good starting point for the development of novel thermoresponsive polymers. Shortcomings are the neglect of temperature and concentration dependence of the enthalpic and entropic contributions. Estimation of the trend of  $T_p$  with polymer concentration and a prediction whether the system could show, for instance, a loop-shaped miscibility gap is not possible.

For simplicity of the qualitative discussion, it is reasonable to assume that the phases separate into pure solvent and pure polymer. Based on this assumption, a polymer dissolves in a solvent when the Gibbs energy of mixing is negative (Equation 4).

$$\Delta G_m = \Delta H_m - T \cdot \Delta S_m \quad (4)$$

According to Equation 4, polymers with UCST must have a positive  $\Delta H_m$  and  $\Delta S_m$  value at the phase-separation temperature  $T_p$ . At  $T_p$ , phase separation and mixing are in equilibrium, hence  $\Delta G_m$  is zero and Equation 4 simplifies to  $T_p = \Delta H_m / \Delta S_m$ . For explaining trends in  $T_p$ , one has to consider all possible contributions to  $\Delta H_m$  and  $\Delta S_m$  for the process of mixing (Table 2).

The relative magnitudes for the enthalpic contributions are based on the relative strength of interactions that increase in the order van der Waals forces < hydrogen bonds < ion–dipole < ion–ion. The strength of hydrogen bonds depends on the specific donor–acceptor pair. For example, alcohol–alcohol hydrogen bonds are weaker than amide–amide hydrogen bonds.<sup>[131]</sup> During the process of dissolution in water, polymer–polymer and water–water hydrogen bonds need to be cleaved while polymer–water hydrogen bonds form. A rough estimation which interactions are favored is possible by a model of Hunter.<sup>[131]</sup> A deficiency of such estimations is that they do not consider that polymer–polymer hydrogen bonding can be prevented by steric hindrance. The relative magnitudes for the entropic contributions are based on the FHS model that explains the only small combinatorial entropy of mixing for polymers compared with a large hydrophobic effect.<sup>[132,133]</sup> The ordered hydration shell of ionic groups does also account for a decrease of entropy depending on the charge density.<sup>[134]</sup>

For the FHS model, it was already mentioned that the interaction is temperature dependent. In terms of

Table 2. Contributions to the enthalpy and entropy of mixing in aqueous polymer solutions. The relative magnitude is indicated by the number of plus or minus signs.

Contribution to $\Delta H_m$	Sign and magnitude
Breaking polymer – polymer hydrogen bonds	++
Breaking water – water hydrogen bonds	++
Breaking polymer – polymer van der Waals forces	+
Formation of polymer – water hydrogen bonds	--
Solvation of ionic groups	---
Avoiding coulomb repulsion between same charges	----
Breaking the coulomb attraction between opposite charges (zwitterionic polymers)	++++
<b>Entropic Contributions:</b>	Contributions to $\Delta S_m$
Combinatorial entropy of mixing	+
Hydrophobic effect	---
Formation of the ordered hydration shell around ionic groups	- (soft ions) -- (hard ions)

Equation 4, it means that  $\Delta H_m$  and  $\Delta S_m$  are temperature dependent. This explains why some polymers can show both UCST and LCST. Both the UCST and LCST of polymers can be tuned by statistical copolymerization. As a general rule, hydrophobic comonomers increase the UCST and lower the LCST while hydrophilic comonomers cause the opposite.<sup>[119,135–137]</sup> In case of nonionic polymers, this effect is mainly attributed to an increase or decrease of the hydrophobic effect and the resulting change of  $\Delta S_m$  because the hydrophobic effect is large compared with the small combinatorial entropy of mixing for polymers. The contribution to the enthalpy of mixing from hydrophobes is usually negligible and close to zero.<sup>[132]</sup> A good example are nonionic copolymers of acrylamide and acrylonitrile.<sup>[119]</sup> Since the positive contributions of polymer–polymer, water–water hydrogen bonding, and polymer–polymer van der Waals forces are greater than the negative contribution of polymer–water hydrogen bonding,  $\Delta H_m$  is positive. Increasing the acrylonitrile content from 10 to 14 mol% increases the cloud point of a 1 wt% solution from 293 to 318 K (20 to 45 °C), which must correspond to the ratio  $\Delta H_m/\Delta S_m$ . Substitution of some acrylamide units by acrylonitrile units slightly diminishes the number of sites available for intermolecular hydrogen bonding, thus slightly diminishing  $\Delta H_m$ . As a consequence, the increase of the  $\Delta H_m/\Delta S_m$  ratio from 293 to 318 K (=  $T_p$ ) can only be explained by a significant decrease of  $\Delta S_m$  caused by the strong negative contribution of the hydrophobic effect, which is large compared to the for polymers small positive combinatorial entropy of mixing.

This qualitative concept can also explain why the UCST of polymers that rely on hydrogen bonding (HB-UCST polymers) is so heavily affected by small amounts of ionic groups while the LCST of poly(NiPAAm) is not. For instance, about 0.2 mol% of acrylic acid units in PNAGA caused the cloud point in pure water to disappear.<sup>[53]</sup> In contrast, 0.8 mol% of acrylic acid units in the

poly(NiPAAm) raised the cloud point by just 3 °C<sup>[138]</sup> as compared to the pure homopolymer.<sup>[120]</sup> For PNAGA, the heat of the phase transition was determined by ultra-sensitive DSC to be  $0.7 \pm 0.4 \text{ J g}^{-1}$ ,<sup>[53]</sup> which is about two magnitudes lower than the heat of the LCST transition of PNiPAAm that was reported to be 42–76 J g<sup>-1</sup>.<sup>[116–118]</sup> If we assume for simplicity of the qualitative discussion that the phases separate into pure solvent and pure polymer then the heat of transition is equal to  $\Delta H_m$ . According to Table 2, it is obvious that the quite strong negative contribution of ionic groups<sup>[136,139]</sup> will affect the  $\Delta H_m/\Delta S_m$  ratio more when  $\Delta H_m$  is already small like it is the case for PNAGA. It should be added that deviations from the general rule that hydrophobic groups increase the UCST and hydrophilic groups decrease it are more likely to occur for hydrophilic comonomers as they usually participate in interpolymer hydrogen bonding. When the two comonomers form stronger hydrogen bonds to each other than to themselves the UCST may increase in contrast to the general rule.

Additionally, this concept can be used to deduce a general rule for the sharpness of the phase transition on the basis of the relation  $\Delta G = -RT \ln(K)$  with  $K$  being the equilibrium constant of the coil-to-globule transition. At constant  $\Delta H_m/\Delta S_m$  ratio, the temperature dependence of  $K$  is stronger for high absolute values of  $\Delta H_m$  and  $\Delta S_m$  resulting in a sharper phase transition. Figure 13 illustrates these trends and this hypothesis is in agreement with experiments.<sup>[117,139]</sup> However, in many cases, the sharpness of transition is more affected by other factors such as the homogeneity of the copolymer composition as discussed in the “Section 3.5.”

## 5. Structure–Property Relationships

### 5.1. Efficiency of Phase Separation

For most applications of thermoresponsive polymers, the phase separation should be as extreme as possible. It

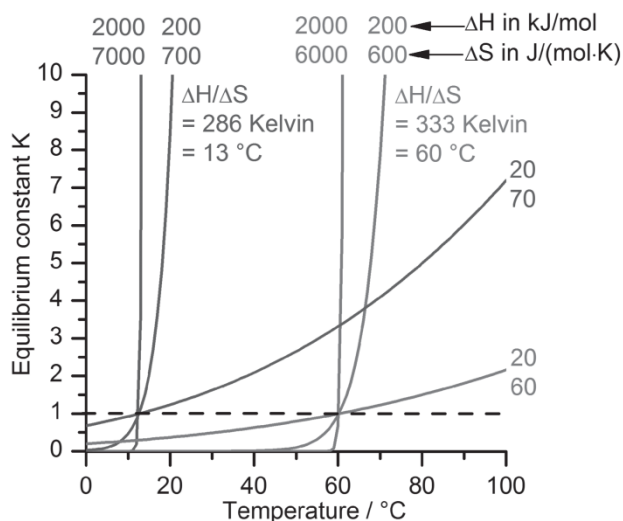


Figure 13. Modeled influence of the absolute magnitude of  $\Delta H_m$  and  $\Delta S_m$  on the equilibrium constant  $K$  of the coil-to-globule transition at two assumed values of  $T_p$  (13 and 60 °C).  $\Delta H_m$  and  $\Delta S_m$  were assumed independent of temperature.

governs the efficiency of separation processes in solution as well as in hydrogels or surface coatings. Considering thermoresponsive hydrogels or surfaces with thermally switchable hydrophilicity, a water-content change between, e.g., 85% and 90% would be of very limited use. For strictly binary polymer solutions, the composition of each phase can be derived from the phase diagram. Ideally, the binodal should be flat and reach far into the high concentration region. This means the attractive polymer–polymer interaction needs to increase monotonically with concentration in a balanced way. Unfortunately, despite the great importance of this aspect, it is the least studied and probably the most difficult to control. Possible handles could be the strength of interpolymer interaction, for example, hydrogen bonds, and the molar mass. Furthermore, the glass transition temperature of the polymer–water mixtures in the high concentration region should be low so the system does not vitrify before complete phase separation. It can be concluded that for evaluation of the possible phase separation efficiency, it is worth obtaining the whole phase diagram including the glass transition temperatures in the high concentration region.

## 5.2. Sharpness of Phase Transition

There is no generally accepted definition for the sharpness of the phase transition of thermoresponsive polymers. For the purpose of this review, it is defined as how strongly the number and compactness of the collective of polymer chains in the collapsed globule state change with temperature. The sharpness is reflected by the suddenness of transmittance change with temperature. The main influences are

the homogeneity of the polymer composition, the dispersity, the absolute magnitude of the enthalpy and entropy of mixing, and the shape of the phase diagram. The first two influences rely on the fact that for a sharp transition, all polymer chains in solution need to possess the same phase-separation temperature. The shape of the phase diagram determines how strongly the compactness and, hence, the refractive indices of the globuli change with temperature. Current results for PNAGA indicate that the homogeneity of the polymer composition is the primary factor. This is most relevant for copolymers.<sup>[119]</sup> In case of disperse low molar mass homopolymers, the endgroups have a marked influence for the same reason.<sup>[111]</sup> The dispersity itself seems to be secondary. Fortunately, several methods should allow precise control of the copolymer composition, molar mass distribution, and endgroups. The copolymer compositions could be controlled by continuous polymerization procedures. Another option would be using controlled radical polymerization (CRP) methods where the compositional drift with conversion is transferred into each individual polymer chain resulting in a gradient copolymer. However, this could have the disadvantage of creating unwanted amphiphilic properties and micelle formation.

## 5.3. Hysteresis

Studies on water-soluble LCST polymers correlated hysteresis with the capability to form additional intra- and interchain hydrogen bonds upon aging in the collapsed state and the magnitude of the glass transition temperature.<sup>[140–142,18]</sup> Same appears to apply for water-soluble UCST polymers. The hysteresis of Poly(AAm-co-AN), PNAGA, and PMAAm increased in the same order as the glass transition temperature.<sup>[119]</sup> As the glass transition is a measure of chain mobility, it is plausible that the kinetics of the phase transition slow down for high  $T_g$  polymers. As expected, the hysteresis of the remixing process increased with aging below the phase-separation temperature which gives rise to the formation of additional hydrogen bonds. However, for poly(NAGA) supercooling below the phase transition temperature before demixing was larger than overheating for remixing. This was probably caused by slow phase separation in the metastable zone between binodal and spinodal. Other factors influencing the hysteresis are the temperature at which the transition occurs and the polymer concentration. As expected, the hysteresis is smaller for higher temperatures and larger at high polymer concentrations due to the increased solution viscosity.<sup>[119,142]</sup>

## 5.4. Sensitivity to pH, Salt, and Other Additives

For a broad application little sensitivity to pH, salt, and other additives is desirable. Since every kind of additive

changes at least the solvent quality, this kind of sensitivity cannot be completely suppressed. However, it is obvious that charged polymers are more sensitive to pH and salts than nonionic polymers. The UCST of cationic or anionic polymers increases upon addition of salts,<sup>[89,125]</sup> the UCST of zwitterionic polymers decreases.<sup>[70–72,79]</sup> Therefore, nonionic UCST polymers based on hydrogen bonding appear to be the most promising candidates for application because they are capable of showing a UCST in both pure water as well as electrolyte solution.<sup>[53,111]</sup> As already found for

nonionic LCST polymers, the effect of salts on nonionic UCST polymers follows the Hofmeister series of ions.<sup>[125,111]</sup>

### 5.5. Type of Phase Behavior

Type II phase separation as observed for PNiPAAm is the most convenient for a broad application because the critical point is independent of the molar mass and the influence on the phase-separation temperature (binodal) is small. For this type of phase behavior,  $\bar{M}_w$ -independent contributions

■ Table 3. Polymers with a UCST in aqueous solution.

Polymer	Inter-polymer interactions	UCST behavior		Remarks	Reference
		Pure water	Physiological conditions <sup>a)</sup>		
PEO (1)	Dipole + bridged HB <sup>b)</sup>	Yes	Yes	Loop-shaped miscibility gap LCST < 200 °C < UCST	[48,49,60–62]
PVME (2)	Dipole + bridged HB	Yes	Yes	2 UCSTs < 0 °C + bimodal LCST	[46,47]
Hydrophobically modified PVA (3)	Weak HB	Yes	Yes	Loop-shaped miscibility gap LCST < 80 °C < UCST; tunable UCST for certain graft polymers	[63,64,130]
PHEMA (4)	Weak HB	Yes	Yes	Loop-shaped miscibility gap for polymers with $\bar{M}_n < 6 \text{ kg mol}^{-1}$ , UCST > 100 °C	[61]
Zwitterionic polymers (5–7)	Zwitterionic interaction	Yes	No		[70–86]
Polyelectrolytes in the presence of multivalent counterions	Bridged ionic interaction	No	Depends on system	Strongly dependent on pH, ionic strength, and ion valency	[87,88]
PAA and copolymers (8)	HB	No	No	UCST behavior at $c(\text{NaCl}) > 400 \times 10^{-3} \text{ M}$ or $\text{pH} < 4$	[89–93]
PAU (10)	HB	Yes <sup>c)</sup>	Yes		[96,97]
PNAGA and derivatives + copolymers (11–14)	HB	Yes <sup>c)</sup>	Yes	Hysteresis of PNAGA and copolymers about 10 °C while only 0.5–0.8 °C for the derivative PNAAAm	[53,105–108, 111,113,119]
Ureido-functionalized polymers (15,16)	HB	Yes <sup>d)</sup>	Yes	hysteresis of 1–2 °C	[125]
Poly(acrylamide-co-acrylonitrile) (17)	HB	Yes <sup>c)</sup>	Yes	Slow hydrolysis, hysteresis of 1–2 °C	[119]
Poly(methacrylamide) (9)	HB	Yes <sup>c)</sup>	?	Broad transition and strong hysteresis; slow hydrolysis	[119]
Copolymers of N-acetylacrylamide (18)	HB	Yes <sup>c)</sup>	?		[126]

<sup>a)</sup>pH 6–8, ionic strength =  $0.1\text{--}0.2 \times 10^{-3} \text{ M}$ ; <sup>b)</sup>HB = hydrogen bonding; PEO and PVME possess only hydrogen bond acceptor units, a water molecule can act as crosslink; <sup>c)</sup>small amounts of ionic groups in the polymer, for example, endgroups or carboxyl groups strongly decrease the UCST so that a cloud point in pure water may be absent. The effect of ionic groups can largely be compensated by the addition of salts; <sup>d)</sup>To observe a cloud point in pure water, the degree of functionalization must be very high because of residual amine groups that are partially protonated at neutral pH.



■ Table 4. Desired properties for a broad applicability of UCST polymers and possible handles for tuning these properties.

Ideal property	Possible handles for tuning
Extreme phase separation, that is, phases separate in almost pure polymer and pure solvent, and little sensitivity of the phase-separation temperature to concentration	The phase diagram should be flat, structure – property relationship not well understood, possible handles are type and strength of interaction as well as molar mass; $T_g$ should be low enough to ensure complete phase separation before vitrification
Sharp phase transition	(a) Homogeneous chain composition: in case of copolymers achievable by continuous polymerization or CRP methods <sup>a)</sup> (b) in case of low molar mass polymers, the end-groups should be similar to the repeating units (c) narrow molar mass distribution (d) high values of $\Delta H_m$ and $\Delta S_m$ by enhancing the polymer – polymer interactions and simultaneously decreasing the hydrophobic effect
Small hysteresis	High chain mobility, low glass transition temperature
Little sensitivity to pH, salts, and other additives	Currently, nonionic UCST polymers appear to be the best option
UCST not dependent on molar mass	Type II phase behavior, molecular origin unclear, possibly cooperativity
Facile tuning of the phase-separation temperature	Choose monomers that can easily be copolymerized or post-modified
Chemically stable <sup>b)</sup>	Choose monomers that are stable under the conditions of intended use

<sup>a)</sup>Using CRP methods, all chains will ideally have the same copolymer composition, however, there will be a gradient within each polymer chain, which might cause unwanted amphiphilic properties like micellation; <sup>b)</sup>for medical applications, where high reversibility is not required biodegradability of the backbone may be intentional.

to  $\Delta H_m$  and  $\Delta S_m$  need to dominate. However, since attractive intermolecular interactions and the positive combinatorial entropy of mixing are the basis of the UCST in water, it is unlikely that type II behavior will be observed.

### 5.6. Facile Tuning of the Phase-Separation Temperature

The phase separation temperature can be tuned by copolymerization or post-modification of the polymer. In case of radical copolymerization, the reaction conditions should provide a homogeneous copolymer composition to achieve a sharp phase transition.<sup>[119]</sup>

### 5.7. Chemical Stability

Chemical stability, especially hydrolysis, is a greater issue than for LCST polymers for two reasons. First, at high temperature when chemical degradation is fast, UCST polymers are in solution and the relevant groups are readily accessible for water or other reagents in solution. Second, UCST polymers appear to have a very small enthalpy of mixing. Therefore, small chemical changes in the polymer composition have a large effect on the phase-separation temperature. To avoid degradation, the monomers should

be chemically stable under the intended conditions. For instance, in the case of hydrolysis, one should prefer acrylamides over acrylates.<sup>[119]</sup> The speed of hydrolysis can be decreased by the addition of sacrificial agents. The hydrolysis of PNAGA for example slowed down considerably by the addition of formamide or other low molar mass amides (unpublished results). The UCST decreasing effect of ester or amide hydrolysis originates from the formation of carboxylate groups. Their effect can largely be neutralized by the addition of salts.

## 6. Conclusions

Polymers with a UCST in water were largely underrepresented in research for a number of possible reasons. (1) The UCST was only observed under practically less relevant conditions, for example, outside the 0 to 100 °C range, only high ionic strength or low pH. Examples are PEO, PVME, hydrophobically modified PVA, PHEMA, PAAc, or carboxylic polymers. (2) The UCST was too sensitive to electrolytes and concentration (e.g., in case of zwitterionic polymers), which is unsuitable for a broad application. (3) Although many hydrogen bonding polymers are capable

of showing a UCST under practically relevant conditions, it remained unobserved because of the strong sensitivity to the (co)polymer composition including endgroups. Examples are PNAGA, poly(methacrylamide), or copolymers of (meth)acrylamide.

All polymers reviewed in this work with their key properties and references are tabulated in Table 3. In order to make UCST polymers suitable for a broad range of applications, one should think about which properties are required and which handles are available to tune these properties. In Table 4, ideal properties for a broad applicability are summarized. Of course, for specific applications, the required properties may vary.

Particularly promising for industrial as well as medical application are UCST polymers that function on the basis of hydrogen bonds (HB-UCST polymers). They show thermoresponsivity in pure water and physiological conditions, allow facile tuning of the phase-separation temperature and can be synthesized from simple building blocks. Since the conditions for a reproducible synthesis and handling have been elaborated HB-UCST polymers are now available for a broader community of scientists. Despite the need for collecting more data on the fundamental properties of these polymers, it will be highly interesting to see how the solution properties will correlate to temperature induced swelling changes of hydrogels or the wetting properties of films. Remaining issues are the chemical stability and yet unknown efficiency of the phase separation. Whatever the outcome, this emerging class of polymers represents a large piece of unclaimed land for physical as well as synthetic polymer chemists and it will help to complete our understanding of the phase behavior of water-soluble polymers.

Acknowledgements: The authors would like to thank the Philipps-University of Marburg for financial support and Michael Salz (University of Hamburg) for advice regarding the calculation of binodals.

Received: June 19, 2012; Revised: July 27, 2012; Published online: DOI: 10.1002/marc.201200433

Keywords: smart polymers; stimuli-responsive polymers; thermoresponse; upper critical solution temperatures

- [1] N. Yamada, T. Okano, H. Sakai, F. Karikusa, Y. Sawasaki, Y. Sakurai, *Macromol. Rapid Commun.* **1990**, *11*, 571.
- [2] N. Mori, H. Horikawa, H. Furukawa, T. Watanabe, *Macromol. Mater. Eng.* **2007**, *292*, 917.
- [3] P. Muthiah, S. M. Hoppe, T. J. Boyle, W. Sigmund, *Macromol. Rapid Commun.* **2011**, *32*, 1716.
- [4] H. Kanazawa, K. Yamamoto, Y. Matsushima, *Anal. Chem.* **1996**, *68*, 100.
- [5] Y. H. Bae, T. Okano, R. Hsu, S. W. Kim, *Macromol. Rapid Commun.* **1987**, *8*, 481.
- [6] Y. Oni, W. O. Soboyejo, *Mater. Sci. Eng., C* **2012**, *32*, 24.
- [7] V. Bulmus, S. Patir, S. A. Tuncel, E. Piskin, *J. Controlled Release* **2001**, *2001*, 265.
- [8] W. L. J. Hinrichs, N. M. E. Schuurmans-Nieuwenbroek, P. van de Wetering, W. E. Hennink, *J. Controlled Release* **1999**, *60*, 249.
- [9] S. Dincer, A. Tuncel, E. Piskin, *Macromol. Chem. Phys.* **2002**, *203*, 1460.
- [10] S. A. Asher, J. M. Weissman, H. B. Sunkura (University of Pittsburgh of the Commonwealth of Higher Education), *U.S. patent 6,165,389*, **2000**.
- [11] J. P. Chen, A. S. Hoffman, *Biomaterials* **1990**, *11*, 631.
- [12] A. Kondo, T. Kaneko, K. Higashitani, *Biotechnol. Bioeng.* **1994**, *44*, 1.
- [13] S. Anastase-Ravion, Z. Ding, A. Pelle, A. S. Hoffman, D. Letourneur, *J. Chromatogr., B: Anal. Technol. Biomed. Life Sci.* **2001**, *761*, 247.
- [14] J. Kobayashi, T. Okano, *Sci. Technol. Adv. Mater.* **2010**, *11*, 014111.
- [15] M. Nakayama, T. Okano, F. M. Winnik, *Mater. Matters* **2010**, *5*, 56.
- [16] Cosmo Biosciences Inc., Online-Shop, [http://www.cosmo-brand.com.cn/product/transplant-medical/22\\_eb9a98e-fc499464b9e88b6d66cc67423.shtml](http://www.cosmo-brand.com.cn/product/transplant-medical/22_eb9a98e-fc499464b9e88b6d66cc67423.shtml) (May 2012).
- [17] Magnabeat Inc., Online-Shop Thermo-Max, [http://www.magnabeat.com/e\\_thermamax.html](http://www.magnabeat.com/e_thermamax.html) (May 2012).
- [18] V. Aseyev, H. Tenhu, F. M. Winnik, *Adv. Polym. Sci.* **2010**, *242*, 29.
- [19] R. Koningsveld, W. H. Stockmayer, E. Nies, *Polymer Phase Diagrams*, Oxford University Press, Oxford **2001**.
- [20] A. D. McNaught, A. Wilkinson, *IUPAC. Compendium of Chemical Terminology (the "Gold Book")*, Blackwell Scientific Publications, Oxford **1997**.
- [21] Note: there is no consent about the scale of phase separation necessary for "UCST-behavior". A typical borderline case are thermoreversible gels that involve microphase separation without further macrophase separation. These were not included in this review. An example are linear poly(ethyleneimine)s that form opaque gels below a critical gelation temperature due to the formation of crystalline domains. See a) J.-J. Yuan, R.-H. Jin, *Langmuir* **2005**, *21*, 3136; b) H. Kakuda, T. Okada, T. Hasegawa, *J. Phys. Chem. B* **2009**, *113*, 13910.
- [22] A. J. Staverman, J. H. van Santen, *Recl. Trav. Chim. Pays-Bas* **1941**, *60*, 76.
- [23] A. J. Staverman, *Recl. Trav. Chim. Pays-Bas* **1941**, *60*, 640.
- [24] M. L. Huggins, *J. Chem. Phys.* **1941**, *9*, 440.
- [25] M. L. Huggins, *Ann. N. Y. Acad. Sci.* **1942**, *43*, 1.
- [26] P. J. Flory, *J. Chem. Phys.* **1941**, *9*, 660.
- [27] P. J. Flory, *J. Chem. Phys.* **1942**, *10*, 51.
- [28] D. B. Keyes, J. H. Hildebrand, *J. Am. Chem. Soc.* **1917**, *39*, 2120.
- [29] A. Nakajima, F. Hamada, S. Hayashi, *J. Polym. Sci., Part C: Polym. Symp.* **1967**, *15*, 285.
- [30] R. Koningsveld, A. J. Staverman, *J. Polym. Sci., Polym. Phys. Ed.* **1968**, *6*, 325.
- [31] A. R. Schultz, P. J. Flory, *J. Am. Chem. Soc.* **1952**, *74*, 4760.
- [32] J. Hashizume, A. Teramoto, H. Fujita, *J. Polym. Sci., Polym. Phys. Ed.* **1981**, *19*, 1405.
- [33] M. Bercea, M. Cazacu, B. A. Wolf, *Macromol. Chem. Phys.* **2003**, *204*, 1371.
- [34] B. A. Wolf, *Macromol. Chem. Phys.* **2003**, *204*, 1381.
- [35] S. Stryuk, B. A. Wolf, *Macromol. Chem. Phys.* **2003**, *204*, 1948.
- [36] R. De Cooman, PhD thesis, Katholieke Universiteit (Leuven), **1994**.

- [37] L. P. Rebelo, W. A. Van Hook, *J. Polym. Sci., Part B: Polym. Phys.* **1993**, *31*, 895.
- [38] L. Aerts, M. Kunz, H. Berghmans, R. Koningsveld, *Makromol. Chem.* **1993**, *194*, 2697.
- [39] J. Arnauts, H. Berghmans, R. Koningsveld, *Makromol. Chem.* **1993**, *194*, 77.
- [40] P. J. Flory, *J. Chem. Phys.* **1944**, *12*, 114.
- [41] R. L. Scott, M. Magat, *J. Phys. Chem.* **1945**, *13*, 172.
- [42] G. Rehage, W. Wefers, *J. Polym. Sci., Polym. Phys. Ed.* **1968**, *6*, 1683.
- [43] R. Koningsveld, *Adv. Colloid Interface Sci.* **1968**, *2*, 151.
- [44] K. Solc, K. Dusek, R. Koningsveld, H. Berghmans, *Collect. Czech. Chem. Commun.* **1995**, *60*, 1661.
- [45] F. Afroze, E. Nies, H. Berghmans, *J. Mol. Struct.* **2000**, *554*, 55.
- [46] K. Van Durme, G. V. Assche, E. Nies, B. Van Mele, *J. Phys. Chem. B* **2007**, *111*, 1288.
- [47] G. V. Assche, B. Van Mele, T. Li, E. Nies, *Macromolecules* **2011**, *44*, 993.
- [48] E. E. Dormidontova, *Macromolecules* **2002**, *35*, 987.
- [49] E. E. Dormidontova, *Macromolecules* **2004**, *37*, 7747.
- [50] Y. Okada, F. Tanaka, *Macromolecules* **2005**, *38*, 4465.
- [51] F. Tanaka, T. Koga, I. Kaneda, F. M. Winnik, *J. Phys.: Condens. Matter* **2011**, *23*, 284105.
- [52] D. E. Bergbreiter, H. Fu, *J. Polym. Sci., Part A: Polym. Chem.* **2008**, *46*, 186.
- [53] J. Seuring, F. M. Frank, K. Huber, S. Agarwal, *Macromolecules* **2012**, *45*, 374.
- [54] C. Wu, X. Wang, *Phys. Rev. Lett.* **1998**, *80*, 4092.
- [55] S. Vshivkov, A. P. Safronov, *Macromol. Chem. Phys.* **1997**, *198*, 3015.
- [56] F. Zeng, Z. Tong, *Polymer* **1997**, *38*, 5539.
- [57] Y. Maeda, T. Nakamura, I. Ikeda, *Macromolecules* **2001**, *34*, 1391.
- [58] F. M. Winnik, *Macromolecules* **1990**, *23*, 233.
- [59] F. M. Winnik, *Macromolecules* **1990**, *23*, 1647.
- [60] G. N. Malcolm, J. S. Rowlinson, *Trans. Faraday Soc.* **1957**, *53*, 921.
- [61] S. Saeki, N. Kuwahara, M. Nakata, M. Kaneko, *Polymer* **1976**, *17*, 685.
- [62] Y. C. Bae, S. M. Lambert, D. S. Soane, J. M. Prausnitz, *Macromolecules* **1991**, *24*, 4403.
- [63] K. Shibatani, Y. Oyanagi, *Kobunshi Kagaku* **1971**, *28*, 361.
- [64] T. Shiomi, K. Imai, C. Watanabe, M. Miya, *J. Polym. Sci., Polym. Phys. Ed.* **1984**, *22*, 1305.
- [65] B. J. Pae, T. J. Moon, *Korea Polym. J.* **1997**, *5*, 126.
- [66] R. Longenecker, T. Mu, M. Hanna, N. A. D. Burke, H. D. H. Stöver, *Macromolecules* **2011**, *44*, 8962.
- [67] S. E. Kudajbergenov, *Polyampholytes*, Kluwer Academic/Plenum Publishers, New York **2002**.
- [68] A. B. Lowe, C. L. Mc Cormick, *Chem. Rev.* **2002**, *102*, 4177.
- [69] S. Kudaibergenov, W. Jaeger, A. Laschewsky, *Adv. Polym. Sci.* **2006**, *201*, 157.
- [70] D. N. Schulz, D. G. Pfeiffer, P. K. Agarwal, J. Larabee, J. J. Kaladas, L. Soni, B. Handwerker, R. T. Garner, *Polymer* **1986**, *27*, 1734.
- [71] M. B. Huglin, M. A. Radwan, *Polym. Int.* **1991**, *26*, 97.
- [72] P. Mary, D. D. Bendejacq, M.-P. Mareau, P. Dupuis, *J. Phys. Chem. B* **2007**, *111*, 7767.
- [73] L. Chen, Y. Honma, T. Mizutani, D. Liaw, J. P. Gong, Y. Osada, *Polymer* **2000**, *41*, 141.
- [74] Y. Chang, W.-Y. Chen, W. Yandi, Y.-J. Shih, W.-L. Chu, C.-W. Chu, R.-C. Ruaan, A. Higuchi, *Biomacromolecules* **2009**, *10*, 2092.
- [75] Y. Maeda, H. Mochiduki, I. Ikeda, *Macromol. Rapid Commun.* **2004**, *25*, 1330.
- [76] H. Tian, J. Yan, D. Wang, C. Gu, Y. You, X. Chen, *Macromol. Rapid Commun.* **2011**, *32*, 660.
- [77] M. Arotcarena, B. Heise, S. Ishaya, A. Laschewsky, *J. Am. Chem. Soc.* **2002**, *124*, 3787.
- [78] J. Virtanen, M. Arotcarena, B. Heise, S. Ishaya, A. Laschewsky, H. Tenhu, *Langmuir* **2002**, *18*, 5360.
- [79] P. Köberle, A. Laschewsky, T. D. Lomax, *Makromol. Chem., Rapid Commun.* **1991**, *12*, 427.
- [80] N. Gonsior, H. Ritter, *Macromol. Chem. Phys.* **2012**, *213*, 382.
- [81] G. S. Georgiev, Z. P. Mincheva, V. T. Georgieva, *Macromol. Symp.* **2001**, *164*, 301.
- [82] I. Kamenova, M. Harrass, B. Lehmann, K. Friedrich, I. Ivanov, G. Georgiev, *Macromol. Symp.* **2007**, *254*, 122.
- [83] P. Ravi, S. Dai, K. C. Tam, *J. Phys. Chem. B* **2005**, *109*, 22791.
- [84] A. Housni, Y. Zhao, *Langmuir* **2010**, *26*, 12933.
- [85] F. Polzer, J. Heigl, C. Schneider, M. Ballauff, O. V. Borisov, *Macromolecules* **2011**, *44*, 1654.
- [86] A. V. Ermoshkin, A. N. Kudlay, M. Olvera de la Cruz, *J. Chem. Phys.* **2004**, *120*, 11930.
- [87] X. Jia, D. Chen, M. Jiang, *Chem. Commun.* **2006**, *42*, 1736.
- [88] F. A. Plamper, A. Schmalz, M. Ballauff, A. H. E. Müller, *J. Am. Chem. Soc.* **2007**, *129*, 14538.
- [89] P. J. Flory, J. E. Osterheld, *J. Phys. Chem.* **1954**, *58*, 653.
- [90] R. Buscall, T. Corner, *Eur. Polym. J.* **1982**, *18*, 967.
- [91] G. Bokias, G. Staikos, I. Iliopoulos, *Polymer* **2000**, *41*, 7399.
- [92] J. Fang, F. Bian, W. Shen, *J. Appl. Polym. Sci.* **2008**, *110*, 3373.
- [93] T. Mori, M. Nakashima, Y. Fukuda, K. Minagawa, M. Tanaka, Y. Maeda, *Langmuir* **2006**, *22*, 4336.
- [94] H. Mori, I. Kato, Saito Shoko; Endo, T. Endo, *Macromolecules* **2010**, *43*, 1289.
- [95] N. M. Brahme, W. T. Smith, *J. Polym. Sci., Polym. Chem. Ed.* **1984**, *22*, 813.
- [96] T. Aoki, K. Nakamura, K. Sanui, N. Ogata, A. Kikuchi, T. Okano, Y. Sakurai, *Proceed. Int. Symp. Control. Rel. Bioact. Mater.* **1996**, *23*, 767.
- [97] T. Aoki, K. Nakamura, K. Sanui, A. Kikuchi, T. Okano, Y. Sakurai, N. Ogata, *Polym. J.* **1999**, *31*, 1185.
- [98] H. C. Haas, N. W. Schuler, *Polym. Lett.* **1964**, *2*, 1095.
- [99] H. C. Haas, R. D. Moreau, N. W. Schuler, *J. Polym. Sci., Polym. Phys. Ed.* **1967**, *5*, 915.
- [100] H. C. Haas, C. K. Chiklis, R. D. Moreau, *J. Polym. Sci., Part A-1: Polym. Chem.* **1970**, *8*, 1131.
- [101] H. C. Haas, M. J. Manning, M. H. Mach, *J. Polym. Sci., Part A-1: Polym. Chem.* **1970**, *8*, 1725.
- [102] O. Marstokk, B. Nyström, J. Roots, *Macromolecules* **1998**, *31*, 4205.
- [103] D. Ostrovskii, P. Jacobsson, B. Nyström, O. Marstokk, H. B. M. Kopperud, *Macromolecules* **1999**, *32*, 5552.
- [104] S. Glatzel, N. Badi, M. Päch, A. Laschewsky, J. Lutz, *Chem. Commun.* **2010**, *46*, 4517.
- [105] H. Nagaoka, N. Ohnishi, M. Eguchi (Chisso Corporation), *US patent 2007/0203313 A1*, **2007**.
- [106] N. Ohnishi, H. Furukawa, K. Kataoka, K. Ueno (National Institute of Advanced Industrial Science and Technology; Chisso Corporation), *US patent 7,195,925 B2*, **2007**.
- [107] N. Ohnishi, H. Furukawa, H. Hideyuki, J. Wang, C. An, E. Fukusaki, K. Kataoka, K. Ueno, A. Kondo, *NanoBiotechnology* **2006**, *2*, 43.
- [108] J. Seuring, S. Agarwal, *Macromol. Chem. Phys.* **2010**, *211*, 2109.
- [109] G. Müller, *Polym. Bull.* **1981**, *5*, 31.
- [110] H. Kheradmand, J. Francois, *Polymer* **1988**, *29*, 860.

- [111] F. Liu, J. Seuring, S. Agarwal, *J. Polym. Sci., Part A: Polym. Chem.* **2012**, DOI: 10.1002/pola.26322.
- [112] F. Hofmeister, *Arch. Exp. Pathol. Pharmacol.* **1888**, *24*, 247.
- [113] M. Eguchi, N. Ohnishi (Chisso Corporation), *EP 2009044A1*, **2008**.
- [114] Y. Zhang, S. Furyk, D. E. Bergbreiter, P. S. Cremer, *J. Am. Chem. Soc.* **2005**, *127*, 14505.
- [115] Y. Zhang, P. S. Cremer, *Curr. Opin. Chem. Biol.* **2006**, *10*, 658.
- [116] H. G. Schild, D. A. Tirrell, *J. Phys. Chem.* **1990**, *94*, 4352.
- [117] P. S. Mumick, C. L. Mc Cormick, *Polym. Eng. Sci.* **1994**, *34*, 1419.
- [118] Y. Ding, X. Ye, G. Zhang, *Macromolecules* **2005**, *38*, 904.
- [119] J. Seuring, S. Agarwal, *Macromolecules* **2012**, *45*, 3910.
- [120] S. Fujishige, K. Kubota, I. Ando, *J. Phys. Chem.* **1989**, *93*, 3311.
- [121] M. Netopilik, M. Bohdanecky, V. Chytry, K. Ulbrich, *Macromol. Rapid Commun.* **1997**, *18*, 107.
- [122] E. Tiktopulo, V. N. Uversky, V. B. Lushchik, S. I. Klenin, V. E. Bychkova, O. B. Ptitsyn, *Macromolecules* **1995**, *28*, 7519.
- [123] M. Kano, E. Kokufuta, *Langmuir* **2009**, *25*, 8649.
- [124] S. Glatzel, A. Laschewsky, J. Lutz, *Macromolecules* **2011**, *44*, 413.
- [125] N. Shimada, H. Ino, K. Maie, M. Nakayama, A. Kano, A. Maruyama, *Biomacromolecules* **2011**, *12*, 3418.
- [126] N. Ohnishi, K. Aoshima, K. Kataoka, K. Ueno (Agency of Industrial Science and Technology MITI; Japan Chemical Innovation Institute), *EP 0 922 715 A2*, **1999**.
- [127] N. Kato, M. Takeda, Y. Sakai, T. Uyehara, *Anal. Sci.* **2001**, *17*, i1137.
- [128] A. Silberberg, J. Eliassaf, A. Katchalsky, *J. Polym. Sci.* **1957**, *23*, 259.
- [129] J. Eliassaf, *J. Appl. Polym. Sci.* **1960**, *3*, 372.
- [130] G. Wu, S.-C. Chen, Q. Zhan, Y.-Z. Wang, *Macromolecules* **2011**, *44*, 999.
- [131] C. A. Hunter, *Angew. Chem., Int. Ed.* **2004**, *43*, 5310.
- [132] T. P. Silverstein, *J. Chem. Edu.* **1998**, *75*, 116.
- [133] T. P. Silverstein, *J. Chem. Edu.* **2008**, *85*, 917.
- [134] J. Burgess, *Metal Ions in Solution*, Ellis Horwood, Chichester **1978**.
- [135] L. D. Taylor, L. D. Cerankowski, *J. Polym. Sci., Polym. Chem. Ed.* **1975**, *13*, 2551.
- [136] H. Feil, Y. H. Bae, J. Feijen, S. W. Kim, *Macromolecules* **1993**, *26*, 2496.
- [137] R. Liu, M. Fraylich, B. R. Saunders, *Colloid Polym. Sci.* **2009**, *287*, 627.
- [138] X. Qiu, C. M. S. Kwan, C. Wu, *Macromolecules* **1997**, *30*, 6090.
- [139] S. Kunugi, T. Tada, Y. Yamazaki, *Langmuir* **2000**, *16*, 2042.
- [140] K. Van Durme, G. V. Assche, B. Van Mele, *Macromolecules* **2004**, *37*, 9596.
- [141] H. Cheng, L. Shen, C. Wu, *Macromolecules* **2006**, *39*, 2325.
- [142] Y. Lu, K. Zhou, Y. Ding, G. Zhang, C. Wu, *Phys. Chem. Chem. Phys.* **2010**, *12*, 3188.

## Lectures

- 12/2010      **Frühjahrssymposium des Jungchemiker Forums** in Rostock, Germany  
*Concealed Properties – Polymers with an Upper Critical Solution Temperature in Water*
- 01/2012      **14<sup>th</sup> IUPAC Conference on Polymers and Organic Chemistry** in Doha, Qatar  
*Concealed Qualities – Polymers with an Upper Critical Solution Temperature in Water*
- 03/2012      **Macro 2010** conference in New Delhi, India  
*Non-Ionic Homo- and Copolymers with an Upper Critical Solution Temperature in Water*



## Summary

In this work polymers with upper critical solution temperature (UCST) in water have been synthesized and characterized. The task was to answer the question why polymers with UCST in water were largely underrepresented in basic and applied research and to develop a universal approach for the synthesis of new polymers with UCST.

Drawing on the example of poly(*N*-acryloylglycinamide) (poly(NAGA)), a polymer that is well known since 1964, it was shown that traces of ionic groups drastically decrease the UCST. In the past ionic groups have been introduced unintentionally by either acrylate impurities in the monomer, hydrolysis of the polymer side chains and/or usage of ionic initiators or chain transfer agents giving a feasible explanation why the UCST of poly(NAGA) remained unreported until 2010 as a part of this work. The synthesis of NAGA was modified in order to yield acrylate free monomer and the crystal structure was determined. A detailed analysis of the UCST suppressing effects of ionic groups followed. Only 1 ionic group in 1000 repeating units of the polymer is sufficient to completely suppress the UCST behavior. Therefore, conventional analytic methods like NMR, IR, elemental analysis, thin layer chromatography, etc. were not sensitive enough. Special methods like capillary electrophoresis and flame atomic absorption spectroscopy had to be employed to prove the hypothesis. The UCST of poly(NAGA) relies on thermally reversible hydrogen bonding. The sensitivity to ionic groups in the polymer may be explained by the very low heat of transition which could be determined by using ultrasensitive differential scanning calorimetry. Furthermore, in a preliminary dynamic and static light scattering study it could be shown that when polymer aggregates collapsed upon cooling below the phase separation temperature their density increased by more than two orders of magnitude. In order to study the effect of polymer endgroups and the molecular weight distribution on the phase transition controlled radical polymerization via the radical addition fragmentation transfer process (RAFT) was performed. As expected, polymers with an ionic endgroup showed no UCST in pure water but in electrolyte solution. The addition of salts influenced the cloud points according to the Hofmeister series of ions.

The phase transition temperature of poly(NAGA) was shifted by copolymerization with hydrophobic comonomers like butyl acrylate and styrene. The choice of monomer turned out to be crucial for the sharpness and reversibility of the phase transition. Fundamental

knowledge obtained from poly(NAGA) and copolymers was subsequently transferred to simple commercially available monomers. A set of rules were established how to obtain polymers with freely tunable UCST in water as well as electrolyte solution. This hypothesis was proven by the synthesis of poly(methacrylamide) and poly(acrylamide-*co*-acrylonitrile), actually very old polymer systems, that showed a UCST. Finally, knowledge gained in this and previous works was condensed into a review article allowing the conclusion of further structure-property-relationships.



## Outlook

UCST polymers that function on the basis of hydrogen bonds (HB-UCST polymers) are promising candidates for industrial as well as medical applications. They show thermo-responsivity in pure water and physiological conditions, allow facile tuning of the phase separation temperature and can be synthesized from simple building blocks. Since the conditions for a reproducible synthesis and handling have been elaborated HB-UCST polymers are now available for a broader community of scientists. Remaining issues are the chemical stability and yet unknown efficiency of the phase separation. So far all nonionic HB-UCST polymers contain amide groups that can hydrolyze. A yet successful application could be based on three strategies. First, one should conduct a thorough analysis of the hydrolysis speed under different conditions for defining a reasonable temperature range for application. Second, protection against hydrolysis can be achieved by sacrificial agents like low molecular weight amides. Third, salts can be added to compensate the effect of a certain amount of hydrolysis. Another option would be the design new HB-UCST polymers featuring H-acceptor and H-donor moieties that are more stable to hydrolysis. For this purpose a list of H-acceptors and H-donors and their relative strength as given by Hunter et al. (*Angew. Chem. Int. Ed.* **2004**, *43*, 5310) could be highly useful. In order to evaluate the possible phase separation efficiency it is worth obtaining the whole phase diagram including the glass transition temperatures in the high concentration region. Moreover, additional data is needed for consolidation and refinement of apparent structure property relationships regarding important features of the phase transition like sharpness of the transition, hysteresis and sensitivity of the phase transition temperature to composition changes.

As reproducible synthesis and handling of UCST polymers is possible first efforts in the direction of material science can be undertaken. In preliminary experiments a crosslinked hydrogel of poly(NAGA) was synthesized. As anticipated it showed reversible swelling and deswelling as a function of temperature in pure water as well as physiologic conditions (Figure 6). Likewise, investigating the temperature dependent wetting properties of such polymer coatings would be promising.

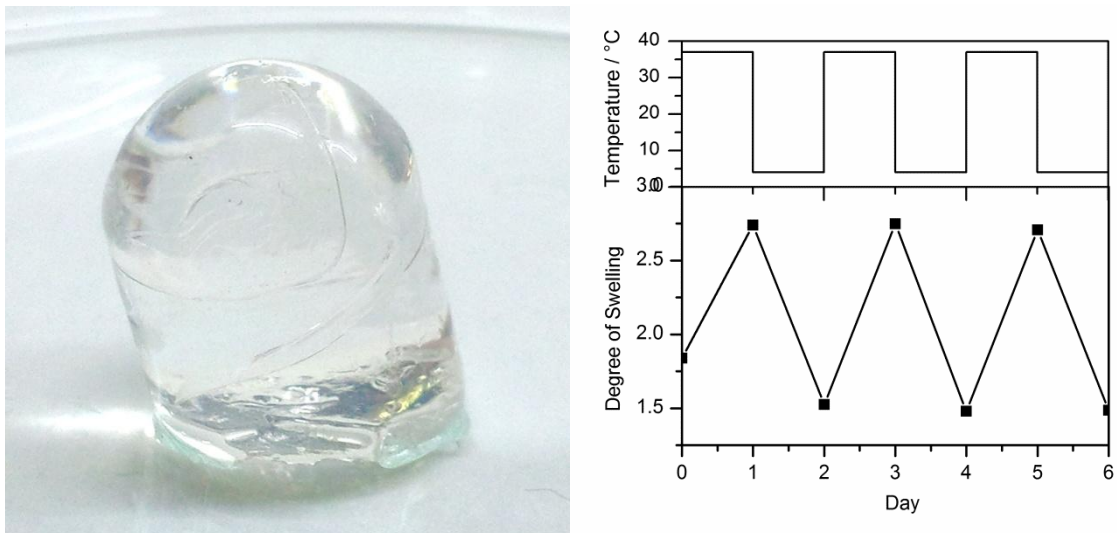


**Figure 6.** left: crosslinked poly(NAGA) hydrogel after preparation in a test-tube and dialysis; right: reversible swelling and deswelling in water as a function of temperature. The degree of swelling at day zero was measured at room temperature.

## Zusammenfassung

Im Rahmen dieser Arbeit wurden Polymere mit oberer kritischer Lösungstemperatur (engl. UCST) synthetisiert und charakterisiert. Das Ziel war die Frage zu beantworten, weshalb Polymere mit UCST in Grundlagen- und angewandter Forschung stark unterrepräsentiert waren und eine universelle Strategie zur Synthese von neuen Polymeren mit UCST in Wasser zu erarbeiten.

Am Beispiel von Poly(*N*-acrylglycinamid) (Poly(NAGA)), welches seit 1964 bekannt ist, wurde gezeigt, dass Spuren von ionischen Gruppen die UCST drastisch erniedrigen. In der Vergangenheit gelangten ionische Gruppen ungewollt in das Polymer durch Acrylat-Verunreinigungen im Monomer, Hydrolyse der Polymerseitenketten und/oder Verwendung von ionischen Initiatoren oder Kettentransferreagenzien. Höchstwahrscheinlich war dies der Grund, weshalb die UCST von Poly(NAGA) erst 2010 im Rahmen dieser Arbeit berichtet wurde. Um acrylatfreies Monomer zu erhalten, wurde die Synthese von NAGA verändert und die Kristallstruktur bestimmt. Es folgte eine detaillierte Analyse der UCST-Erniedrigung durch ionischen Gruppen. Eine ionische Gruppe auf 1000 Wiederholungseinheiten des Polymers reicht aus, um das UCST-Verhalten vollständig zu unterdrücken. Aus diesem Grund war es nicht möglich, die Verunreinigungen durch konventionelle Methoden wie NMR, IR, Elementaranalyse, Dünnschichtchromatographie oder Ähnliches zu detektieren. Spezielle Methoden wie Kapillarelektrophorese und Flammenabsorptionsspektroskopie mussten eingesetzt werden, um die Hypothese zu bestätigen. Die UCST von Poly(NAGA) basiert auf der Bildung thermisch reversibler Wasserstoffbrückenbindungen. Die Sensitivität der Phasenübergangstemperatur im Bezug auf ionische Gruppen könnte durch die geringe Phasenübergangswärme erklärt werden, welche durch ultrasensitive Differentialkalorimetrie gemessen werden konnte. Weiterhin wurde in einer vorläufigen Untersuchung mit dynamischer und statischer Lichtstreuung gezeigt, dass, wenn Polymeraggregate beim Abkühlen unterhalb der Phasenübergangstemperatur kollabieren, die Dichte dieser Partikel um mehr als zwei Größenordnungen zunimmt. Um den Effekt der Polymerendgruppen und der Molekulargewichtsverteilung auf den Phasenübergang zu untersuchen, wurde kontrollierte radikalische Polymerisation mit Hilfe des „radical addition fragmentation transfer“ (RAFT) Prozesses durchgeführt. Wie erwartet zeigten die Polymere mit ionischen Endgruppen eine UCST in Elektrolytlösung, nicht jedoch in reinem Wasser. Der Zusatz von

Salzen beeinflusste den Trübungspunkt in Übereinstimmung mit der Hofmeister-Reihe der Ionen.

Die Phasenübergangstemperatur von Poly(NAGA) wurde gezielt durch Copolymerisation mit hydrophoben Comonomeren wie Butylacrylat und Styrol erhöht. Die Wahl des Monomers war entscheidend für Schärfe und Wiederholbarkeit des Phasenübergangs. Die grundlegenden Erkenntnisse, die für Poly(NAGA) und Copolymere erlangt wurden, wurden auf simple, kommerziell erhältliche Monomere übertragen. Es wurden Bedingungen formuliert, welche für die Synthese von neuen UCST-Polymeren erfüllt werden müssen. Diese Hypothesen wurden durch die Synthese von Poly(methacrylamid) und Poly(acrylamid-*co*-acrylnitril) bestätigt. Diese eigentlich lange bekannten Polymersysteme zeigten unter den gewählten Synthesebedingungen eine UCST in Wasser. Schließlich wurden die hier erlangten Erkenntnisse mit zuvor bekanntem Literaturwissen in einem Übersichts-Artikel zusammengeführt. Dadurch konnten viele Struktur-Eigenschafts-Beziehungen aufgezeigt werden.

# Curriculum Vitae

since 03/2009	<p><b>Professional Experience</b></p> <p><b>Scientist for research and teaching</b>            Philipps-Universität Marburg  <i>Lecturer of “Übung zur Vorlesung: Chemie für Biologen und Humanbiologen“ and “Seminar zum chemischen Praktikum für Biologen und Humanbiologen“ for undergraduate students in biology and human biology</i>  <i>Supervision and guidance of students in practical work and research projects</i>  <i>2010 and 2011 group leader in the educational project “Erfinderlabor Faszination Nanotechnologie“</i></p>
	<p><b>Education</b></p>
since 03/2009	<p><b>Doctoral studies</b>            Workgroup of Seema Agarwal, macromolecular chemistry, Philipps-Universität Marburg  <i>Polymers with Upper Critical Solution Temperature in Aqueous Solution</i></p>
01/2009	<p><b>Diploma</b> in chemistry, grade <b>1.1</b></p>
05/2008-01/2009	<p><b>Diploma thesis</b>            Work group of Prof. Seema Agarwal, macromolecular chemistry, Philipps-Universität Marburg  <i>Synthese, Charakterisierung und Polymerisation eines neuen polymerisierbaren Tensids – Wege zu biomimetischen Oberflächen,</i>            grade <b>1.0</b></p>
09/2006-04/2007	<p><b>Semester abroad</b>            University of Sydney, Australia</p>
10/2005-02/2008	<p><b>Studies in chemistry</b>, Philipps-Universität Marburg            Main focus: inorganic, organic, and physical chemistry            Elective subject: macromolecular chemistry</p>
06/2003	<p><b>Abitur</b> at Main-Taunus-Schule in Hofheim am Taunus, grade <b>1.8</b></p>
	<p><b>Experience Abroad</b></p>
09/2006-04/2007	<p><b>Research project</b>            Research in the workgroup of Prof. Peter Lay, University of Sydney, <b>Australia</b>, with a period of research at the synchrotron of the Photon Factory, Tsukuba, <b>Japan</b>  <i>Reactivity of potential anti-diabetic molybdenum(VI) complexes in biological media: A XANES spectroscopic study</i></p>

## List of Publications and Presentations

### Publications

- 09/2012 **Jan Seuring**, Seema Agarwal  
Review Article: *Polymers with Upper Critical Solution Temperature in Aqueous Solution*  
*Macromolecular Rapid Communications* **2012**  
DOI: 10.1002/marc.201200433
- 08/2012 Fangyao Liu, **Jan Seuring**, Seema Agarwal  
*Controlled Radical Polymerization of N-Acryloylglycinamide and UCST-type Phase Transition of the Polymers*  
*Journal of Polymer Science, Part A: Polymer Chemistry* **2012**,  
DOI: 10.1002/pola.26322
- 04/2012 **Jan Seuring**, Seema Agarwal  
*First Example of a Universal and Cost-Effective Approach: Polymers with Upper Critical Solution Temperature in Water*  
*Macromolecules* **2012**, 45, 3910-3918
- 12/2011 **Jan Seuring**, Frank M. Bayer, Klaus Huber, Seema Agarwal  
*Upper Critical Solution Temperature of Poly(N-acryloyl glycinamide) in Water: A Concealed Property*  
*Macromolecules* **2012**, 45, 374-384
- 07/2011 **Jan Seuring**, Seema Agarwal, Klaus Harms  
*N-Acryloyl glycinamide*  
*Acta Crystallographica Section E* **2011**, E67, o2170
- 09/2010 **Jan Seuring**, Seema Agarwal  
*Non-Ionic Homo- and Copolymers with H-Donor and H-Acceptor Units with a UCST in Water*  
*Macromolecular Chemistry and Physics* **2010**, 211, 2109-2117
- 03/2010 **Jan Seuring**, Philipp Reiss, Ulrich Koert, Seema Agarwal  
*Synthesis, characterization and properties of a new polymerisable surfactant: 12-Methacryloyloxy dodecylphosphocholine*  
*Chemistry and Physics of Lipids* **2010**, 163, 367-372
- 07/2007 Aviva Levina, Andrew I. McLeod, **Jan Seuring**, Peter A. Lay  
*Reactivity of potential anti-diabetic molybdenum(VI) complexes in biological media: A XANES spectroscopic study*  
*Journal of Inorganic Biochemistry* **2007**, 101, 1586-1593

### Conference Presentations

- 03/2012      **Frühjahrssymposium des Jungchemiker Forums** in Rostock, Germany  
*Concealed Properties – Polymers with an Upper Critical Solution Temperature in Water*
- 01/2012      **14<sup>th</sup> IUPAC Conference on Polymers and Organic Chemistry** in Doha, Qatar  
*Concealed Qualities – Polymers with an Upper Critical Solution Temperature in Water*
- 12/2010      **Macro 2010** conference in New Delhi, India  
*Non-Ionic Homo- and Copolymers with an Upper Critical Solution Temperature in Water*





## Acknowledgments

I would like to thank my supervisor Prof. Seema Agarwal for the highly interesting topic that started with her discovery of an important patent that had slipped notice of the scientific community. I am thankful for her supervision of my thesis, especially for the great degree of freedom I enjoyed regarding the engagement in cooperations and presentation on conferences.

I thank Prof. Andreas Greiner for the second opinion on this work and his great support regarding my teaching efforts.

I am grateful to Prof. Klaus Huber and his workgroup for the fruitful cooperation.

For the perfect cooperation and good working atmosphere I like to thank my Labmates Anna Katharina Bier and Fangyao Liu. Moreover, Anna was an excellent travel companion.

I like to thank Rüdiger Ellinghaus, Kai Krannig, Simon Helmstetter, Fangyao Liu, Anna Fichtner, Dominic Keller, Ziyin Fan, Beatrice Amanda Pineda and Johannes Martin for their motivated assistance during their research training.

I am indebted to Dr. Michael Bognitzki for indispensable advice regarding extraction and crystallization methods.

I express my gratitude to the NMR department for being friendly and cooperative despite being bothered by over 200 high temperature measurements.

The workgroups of Prof. Seema Agarwal and Prof. Andreas Greiner have been an inseparable unity. I thank all members for their everlasting willingness to help and the fun we had especially in Hirscheegg and Freiburg.

Happiness and self-motivation are intertwined. I like to thank my love Kira, my friends and parents for the provision of happiness.

## *Acknowledgments*

---

Finally, I like to thank my parents for their never-ending support at all levels during the last 28 years.